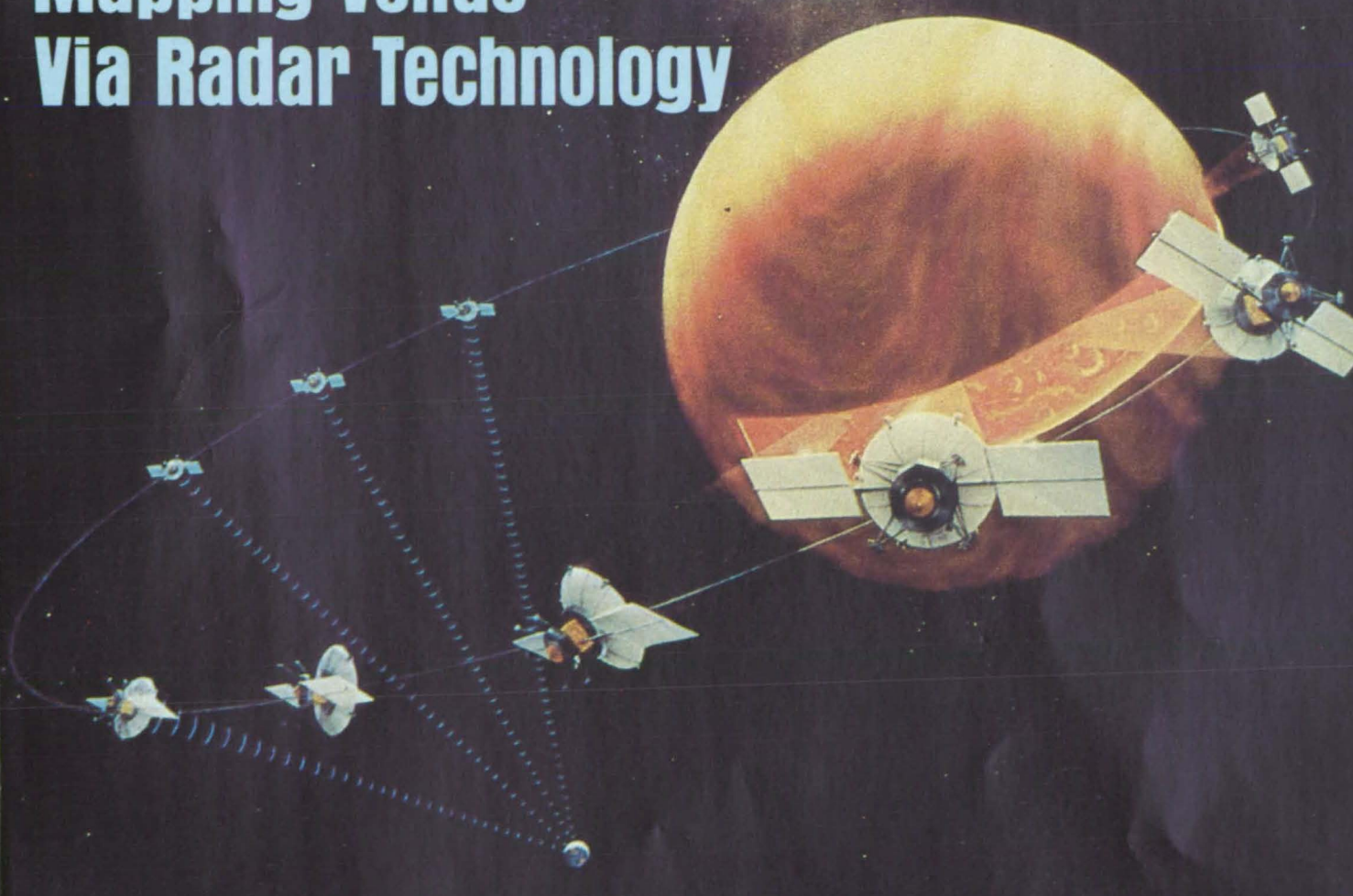


NASA Tech Briefs

National
Aeronautics and
Space
Administration

Summer 1985
Volume 9 Number 2

Mapping Venus Via Radar Technology



Good news

For humans, a better life on Earth.

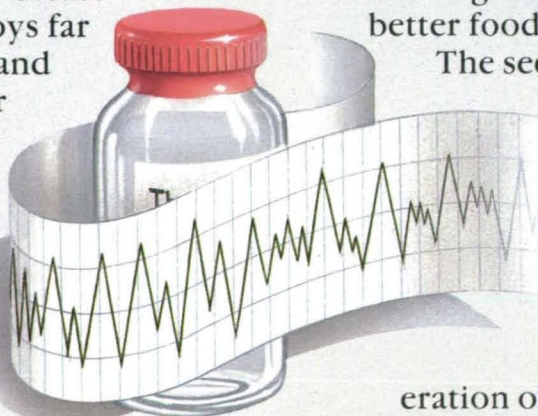
Soon, 26 years of space exploration will begin to pay off in ways few Americans can imagine. When America's first permanent space station goes into orbit, here is what NASA expects to learn:

How to manufacture purer vaccines and new drugs impossible to make on Earth.

How to manufacture computer chips with capacities that are one hundred times greater than the best we have now.

How to create metal alloys far stronger and far lighter than any made on Earth.

How to create metals that can transmit electrical energy with no



appreciable loss of power. (The savings to consumers could be billions of dollars every year!)

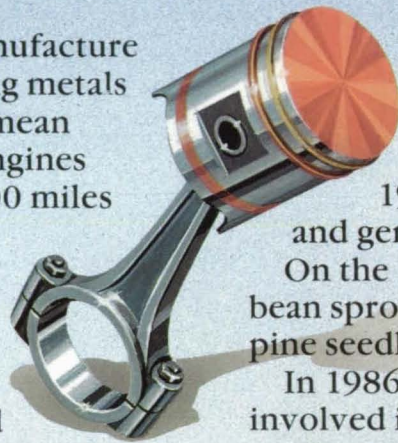
How to manufacture self-lubricating metals which could mean automobile engines lasting 500,000 miles and more.

These are only a few of over 150 experiments being planned right now that will be made possible by NASA and companies such as General Electric.

Planting the seeds of knowledge 25 years ago.

Work NASA began long ago will soon teach us not only how to grow food in space, but perhaps even how to grow more and better food on Earth.

The seeds General Electric helped send into space on Discoverer 32 in 1960 propagated a new generation of increasingly sophisticated — and fruitful — experiments.



On Bio-satellite II, wheat and peppers were successfully germinated.

On Apollo 16 in 1972, beans and watercress were studied.

On Skylab 3 in 1973, the growth and germination of rice.

On the 1982 shuttle, bean sprouts, oats, and pine seedlings.

In 1986, GE will be involved in further work on the Space Shuttle with wheat and oats.

One thing NASA hopes to learn is whether it's possible to grow more from every seed.

Good news for heart patients on Earth.

For fourteen years, GE has worked with NASA on the effects of weightlessness on the cardiovascular system. A new device GE has helped develop for use on America's permanent space station may soon make it possible for doctors on Earth to use a noninvasive

from space:

technique instead of catheterization in the treatment of heart patients.

The GE device uses a trace gas inhaled and then measured during exhalation and monitored exercise.

This permits heart

behavior experimentation in space without catheterization. And for heart patients on Earth this technique would be a welcome benefit.

A major achievement for the 20th century.

General Electric has been committed to NASA and to the exploration of space for the benefit of humanity for over 25 years. We are now building NASA's Upper Atmosphere Research

Satellite (UARS) to develop our understanding of the Earth's atmosphere on which all life depends. We look forward to working on what will be one of the most important scientific endeavors of the 20th Century — America's first permanent space station.

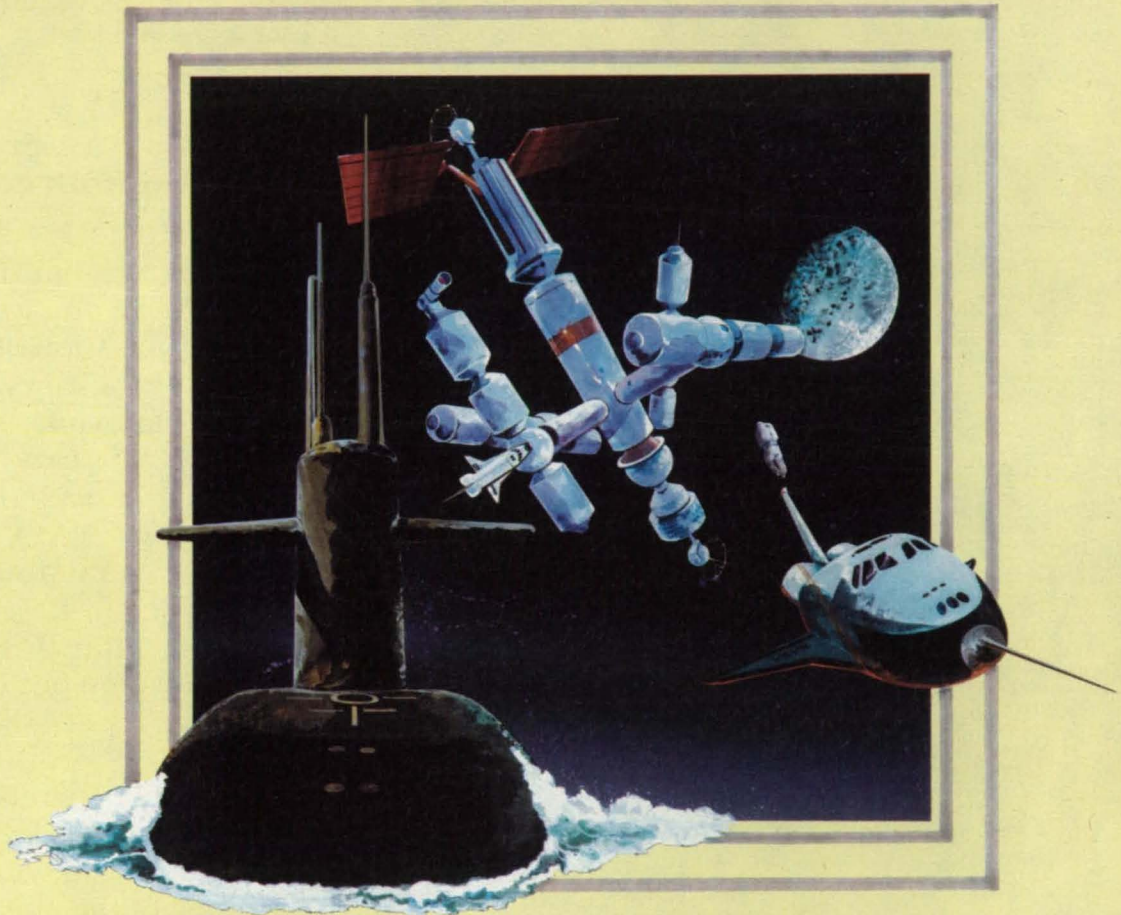
Space Systems Division,
Valley Forge, PA.

Leading from the start ...
and working on the future.

Join the GE Team: Find out about opportunities at GE Space Systems Division. Write: Professional Staffing, General Electric Company, 234 Goddard Blvd., King of Prussia, PA 19406.



Excellence



What do Space Stations and Submarines Have in Common?

Space stations will be required to be self-sufficient for long periods . . . just like submarines. Vitro Corporation has long ensured the sustained on-station operation of the submarine fleet.

How does Vitro make this happen?

Full Support - Vitro provides the logistics support, maintainability support, and systems engineering necessary to keep a submarine on patrol for extended periods.

Long Experience - Vitro support capability is founded upon over 35 years of systems engineering experience. Our engineers are well-versed in the techniques that ensure optimum systems operation in a demanding environment. With

over 6,200 employees, Vitro provides mission support analysis, quality assurance, software, and modern management information systems to ensure system operability.

Extensive Resources - Yes, a space station orbiting our planet and a submarine patrolling our oceans have many needs in common. Vitro has and will continue to meet those needs. Our combination of experience, technical capability, and resources is unmatched.

This capability is available to you. Vitro Corporation stands ready now to work with you to ensure a long and successful Space Station Program . . . to continue a tradition of excellence.

Vitro
CORPORATION

14000 Georgia Avenue, Silver Spring, Maryland 20910
For information call our Marketing Manager, (301) 231-1300

Circle Reader Action No. 394

National Aeronautics and
Space Administration

NASA Tech Briefs:

Published by:

Associated Business Publications
Editor-in-Chief/Publisher: **Bill Schnirring**
Managing Editor: **Rita Nothaft**
Assistant Editor: **Judith Mann**
Creative Director: **Varda Gersten Geller**
Art Director: **Virginia Ferrara**
Assistant Art Director: **Melanie Gottlieb**
Production Manager: **Rita Nothaft**
Traffic Manager: **Jack Doxey**
Circulation Manager: **Anita Weissman**
Fulfillment Manager: **Elizabeth Kuzio**
Controller: **Nell B. Rose**

Technical Staff:

Briefs prepared for National Aeronautics and Space Administration by **Logical Technical Services Corp.**:

Technical Editor: **Jay Kirschenbaum**
Art Director: **Ernest Gillespie**
Managing Editors: **Jerome Rosen, Ted Selinsky**
Administrator: **Agnes Chastain**
Chief Copy Editor: **Melanie Tarka**
Staff Editors: **James Boyd, Larry Grunberger, Paul Johnson, Jordan Randjelovich, George Watson**
Graphics: **Andrew Abramoske, Luis Martinez, Huburn Proffitt**
Editorial & Production: **Camille McQueen, Trudy Cavallo, Sabrina Gibson, Henry Lai, Frank Ponce, Joe Renzler, Elizabeth Teixeira**

NASA:

NASA Tech Briefs are provided by the National Aeronautics and Space Administration, Technology Transfer Division, Washington, DC:
Administrator: **James M. Beggs**
Assistant Administrator for Commercial Programs: **Isaac T. Gillam IV**
Deputy Administrator for Commercial Programs: **L.J. Evans, Jr.**
Acting Director Technology Utilization Division: **Henry J. Clarks**
Publications Manager: **Leonard A. Ault**

Associated Business Publications
41 East 42nd Street, Suite 921
New York, NY 10017-5391
(212) 490-3999

President: **Bill Schnirring**
Executive Vice President: **Frank Nothaft**
Vice President—Sales: **Wayne Pierce**
Vice President: **Patricia Neri**

Special Features and Departments

Editorial Notebook	6
New Technology and NASA Tech Briefs	10
by Len Ault , Deputy Director Technology Utilization Division	
Ames—A History of Looking Forward	14
Letters	170
Classified Advertising	171
Advertising Index	171
About This Publication	172
Mission Accomplished	173













ON THE FRONT COVER:

The Venus Radar Mapper, scheduled for launch in 1988, will utilize advanced high-resolution radar to map—over a span of eight months—virtually all of Venus' surface. The Radar Mapper is expected to generate resolutions more than 10 times better than those obtained by the Pioneer Venus Orbiter in the late 1970s, and to provide the clarity of detail essential to further scientific study of the planet. Both the Venus Radar Mapper and the Pioneer Orbiter missions are managed by Ames Research Center, Moffett Field, California. For more on Ames, see page 14, this issue.

Advertising:

New York Office: (212) 490-3999
Vice President—Sales: **Wayne Pierce**
Sales Manager: **Robin DuCharme**
Account Executive: **Dick Soule**
Chicago Office: (312) 848-8120
Account Executive: **Irene Froehlich**
Los Angeles Office: (213) 822-1205
Account Executive: **Robert Bruder**

Technical Section Thumb Index

NASA TU Services	20	
New Product Ideas	24	
Electronic Components and Circuits	30	
Electronic Systems	56	
Physical Sciences	68	
Materials	88	
Life Sciences	106	
Mechanics	108	
Machinery	128	
Fabrication Technology	152	
Mathematics and Information Sciences	162	
Subject Index	166	

This document was prepared under the sponsorship of the National Aeronautics and Space Administration. Neither Associated Business Publications, Inc., nor anyone acting on behalf of Associated Business Publications, Inc., nor the United States Government nor any person acting on behalf of the United States Government assumes any liability resulting from the use of the information contained in this document, or warrants that such use will be free from privately owned rights. The U. S. Government does not endorse any commercial product, process, or activity identified in this publication.

NASA Tech Briefs, copyright © 1985 in U.S., is published quarterly by Associated Business Publications, Inc. The copyrighted information does not include the individual Tech Briefs which are supplied by NASA. Editorial, sales, production and circulation offices at 41 E. 42nd Street, New York, NY 10017-5391. Subscriptions for non-qualified subscribers in the U.S., Panama Canal Zone, and Puerto Rico, \$50.00 for 1 year; \$100.00 for 2 years; \$150 for 3 years. Single copies \$15.00. Remit by check, draft, postal or express orders. Other remittances at sender's risk. Address all communications for subscriptions or circulation to NASA Tech Briefs, 41 E. 42nd Street, New York, NY 10017-5391. Application to mail at second-class postage rates is pending at New York, NY 10017 and additional mailing offices.

POSTMASTER: please send address changes to 41 E. 42nd Street, Suite 921, New York, NY 10017-5391.



DATA GENERAL ASKS RUSSIAN ROULETTE WITH

FOR ADVANCED COMPUTER SYSTEMS, TALK TO US. IT'S WHY SO
MANY GOVERNMENT DEPARTMENTS HAVE CHOSEN DATA GENERAL.

Government business is too critical to be taken for granted. Too much depends on it.

No wonder nineteen of the top twenty U.S. defense contractors have bought a Data General system. As have all the Armed Services and most major departments of the federal

government.

And to date, nearly thirty U.S. Senate offices and committees have chosen Data General.

TODAY'S BEST VALUE

Why such unanimity? Because Data General offers a complete range of computer solutions for government

programs, with one of the best price/performance ratios in the industry.

From our powerful superminis to the DATA GENERAL/One™ portable. From unsurpassed software to our CEO® office automation system. Plus complete systems for Ada® and Multi Level Secure Operating Systems, and a



ARE YOU PLAYING YESTERDAY'S TECHNOLOGY?

strong commitment to TEMPEST.

All Data General systems have full upward compatibility. And because they adhere to international standards, our systems protect your existing equipment investment. We give you the most cost-effective compatibility with IBM outside of IBM—and the easiest to set up and use.

**SOLID SUPPORT
FOR THE FUTURE**


We back our systems with com-

plete service and support. As well as an investment in research and development well above the industry norm.

So instead of chancing yesterday's technology, take a closer look at the

computer company that keeps you a generation ahead. Write: Data General, Federal Systems Division, C-228, 4400 Computer Drive, Westboro, MA 01580. Or call 1-800-DATAGEN.



 **Data General**
a Generation ahead.



THANKS!

Your response to our first commercial issue of *NASA Tech Briefs* has ranged from gratifying to overwhelming. Our inbox runneth over with suggestions for the future. You have sent us some 7,000 requests for further information on the projects and services advertised in the charter issue and over 12,000 requests for

Technical Support Packages. We are all delighted by your support and ideas.

The hardest part of my job used to be facing a blank sheet of paper and knowing I had to put words on it. The good news is that is no longer a problem. The bad news is that now the hardest part of my job is facing a blank CRT screen

with a cursor that keeps blinking at me until I get the writing done. Feedback like yours makes it a lot easier, both because I know that you read and enjoy NTB, and because it enables me, at least for this month, to devote part of this page to sharing the mail with you.

Before I wriggle entirely off the hook, I'd like to thank L.G. Dillon, Jon Ramer, and David Ratti for the correct spelling of TANSTAAFL, the acronym for "There Ain't No Such Thing As A Free Lunch." We've taken Leo Dillon's suggestion and reprinted the parable on page 89. Hope you enjoy it as much as I do. □

Bill Schnirring
Editor-in-Chief/Publisher

LETTERS

... OF APPLAUSE FOR NASA TECH BRIEFS

Applause, applause!! Your joint venture is a master stroke. Do you think they could ferret out the right kinds of advertisers to publish the Congressional Record at a profit?

Carl T. Steigerwald
Kendall Research
Barrington, IL

I think it's a great step forward putting high-tech advertising in Tech Briefs. Great new format!

Congratulations—my hat is off to whom-ever thought this up.

J.G. Aronson
ERT
Ft. Collins, CO

Congratulations! The charter issue of NASA Tech Briefs was a welcome surprise. The color was outstanding. The features were both well written and informative. The advertising layouts were superior. I hope the public/private sector marriage is a long one.

Bill Bradford
Fla. Dept. Environmental Reg.
Tallahassee, FL

As a principal researcher for advanced product development at Fairchild Republic Company, I find Tech Briefs an ultimate source of technology development conducted at NASA. I am impressed.

Dr. Tahm Sadeghi
Fairchild Republic Co.
Farmingdale, NY

Just a note to let you know that I am glad to see the new format of Tech Briefs and the judicious placement of the ads (not page after page of them).

As a taxpayer, I applaud your efforts to reduce costs. Would that more agencies follow your lead.

I think the whole story of "TANSTAAFL" should be printed, rather than just a passing reference to it as in your editorial.

Keep up the good work.
L.G. Dillon

I think the new NASA Tech Briefs is great! Mr. Schnirring and those involved in saving the taxpayers' dollars but still meeting our needs are to be congratulated. The ads from various companies are helpful, too. I hope many companies will take advantage of it, since that increases the chances of people like me getting new ideas and sources of products.

David Belden
RMI
Verona, WI

Your new format is excellent. Whatever it takes to make it go, do it! I like the short, capsulated items you present of product ideas and innovations, especially in the photovoltaic thin film stacked technology. Keep it up.

Fred Rice
Fred Rice Productions
LaQuinta, CA

... AND SUGGESTIONS

A good start in getting responses would be to make the feedback card easier to remove.

When I was a boy I would read a book called The Boy Mechanic, published by Popular Mechanics, I think, on all sorts of things a boy could do and make. It filled my head with a continuous flow of new ideas by the combining of those I read about. Tech Briefs does that for me now.

Richard Stouffer
Avondale Electro-Mechanics
Auburn Hills, MI

It is good news to know that NASA Tech Briefs will still be published—free! We have indirectly used NTB either to increase our knowledge in design areas of our products or to generate design methods used in our products.

I don't particularly like the ads, but I can live with them...

You should add a Readers' Design Ideas section for those who have utilized NTB.

There is another concept that may give much wider use to NTB. Put a permuted index of all past NTB titles in a computer and give terminal access to any user to search

a key word, i.e., "transceiver." On a hit, an abstract would be displayed or printed out, followed by a question asking if a full report is desired. If yes, then the computer would ask for the NTB mailing label ID number. The computer could look up the ID number, get the subscriber's name and address, and inform the "system" to send the TSP report to the requestor. This should double the use of NTB.

I enjoy NTB, it helps my company, and I wish you good luck in your joint venture.

Peter J. Scola
Honeywell Inc./Process
Management Systems Div.
Phoenix, AZ

... AND CORRECTIONS

As a consulting engineer and retired NASA employee, I was pleased with the Spring 1985 issue of NASA Tech Briefs. Enclosure A is a copy of the Reader Response Card that I mailed to the Technology Transfer Division.

The whole content of the Spring 1985 issue was excellent and well up to the standards set by the prior issues. The Langley story (pp. 22ff) was especially interesting to me. It did contain one minor, questionable item in the reference to Project Mercury and Little Joe. The author, to use an old saying, "The cart before the horse put." Project Mercury grew out of a vast amount of aeronautical research—much of it centered around the Langley Pilotless Aircraft Research Division and its work at Wallops Island, but drawing heavily on work in other Langley divisions and at Ames and Lewis. Little Joe was conceived as, and used as, a test vehicle for the Mercury capsule (spacecraft); thus it was born out of Project Mercury, not vice versa.

Congratulations on keeping up the good work and on finding a way to keep Tech Briefs coming to those who need them.

Paul E. Purser
Consulting Engineer
Humble, TX

Editor's note: Mr. Purser was Special Assistant to the Director of NASA-Johnson Space Center in Houston from 1958—71.



Wyle at work.

Helping explore the new commercial frontier.

Our nation's growth was possible because of the individual's opportunity to excel. The first frontier was broken when our country's founders moved westward. Frontiers have fallen rapidly ever since.

Today we are seeing the development of one of the most exciting commercial frontiers yet. Space itself. Wyle is playing a vital part in that development. We've had an active role in all of our nation's space programs, including the Space Shuttle. We're already at work on the Space Station. We're identifying commercial opportunities in space, including materials processing in microgravity environments. And we're starting in on projects that as yet are still unnamed.

Wyle Laboratories has excelled in aerospace testing since 1949. We're the nation's leading independent testing laboratory. We have the testing facilities, experience, and scientific specialists to conduct any kind of developmental or test program. Our standards of performance are unsurpassed.

For more information on Wyle's testing programs, call collect: Drexel Smith in Norco, California, (714) 737-0871, Don McAvin in Huntsville, Alabama, (205) 837-4411, John Wood in Hampton, Virginia, (804) 865-0000, or Paul Turkheimer in El Segundo, California, (213) 322-1763.

WYLE SCIENTIFIC SERVICES
LABORATORIES & SYSTEMS
GROUP

Huntsville, AL Arlington, VA Norco, CA
Lanham, MD El Segundo, CA Hampton, VA

Circle Reader Action No. 396

GRUMMAN SYSTEMS

OUR COMPETITORS TO TAKE US

In an industry traditionally dominated by giants, one mid-sized company is beginning to create quite a stir.

Grumman Data Systems.

Not only were our sales up 26% in 1984, but we kicked off 1985 with a \$42 million contract for a large-scale, computerized engineering analysis and data system at the Marshall Space Flight Center. A fact, you can be sure, our competition hasn't overlooked.

Why are we enjoying such success?

Perhaps it's because as a hardware-independent systems integrator, we base our solutions solely upon delivering the best performance at the lowest cost, with the most efficient future upgrade. It could also be our experience with emerging information processing technologies, such as

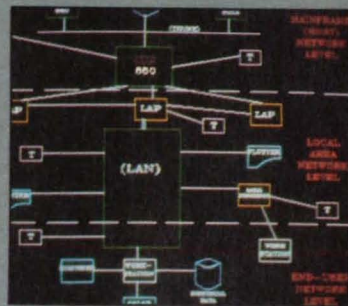


LAN, computer graphics, Ada® software, and machine intelligence. Or our ability to provide complete life-cycle support.

Whatever the reasons, it's certainly paying off. For us. And for our customers.

Command, Control, Communications, Intelligence

Grumman Data Systems has developed decision support systems for all levels of the command chain, from real-time control systems to tactical and strategic planning tools. Whether the system requires the acquisition, correlation and presentation of real-time data streams, or the organization, retrieval and presentation of complex information, we can satisfy the most stringent C³I requirements.



AN DATA SYSTEMS

ION IS STARTING SERIOUSLY

Engineering and Scientific Systems The more sophisticated the requirements of large-scale engineering and scientific centers, the more Grumman Data Systems has to offer. We're fully conversant with the design and implementation of super computer facilities, telecommunications systems, on-line interactive graphics systems and multi-level security systems. We've created modelling and simulations programs for large-scale data systems, and developed procedures for computer performance evaluation and testing.

Management Information Systems Our systems integration services for organizations with large-scale, computer-based administrative, management and logistics control systems, are extensive. They include in-depth expertise in custom software development, existing software modification, systems programming, hardware evaluation and installation, and system testing. We can develop data bases, or even complete communications networks.

Computerized Test Systems For over 15 years, Grumman Data Systems has successfully designed and developed information systems to achieve real-time sig-

nal analysis and integration. In fact, we built the first real-time data acquisition system for flight tests; and we're raising that technology to new levels with an advanced telemetry system for flight testing the Grumman X-29.

Integrated Manufacturing Systems Grumman Data Systems focuses on four components of the manufacturing process: manufacturing cells, material handling systems, maintenance management software, and integrated manufacturing systems. We design, develop, test and install customized systems to suit specific customer needs.

For further information about any of our services, please contact Wesley Stout, Director of Technical Services at (516) 349-5541.

Grumman Data Systems
CUSTOM SOLUTIONS
for Managing Information



*Grumman is a registered trademark of the Grumman Corporation.
*Ada is a registered trademark of the U.S. Government.

Circle Reader Action No. 363



New Technology and NASA Tech Briefs

By Leonard A. Ault,
Deputy Director Technology Utilization Division

The wealth of aerospace technology generated in the course of NASA research and development programs is an important asset in that it offers potential for secondary applications—new products and processes that collectively represent a valuable contribution to the U.S. economy. The task of moving the results of research and development from the laboratory to practical uses in the economy is not, however, an easy one, and requires conscious effort throughout all organizations involved.

For its part, NASA aggressively and continuously surveys its ongoing R&D programs for new technological advances that may have potential utility beyond the purposes for which those technologies are intended. The National Aeronautics and Space Act of 1958 requires that contractors promptly furnish to NASA "full and complete technical information concerning any invention, discovery, improvement, or innovation which may be made" in performance of research and development work for the Agency. Similar reporting requirements also extend to NASA scientists, engineers and technicians conducting in-house technical work in NASA laboratories. New technology, so reported, provides the basic input to *NASA Tech Briefs* which is broadly disseminated to U.S. industry for its potential use.

The process for new technology acquisition, evaluation and publication is managed by the NASA Technology Utilization Officer (TUO) in close coordination with the Patent Counsel in each NASA field center laboratory. With the assistance of Center project personnel, the TUO stays abreast of all R&D programs conducted by its Center, including the administration of the new tech-

nology reporting clause in all R&D contracts. NASA typically maintains about 4,000 active R&D contracts agency-wide at any one point in time. Effective coverage of these efforts to assure appropriate qualitative and quantitative reporting throughout NASA is, at best, difficult and time consuming but is one of the most fundamental activities required to support NASA's technology utilization and transfer efforts.

Over the past twenty years nearly 50,000 reports of new technology have been processed by NASA. Of these, approximately 40 percent have been selected for publication and dissemination to a broad range of potential users in business and industry through *NASA Tech Briefs*. Prior to publication, however, NASA evaluates reported technologies for their novelty, technical significance, and potential utility.

New technologies which meet these criteria are then forwarded to LTS, Incorporated, a NASA contractor, to be prepared in tech brief format. LTS, located in New York City, expends considerable energy in the writing of tech brief articles in order to focus on the new and unique features of any given advancement. It is frequently difficult to ascertain the core of the idea or concept developed and its potential contribution to nonaerospace use. To do this successfully the writer must concentrate on the fundamental scientific or engineering principles in order to broaden the application context of the innovation. Technical completeness and accuracy are, of course, of primary concern. Frequently, well-designed graphical presentations, also prepared by LTS, aid in the process and assist the reader in capturing the essential features of the reported technology.

Prior to publication, prepared draft materials are then reviewed for technical accuracy by the originating NASA laboratory or innovator. Once approved, the material is then finalized for publication at LTS and then forwarded to Associated Business Publications, Inc., for incorporation

in the next issue of *NASA Tech Briefs*.

As raw material is being processed for publication in *NASA Tech Briefs*, the cognizant TU Officer coordinates each item with his Patent Counsel to determine the patent status of the new advancement. Disclosures being processed for patent application by NASA are given special attention so as not to establish a statutory bar through early publication. Patented items or items being processed for patent application are so noted at the end of each article, and the reader is asked to contact the appropriate NASA Patent Counsel concerning rights for the commercial use of the invention. In addition, the TU Officer compiles all appropriate details concerning each tech brief article and prepares a Technical Support Package (TSP). Interested readers may obtain a copy of the TSP for any given article by using the Request Card found in each issue of the journal.

NASA encourages readers of *NASA Tech Briefs* to follow-up even further with the appropriate TU Officer if they have any questions concerning the published technological advancement. The TU Officer can put you in direct contact with the innovator, or can arrange a meeting with the innovator if necessary. Such follow-up discussions or meetings frequently aid in a more comprehensive understanding of the reported technology and offer the user increased insight concerning the potential application in mind.

The process of technology transfer is therefore an iterative one, sometimes requiring that a number of steps be taken to assure effective and tangible end uses. While person-to-person contact is not always needed, it frequently aids in bringing about fruitful results. The publication of new technological advancement in *NASA Tech Briefs* is not a final, but a *first*, step in the process. *NASA Tech Briefs* readers are, thus, encouraged to contact NASA for further information or assistance if such help is felt to be necessary in applying the technology to their specific needs. □

Gould... Innovation and Quality in Data Acquisition



Here's how to start analyzing data in minutes instead of weeks.

Buy the Gould DASA 9000. It's the only data acquisition system with turnkey, menu-driven software for signal acquisition; with multi-channel, high-resolution color graphics; and with data file management. You don't spend weeks or months writing your own programs. You can begin to use this versatile, easy-to-operate system immediately.

Response of the system's multichannel signal digitizer is from dc to 50 kHz per channel providing for high speed signal acquisition for up to 32 channels. Also, hardware trigger and a large internal memory with up to 100% pre-trigger capability make the DASA 9000 ideal for single shot or transient recording.

The signal digitizer also allows realtime record-



ing using oscillographs or instrumentation tape recorders. In addition, test data can be automatically outputted to disk or graphed by Gould's multipen digital plotters.

Gould uses its more than 40 years experience in signal conditioning, acquisition and display to make it easy for users of analog instruments to digitize, store, retrieve and analyze test results.

For complete literature, write Gould Inc., Recordings Systems Division, 3631 Perkins Avenue, Cleveland, Ohio 44114. In the U.S. and Canada, call toll-free 800-447-4700, operator 100.

Nobody else comes close.

 **GOULD**
Electronics

THE HEREAFTER NAMED SUBSIDIARIES OF
UNITED STATES INTERNATIONAL TRADING CO., INC.

760 N. US HIGHWAY 1, SUITE 101, N. PALM BEACH, FL 33408
(305) 627-4510

Propose to register with the
Securities and Exchange Commission

A Public Offering of \$3,960,000
on Form S-1
of 6000 Jumbo Units @ \$660 per unit
Each Jumbo Unit consisting of 26
\$25 Subordinated Convertible
Debentures and 1000 Shares of
Common Stock @ \$.001 par value.

THE OFFERING WILL BE MADE ONLY BY MEANS OF PROSPECTUS

ANTICIPATED TIME OF OFFERING

NOVEMBER 15, 1985

Circle Reader Action No. 397

ZERO GRAVITY ENTERPRISES, INC.

The purpose of the Offering is to capitalize the Company to conduct the business of developing commercial products based on existing and future technology derived from space programs and to develop new technology under weightless environments.

Circle Reader Action No. 387

SPACE METALURGY, INC.

The purpose of the Offering is to capitalize the Company to conduct the business of commercializing existing metalurgical technology and developing new metals technology related to international aerospace activities.

Circle Reader Action No. 376

**OUTER SPACE
LABORATORIES, INC.**

The purpose of the Offering is to capitalize the Company to conduct the business of developing products and services which can be used in governmental and private space environments and to contract for private, commercial experimentation related to space programs.

Circle Reader Action No. 386

**SPACE GENETICS
RESEARCH CORPORATION**

The purpose of the Offering is to capitalize the Company to conduct the business of experimenting and productivity in the fields of human, animal and plant life relating to bacteriological, geobiology, aging, gene splicing, disease control, chemo-remedial chemistry and waste control.

Circle Reader Action No. 388

**SPACE SHUTTLE
CARGO CORPORATION**

The purpose of the Offering is to capitalize the Company to conduct the business of providing international transportation systems and services related to aerospace research and development activities with governmental and private entities.

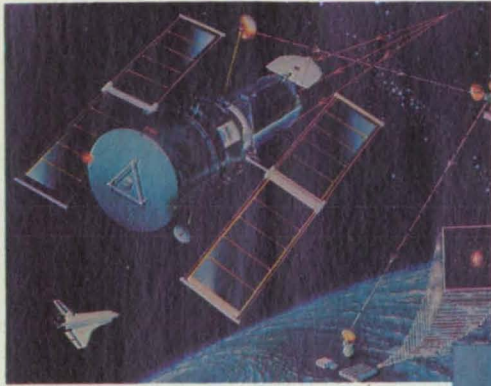
Circle Reader Action No. 366

**INTERSTELLAR COMMUNICATIONS
CORPORATION**

The purpose of the Offering is to capitalize the Company to conduct the business of commercializing existing technology from past governmental space programs and to develop new technologies of international earth and space communications.

\$300,000,000,000.00

\$300 BILLION.



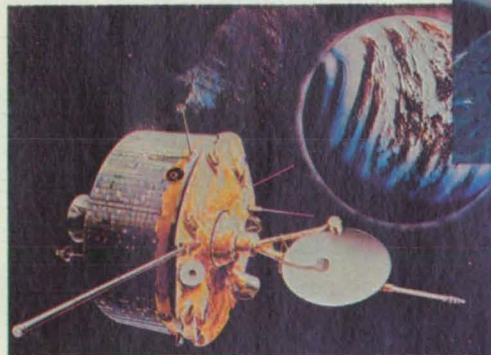
Zero Gravity Enterprises

That's the projected Gross National Product of U.S. business in space in just fifteen years, according to the Congressional Space Caucus.

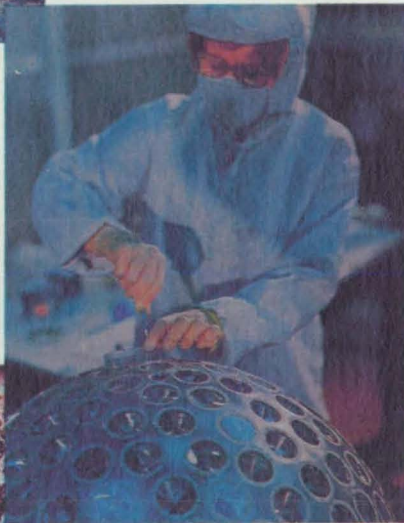
\$300 billion . . . and ten million new jobs for space construction, manufacturing, materials, medical products, metallurgy, and communications.

And that's where we come in. We're United States International Trading Co., Inc. and we're developing investment programs today, to fund research and development for the industries of tomorrow.

We're taking stock in America.
On its final frontier.



Outer Space Laboratories, Inc.



Space Metallurgy, Inc.



Space Genetics Research Corporation



Space Shuttle Cargo Corporation

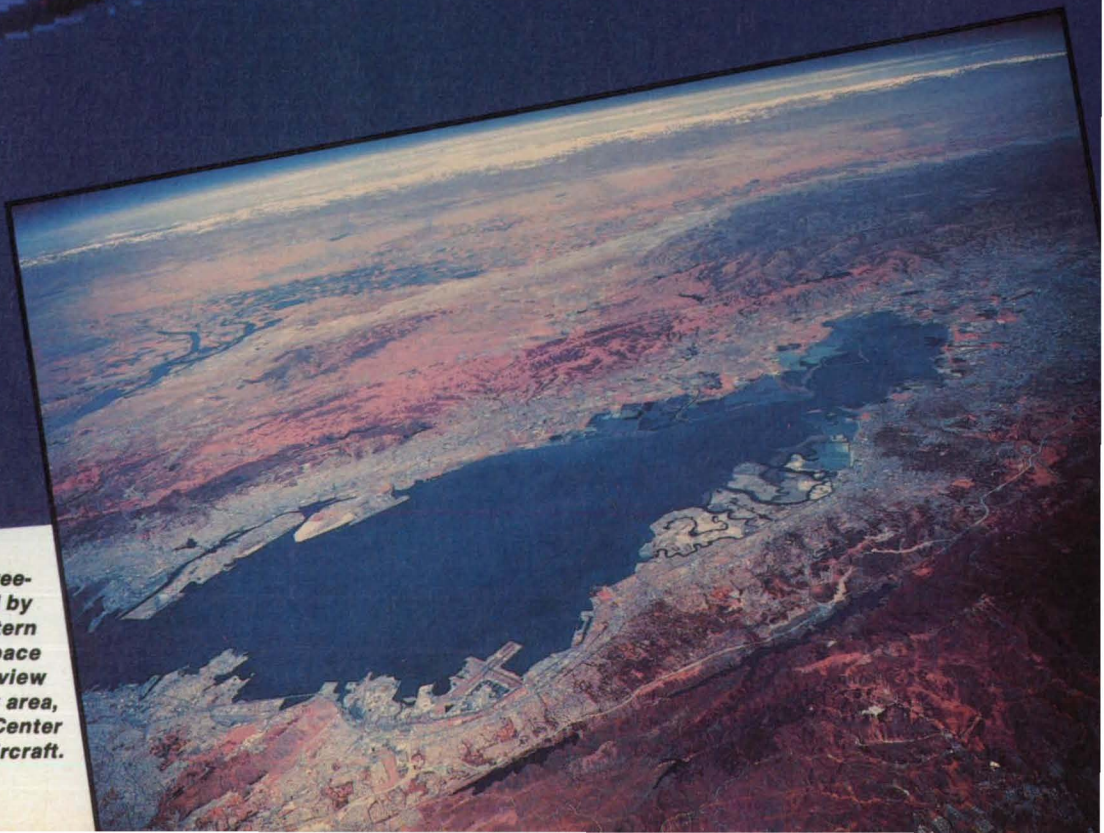
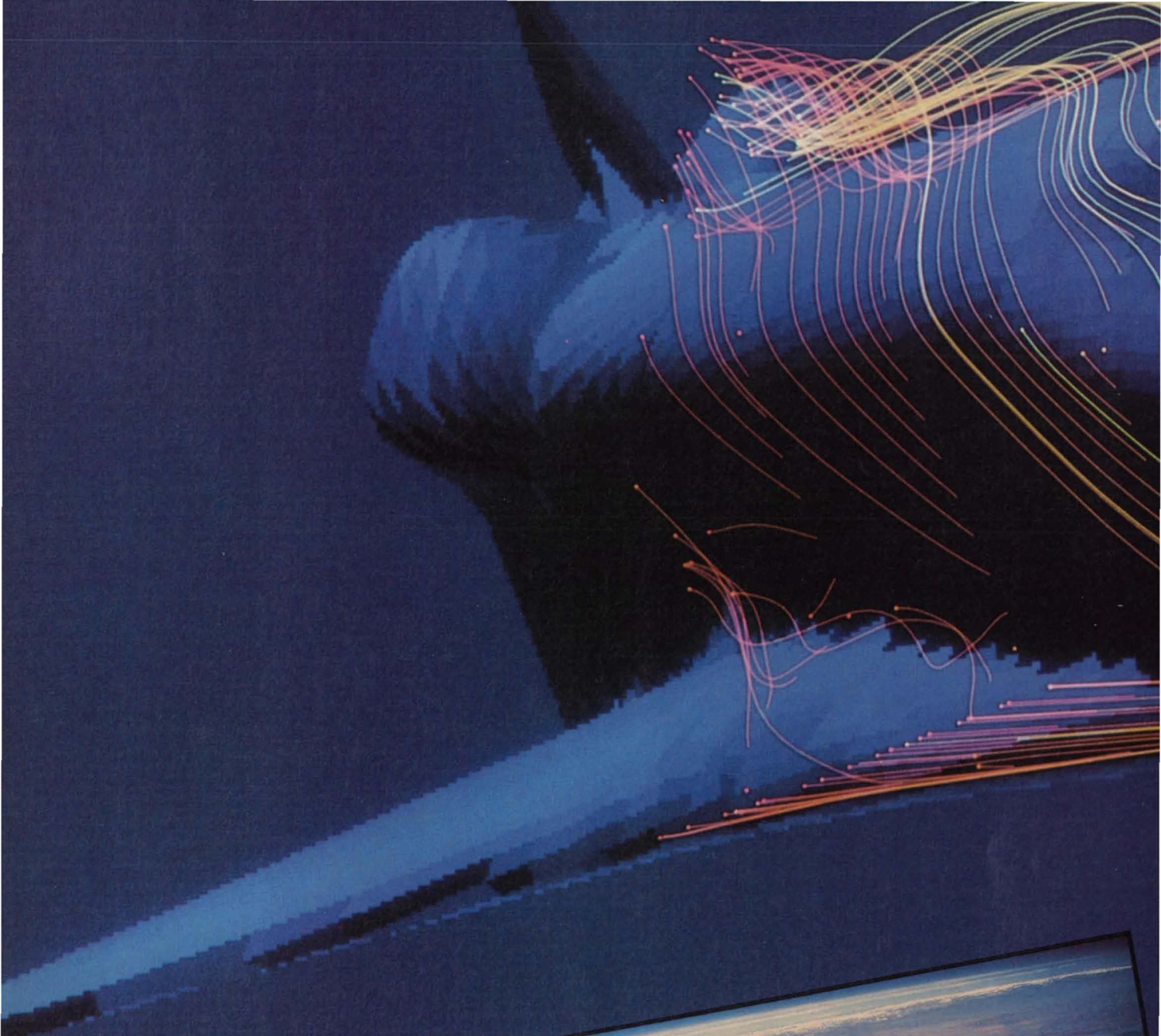


Interstellar Communications Corporation

We're the Business End of Space.

We're United States International Trading Co., Inc.

For more information, please call or write to James Miller, Chief Operations Officer, United States International Trading Co., Inc. 760 N. US Highway 1, Suite 101, N. Palm Beach, FL 33408 (305) 627-4510



GRAPHIC INSIGHT: Above, a three-dimensional image generated by a computer depicts the pattern of air flow around the space shuttle. At right, an infrared view of the San Francisco Bay area, taken from an Ames Research Center U-2 aircraft.



AMES-

A History of Looking Forward

By C.A. Syvertson, Ames
Director 1978—1984

This is the second installment in a series profiling NASA's field research centers, and part of *NASA Tech Briefs'* effort to acquaint its readers with NASA itself, in addition to its technology transfer process.

One of the first high-technology organizations to arrive in the Santa Clara Valley was the federal laboratory at Moffett Field now known as the Ames Research Center. Led for 25 years by its first director, Smith J. DeFrance, it was originally known as the Ames Aeronautical Laboratory and it was the second field laboratory of the National Advisory Committee of Aeronautics (NACA). A panel of experts including Charles Lindbergh selected the site in the late 1930s because the Santa Clara Valley provided good flying weather, low cost and plentiful electric power, and proximity to major universities. Ground was broken for Ames on December 20, 1939, and its first research facilities, including several wind tunnels, were dedicated in the spring of 1940. Eighteen years later, Ames became part of the National Aeronautics and Space Administration when NASA was formed in 1958 and absorbed the NACA.

With the advent of the space program, Ames' mission broadened to include such areas as life sciences, space physics, astronomy, material sciences, space project management, operating airborne platforms

AMES

and, more recently, computational physics. Ames' mission expanded again in 1981 when it took over management of the Dryden Research Facility, NASA's installation at Edwards Air Force Base in the Mojave Desert. With the addition of Dryden, Ames' role in flight testing was greatly

expanded and responsibilities associated with landing the Space Shuttle were added.

Aeronautical Research— World War II

Over the 40 plus years of its existence, Ames has been involved in, and contributed to, a wide variety of aerospace projects. The early years

were dominated by WW II and the laboratory was totally dedicated to the support of the nation's war effort. Ames' staff and facilities were necessarily applied to solving the immediate problems encountered by the nation's rapidly expanding fleet of military and naval aircraft. One key example serves to characterize this effort.

When flying at high speeds, pilots of early versions of the P-51 Mustang fighter encountered a powerful and disconcerting rumble immediately underneath the cockpit. The source of the problem was difficult to establish, so one P-51 had the outboard sections of its wings chopped off to permit it to fit into a 16-foot diameter, high-speed wind tunnel at Ames. Test engineers soon determined that the rumbling came from an unsteady flow in a large ducting under the fuselage, which carried air to the engine. The engineers devised a modified shape for the inlet to the duct that eliminated the rumble. The P-51 went on to become one of America's premier fighters in WW II. Its very long range, a result of superior aerodynamic performance, permitted the P-51 to escort our long-range B-17 and B-24 bombers over Nazi Germany.

Later, the P-51 and other high-speed aircraft of WW II encountered severe problems when they were flown at speeds approaching the speed of sound. Immediately after WW II, Ames scientists turned their attention to developing an understanding of these high-speed problems. Ames built new wind tunnels capable of operating at very high speeds, both near, at and well in excess of the speed of sound. With these new facilities and complementary theoretical studies, Ames scientists helped develop an understanding of flight at high subsonic, transonic and supersonic speeds. One of the key contributors to this fundamental research was Robert T. Jones, a scientist who conceived of the concept of using swept back wings to delay the effects of high-speed flight. The designs of nearly all modern jet aircraft are based on this fundamental knowledge that Ames scientists helped develop. Two military aircraft, the B-58 and B-70, which were among the earliest capable of sustained supersonic flight, were based on specific work done at Ames.

Ames scientists continued to probe the problems of flight at higher and higher speeds, always approaching problems in a basic way, in order to develop a fundamental understanding of the phenomena involved. The foundations thus established proved to be important when interest turned to problems of entering the earth's atmosphere at the very high speeds attained by ballistic missiles and returning spacecraft. Here the laboratory

SPOTLIGHT: Ames

One of the most exciting and potentially far-reaching developments at NASA-Ames took place at the March 14, 1985, ground-breaking ceremony for the Numerical Aerodynamic Simulator (NAS) facility. The multicomponent NAS Processing System Network, whose initial components will become operable in 1986, will constitute the world's largest computer complex. The NAS will provide a computational complement to NASA's experimental facilities, allowing for swifter and more economical development of new aircraft, and ensuring continued national preeminence in aeronautical research.

Other disciplines which will be supported by NAS capabilities include computational materials and structures, weather prediction, computational chemistry, genetic engineering and computational astrophysics. To make the NAS supercomputer, a national facility, available to remote users in universities, private industry and other government agencies, an already extensive satellite and telecommunications network will be expanded.

Cray Research's Cray 2 supercomputer will be at the heart of the initial NAS network. With an expected operating speed of 250 million calculations per second for aerodynamic problems, the Cray 2 is one of the fastest computers in the world. The NAS system will reach continuous high speeds of one billion computations per second (one "gigaflop") in 1988, and the goal for the system in the 1990s is ten billion calculations per second. NASA intends to incorporate even faster supercomputers as they become commercially available, and hopes its NAS program will provide private industry with an incentive to develop and build them.

Advances in logic and memory chips have paved the way for these incredible computing rates. Since the rate of calculation is determined by the time it takes for impulses to pass from one chip to another, packing the chips close together with short interconnecting cables allows for faster computations. Closely-packed chips, however, can generate enough heat to damage one another.

The Cray 2 will be the first computer to have its chips totally immersed in a fluid coolant. Since the fluid is inert, it will not damage or corrode the chips. Incidentally, the same fluid is used by hospitals as an artificial plasma to replace human blood. "Supercomputers are like big brains, and now we have to give them blood to keep them cool," quipped Don Senzig of the NAS project at Ames.

That Ames should be the site for the NAS supercomputer facility is fitting. According to Ames Technology Utilization Officer Stanley A. Miller, research engineers there have "advanced the science of simulation art to a degree it might never have reached otherwise, making the U.S. preeminent in that particular field." And finally, Ames Director William F. Ballhaus, Jr., has "put a lot of interest, energy and skill into making Ames the focal point of new, large computer technology. This is the kind of thrust he is giving Ames, a boost into the '90s for NASA." □



Stan Miller and William Ballhaus, Jr.

When the challenge is handling propellants in space...



Fairchild Control Systems Company has the answers.

Fairchild Control Systems Company has provided disconnects for every major space program requiring storable propellants, cryogenics, and gases. Our reliability and safety record is second to none.

If your system requires light weight, long life, low leakage, self-alignment, minimal pressure drop, manual or remote actuation, give the challenge to Fairchild Control Systems Company. Go with the leader in fluid transfer technology . . . with more QD's in

space than all other competitors combined.

Fairchild's fluid transfer couplings used aboard:

- VOYAGER (Hypergolic)
- SATURN/APOLLO (Cryogenic)
- LUNAR MODULE (Oxygen and EGW)
- TITAN (Hypergolic)
- SPACE SHUTTLE (Hypergolic, Cryogenic, Pneumatic)
- SHUTTLE/CENTAUR (Cryogenic)

Fairchild Control Systems Company . . . meeting the aerospace challenges of today and tomorrow.



FAIRCHILD
CONTROL SYSTEMS COMPANY

Fairchild Control Systems Company
1800 Rosecrans Avenue
Manhattan Beach, California 90266
Tel.: (213) 643-9222
Telex: 910-325-6216

AMES

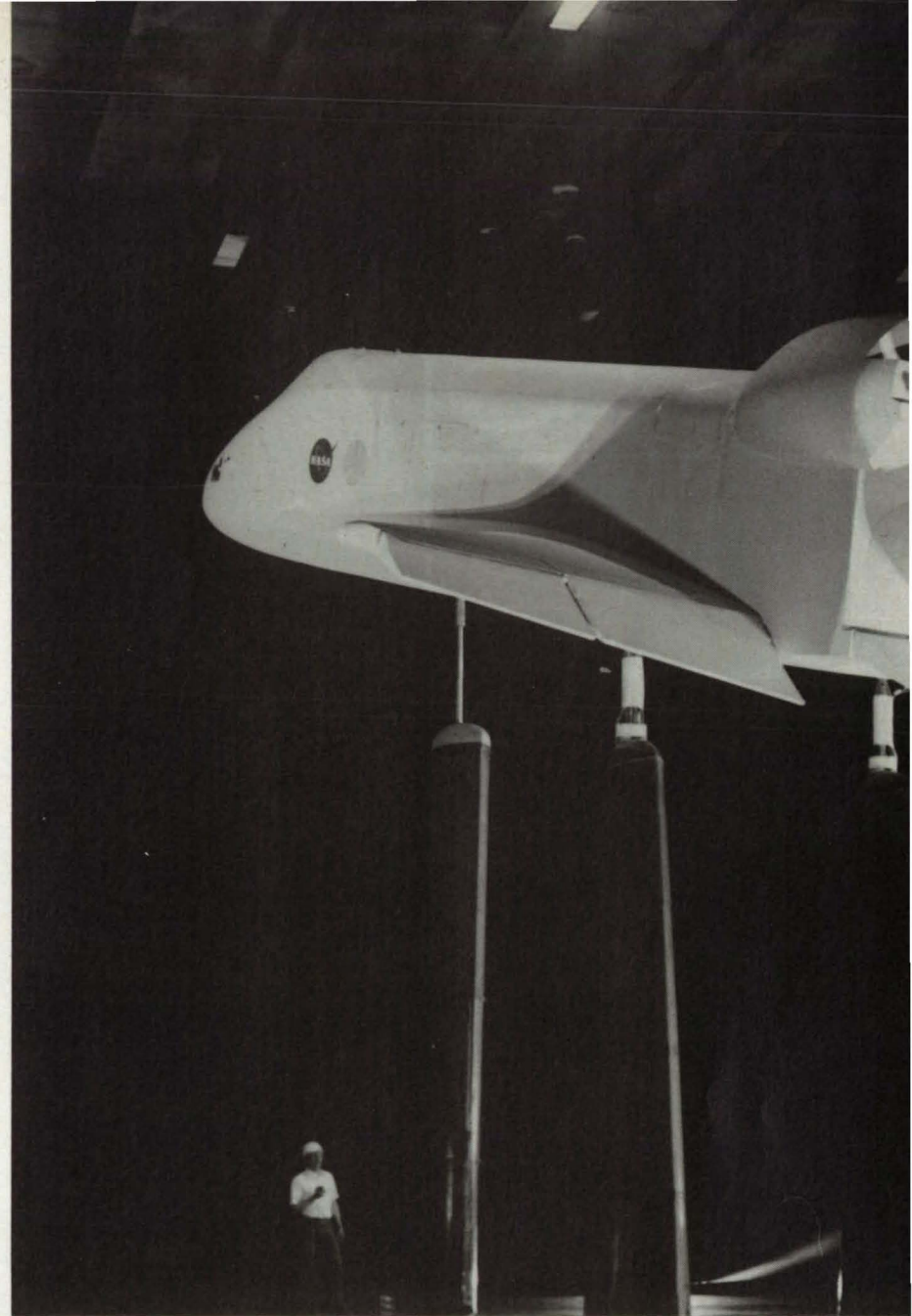
made one of its most significant contributions when, in the early 1950s, Ames scientist H. Julian Allen working with colleague Alfred J. Eggers, Jr. developed the "blunt-body" concept. With this approach, vehicles entering the atmosphere are made blunt with high drag and, thus, as aerodynamically inefficient as possible. As a result, most of their energy is dissipated heating the atmosphere rather than heating the vehicles themselves. The blunt-body concept was the basis for the design of manned capsules for Mercury, Gemini and Apollo, as well as probes sent into the atmospheres of other planets.

Space Technology

Ames became a leading center in the field of atmosphere entry, and in the 1950s and 1960s developed powerful facilities such as arc jets and ballistic ranges to support the related research. The effort included the study of materials suitable for heat shields to protect entry vehicles. Many of the materials used in the thermal protection tiles for the Space Shuttle were developed and tested at Ames in the mid-1970s. Ames provided more tests in the development of the Shuttle than any other installation.

Ames extended its activities beyond the earth's atmosphere when, in the early 1960s, it took over management of the Pioneer program. Ames' Pioneer spacecraft have included three series. Pioneer 6, 7, 8 and 9 were launched in 1965 to 1967 to explore the solar system in regions away from the influence of the planets. All four of these Pioneers are still in orbits about the sun, either just inside or just outside the earth's own orbit. Several still send back data although they have been in space for almost 20 years.

The next series included Pioneers 10 and 11, which were launched in 1972 and 1973 to explore the outer reaches of the solar system. Pioneer 10 was the first spacecraft to pass through the asteroid belt, the first to explore Jupiter, the largest planet, and the first man-made object to leave the known solar system. Pioneer 11 followed its sister 13 months later and was the first spacecraft to explore Saturn and penetrate its rings. Pioneer 10 and 11 were true to their name, pioneering the way for the more sophisticated spacecraft which were to follow. Pioneer Venus was the third member of the Ames Pioneer family. The Pioneer Venus project sent several spacecraft to earth's sister planet, Venus, in 1978. One spacecraft orbited the planet and still sends back data. The second spacecraft sent a set



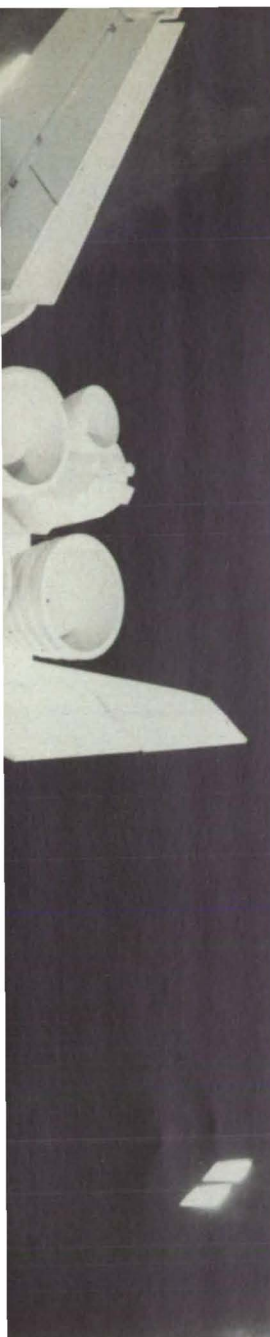
of five vehicles into the Venusian atmosphere to determine its properties. Although not designed to do so, one of these probes survived landing on the planet surface and continued to transmit for an hour after impact.

Better Tools for Aeronautic Research

The good weather of the Santa Clara Valley permitted Ames to conduct extensive flight research from contiguous Moffett Field Naval Air Station. More than 160 aircraft have been flight tested by Ames over the years. Several were modified to operate as "variable stability" aircraft. A computer was added to these aircraft and programmed to make the aircraft fly as it would if it had a different shape (e.g., a different wing) or different controls. This flexibility allowed test pilots and resea-

chers to explore, in flight, different aircraft design characteristics, and the results were valuable in developing new aircraft designs. For example, results from the variable stability aircraft led designers to give the F-104 Starfighter of the 1960s negative dihedral (i.e., drooped) wings.

Ames flight research led to several new and important activities at the center. Flight research specialists desired a safer and a more controlled way to study how advanced aircraft respond to a pilot's handling. This desire led to the development, starting about 1958, of a family of research flight simulators which a pilot could operate and experience most of the cues he would experience in flight—motion, visual, sound, control forces, etc. The simulators are controlled by computers which can be programmed to represent any desired aircraft and to make



Scale model of the Space Shuttle Orbiter undergoing tests in an Ames wind tunnel.

gists and other life scientists. At first the numbers were small, but in the early 1960s when NASA desired to establish a life sciences research organization, this staff nucleus made Ames the logical site. Since then the life sciences program at Ames has grown and now includes such fields as exobiology, biomedical research, and an expanded aeronautical human factors program. Exobiology covers the search for life elsewhere in the universe and, as part of that, an improved understanding of how life began on earth. Ames scientists were key participants in the life detection experiments landed on the surface of Mars in 1976 by the Viking spacecraft. Biomedical research at Ames is primarily concerned with the effect of the space environment on humans. The research seeks an understanding and potential corrective action for such problems as deconditioning of the cardio-vascular system, loss of bone calcium, and space sickness or malaise. Ames scientists and engineers will fly many related experiments as part of Space Shuttle payload.

The role of life sciences in aeronautics has grown and permitted increased understanding of how humans function as pilots. Since 1976 Ames has operated the Aviation Safety Reporting System (ASRS) for the Federal Aviation Administration. The ASRS is designed to permit anyone operating in the country's air system—pilot, air traffic controller, passenger, etc.—to report problems, hopefully before they become sufficiently serious to cause an accident. In the years since it was started, the ASRS has collected over 30,000 reports, and analysis shows that in roughly 75 percent of the cases, humans are key contributors to the problems.

Airborne Science

Still another outgrowth of flight research occurred about 1960, when Ames combined this capacity and its interest in space sciences to develop the use of high flying jet aircraft as platforms to carry scientific instruments for observations of space, as well as of the earth and its atmosphere. The first aircraft in the airborne science fleet was a Convair 990 jet transport modified to carry as many as 12 different experiments and technicians. Other aircraft now include a Lockheed C-141 military transport, added in 1974 and modified to carry a 36-inch telescope above much of the earth's obscuring atmosphere. The fleet also includes three high flying U-2 reconnaissance aircraft.

Aeronautics remains the primary mission of Ames and today represents about 60 percent of the center's ef-

forts. Over the years since 1940, new wind tunnels have been added and old ones modified and improved. They now include some of the largest, most powerful and most refined in the world. As Ames' capabilities grew, the attention of other organizations was attracted. In 1965, Ames and the U.S. Army entered into an agreement to cooperate in aeronautical research at low speeds, especially as it relates to helicopters. The Army agreed to station scientists, engineers, and other personnel at Ames to carry out both joint and Army-specific research and Ames agreed to give the Army special access to some of its facilities. The joint venture has worked very well and today is a fine example of cooperation between federal agencies. The joint NASA-Army operation has produced some highly valuable results including two unique aircraft. One added about 1980 is the Tilt Rotor Research Aircraft which takes off and lands as a helicopter, but transitions in flight, by rotating engine-rotor combinations at each wing tip, to a turbo-prop airplane. The other is a highly-instrumented research helicopter operating like a flying wind tunnel to test advanced rotors for future helicopters.

In addition to its wind tunnels, flight research and simulators, Ames has developed a major set of computer facilities. The first digital computers appeared at Ames in the late 1950s and the computing capacity has grown steadily ever since. In the early 1970s, the growth accelerated when Ames began to accent a new field called Computational Fluid Dynamics (CFD). With advanced computers and CFD techniques, scientists foresee the ability to calculate, in fine detail, air flow over complicated advanced aircraft, a capability which had not existed in the past due to the extreme complexity of the mathematics involved. Already scientists have used CFD techniques to modify the design of several aircraft, including an unmanned research aircraft known as HIMAT (Highly Maneuverable Aircraft Technology). The modifications developed with CFD were essential in permitting HIMAT to achieve its desired performance.

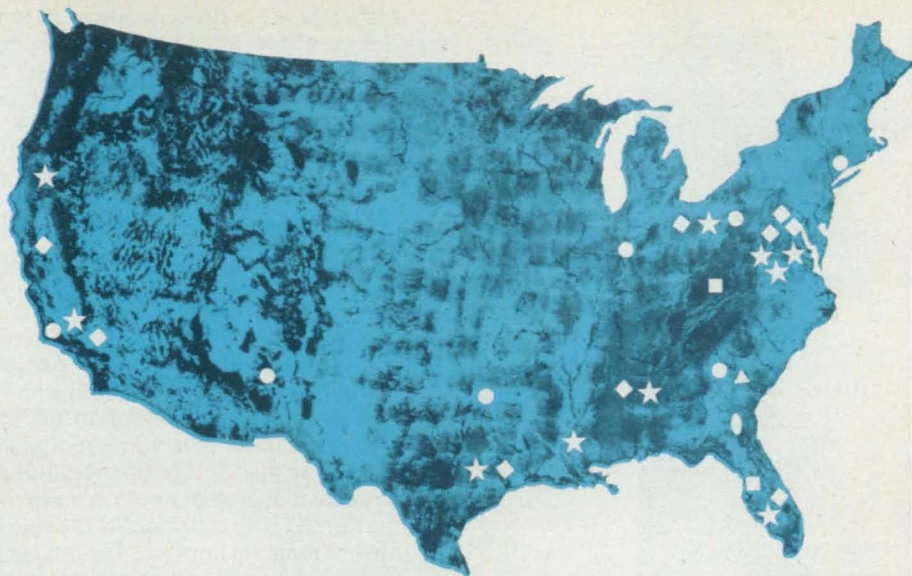
Ames' future promises to be as productive as its past. Each year outstanding new scientists and engineers join the Ames staff, fresh from universities and colleges all over the country. They bring new expertise and ideas to augment the capabilities at the center. Each year the research staff devises new technical approaches with applications to aerospace programs. With its outstanding staff and unique facilities, Ames will continue to support national programs in both aeronautics and space. □

the simulators respond accordingly. With this tool available, research engineering test pilots can, in effect, fly advanced aircraft before they are built. The pilots give important input for the design of new aircraft and also identify any piloting deficiencies so corrections can be made before changes involve expensive aircraft modifications. Ames' simulation results have affected the design of advanced fighters, transports, bombers, helicopters, and even the Space Shuttle.

Life Sciences

Work in flight, and with the simulators, led Ames researchers to seek an improved understanding of how a pilot functions when flying an aircraft. The center thus sought the services of scientists in disciplines non-traditional for Ames—flight surgeons, physiolo-

NASA Technology Utilization Services



TECHNOLOGY UTILIZATION OFFICERS

Technology transfer experts can help you apply the innovations in NASA Tech Briefs.

The Technology Utilization Officer

at each NASA Field Center is an applications engineer who can help you make use of new technology developed at his center. He brings you NASA Tech Briefs and other special publications, sponsors conferences, and arranges for expert assistance in solving technical problems.

Technical assistance,

in the form of further information about NASA innovations and technology, is one of the services available from the TUO. Together with NASA scientists and engineers, he can often help you find and implement NASA technology to meet your specific needs.

Technical Support Packages (TSP's)

are prepared by the center TUO's. They provide further technical details for articles in NASA Tech Briefs. This additional material can help you evaluate and use NASA technology. You may receive most TSP's free of charge by using the TSP Request Card found at the back of this issue.

Technical questions about articles

in NASA Tech Briefs are answered in the TSP's. When no TSP is available, or you have further questions, contact the Technology Utilization Officer at the center that sponsored the research [see facing page for details].



COSMIC®

An economical source of computer programs developed by NASA and other government agencies.

A vast software library

is maintained by COSMIC—the Computer Software Management and Information Center. COSMIC gives you access to approximately 1,600 computer programs developed for NASA and the Department of Defense and selected programs for other government agencies. Programs and documentation are available at reasonable cost.

Available programs

range from management (PERT scheduling) to information science (retrieval systems) and computer operations (hardware and software). Hundreds of engineering programs perform such tasks as structural analysis, electronic circuit design, chemical analysis, and the design of fluid systems. Others determine building energy requirements and optimize mineral exploration.

COSMIC services

go beyond the collection and storage of software packages. Programs are checked for completeness; special announcements and an indexed software catalog are prepared; and programs are reproduced for distribution. Customers are helped to identify their software needs; and COSMIC follows up to determine the successes and problems and to provide updates and error corrections. In some cases, NASA engineers can offer guidance to users in installing or running a program.

Information about programs

described in NASA Tech Briefs articles can be obtained by completing the COSMIC Request Card at the back of this issue. Just circle the letters that correspond to the programs in which you are interested.



★ TECHNOLOGY UTILIZATION OFFICERS

Stanley A. Miller
Ames Research Center
Mail Code 234-B
Moffett Field, CA 94035
(415) 694-6471

Donald S. Friedman
Goddard Space Flight Center
Mail Code 702.1
Greenbelt, MD 20771
(301) 344-6242

William Chmylak
Lyndon B. Johnson Space Center
Mail Code AL32
Houston, TX 77058
(713) 483-3809

U. Reed Barnett
John F. Kennedy Space Center
Mail Stop: PT-TPO-A
Kennedy Space Center, FL 32899
(305) 867-3017

John Samos
Langley Research Center
Mail Stop 139A
Hampton, VA 23665
(804) 865-3281

Dan Soltis
Lewis Research Center
Mail Stop 7-3
21000 Brookpark Road
Cleveland, OH 44135
(216) 433-4000, Ext. 422

Ismail Akbay
George C. Marshall Space Flight Center
Code AT01
Marshall Space Flight Center,
AL 35812
(205) 453-2223

Leonard A. Ault
NASA Headquarters
Code IU
Washington, DC 20546
(202) 453-8415

James T. English
Jet Propulsion Laboratory
Mail Stop 201-110
4800 Oak Grove Drive
Pasadena, CA 91109
(818) 354-2240

Robert M. Barlow
National Space Technology Laboratories
Code GA-10
NSTL Station, MS 39529
(601) 688-1929

Aubrey D. Smith
NASA Resident Office-JPL
Mail Stop 180-801
4800 Oak Grove Drive
Pasadena, CA 91109
(818) 354-4849

● INDUSTRIAL APPLICATIONS CENTER

Aerospace Research Applications Center (ARAC)
Indianapolis Center for Advanced Research
611 N. Capitol Avenue
Indianapolis, IN 46204
John M. Ulrich, Director
(317) 262-5003

Kerr Industrial Applications Center (KIAC)
Southeastern Oklahoma State University
Station A, Box 2584
Durant, OK 74701
Tom J. McRorey, Director
(405) 924-6822

NASA Industrial Applications Center
823 William Pitt Union
University of Pittsburgh
Pittsburgh, PA 15260
Paul A. McWilliams, Executive Director
(412) 624-5211

New England Research Application Center (NERAC)
Mansfield Professional Park
Storrs, CT 06268
Daniel U. Wilde, Director
(203) 486-4533

North Carolina Science and Technology Research Center (NC/STRC)
Post Office Box 12235
Research Triangle Park, NC 27709
James E. Vann, Director
(919) 549-0671

Technology Application Center (TAC)
University of New Mexico
Albuquerque, NM 87131
Stanley A. Morain, Director
(505) 277-3622

NASA Industrial Applications Center (WESRAC)
University of Southern California
Research Annex
3716 South Hope Street
Room 200
Los Angeles, CA 90007
Robert Mixer, Director
(213) 743-8988

◆ PATENT COUNSELS

Robert F. Kempf, Asst. Gen.
Counsel for Patent Matters
NASA Headquarters
Code GP
Washington, DC 20546
(202) 453-2424

Darrell G. Brekke
Ames Research Center
Mail Code: 200-11A
Moffett Field, CA 94035
(415) 694-5104

John O. Tresansky
Goddard Space Flight Center
Mail Code: 204
Greenbelt, MD 20771
(301) 344-7351

Marvin F. Matthews
Lyndon B. Johnson Space Center
Mail Code: AL3
Houston, TX 77058
(713) 483-4871

James O. Harrell
John F. Kennedy Space Center
Mail Code: PT-PAT
Kennedy Space Center, FL 32899
(305) 867-2544

Howard J. Osborn
Langley Research Center
Mail Code: 279
Hampton, VA 23665
(804) 865-3725

Norman T. Musial
Lewis Research Center
Mail Code: 60-2
21000 Brookpark Road
Cleveland, OH 44135
(216) 433-4000, Ext. 346

Leon D. Wofford, Jr.
George C. Marshall Space Flight Center
Mail Code: CC01
Marshall Space Flight Center, AL
35812
(205) 453-0020

Paul F. McCaul
NASA Resident Office-JPL
Mail Code: 180-801
4800 Oak Grove Drive
Pasadena, CA 91109
(818) 354-2700

□ APPLICATION TEAM

Technology Application Team
Research Triangle Institute
Post Office Box 12194
Research Triangle Park, NC 27709
Doris Rouse, Director
(919) 541-6980

■ STATE TECHNOLOGY APPLICATIONS CENTERS

NASA/Florida State Technology Applications Center
State University System of Florida
307 Weil Hall
Gainesville, FL 32611
J. Ronald Thornton, Director
(904) 392-6626

NASA/UK Technology Applications Program
University of Kentucky
109 Kinkead Hall
Lexington, KY 40506-0057
William R. Strong, Program Director
(606) 257-6322

● COMPUTER SOFTWARE MANAGEMENT & INFORMATION CENTER

COSMIC®
112 Barrow Hall
University of Georgia
Athens, GA 30602
John A. Gibson, Director
(404) 542-3265

◆ CENTRALIZED TECHNICAL SERVICES GROUP

NASA Scientific and Technical Information Facility
Technology Utilization Office
P.O. Box 8757
BWI Airport, MD 21240
Walter M. Helland, Manager
(301) 859-5300, Ext. 242, 243

STATE TECHNOLOGY APPLICATIONS CENTERS

Technical information services for industry and state and local government agencies

Government and private industry in Florida and Kentucky can utilize the services of NASA's State Technology Applications Centers (STAC's). The STAC's differ from the Industrial Applications Centers described on page 21, primarily in that they are integrated into existing state technical assistance programs and serve

only the host state, whereas the IAC's serve multistate regions.

Many data bases, including the NASA base and several commercial bases, are available for automatic data retrieval through the STAC's. Other services such as document retrieval and

special searches are also provided. (Like the IAC's, the STAC's normally charge a fee for their services.)

To obtain information about the services offered, write or call the STAC in your state [see above].

NASA INVENTIONS AVAILABLE FOR LICENSING

Over 3,500 NASA inventions are available for licensing in the United States—both exclusive and nonexclusive.

Nonexclusive licenses

for commercial use of NASA inventions are encouraged to promote competition and to achieve the widest use of inventions. They must be used by a negotiated target date.

Exclusive licenses

may be granted to encourage early commercial development of NASA inventions, especially when considerable private investment is required. These are generally for 5 to 10 years and usually require royalties based on sales or use.

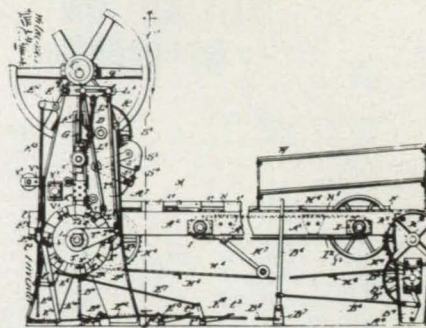
Additional licenses available

include those of NASA-owned foreign patents. In addition to inventions described in NASA Tech Briefs, "NASA Patent

Abstract Bibliography" (PAB), containing abstracts of all NASA inventions, can be purchased from National Technical Information Service, Springfield, VA 22161. The PAB is updated semiannually.

Patent licenses for Tech Briefs

are frequently available. Many of the inventions reported in NASA Tech Briefs are patented or are under consideration for a patent at the time they are published. The current patent status is described at the end of the article; otherwise, there is no statement about patents. If you want to know more about the patent program or are interested in licensing a particular invention,



contact the Patent Counsel at the NASA Field Center that sponsored the research [see page 21]. Be sure to refer to the NASA reference number at the end of the Tech Brief.

INDUSTRIAL APPLICATIONS CENTERS

Computerized access to over 10 million documents worldwide

Computerized information retrieval

from one of the world's largest banks of technical data is available from NASA's network of industrial Applications Centers (IAC's). The IAC's give you access to 1,800,000 technical reports in the NASA data base and to more than 10 times that many reports and articles found in nearly 200 other computerized data bases.

The major sources include:

- 750,000 NASA Technical Reports
- Selected Water Resources Abstracts
- NASA Scientific and Technical Aerospace Reports
- Air Pollution Technical Information Center
- NASA International Aerospace Abstracts

- Chem Abstracts Condensates
- Engineering Index
- Energy Research Abstracts
- NASA Tech Briefs
- Government Reports
- Announcements

and many other specialized files on food technology, textile technology, metallurgy, medicine, business, economics, social sciences, and physical science.

The IAC services

range from tailored literature searches through expert technical assistance:

- **Retrospective Searches:** Published or unpublished literature is screened and documents are identified according to your interest profile. AIC engineers tailor results to your specific needs and furnish

abstracts considered the most pertinent. Complete reports are available upon request.

- **Current-Awareness Searches:** IAC engineers will help design a program to suit your needs. You will receive selected monthly or quarterly abstracts on new developments in your area of interest.
- **Technical Assistance:** IAC engineers will help you evaluate the results of your literature searches. They can help find answers to your technical problems and put you in touch with scientists and engineers at appropriate NASA Field Centers.

Prospective clients can obtain more information about these services by contacting the nearest IAC [see page 21]. User fees are charged for IAC information services.

APPLICATION TEAMS

Technology-matching and problem-solving assistance to public sector organizations

Application engineering projects

are conducted by NASA to help solve public-sector problems in such areas as safety, health, transportation, and environmental protection. Some application teams specialize in biomedical disciplines;

others, in engineering and scientific problems. Staffed by professionals from various disciplines, these teams work with other Federal agencies and health organizations to identify critical problems amenable to solution by the application of existing

NASA technology.

Public-sector organization

representatives can learn more about application teams by contacting a nearby NASA Field Center Technology Utilization Office [see page 21].

TECHNOLOGY UTILIZATION OFFICE, NASA SCIENTIFIC & TECHNICAL INFORMATION

Centralized technical facility to provide service to the U.S. professional community and general public

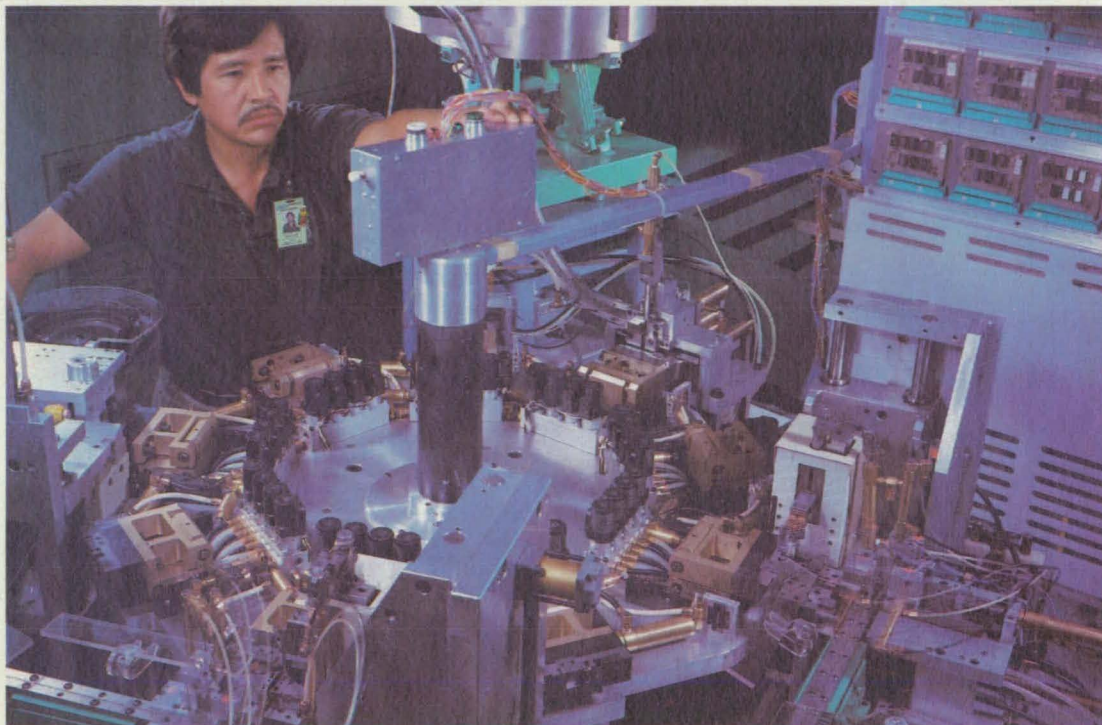
Missing a copy of NASA Tech Briefs?

Not received Technical Support Package requested? Want to check on Tech Briefs status? Have urgent request for subscription address change? Wish to receive other

Tech Brief in area of interest? Simply confused as to whom to contact within the NASA Technology Utilization Network? Have general or specific question about the Technology Utilization Program, its

services and documents?

We are here to help you. Write or call. We have the right answer, the correct document, or the proper referral [see page 21].



INNOVATIVE METHODS FOR RELAY RELIABILITY

Reliable performance. That's the assurance you dare not compromise. And with Leach, you don't. Here, innovative manufacturing methods like the Leach-designed Header Assembly Machine, shown above, assure unerring precision. And other innovations, like fine leak testing using radioactive Krypton 85, and automated 100% testing of

subminiature relays before and after sealing, assure relay reliability exceeding MIL-R-6106. Reliability is why virtually every military and commercial aerospace program has chosen Leach. To learn more just call us. Or send for our new capabilities brochure. Leach Relay Division, 5915 Avalon Blvd., Los Angeles, CA 90003. Phone (213) 232-8228.

LEACH RELAYS GO ON AND ON



Automate DOD, DOE & NASA Reporting with VISION's Performance Management System

C/SSR

COST/SCHEDULE STATUS REPORT - BY WBS

CONTRACTOR: SYSTEMETICS INC | CONTRACT TYPE/NO: | PROGRAM NAME/NUMBER: | REPORT PERIOD: | SIGNATURE, TITLE & DATE: |
 LOCATION: FULLERTON CA | OFF: | HOME: | FROM: 12/1/1981 | TO: 1/1/1982 |
 TOTAL: PRODUCTION: |
 *** CONTRACT DATA ***
 ORIGINAL CONTRACT TARGET COST: | MODIFIED CONTRACT CHANGES: | CURRENT TARGET COST: | ESTIMATED COST OF AUTHORIZED UNPRICED WORK: | CONTRACT BUDGET BASE: |
 K2950 A | 40 | K2950 A | 40 | K2950 X

*** PERFORMANCE DATA ***

WBS BREAKDOWN STRUCTURE	SCHEDULED COST - MONTH		ACTUAL COST MONTH		VARIANCE		LATEST REVISION		VARIANCE
	SCHEDULED	PERFORMED	SCHEDULED	PERFORMED	COST	COST	ESTIMATE		
3211	0	0	0	0	0	0	186	186	0.0
3221	104	140	26	34	0	104	142	142	0.0
3224	26	15	17	-9	0	-2	325	327	-2.0
3229	0	0	0	0	0	0	306	306	0.0
GENERAL AND ADMINISTRATIVE	15	18	4	3	0	12	277	277	0.0
UNDISTRIBUTED RESERVE							240	240	0.0
MANAGEMENT RESERVE							350	350	0.0
TOTAL	145	173	54	28	0	251	250	250	0.0

CPR

COST PERFORMANCE REPORT - BY WBS

CONTRACTOR: SYSTEMETICS INC | CONTRACT TYPE/NO: | PROGRAM NAME/NUMBER: | REPORT PERIOD: | SIGNATURE, TITLE & DATE: |
 LOCATION: FULLERTON CA | OFF: | HOME: | FROM: 12/1/1981 | TO: 1/1/1982 |
 BASIC: PRODUCTION: |
 QUANTITY/THEORY/TARGET COST/EST COST/AUTH UNPRICED WORK/EST FROM/TARGET PRICE/EST PRICE/UNPRICED BUDGET/DATE/CONT. DECLINE/EST. DECLINE
 K2950 A | 40 | 40 | 10 | 10 | 2930 A | 3000 A | 86/20 | 74200 A | 4200 A |

CURRENT PERIOD | CUMULATIVE TO DATE | REPROGRAMMING ADJUSTMENTS | AT COMPLETION

WBS	BUDGETED COST		ACTUAL COST		VARIANCE		SCHEDULE		COST		LATEST REVISION	VARIANCE	
	MONTH	PERFORMED	MONTH	PERFORMED	MONTH	PERFORMED	MONTH	PERFORMED	MONTH	PERFORMED			
3211	0	0	0	0	0	0	0	0	0	0	186	186	0.0
3221	104	140	26	34	0	104	142	26	34	0	142	142	0.0
3224	26	15	17	-9	0	-2	24	15	17	-9	325	327	-2.0
3229	0	0	0	0	0	0	0	0	0	0	306	306	0.0
GENERAL AND ADMINISTRATIVE	15	18	4	3	0	12	15	18	4	3	277	277	0.0
UNDISTRIBUTED RESERVE											240	240	0.0
SUBTOTAL	145	173	54	28	0	114	143	54	28	0	251	250	0.0
RESERVE											350	350	0.0
TOTAL	145	173	54	28	0	114	143	54	28	0	251	250	0.0

NASA533M

NATIONAL AERONAUTICS AND SPACE ADMINISTRATION MONTHLY CONTRACT FINANCIAL MANAGEMENT REPORT

FROM: SYSTEMETICS INC | 2 REPORT FOR MONTH ENDING: |
 801 E CHAPMAN AVE | FULLERTON CA | CA | * COSTS | * FEE |
 92631 | * 7000000 | * 3000000

CONTRACT AND LATEST AMENDMENT NUMBER: AF1952025 | FUND LIMITATION: 30000000

DESCRIPTION OF CONTRACT: CPFF | CONTRACT AND LATEST AMENDMENT NUMBER: AF1952025 | FUND LIMITATION: 30000000

SCOPE OF WORK: | CONTRACT AND LATEST AMENDMENT NUMBER: AF1952025 | FUND LIMITATION: 30000000

REPORTING CATEGORY: | COST INCURRED: | ESTIMATED COST/HOURS TO COMPLETE: | EST. FUND COST/HOURS TO COMPLETE: |

ACTUAL	MONTH		CUMULATIVE TO DATE		DETAIL		CONTRACT	CONTRACT VALUE
	PLANNED	ACTUAL	MONTH 1	MONTH 2	MONTH 1	MONTH 2		
ENGINEERING	670	1870	670	0	942	1214	22980	23007
MANUFACTURING	85	48	85	0	28	277	11700	12130
SUPPORT	93	128	93	0	82	156	2652	26470
TOTAL	1348	2125	1348	0	1052	2057	36652	41607
ENGINEERING	3528	7853	3528	7853	4080	8212	1008717	1143620
MANUFACTURING	249	123	249	123	54	473	21227	20641
SUPPORT	11274	38843	11274	38843	26498	32449	742657	813389
TOTAL	47051	118728	47051	118728	47732	11454	2042613	2256689
LABOR OVERHEAD DOLLARS	71054	137154	71054	137154	81780	103004	2017438	2273202
ENGINEERING	872	488	872	488	2674	2261	131708	144891
MANUFACTURING	14973	48840	14973	48840	35231	40811	101720	101496
SUPPORT	132072	209891	132072	209891	19480	22915	601902	636791
TOTAL	144549	215419	144549	215419	166885	165807	1743010	1763378
OTHER CHARGES	8426	4591	8426	4591	4764	8149	38129	37781
GENERAL & ADMINISTRATIVE	14522	34871	14522	34871	17780	27792	627210	691842
APPLIED FEES	14522	34871	14522	34871	17780	27792	627210	691842
TOTAL CHARGES	149744	363290	149744	363290	170574	26714	4899321	5403061

NASA533Q

NATIONAL AERONAUTICS AND SPACE ADMINISTRATION QUARTERLY CONTRACT FINANCIAL MANAGEMENT REPORT

FROM: SYSTEMETICS INC | 2 REPORT FOR QUARTER BEGINNING: |
 801 E CHAPMAN AVE | FULLERTON CA | CA | * COSTS | * FEE |
 92631 | * 7000000 | * 3000000

CONTRACT AND LATEST AMENDMENT NUMBER: AF1952025 | FUND LIMITATION: 30000000

DESCRIPTION OF CONTRACT: CPFF | CONTRACT AND LATEST AMENDMENT NUMBER: AF1952025 | FUND LIMITATION: 30000000

SCOPE OF WORK: | CONTRACT AND LATEST AMENDMENT NUMBER: AF1952025 | FUND LIMITATION: 30000000

REPORTING CATEGORY: | COST INCURRED: | ESTIMATED COST/HOURS TO COMPLETE: | EST. FUND COST/HOURS TO COMPLETE: |

ACTUAL	MONTH		CUMULATIVE TO DATE		DETAIL		CONTRACT	CONTRACT VALUE
	PLANNED	ACTUAL	MONTH 1	MONTH 2	MONTH 1	MONTH 2		
ENGINEERING	670	1870	670	0	942	1214	22980	23007
MANUFACTURING	85	48	85	0	28	277	11700	12130
SUPPORT	93	128	93	0	82	156	2652	26470
TOTAL	1348	2125	1348	0	1052	2057	36652	41607
ENGINEERING	3528	7853	3528	7853	4080	8212	1008717	1143620
MANUFACTURING	249	123	249	123	54	473	21227	20641
SUPPORT	11274	38843	11274	38843	26498	32449	742657	813389
TOTAL	47051	118728	47051	118728	47732	11454	2042613	2256689
LABOR OVERHEAD DOLLARS	71054	137154	71054	137154	81780	103004	2017438	2273202
ENGINEERING	872	488	872	488	2674	2261	131708	144891
MANUFACTURING	14973	48840	14973	48840	35231	40811	101720	101496
SUPPORT	132072	209891	132072	209891	19480	22915	601902	636791
TOTAL	144549	215419	144549	215419	166885	165807	1743010	1763378
OTHER CHARGES	8426	4591	8426	4591	4764	8149	38129	37781
GENERAL & ADMINISTRATIVE	14522	34871	14522	34871	17780	27792	627210	691842
APPLIED FEES	14522	34871	14522	34871	17780	27792	627210	691842
TOTAL CHARGES	149744	363290	149744	363290	170574	26714	4899321	5403061

CUTS PREPARATION TIME FROM DAYS TO MINUTES.

If you're preparing and updating DOD, DOE and NASA Performance Management Reports manually, you're losing days or weeks of valuable time and manpower. You need VISION... the comprehensive, interactive project management information system.

VISION does it automatically.

- Integrates cost/schedule information from a single data base.
- Produces C/SSR, CPR, NASA533M, and NASA533Q reports to approved formats in minutes.
- Reduces errors.
- Updates reports in minutes.
- Quickly generates "what if" simulations using actual reports for analysis.
- Produces cost/schedule variances and impact analysis as well as other reports.
- Saves time and money—Reduces days and weeks of preparation time to minutes.
- Easy to use—No data processing experience required. GSA approved.

FREE BOOKLET



"Performance Measurement System Description"

This useful booklet can save you days in writing a System Description. Basically, the work's all done; you just fill in the blanks. To get a free copy just drop us a note on your company letterhead or call your local field office listed below.

SYSTONETICS

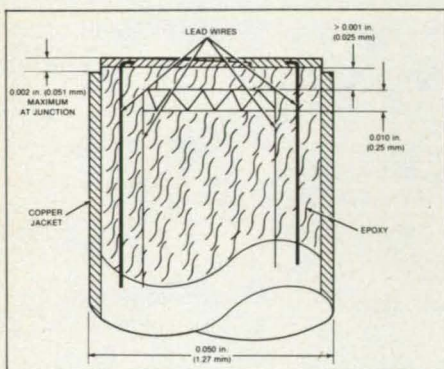
801 E. Chapman Ave., Fullerton, CA 92631
(714) 680-0910 • Telex 692-327

OFFICE LOCATIONS: Fullerton, CA (714) 680-0910 • San Jose, CA (408) 353-2916
 • Seattle, WA (206) 455-3374 • Denver, CO (303) 740-6681 • Houston, TX (713) 461-3905 • Atlanta, GA (404) 955-7740 • Oakland, VA (703) 359-2982

Combination Heat-Flux and Temperature Gage

A new gage combines the functions of temperature measurement and heat-flux measurement in a miniature package. Its small size makes it suitable for testing scale models of aircraft and monitoring thermal effects in automobile engines, turbines, and heat exchangers. The gage contains a surface thermocouple and a thermopile heat-flux gage near the surface. The unit is mounted so that the thermocouple is flush with the surface of the object to be monitored. The small size of the new gage overcomes the awkwardness of older, larger devices. The new gage design also reduces measurement errors by ensuring that the thermal conditions at the flux and thermocouple are nearly the same.

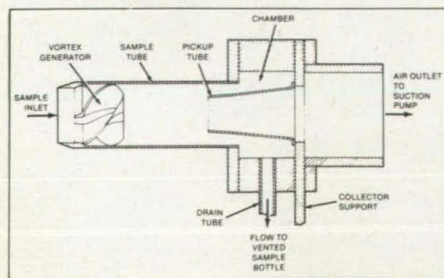
(See page 112)



Accurate Airborne Particle Sampler

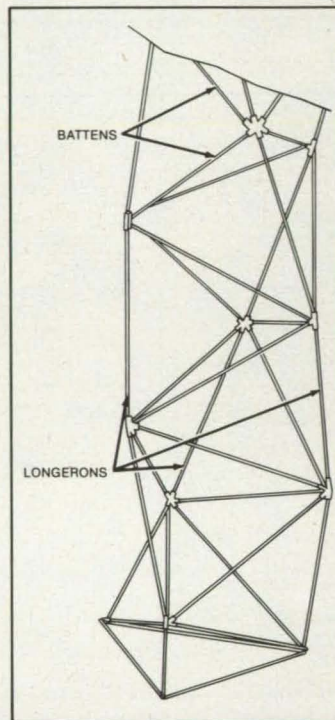
An airborne sampler gathers water droplets from clouds to form bulk liquid samples for chemical analysis of trace constituents. Ambient air is sucked in past vanes that impart a whirling motion; the resulting centrifugal force flings the droplets toward an outer wall, where the airflow drives them toward a drain tube. These samplers can be connected in series, each designed to collect droplets in a different size range. By analyzing each size fraction, the chemical composition of cloud droplets can be related to droplet size.

(See page 110.)



Sequentially-Deployable Tetrahedral Beam

A sequentially-deployable beam consists of a tandem series of interconnected tetrahedra. The beam can become a crane, manipulator arm, antenna-feed support, or other structure. The beam can be retracted into a compact package or extended to full length automatically. It consists of interconnected tetrahedra, with adjacent tetrahedra sharing triangular common sides. The triangles are connected by longerons that can be folded, telescoped, or otherwise changed in length to store, deploy, or manipulate the shape of the beam. (See page 113.)



Diffusely Reflecting Paints Containing TFE

Diffusely reflective paints have been developed by incorporating polytetrafluoroethylene (TFE) pigment with alcohol-soluble binders. These highly reflective coatings are useful on reflectance-standard surfaces for calibrating radiometric instruments. The paints can be used on many substrates including metals, plastics, and ceramics. Surfaces are prepared by degreasing, roughening, and priming. The paint is applied by spraying. The cured paint has a matte finish and a reflection characteristic that is more nearly lambertian than that of other optical-reference paints. Typically, the paint exhibits 90 percent reflective efficiency in ultraviolet light and 95 percent in visible light.

(See page 92.)

Intercalated-Carbon Low-Resistivity Fibers

Experiments have shown that light-weight, electrically conductive fibers can be made from graphite intercalation compounds. When the intercalant is CuCl_2 , the fibers are thermally stable in air up to 100°C . The fibers might be used as ingredients in composite enclosures for electronic equipment, especially where the enclosures must be light in weight and conductive for radio-frequency or static suppression. In the experiments, pitch-based fibers were first heat-treated, then intercalated by sublimation and vapor transport of the intercalant. For one type of fiber, this process yielded a resistivity of $12.9\ \Omega\text{-cm}$, representing a reduction of almost 14 times below the starting value.

(See page 94.)

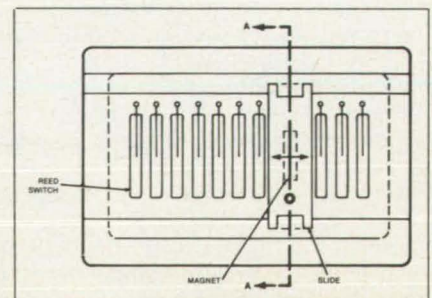
Intercalant	Fiber	Resistivity in $\mu\Omega\text{-cm}$
None	P100-4	200 ± 30
ICl	P100-4	42 ± 7
Br_2	P100-4	30 ± 5
CuCl_2	P100-4	15 ± 3
CuCl_2	P100-3	22 ± 4
CuCl_2	HTT 3,000	12.9

NOTE: Fibers in the P-100 series have the radial structure.

Reed-Switch Position Indicator

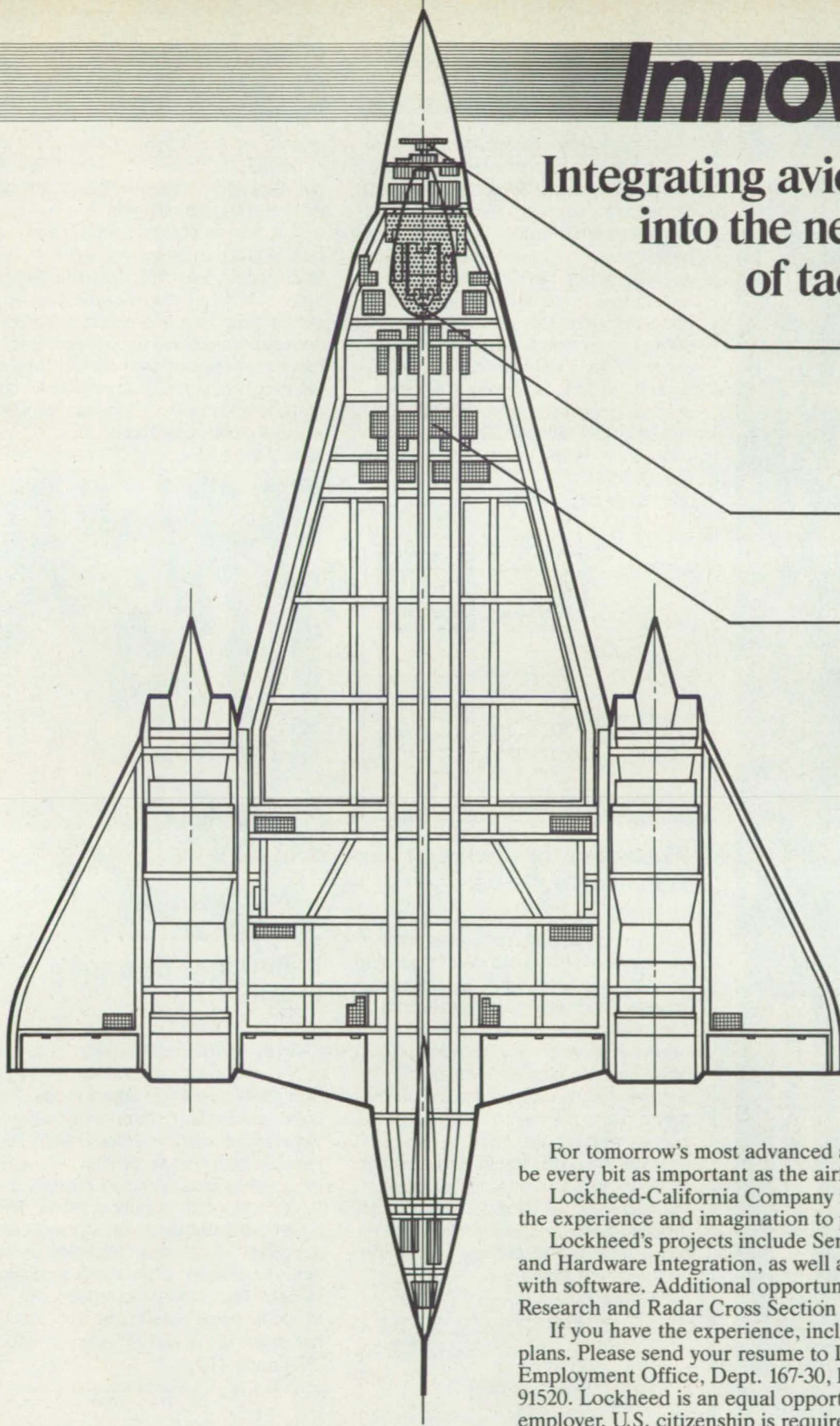
A position transducer is easy to mount, reliable, and explosionproof. The transducer, which can be used on valves and other mechanisms, includes a magnet that sequentially opens or closes reed switches as the valve stem or other part moves. In combination with resistors, the reed switches constitute a voltage divider, the output voltage of which changes in steps depending on the position of the magnet. The transducer has been used in controlling highly flammable fuels and can readily be adapted to oil-refining and other chemical-processing plants.

(See page 49.)



Innovation

Integrating avionics systems
into the next generation
of tactical aircraft.



Sensor Systems

- Antenna/Radome Design
- Radar
- IR/EO
- ESM/ECM

Cockpit Design

- Displays
- Real-Time Software

Hardware Integration



- Inertial Navigation
- Digital Computers
- Armament Support Management
- Microwave/RF

For tomorrow's most advanced aircraft, what goes inside will be every bit as important as the airframe in which it rides.

Lockheed-California Company is looking for individuals with the experience and imagination to put the pieces together.

Lockheed's projects include Sensor Systems, Cockpit Design, and Hardware Integration, as well as the integration of all systems with software. Additional opportunities exist in Operations Research and Radar Cross Section Technology.

If you have the experience, include Lockheed in your career plans. Please send your resume to Lockheed-California Company, Employment Office, Dept. 167-30, P.O. Box 551, Burbank, CA 91520. Lockheed is an equal opportunity, affirmative action employer. U.S. citizenship is required.

 **Lockheed-California Company** 

Giving shape to imagination.

SKUNK WORKS and the skunk design are registered service marks of the Lockheed Corporation. © 1985 Lockheed Corporation

fisher
SPACE PEN

**...DEVELOPED FOR
N.A.S.A.
...USED BY
ASTRONAUTS ON
SPACE FLIGHTS**

Probably the world's most dependable pen. The patented pressurized cartridge developed for NASA permit these pens to write at any angle (even upside down) in severe temperatures 50° to +400° F. over glossy or greasy surfaces, under water and up to 3 times longer than ordinary pens.



Chrome Space Pen with flight button point retraction. Refills readily available.

\$10.00



Chrome pocket purse pen with distinctive Space Shuttle emblem. Unique compact design.

\$12.50

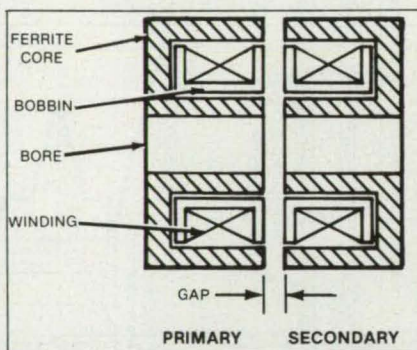
Fisher Space Pens are available wherever better pens are sold. Corporate logos and emblems are available. You may order or request further information by contacting:

PAUL C. FISHER
743 Circle Avenue
Forest Park, IL 60130
(312) 366-5030

Rotary Power Transformer and Inverter Circuit

A rotary transformer transfers electrical power between a stationary primary winding and a rotating secondary winding. Since there are no sliprings or other sliding contacts, there is no contact wear, contact noise, or contamination from lubricants and wear debris. The windings are placed face to face on separate ferrite cores. A pulse-width-modulated inverter supplies power to the primary. A resonant tank circuit on the secondary side converts the alternating rectangular pulses to sinusoidal alternating current. A prototype model operating at 20 kHz delivered 539 W output with 580 W input. Power ratings of 20 to 50 kW are possible.

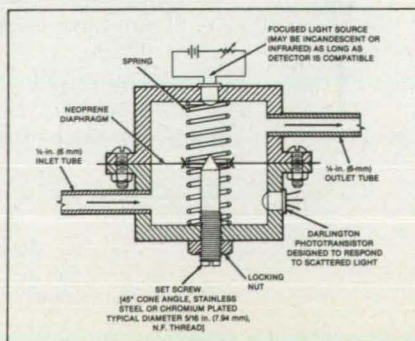
(See page 52.)



Flowmeter for Clear and Translucent Fluids

A transducer with only three moving parts senses the flow of a clear or translucent fluid. The force of the flow displaces a spring-loaded diaphragm away from a cone that normally seats in a hole in the diaphragm at zero flow. The hole is illuminated from the upstream side of the diaphragm, while a photodetector on the downstream side senses the light that passes through the opening, thereby measuring the diaphragm displacement and the flow rate. A transducer system of this kind might be used, for example, to measure the flow of gasoline to an automobile engine and to provide one of the engine-control inputs.

(See page 117.)



Communications Headgear With Protective Features

A headgear for use in noisy and hazardous areas protects the face and hearing while enabling the wearer to communicate with a remote operator. An inexpensive prototype of the headgear was made from stock parts. A helmet and face shield were adapted to an intercom headset. The unit should have uses where communication and head protection are required while the hands must remain free to work. For example, it might be worn during wind-tunnel operations, chemical handling, mining, blasting, and military operations.

(See page 63.)



High-Output Injection Laser

A new semiconductor laser puts out continuous-wave radiation at relatively high power in a single optical mode. The device is a single crystal of semiconductor material deposited in terraced layers. The terraces form a weak, positive-refractive-index optical guide that supports only the fundamental lateral optical mode. The power is supplied by a metal contact over the portion of maximum thickness of the active layer. At 20° C, the lateral and transverse far-field output patterns are stable up to about 50 mW output, with full widths at half power of 23° and 26°, respectively.

(See page 45.)

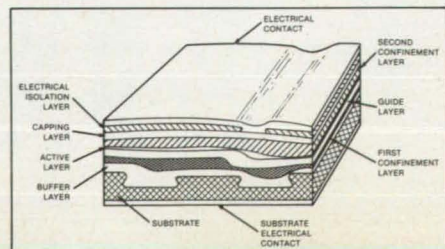


Photo: courtesy of NASA.

ON SOME TRIPS, YOU CAN'T JUST TOSS YOUR LUGGAGE IN THE TRUNK

When you're sending important cargo into space, you have to pack carefully.

It's called space cargo processing and McDonnell Douglas does it.

Space cargo is precision machines, laboratories, instruments, factories, satellites, rockets and experiments. Space cargo is intricate, delicate and expensive. It must be planned for, integrated, and guarded. Some must be refrigerated; some must be heated. Some is put in place with tweezers and some with cranes. All must be packaged to fit the cargo hold of NASA's shuttles, attached to their operating controls and carefully fitted to withstand the forces of the journey.

And when the journey's over, the results must be harvested. Unloaded, preserved, packaged and delivered.

We've been sending spacecraft and launch systems into space for thirty-five years—that's why we know that when going to work in space, it's important how you pack.

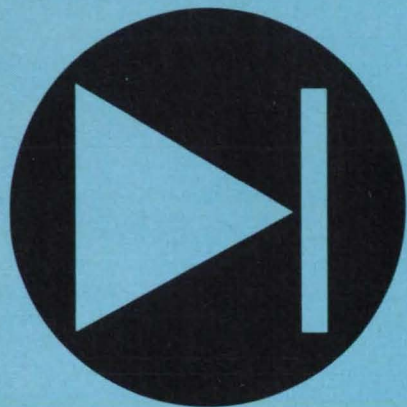
For further information, contact:
George Faenza, McDonnell Douglas Technical
Services Company, P.O. Box 21233, Kennedy
Space Center, FL 32815.

MCDONNELL DOUGLAS

© 1985 McDonnell Douglas Corporation

Circle Reader Action No. 373

Electronic Components and Circuits



Hardware, Techniques, and Processes

- 30 Ferroresonant Circuit With Increased Efficiency
- 32 Power Supply for 25-Watt Arc Lamp
- 35 Portable Temperature Set-Point Controller
- 35 Recharging Batteries Chemically
- 36 Rolling-Contact Rheostat
- 38 Incrementally Variable High-Voltage Supply
- 42 Low-Voltage Protection for Volatile Computer Memories
- 43 Comparator With Noise Suppression
- 44 Remote Power Controllers for High-Power dc Switching
- 45 High-Output Injection Laser
- 46 Commutating Permanent-Magnet Motors at Low Speed
- 48 Remotely-Adjustable Solid-State High-Voltage Supply
- 49 Reed-Switch Position Indicator
- 50 Retrodirective-Optical-Transponder Concept
- 51 Electrically Connecting to Pressure Vessels
- 51 Orienting Arc Lamps for Longest Life
- 52 Rotary Power Transformer and Inverter Circuit
- 53 Pulse-Width-to-Analog-Voltage Converter

Books and Reports

- 54 Modeling "Soft Errors" in Bipolar Integrated Circuits
- 54 Study of Contact Resistances in Integrated Circuits

Ferroresonant Circuit With Increased Efficiency

An additional inductor reduces heating and increases stability.

NASA's Jet Propulsion Laboratory, Pasadena, California

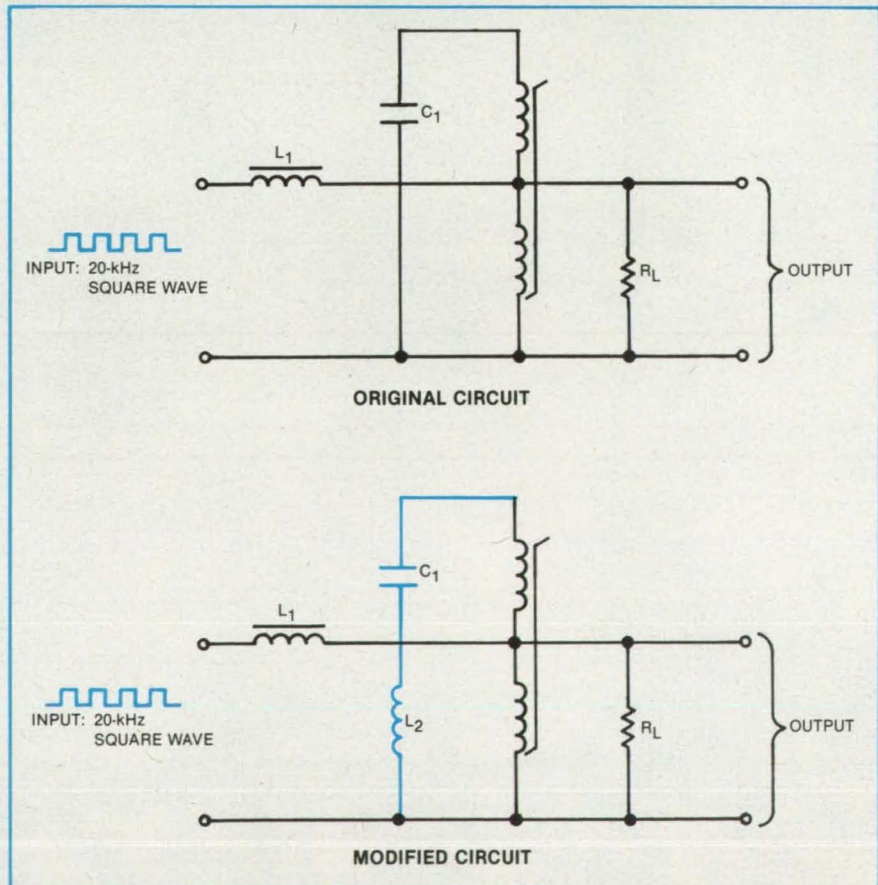
The efficiency of a ferroresonant voltage regulator operating at about 20 kHz is increased by the addition of a small inductor in series with the tuning capacitor. In comparison with the unmodified regulator, the regulator input voltage and the power consumption of the load can be varied over a wider range without degradation of performance.

A typical ferroresonant voltage regulator reduces a square-wave input to a regulated square-wave output. The original circuit includes a tuning capacitor in series with a saturating transformer (see upper part of figure). For correct operation, the capacitance must be selected for the frequency and the expected load: A single capacitance value does not insure correct operation over a wide input-voltage swing or a wide load variation. Furthermore, transformer heating is caused by the large capacitor commutating current that occurs during the polarity change of the square wave.

In the modified circuit (see lower part of figure), a small inductor in series with the capacitor reduces the criticality of tuning. It broadens the commutating interval but decreases the peak commutating current sufficiently to reduce the net heating over a complete cycle.

In one 20-kHz circuit, a tuning capacitor of $C_1 = 0.08 \mu\text{F}$ was replaced by a series combination of $C_1 = 0.05 \mu\text{F}$ and $L_2 = 100 \mu\text{H}$. With this change, the circuit showed no instability and the output voltage varied ± 1.5 percent when the input was varied between 100 and 130 V or when the load power was varied from 0.05 to 160 W. The temperature rise of the saturating transformer was reduced from the original value of 130° to 75° C.

This work was done by Colonel W. T. McLyman of Caltech for NASA's Jet Propulsion Laboratory. For further information, Circle 18 on the TSP Request Card.
NPO-16326



In the **Modified Ferroresonant Voltage Regulator**, the tuning capacitance is replaced by a series combination of inductance and capacitance for greater operating stability and less heat dissipation.

Tomorrow's Engineering Tool

Today

The C1200 computational system brings mainframe performance and features to the individual user. It provides the power and local control needed for today's most compute-intensive engineering and scientific applications, including modeling, analysis, and simulation.

A true UNIX 4.2 BSD implementation complements the register-intensive 32-bit advanced architecture providing 2.3 million Whetstones/second speed. Up to 24 Mbytes physical memory, 4 Gigabytes virtual memory, high performance disks and I/O subsystems enable the C1200 to deliver multi-user capability at a single user price.

The C1200 offers high resolution bit mapped color graphics and incorporates industry-standard compilers, networking, communications, and interconnection options to complement other systems from PC's to Supercomputers.

The C1200—Proof of Celerity's Dedication to Performance Technology.

**Get in touch with tomorrow today.
Contact Celerity Computing.**

CELERITY COMPUTING



Corporate Headquarters 9692 Via Excelencia, San Diego, CA 92126, (619) 271-9940

Sales/Support Offices Framingham, MA/(617) 872-1552; Houston, TX/(713) 496-2128; Farmington Hills, MI/(313) 553-7833;
Woodland Hills, CA/(818) 703-5141 and Santa Clara, CA/(408) 986-8466

UNIX is a registered trademark of AT&T Bell Laboratories.

Circle Reader Action No. 352

Power Supply for 25-Watt Arc Lamp

Dual-voltage circuitry both strikes and maintains the arc.

Langley Research Center, Hampton, Virginia

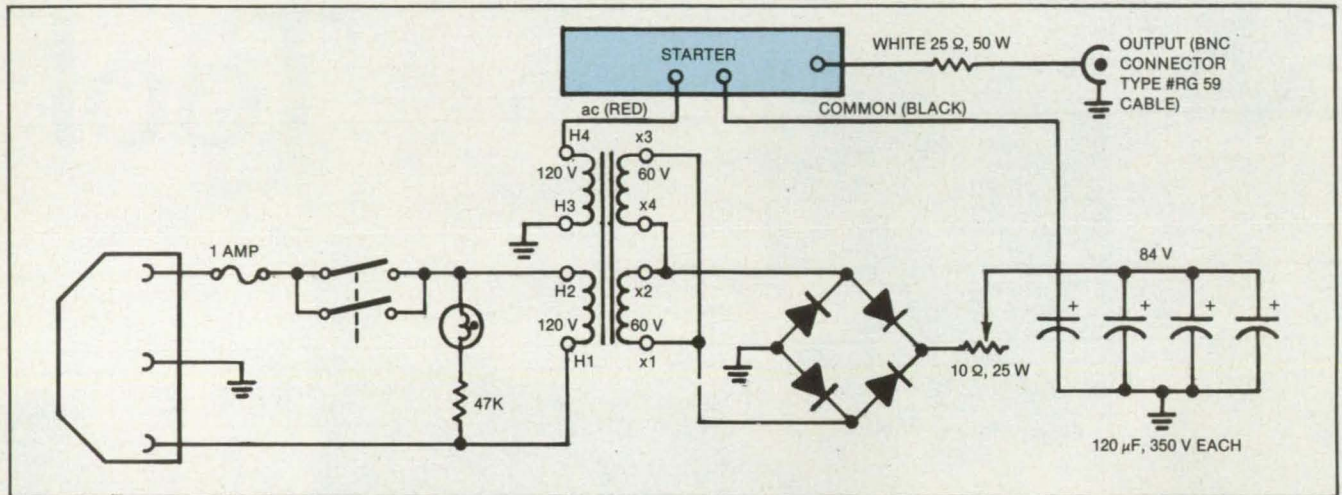


Figure 1. The **Low-Voltage Power Section** makes the arc. This section is an 84-volt direct-current supply.

Twenty-five-watt concentrated arc lamps have found widespread applications at Langley Research Center and elsewhere. They are used as light sources for schlieren, shadowgraph, and other flow-visualization techniques. One drawback to their operation has been the intermittent or unreliable performance of the associated power supplies.

The lamps require a starting voltage in excess of 1,000 volts. Once stabilized, the voltage drop across the lamp is near 20 volts. The recommended operating technique is to supply the lamp from a constant voltage in excess of 50 volts with a series resistor limiting the current to 1.25 amperes. The series resistance serves to eliminate the negative resistance of the arc. The starting voltage is derived from a relay/choke that generates high-voltage spikes by inductive kickback. The generation of the starting voltage is the weakest feature of these supplies.

A new power supply has been designed (and several units are already in use) that replaces the relay/choke combination with a solid-state starter. The new power supply consists of two main sections. The first section, the low-voltage power supply section, is an 84-volt direct-current supply. This supply powers the stabilized arc. As shown in Figure 1, the current is limited by the 10-ohm adjustable and 25-ohm fixed resistance. The second section, the high-voltage starter circuit, is a Cockcroft-Walton voltage multiplier (see Figure 2). With no load, the output voltage is 2,036 volts. However, when the arc is established, the heavy current drain maintains a forward bias on all of the diodes, and the circuit becomes a straight path with a voltage drop of 7.2 volts. The small value of

the capacitors used in the multiplier guarantees that the diodes will be forward-biased once the arc is established. If the arc is broken due to a power interruption or other cause, the multiplier will again become functional, automatically generating a high voltage to restart the arc.

Several units have been constructed entirely from stock components and are in use. It was found that adequate ventilation must be maintained for the 25-ohm resistor that dissipates approximately 40 watts. Also, the cable from the supply to the lamp

must be kept short to reduce distributed capacitance. With a large cable capacitance, the nonlinear arc can form a relaxation oscillator and operate in a self-pulsing mode. Cable lengths of 4 ft (1.2 m) with RG 59 coaxial cable present no problem. The new unit is entirely solid state and eliminates formerly used troublesome electromechanical components.

This work was done by Bradley D. Leighty of Langley Research Center. No further documentation is available. LAR-13202

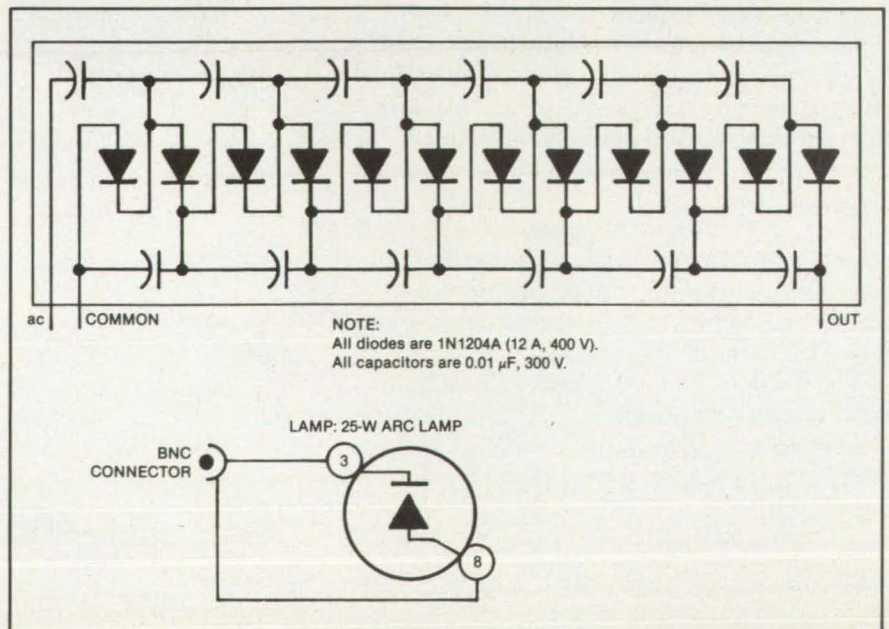


Figure 2. The **High-Voltage Starter Circuit** is used to strike the arc. Should the arc be broken, this circuit will automatically generate a high voltage to restart the arc.



The TI Professional Computer takes CAD where no PC CAD has gone before.

Now the TI Professional Computer and AutoCAD™ 2 software from Autodesk, Inc. team up to bring you the best of both worlds in CAD and personal computing.

You'll put true CAD on your desktop at an affordable price. And you'll have a superior PC system for all your computing needs—available in a package of hardware, software and exclusive service and support options *no other PC offers*.

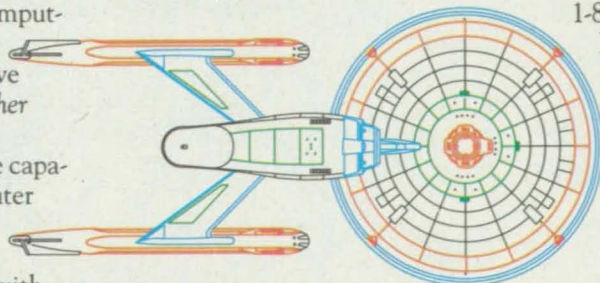
You get top-quality mainframe capabilities that let you explore the outer limits of your imagination. Like multilayering and precise dimensioning. Isometric design. Zoom with trillion-to-one precision. The ability to create your own symbol libraries. And to move, copy, rotate or delete any part of any drawing.

You also get the perfect match of CAD and machine. TI gives you superb high-resolution graphics, a palette of up to 8 simultaneous colors, fast processing speed, and more. Including top performance

from the best-selling software for other applications. And you can choose from a wide range of options to put together a system that precisely fits your needs.

Draw your own conclusions. For the TI-authorized reseller nearest you, call 1-800-527-3500, extension TBA.

In Canada call 416-884-9181. Or, for more information, write Texas Instruments Incorporated, Dept. DBY00000, P.O. Box 809063, Dallas, TX 75380-9063. We'll show you out-of-this-world CAD you can afford.



Create drawings of any size to any scale.

AutoCAD is a trademark of Autodesk, Inc. "Star Trek" elements used with permission of Paramount Pictures Corp., the copyright owner.

TEXAS INSTRUMENTS

Creating useful products and services for you.

For Government Sales and GSA Schedule Information, Please Call: 1-800-527-3500, Operator 602. Circle Reader Action No. 393

2775-23
© 1985 TI



**FOR
SALE**

SPACE

on board NASA Tech Briefs' next launch

"NASA Tech Briefs WORKS for advertisers."

That's according to Bill Waske, Director of New Business Development for Fairchild Industries' Control Systems Division, and other executives now advertising in NASA Tech Briefs.

Companies like Rockwell, Amoco, Data General, and DuPont have already received more than 6200 top-quality responses to their ads in NASA Tech Briefs. If your company is on the leading edge of technology, shouldn't you be marketing in the #1 magazine on the leading edge of technology?

Confirm Your Space on Board.

To find out how you can be on board the next launch of NASA's official magazine, call Robin DuCharme, Bill Schnirring, Wayne Pierce, Bob Bruder or Dick Soule at U.S. (212) 490-3999.

NASATechBriefs

is published by
Associated Business Publications
41 East 42nd Street, Suite 921

Portable Temperature Set-Point Controller

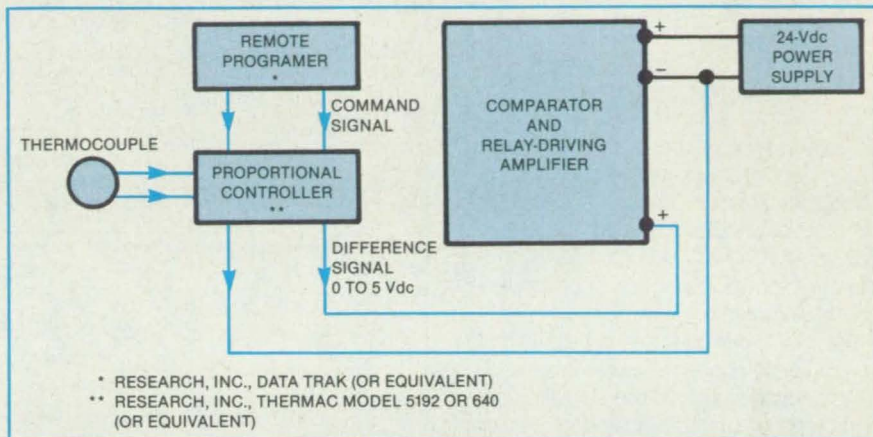
Two off-the-shelf instruments combine to control chamber temperature over a wide range.

Lyndon B. Johnson Space Center, Houston, Texas

A portable controller for environmental test chambers changes temperatures automatically over the range of -300° to $+400^{\circ}$ F (-184° to $+204^{\circ}$ C). The unit controls the rate of temperature change and the time at a given temperature.

The controller, developed to meet NASA Shuttle test requirements, combines two pieces of commercial test equipment plus some auxiliary lamps and relays. The two pieces of hardware include a proportional controller and a remote programmer (see figure). The proportional controller compares the thermocouple output to a reference signal, amplifies the error voltage, and applies it to a temperature-control element such as a heater or liquid-nitrogen pump. This feedback loop is normally used to keep the chamber at a constant operating temperature. It does not, however, program a changing temperature profile.

The remote programmer is used to vary the temperature set point. A command signal sent from the remote programmer to the proportional controller changes the reference temperature signal. The magnitude and duration of the command signal is pro-



The **Portable Temperature Set-Point Controller** combines two commercial instruments: A remote programmer and a proportional controller. The difference signal is used to actuate heaters or liquid-nitrogen flow.

gramed by the user for each application.

The portable controller includes safety switches that automatically shut down the test chamber if preselected high and low temperatures are exceeded. This feature allows the controller to be used for unat-

tended tests without the danger of damage to test specimens or equipment.

This work was done by James F. Milner of Rockwell International Corp. for **Johnson Space Center**. No further documentation is available.
MSC-20056

Recharging Batteries Chemically

Iron/air electrochemical cells might be regenerated with little electric power.

NASA's Jet Propulsion Laboratory, Pasadena, California

Iron/air batteries can be partly recharged chemically by a solution of a strong base in an alcohol or by a basic alcohol solution of a reducing agent. Although the chemical recharging method is still experimental, it has potential for batteries in electric automobiles, or it may be used as an energy storage system in remote applications. It may also be used in "quiet" operations where the noise or infrared signature of a diesel engine is not desired. Instead of relying on relatively slow electrical recharging, a recharging solution might be circulated through the battery in somewhat less time.

A discharged iron electrode — that is, one that has changed to ferrous hydroxide in the process of producing electric current —

NASA Tech Briefs, Summer 1985

can be partly reconverted to iron by immersion in a 4-molar solution of potassium hydroxide in methanol at 60° to 80° C. With the addition of a platinized nickel counterelectrode at a small dc bias, the iron electrode is more completely reconstituted: At 80° C, the degree of recharge ranges from 10 to 20 percent at zero bias to nearly 100 percent at 0.5 V bias.

The recharging system works best at temperatures of 35° to 40° C. Precise temperature control is not needed, however, since the reaction tolerates a wide temperature range. Below 25° C, the reaction is sluggish, and the reactants should be heated. One important safety feature of the basic alcohol solution is that it not only

serves as a reducing agent but also protects against the evolution of hydrogen during the recharging reaction.

This work was done by Roger M. Williams, John Rowlette, and James Graf of Caltech for **NASA's Jet Propulsion Laboratory**. For further information, Circle 46 on the TSP Request Card.

Title to this invention has been waived under the provisions of the National Aeronautics and Space Act [42 U.S.C. 2457(f)], to the California Institute of Technology, Pasadena, CA 91125. (Contact Edward O. Ansell, Dir., Patents & Licensing.)
NPO-16024

Rolling-Contact Rheostat

Noise should be suppressed.

NASA's Jet Propulsion Laboratory, Pasadena, California

Contact noise in rheostats and potentiometers is expected to be reduced by a proposed rolling-contact design. The smooth rolling action should eliminate the sporadic variations in resistance caused by the bouncing and stick/slip motion of conventional sliding contacts.

The principle of operation is illustrated at the top of the figure. A flexible resistance band is wrapped around two insulating cylinders, one of which is coated or permanently wrapped with another resistance band. Ordinary low-resistance flexible wires connect the outer ends of the two bands to the external circuitry.

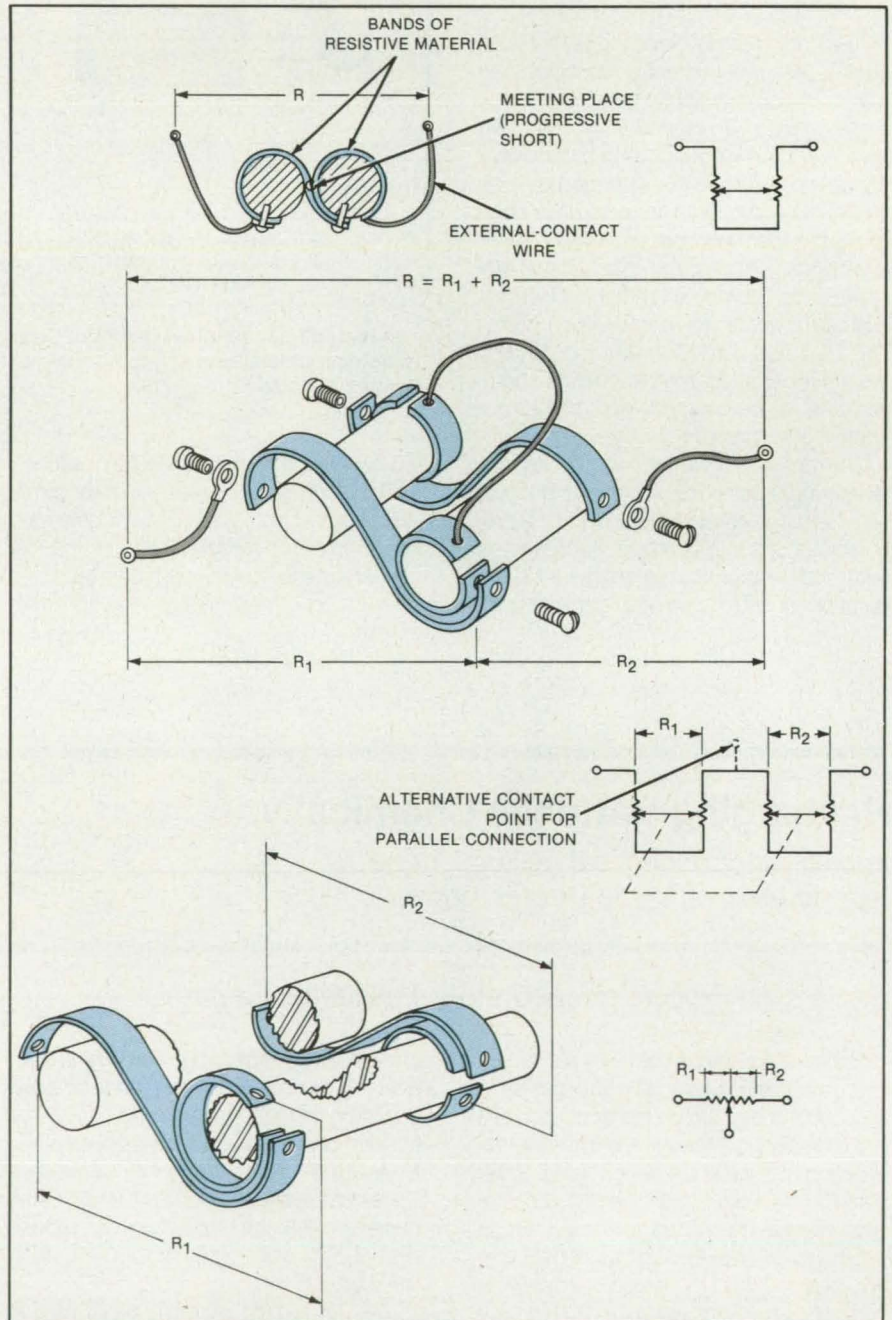
The two cylinders are pressed together by sprung bearings (not shown) to assure steady, intimate electrical contact between the bands at their meeting place between the cylinders. As one cylinder rotates, it turns the other in the opposite direction. The flexible band wraps or unwraps about the permanently wrapped band (depending on the direction of rotation), progressively shorting the bands together at the meeting place and thereby changing the resistance along the path between the external contact wires.

In the more elaborate version shown at the middle of the figure, two sets of oppositely wound bands are used so that both clockwise and counterclockwise motions are communicated by ribbon tension, without having to rely on the contact friction alone to transmit the torque between the cylinders. In addition, the two flexible bands maintain each other in tension, preventing slippage out of the proper wrapping configuration. The two sets of bands can be connected in series or parallel.

With the arrangement shown at the bottom of the figure, turning the rollers causes R_1 to decrease while R_2 increases, or vice versa. Thus, the two sets of bands can be connected as a three-terminal potentiometer.

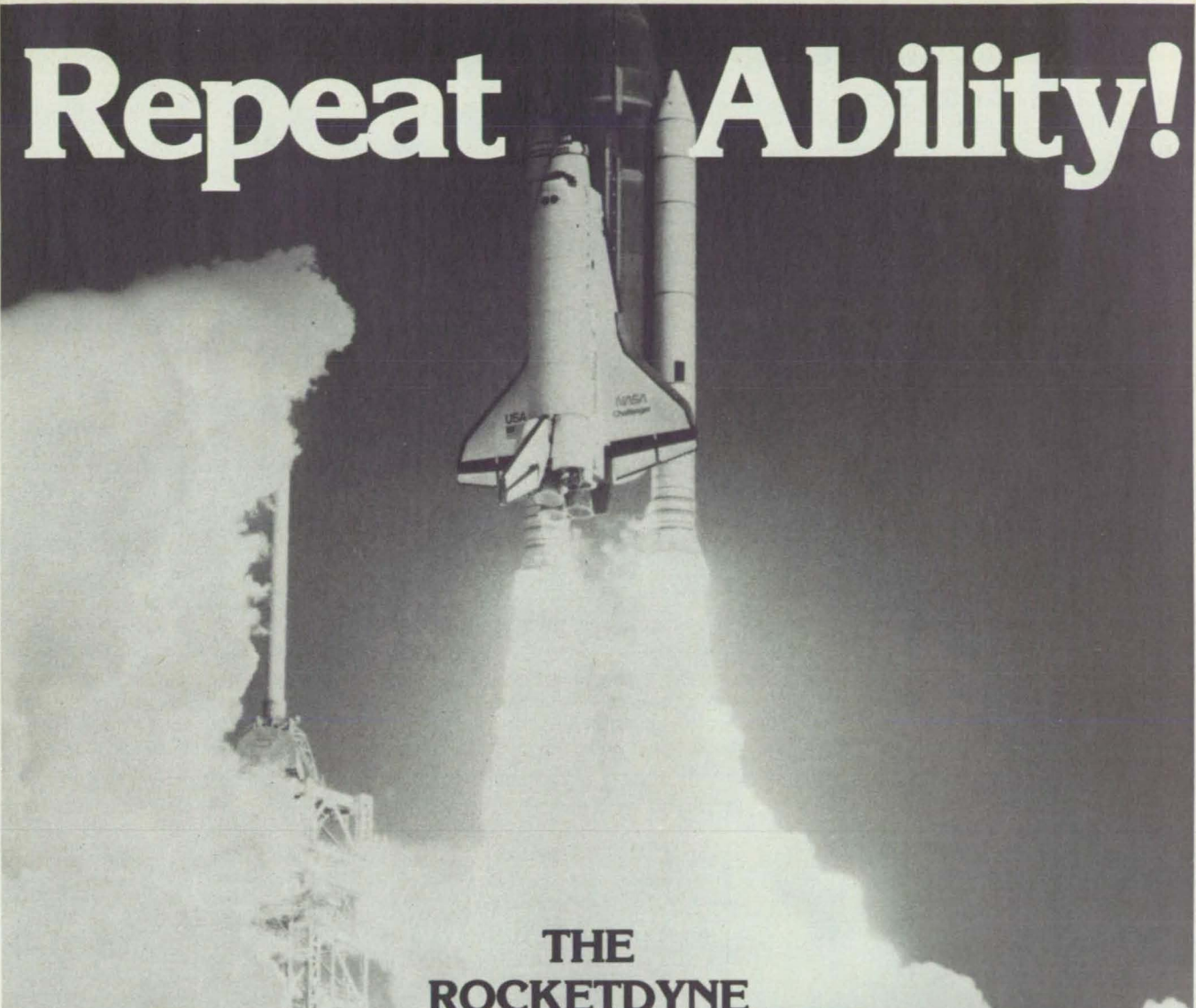
This work was done by Carl F. Ruoff of Caltech for NASA's Jet Propulsion Laboratory. For further information, Circle 51 on the TSP Request Card.

Inquiries concerning rights for the commercial use of this invention should be addressed to the Patent Counsel, NASA Resident Office-JPL [see page 21]. Refer to NPO-15567.



Rolling Contact Between Strips of Resistive Material should assure a low-noise connection. The resistance should vary smoothly with contact position.

Repeat Ability!



**THE
ROCKETDYNE
TEAM
SCORES
AGAIN!**

America's Shuttles have made many spectacular flights into space and back.

The Rockwell-built Shuttles are the latest in the long list of space vehicles powered by rocket engines designed, built, tested, and proven by the Rocketdyne team—for almost 30 years, the world's leader in space propulsion.



**Rockwell
International**

... where science gets down to business

Aerospace/Electronics
Automotive/General Industries



Incrementally Variable High-Voltage Supply

Output varies from 2.5 V to 2.5 kV in small steps.

Marshall Space Flight Center,
Alabama

A proposed programable power supply would provide a regulated output ranging from 2.5 to 2,500 volts. Under control of a digital signal, the output would be increased or decreased in increments of about 4 percent. The entire voltage range would be covered in 169 steps.

As directed, the unit would provide the complete sequence of incremental steps, a limited range of steps, or any individual step. The power-supply concept was developed for an energetic-particle spectrometer in which an exponentially varying voltage is needed to deflect particles having a wide range of energies. A prototype circuit with 64 steps has been tested, and production models are planned.

Positive and negative outputs over the full voltage range are available from the unit. In the prototype, the output settles to a steady

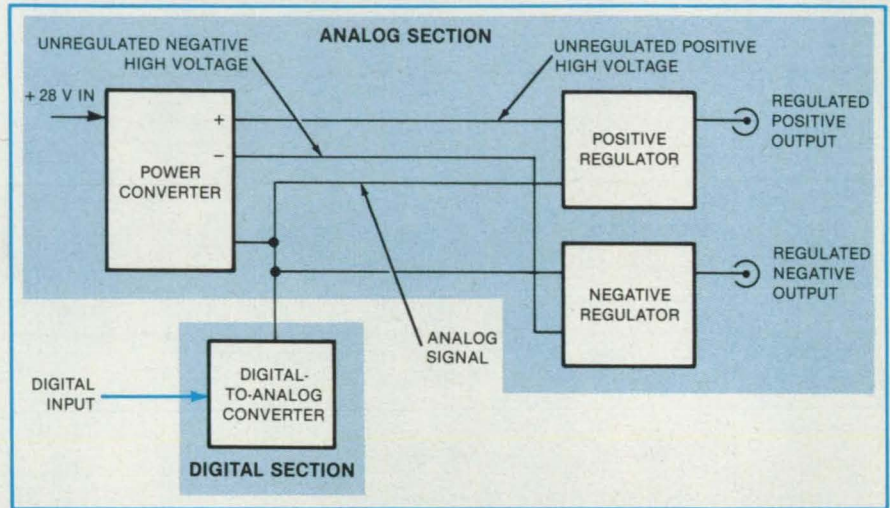


Figure 1. The **Exponential Digital-to-Analog Converter** provides a low-voltage analog signal to a power converter and to negative and positive high-voltage regulators. In response, the converter furnishes a voltage of the approximate magnitude represented by the analog signal, and the regulators adjust this voltage to the precise magnitude.

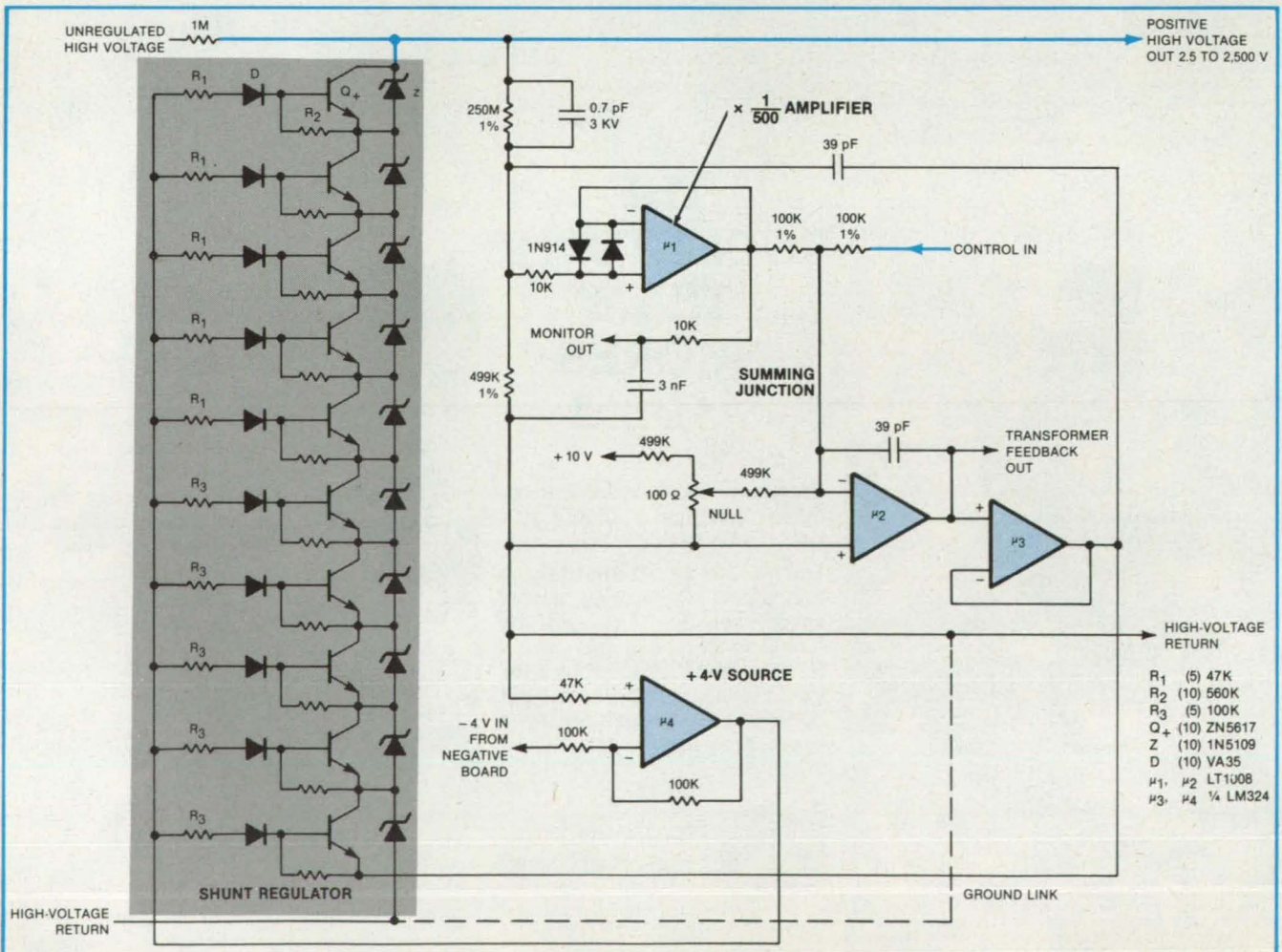


Figure 2. In the **Positive High-Voltage Regulator**, successive stages are turned on by the control signal, thereby varying the output voltage.



Ad
Council

Photo: Peter B. Kaplan

If you still believe in me, save me.

For nearly a hundred years, the Statue of Liberty has been America's most powerful symbol of freedom and hope. Today the corrosive action of almost a century of weather and salt air has eaten away at the iron framework; etched holes in the copper exterior.

On Ellis Island, where the ancestors of nearly half of all Americans first stepped onto American soil, the Immigration Center is now a hollow ruin.

Inspiring plans have been developed to restore the Statue and to create on Ellis Island a permanent museum celebrating the ethnic diversity of this country of immigrants. But unless restoration is begun now, these two landmarks in our nation's heritage could be closed at the very time America is celebrating their hundredth anniversaries. The 230 million dollars needed to carry out the work is needed now.

All of the money must come from private donations; the federal government is not raising the funds. This is consistent with the Statue's origins. The French people paid for its creation themselves. And America's businesses spearheaded the public contributions that were needed for its construction and for the pedestal.

The torch of liberty is everyone's to cherish. Could we hold up our heads as Americans if we allowed the time to come when she can no longer hold up hers?

Opportunities for Your Company.



You are invited to learn more about the advantages of corporate sponsorship during the nationwide promotions surrounding the restoration project. Write on your letterhead to: The Statue of Liberty-Ellis Island Foundation, Inc., 101 Park Ave., N.Y., N.Y. 10178.



In 1992, we set sail for a New World.

In 1492, a Genoese navigator and an intrepid crew crossed uncharted waters in search of a west passage to India. In the process, they uncovered the vast resources of two continents. And they opened up a new base for exploration, progress, and the hopes of mankind.

In 1992, coincident with the 500th anniversary of Columbus's voyage, we plan to set sail for another New World. That year, or shortly thereafter, the United States and the world will begin benefiting from the first manned Space Station. The Station will be more than another giant step for mankind. It will be our stepping stone to living in new realms, and it will result in thousands of discoveries that will benefit earth.



This New World, free from gravity and atmospheric impurity, will provide that ideal environment for experimentation and production that is impossible on earth. Simultaneously we will have a permanent station for scanning the earth and the heavens — an unparalleled vantage point for predicting weather, aiding agriculture, and understanding the universe.

Of course, like Columbus, we cannot foresee all the benefits ahead. But we do know that we will have a new arena in which to conquer disease, transform the materials of earth, and generate precious energy. The resulting knowledge from countless discoveries will come down to earth for our well-being.

But, unlike Columbus, our craft will be in constant contact with the Old World. Harris Aerospace, as a member of the Rockwell, Grumman and Sperry team, is responsible for the Space Station's communications and tracking system. We are totally committed to this great endeavor, and we bring to the challenge the capabilities and experience necessary for success.

Harris has had 27 years of successful involvement with the kind of space communications and tracking required for the manned Space Station. Our space experience includes programs from Telstar to the Tracking and Data Relay Satellite as well as the manned programs of Apollo, Lunar Module, and Space Shuttle. We are also a leader in the architecture and design of large communication networks.

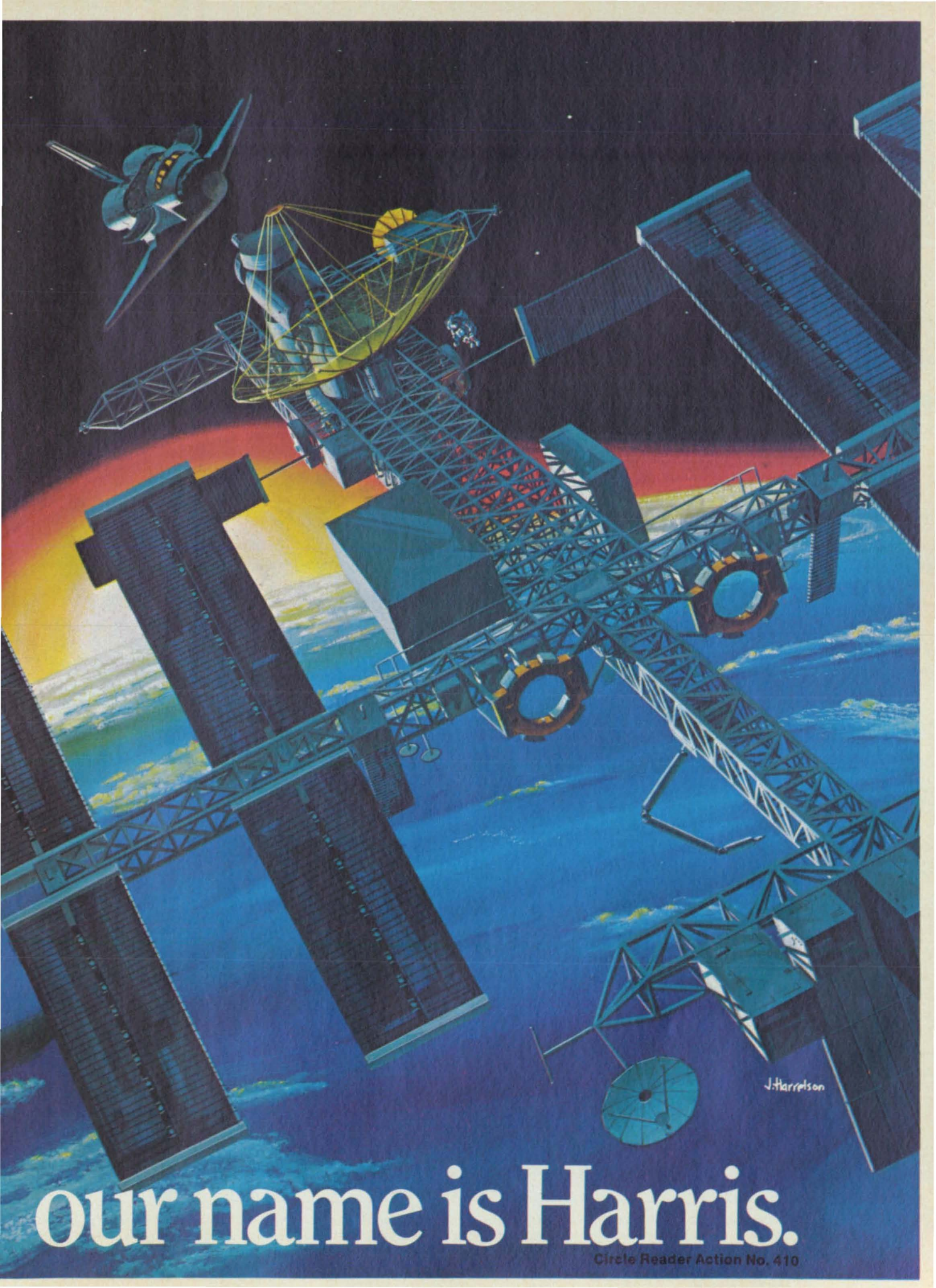
Now Harris is ready for the Space Station. Over the next years and centuries, the scope of scientific, commercial and technological opportunities and breadth of results are sure to exceed our wildest expectations.

For in 1992, we, too, will be very much like Columbus: carrying the sum of our knowledge into the unknown. And, like him, we, too, shall return with the bountiful gifts of a New World.



HARRIS

For your information,



our name is Harris.

Circle Reader Action No. 410

value at a new step in about 0.4 milliseconds. Despite variations in temperature, input voltage, and current, the output voltage varies no more than half a step (that is, ± 2 percent) except in the last 10 steps near zero, where a 3-percent deviation occurs.

The supply consists of two parts: A digital section and an analog section (see Figure 1). The digital section converts the 8-bit parallel input for each step into a low-level analog signal representing the output voltage at that step. This exponential-response feature is best handled digitally, rather than in the analog section because analog exponential amplifiers are notoriously sensitive to temperature changes.

The analog section converts the analog output of the digital-to-analog converter into high output voltages. It contains two regulators — one for the negative output and the other for the positive output. Each, in effect, has a gain of 500 and must respond linearly

to an input that ranges from 0 to -5 volts.

The control signal put into each regulator is added to the output of a divide-by-500 amplifier stage operating from the high-voltage output (see Figure 2). The resulting error signal is fed through an operational amplifier to a high-voltage shunt regulator.

The high-voltage shunt regulator consists of 10 stages, each composed of a transistor, a Zener diode, a high-voltage diode, and a pair of resistors. The output voltage is controlled by turning on successive stages of the shunt regulator and operating the highest one in the active region.

The power converter transforms 28 volts from the line to the voltages required by the operational amplifiers (± 10 volts) and to the unregulated high voltage used by the regulators. A feedback signal from the regulators keeps the unregulated high voltage at about 100 volts above the regulated value. This reduces the power that must be dissipated

by the shunt regulator stages and hence the power consumed by the circuit. The total power consumption is expected to be less than 2 watts.

This work was done by Douglas W. Potter and John Chin of the University of Washington and Hugh R. Anderson and Robert L. Loveless of Science Applications, Inc., for Marshall Space Flight Center. For further information, Circle 49 on the TSP Request Card.

Inquiries concerning rights for the commercial use of this invention should be addressed to the Patent Counsel, Marshall Space Flight Center [see page 21]. Refer to MSC-28018.

Low-Voltage Protection for Volatile Computer Memories

Short-circuit current provides minimum memory power.

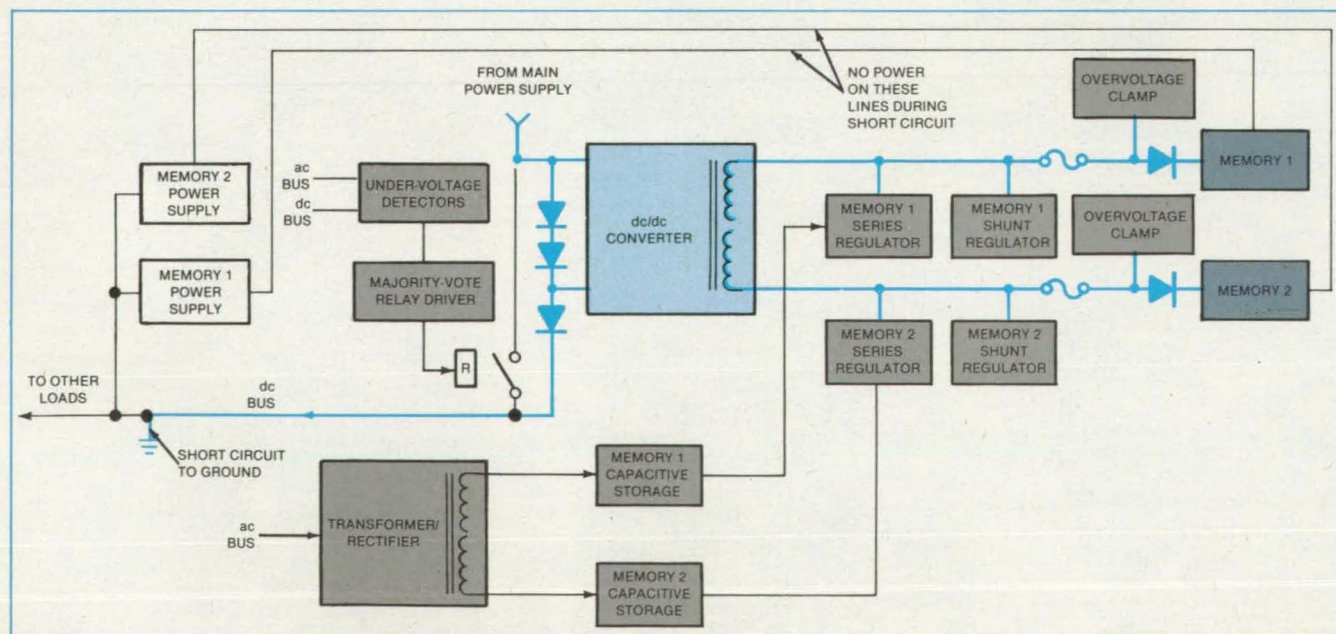
NASA's Jet Propulsion Laboratory, Pasadena, California

The contents of two semiconductor computer memories are preserved by a circuit that supplies the minimum "keep-alive" voltage in case of a short circuit elsewhere in the computer system. A simplified version of the protective circuit may be useful wher-

ever it is necessary to improve the reliability of volatile memories or other circuits that must not lose power. In addition, the circuit includes a unique low-input-voltage dc-to-dc converter that may have other uses.

A short circuit in one or more loads fed by

the main 30-Vdc power bus is signaled by undervoltage detectors at critical system locations that are connected to a majority-vote relay driver (see figure). In normal operation, the relay switch is closed to divert the dc bus current around the three series isola-



The Protective Circuit includes a dc-to-dc converter that supplies keep-alive voltage to the memories when a short circuit occurs in any of the system loads. The converter is powered by the low voltage across two of the three series diodes that is generated by the short-circuit bus current. The relay switch is shown in open (short-circuit-detected) position.

tion diodes. When a short is detected, the relay switch is driven to the open position, forcing the short-circuit bus current through the diode string. During the detection-and-switching interval of about 0.1 second, the memory voltage is maintained by a small storage-capacitor supply (not shown).

The short-circuit bus current of 8.75 to 20 A produces 0.8 to 2.0 Vdc across the two series diodes at the dc-to-dc converter input

terminals. With the worst-case combinations of fault currents and voltages, the regulated converter outputs are 7.779 to 9.283 V for memory 1 and 6.804 to 7.978 for memory 2. Both voltages are above their respective memory keep-alive levels, yet are below the minimum excursions of the memory operating voltage under normal conditions.

The dc-to-dc-converter outputs are fused and equipped with 12-V Zener-diode voltage

clamps for additional protection. This is necessary to insure that no single failure will result in overvoltage damage to the memories and that a failure in one memory will not harm the other memory.

This work was done by Robert C. Detwiler of Caltech for NASA's Jet Propulsion Laboratory. For further information, Circle 52 on the TSP Request Card. NPO-15909

Comparator With Noise Suppression

A comparator continuously and automatically adjusts the noise immunity period.

Langley Research Center, Hampton, Virginia

A new level comparator prevents the multiple triggering that occurs when conventional comparators are driven with noisy sinusoidal inputs. The comparator continuously and automatically adjusts the noise immunity period to accommodate the existing pulse width of the input signal.

The output of multivibrator 1 (see figure) is set high by the first negative-going output pulse of the (+) comparator, indicating the comparator input has exceeded the reference level. Subsequent comparator output pulses between t_0 and t_1 caused by the noise present on the sinusoidal input are ignored by multivibrator 1, since its timing is set with sufficient duration to make it independent of further transitions until it receives an overriding clear pulse. The timing components are selected to provide an output

pulse duration equal to or greater than the period ($t_1 - t_0$) of the lowest frequency of interest. For example, if the pulse duration is 0.5 seconds, the lowest noise-free operation is 1 Hz. The upper limit is typically the upper frequency limit of the amplifiers and comparators.

A high-gain amplifier is used in conjunction with multivibrator 4 to provide a clear pulse to multivibrator 1 at the first negative-going zero crossing ($\cong t_1$) of the input signal. Once multivibrator 1 is cleared, its output goes to zero volts, and it will not be retriggered until the next time a positive input exceeds the reference level. Since the input-signal noise at the zero crossing ($\cong t_1$) does not exceed the reference level, it has no effect on multivibrator 1 operation.

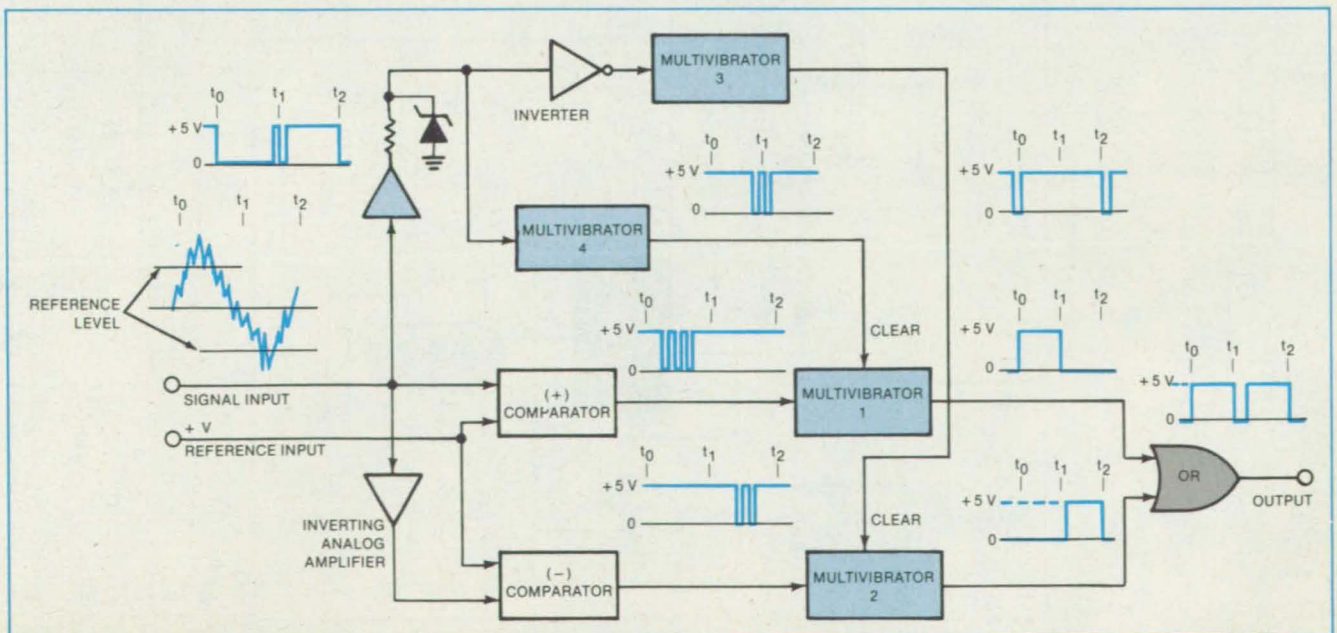
The (-) comparator and multivibrator 2

are sensitive to the negative portions of the sinusoidal input signal and respond in the same manner described for the (+) comparator and multivibrator 1. An OR gate combines the outputs of multivibrators 1 and 2 to provide a total pulse count.

The circuit was fabricated using standard solid-state operational amplifiers, multivibrators, OR gates, and passive elements.

This work was done by Colossie N. Batts of Langley Research Center. No further documentation is available.

This invention is owned by NASA, and a patent application has been filed. Inquiries concerning nonexclusive or exclusive license for its commercial development should be addressed to the Patent Counsel, Langley Research Center [see page 21]. Refer to LAR-13151.



A High-Gain Amplifier Is Used With Four Multivibrators and an OR gate, which combines multivibrator outputs to discriminate against noise.

Remote Power Controllers for High-Power dc Switching

They combine the functions of a remotely controlled switch and a circuit breaker.

Lewis Research Center, Cleveland, Ohio

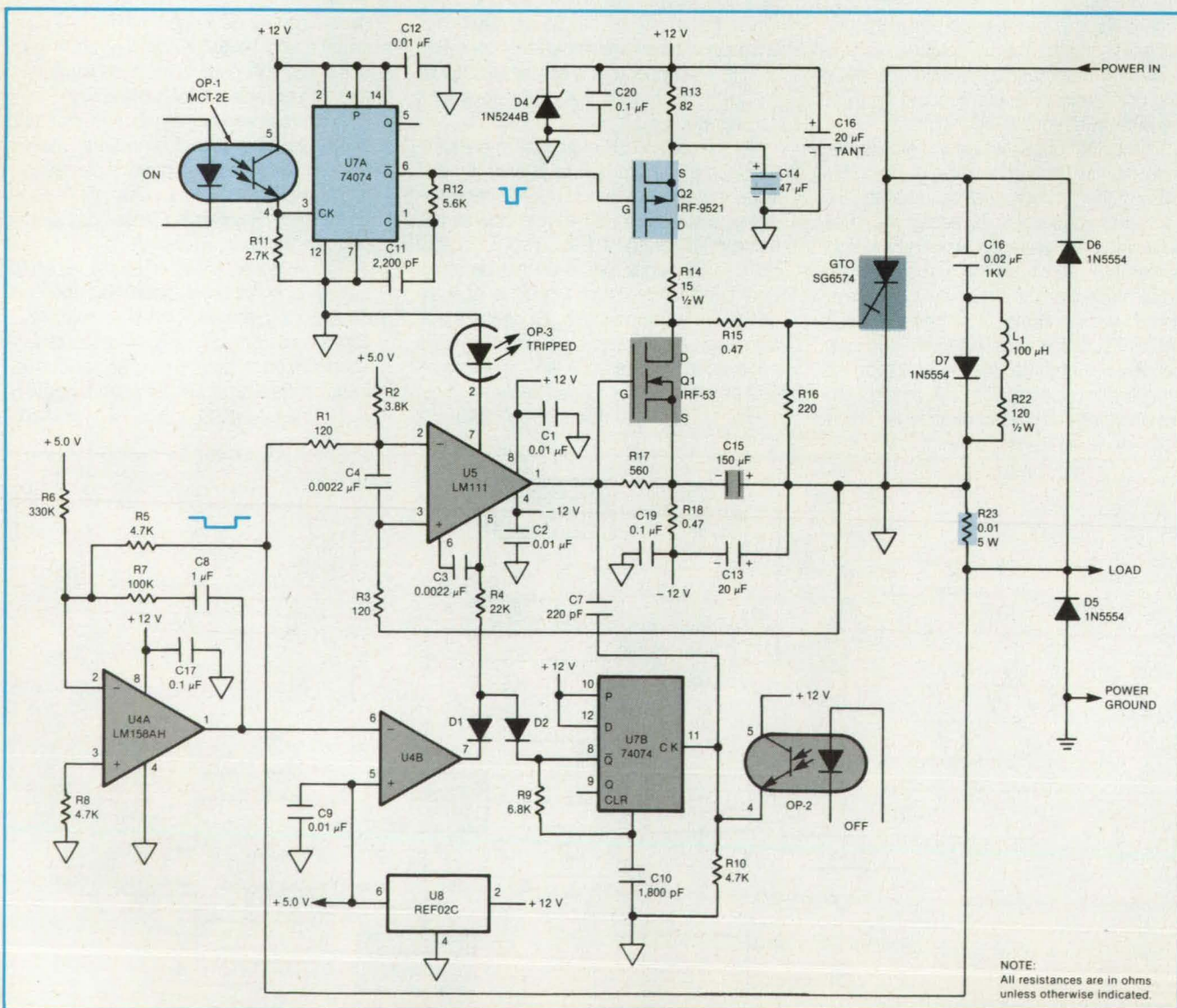
Circuit designs, covering a wide range of power levels, were developed for two general types of Remote Power Controllers (RPC's). They all combine circuit breaker and remote switching functions with very fast overload protection. The power switching devices used in these designs are the gate turnoff thyristor (GTO) or power MOSFET transistors. Both have faster response times than junction transistors, particularly at turnoff. This facilitates the design of fast-tripping RPC's, which can protect against severe overloads.

Specific circuits were developed at different power levels but conceptually are very similar. By selection of appropriate switching devices and minor modifications, these circuits can be used to build RPC's covering a range of voltage and power levels limited only by the switching devices chosen. Those RPC's using GTO's have a power capability that ranges from 7.8 to 52 kW, while those using MOSFET's range from 8 to 15 kW.

There is a recognized need for RPC's that can provide both efficient switching

and overcurrent protection in dc power systems. Potential applications include satellites, the Space Station, commercial aircraft, naval vessels, and numerous industrial areas. The RPC's combine the functions of a remotely controlled switch and a circuit breaker. Because they are all solid state, there are no contacts to arc and wear out when the switch opens and closes. This is also important for operation in areas having fire or explosion hazards.

To be effective in protecting systems using semiconductor devices, an RPC must



This Gate Turnoff Thyristor Remote Power Controller switches efficiently and protects from overload. The circuit can apply turnoff gate drive in less than 2 µs after application of a large overload.

interrupt large overloads very rapidly or limit the current that it will pass. This requirement was incorporated in the circuit designs.

The schematic shows a typical GTO-RPC circuit. Switch turn-on is initiated by optoisolator OP-1, which triggers flip-flop U7A, which is used as a one-shot multivibrator. Flip-flop U7A turns on transistor Q2, discharging capacitor C14 into the gate of the GTO thyristor to turn it on. Direct current flows through the GTO, current shunt R23, and out the load terminal.

Turnoff can be initiated in three ways. A large overcurrent will produce sufficient voltage across R23 to trigger comparator U5. Its output then turns on Q1, discharging capacitor C15, which is charged to a negative voltage, into the gate of the GTO, turning it off. The action of this circuit is very fast. It can apply turnoff gate drive in less than two microseconds after application of

a large overload. For smaller overloads, the voltage from R23 is integrated by operational amplifier U4A, the output of which is a step function with a superimposed linear ramp. The second operational amplifier, U4B, is used as a comparator that detects when the ramp exceeds a preset threshold. At that time it drives U5 on, causing a shutdown as before. This provides a tripout function approximately proportional to I^2T , where I is output current and T is time. A normal shutdown is initiated by optocoupler OP-2, which triggers the one-shot U7B. Its output turns on U5 as in the previous cases.

All of this circuit is built on one printed-circuit card that floats at the output voltage. Signals to and from the ground referenced controls are via the optoisolators.

Control circuits for the MOSFET RPC's are very similar to the above, except that a latching output is used to keep the MOSFET's on or off. A small switching-type

power supply, with transformer isolation, powers the control circuitry in either case.

An important feature of the control circuit is the programmable overcurrent tripout that can be adjusted for both current level and time. Various current/trip-time curves can be set with a simple RC network. For slight overloads, tripout typically takes several seconds. As the overload increases, the trip time decreases. At two to three times rated current, tripout occurs in 50 ms. For even higher currents, the fast trip circuit is initiated, and the RPC opens in less than 3 microseconds.

The basic technology has been developed to a level that enables an engineer to design RPC's for nearly any required power level or application.

This work was done by John C. Sturman of Lewis Research Center. No further documentation is available.
LEW-14109

High-Output Injection Laser

A terraced double-heterojunction large optical cavity laser features high output in a single optical mode.

Langley Research Center, Hampton, Virginia

A new semiconductor laser has high output power in a single optical mode. The deposition of the active layer (see figure) of the semiconductor laser over a terraced confinement layer results in an active layer that has its maximum thickness and recombination region over the concave portion of the terrace and tapers in decreasing thickness in the lateral direction. A weak, asymmetric positive-index optical guide is thus formed that supports only the fundamental lateral optical mode. A guide layer may be interposed between the confinement layer and the active layer with the thickest portion of the active layer over the terrace in the guide layer.

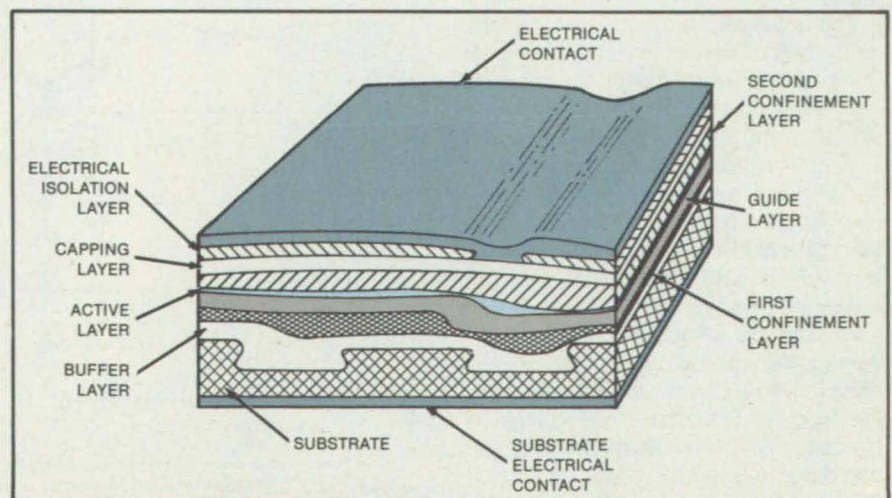
The semiconductor laser consists of a body of single-crystal semiconductor material, typically composed of Group III to V compounds, in the form of a rectangular parallelepiped. One of the laser end faces is partially transparent so that light may be emitted from it.

The laser body is built up from several layers, each layer having a unique shape. As shown in the figure, the substrate has a pair of spaced, substantially parallel grooves with a mesa between the grooves.

A buffer layer with a terraced surface overlies the substrate and fills the grooves. Over the buffer layer is a terraced first confinement layer. On top of the first confinement layer are the guide layer and the active layer.

A second confinement layer overlies

the active layer, and a capping layer covers the confinement layer, which in turn is covered by an electrical isolation layer. This layer has an opening extending through it in the form of a stripe over the portion of maximum thickness of the active layer. An electrical contact covers the



The Lateral Thickness Variation of the Active and Guide Layers in the semiconductor laser produces a confinement of the propagating laser beam in the lateral direction.

electrical isolation layer and the portion of the capping layer in the region of the opening. An electrical contact underlies the substrate.

The semiconductor laser also includes a protective coating on one end face. The coating is substantially transmissive at the wavelength of the light emitted by the laser. On the opposite face, a reflector reflects light at the laser wavelength.

Continuous-wave lasing was obtained up to about 60 milliwatts at room tem-

perature and up to about 15 milliwatts at a 70° C ambient temperature. The pulsed threshold current temperature coefficient T_0 was 190° C in the -30° to 20° C temperature range and 105° C in the 20° to 50° C temperature range. The lateral and transverse far-field patterns of the output laser beam were stable up to 50 milliwatts output power with full widths at half power of about 23° and 26°, respectively, at 20° C. About 70 percent of the operative devices exhibited single longitudinal, lateral, and

transverse mode operation up to about 50 milliwatts power output at 20° C.

This work was done by John C. Connolly and Dan Botez of RCA Laboratories for Langley Research Center. For further information, Circle 44 on the TSP Request Card.

Title to this invention has been waived under the provisions of the National Aeronautics and Space Act (42 U.S.C. 2457(f)) to RCA Corp., Princeton, NJ 08540. LAR-13213



Commutating Permanent-Magnet Motors at Low Speed

A circuit provides forced commutation during starting.

Marshall Space Flight Center, Alabama

A circuit for brushless permanent-magnet motors provides a variable commutation time as the motor comes up to speed. At sufficiently high speed, the circuit becomes inoperative and normal commutation takes over.

A permanent-magnet motor generates a sinusoidal back-electromotive force that can commutate the silicon-controlled rectifier (SCR) switches in the inverter that supplies power to the motor. However, when the motor is just starting up, its back-electromotive force is too low for commutation, and some other means of turning off the SCR's for brief periods must be provided. The new circuit furnishes the requisite forced commutation with only three additional components: An SCR, the rating of which need be no higher than that of the inverter SCR's; a low-voltage, high-current transistor; and a capacitor.

The circuit was designed for a brushless dc motor that drives the compressor of a 25-ton solar-powered heater and cooler. It has no adverse effects on the power factor, efficiency, and capacity of the motor.

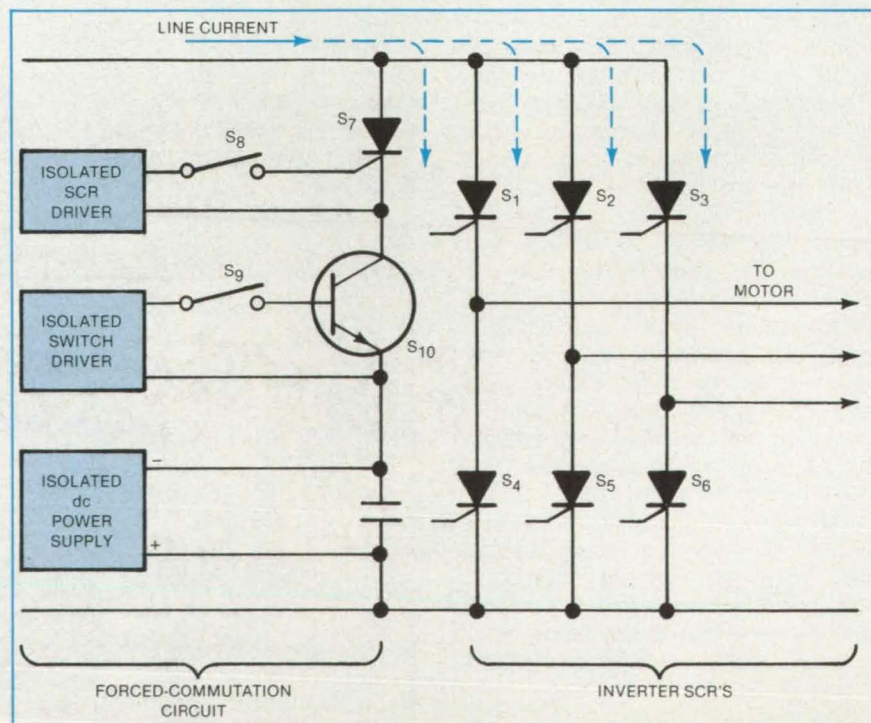
At the instant the motor starts, the capacitor of the forced-commutation circuit is charged to a predetermined voltage greater than 10 volts (see figure) by an isolated dc supply. An isolated SCR driver S_8 turns on, allowing SCR switch S_7 to turn on. When commutation is required, the inverter position-sensor logic turns on isolated switch driver S_9 , diverting the line current into the capacitor. Since the -10-V charge on the capacitor overcomes the forward voltage drops in S_7 and S_{10} that occur when these two switches conduct the line current, the voltage across the inverter SCR's S_1 through S_6 becomes negative enough to

shut them off during the commutation period of about 100 μ s.

When the motor comes up to about 10 percent of full speed, its back-electromotive force is sufficient to support commutation. At this point, S_{10} is turned off for about 300 μ s, allowing S_7 to turn off and block the line voltage. S_{10} is then turned on to provide a path for the leakage current from S_7 , and normal commutation begins.

This work was done by Carlisle Dolland of AiResearch Manufacturing Co. for Marshall Space Flight Center. No further documentation is available.

Inquiries concerning rights for the commercial use of this invention should be addressed to the Patent Counsel, Marshall Space Flight Center [see page 21]. Refer to MFS-25207.



The **Forced-Commutation Circuit** diverts current from the inverter SCR's and turns the SCR's off during the commutation intervals. The silicon-controlled rectifier in the circuit will be unnecessary when switch S_{10} can be replaced by a high-current, high-voltage transistor. At present, a high-current, low-voltage device must suffice.

This is not an ad for the world's finest helicopter. It is an opportunity for the world's finest engineers.

At Bell, our engineers have proven that a challenging and advanced work environment encourages the most creative engineering thinking.

It's that kind of thinking which has involved Bell in projects like the V-22 Osprey program using tilt-rotor design, the advancement in redundant 'fly-by-light' and 'fly-by-wire' technology and many other progressive R&D programs. Bell currently employs engineers in 75 distinct disciplines, and we have many openings for experienced engineering professionals now.

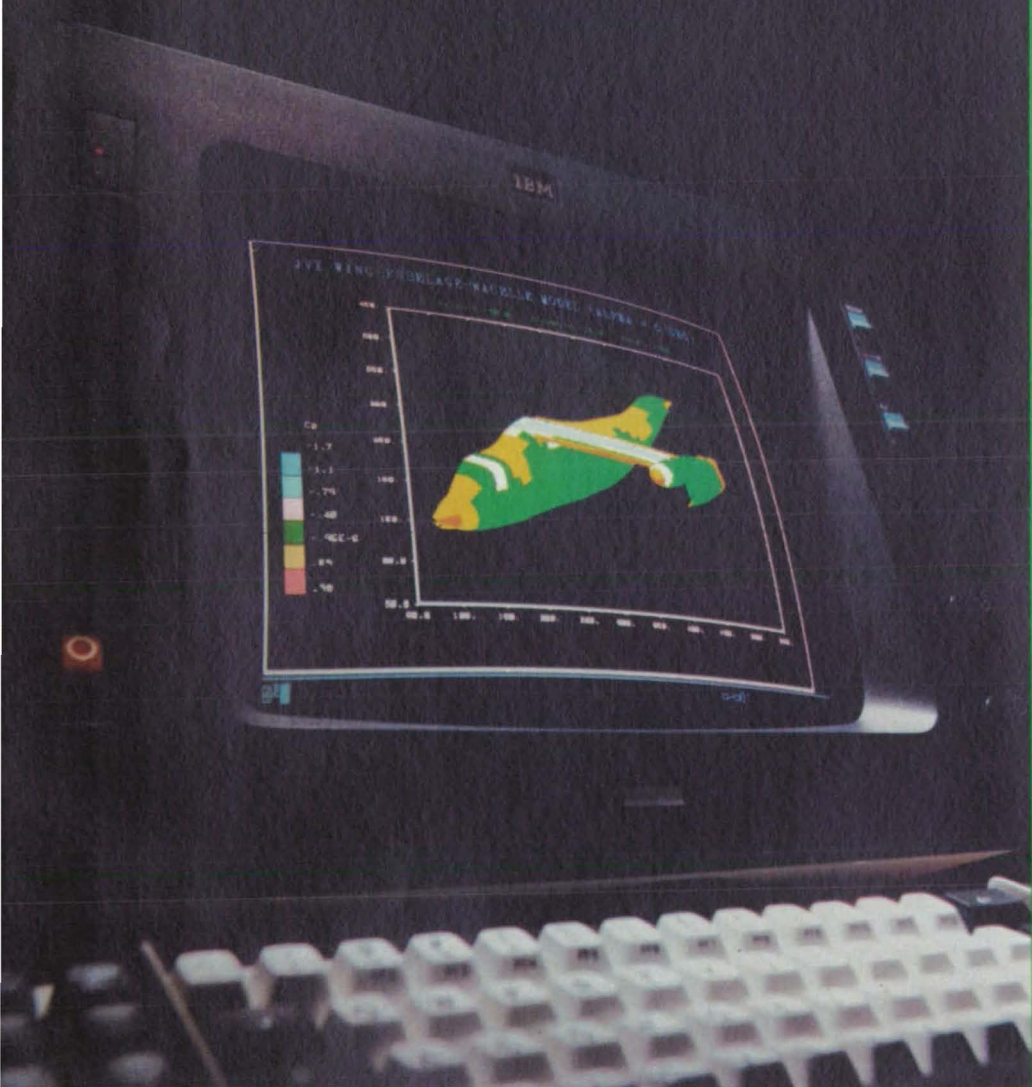
Your chance to enhance your career potential begins today with a call to Bell Helicopter.

Help us make tomorrow unlike anything today.

Here's what we'd like: if you have appropriate degrees and three or more years experience in your specialty, our engineers are eager to meet you and detail the positions open in these areas now at Bell:

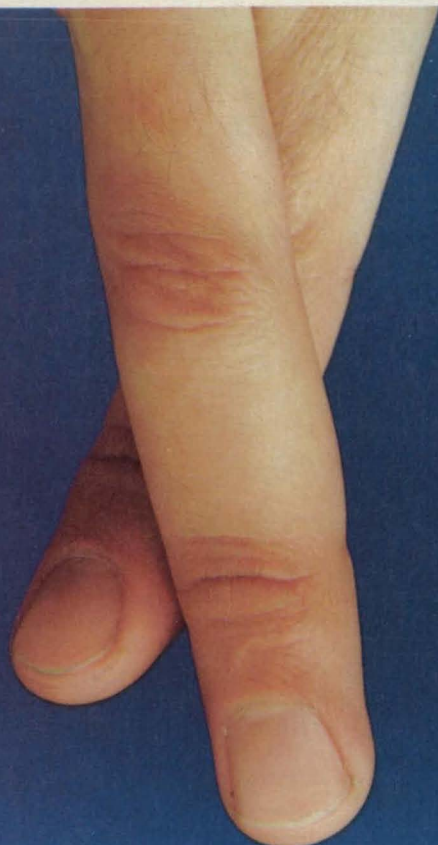
**AIRBORNE SOFTWARE
SUBSYSTEMS INTEGRATION
OPERATION ANALYSIS
COUNTERMEASURES
AERODYNAMICS
STRUCTURAL DYNAMICS
AEROACOUSTICS**

Here's what you'll like: the competitive salary ranges, superior benefit package, liberal vacation programs and sunny Texas location. But most of all, the hands-on responsibility and the opportunity to be involved with people who challenge themselves to the fullest: the best, creating the best. To learn more, call David McDavid at (817) 280-2377 today, or send your resume to him at Bell Helicopter, P.O. Box 482, Dept. NTB-1, Fort Worth, TX 76101.



Bell Helicopter

an equal opportunity employer m/f/h/v



it's this...
OR
LAKE SHORE

For Cryogenic Temperature Accuracy.

Trusting expired cryogenic sensor calibrations? Or calibration data from a jury-rigged system? Lake Shore sensor recalibrations can renew your measurement confidence.

Lake Shore's uniquely-equipped cryogenic cal lab is maintained traceable in accord with MIL-STD-45662. Calibration runs are computer-controlled, scientist-supervised. We automatically test for stability, double intercompare standards & unknowns, exchange polarities to negate thermal emfs, and certify the results in a complete documentation package.

With Lake Shore calibrations you get accuracy you can rely on...rather than data you can only cross your fingers over. Service is prompt, efficient, economical...because at Lake Shore, we know cryogenics COLD!

Cryogenic Thermometry • Instrumentation • Calibrations



64 E. Walnut St., Westerville, OH 43081 • (614) 891-2243

In Europe: Cryophysics: Witney, England • Jouy en Josas, France
Darmstadt, W. Germany • Geneva, Switzerland

In Japan: Niki Glass Co., Shiba Tokyo

Circle Reader Action No. 369

Remotely-Adjustable Solid-State High-Voltage Supply

Pulsed or steady outputs up to 20 kV are produced by commercial components.

*NASA's Jet Propulsion
Laboratory, Pasadena, California*

A new circuit produces an adjustable high-voltage output in response to a low-voltage input. The output voltage changes approximately linearly up to 20 kilovolts as the input voltage is varied from 0 to 5 volts. The output can be steady, or it can be sine wave varied at rates up to 100 pulses per second. Output current is about 100 microamperes.

The high output voltage is varied through a feedback loop in which the input serves as the control signal. Basically, the input voltage establishes the amplitude of an oscillator. This amplitude controls the output voltage.

The oscillator is tuned by a 5-kilohm potentiometer to peak the output voltage (see figure) at the frequency of maximum transformer response: This oscillator frequency lies between 45 and 55 kHz. The half-wave rectified output of the transformer is applied to a voltage divider, from which a feedback voltage is derived. The feedback voltage is applied through a 100-kilohm resistor, an operational amplifier, and a comparator to a high-voltage amplifier. The feedback loop thus maintains the high-voltage output at a level determined by the buffered input signal that is fed to one of the inputs of the comparator. A diode and varistors on the primary side of the transformer protect the output transistor.

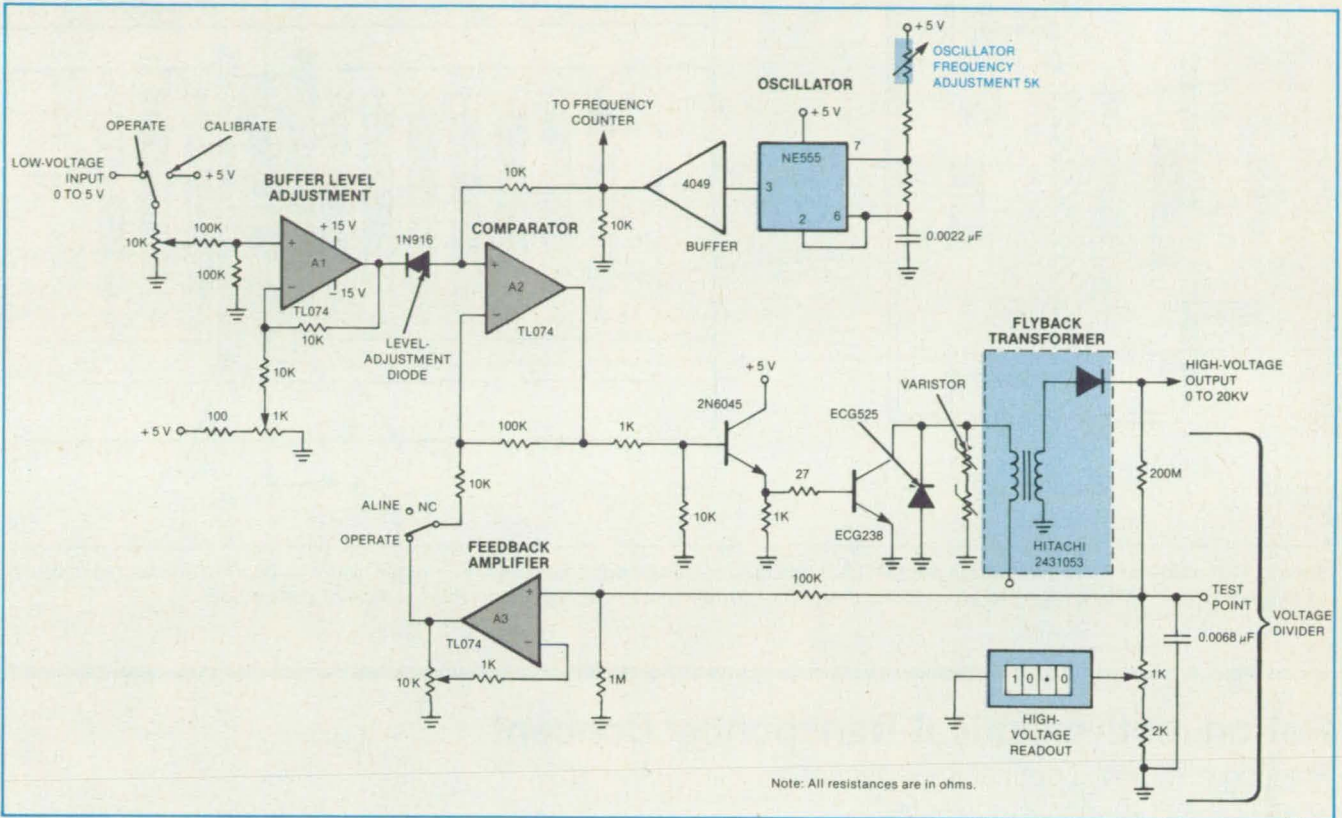
The constant output of the oscillator amplifier is used in conjunction with the buffer level adjustment to bias the level-adjustment diode. This bias clamps the amplitude of the oscillator output to a level related to the input.

The transformer is a flyback transformer of the type used in color-television sets. It was selected because its output is in the required range, it has a wide frequency response, its components are completely encapsulated in potting compound, and it requires no tripling circuits. Since the yoke portion of the transformer is not used in this application, the transformer can be driven at a much higher frequency — about 51 kHz instead of the 15.750 kHz used in television. This high operating frequency helps to reduce ripple voltage: Only a small amount of capacitance need be added to filter out the high frequency. The reduction in output-filter capacitance confers an additional

NASA Tech Briefs, Summer 1985

benefit by reducing pulse rise time.

This work was done by William T. Simms of Caltech for NASA's Jet Propulsion Laboratory. For further information, Circle 41 on the TSP Request Card.
NPO-15719



A **Feedback Loop** between the high-voltage output and the low-voltage input maintains a proportionality between the two. Components in the shaded area are mounted on a high-voltage insulated chassis. The other components are on a conventional circuit board.

Reed-Switch Position Indicator

Switches in a row are actuated one at a time.

John F. Kennedy Space Center, Florida

A position indicator for valves or other control mechanisms is easy to mount, reliable, and explosionproof. The indicator is based on magnetic reed switches. The device replaces slidewires, which are expensive and can sometimes be difficult to mount.

A magnet closes or opens reed switches sequentially as the valve stem or other part moves past them to change the control set-NASA Tech Briefs, Summer 1985

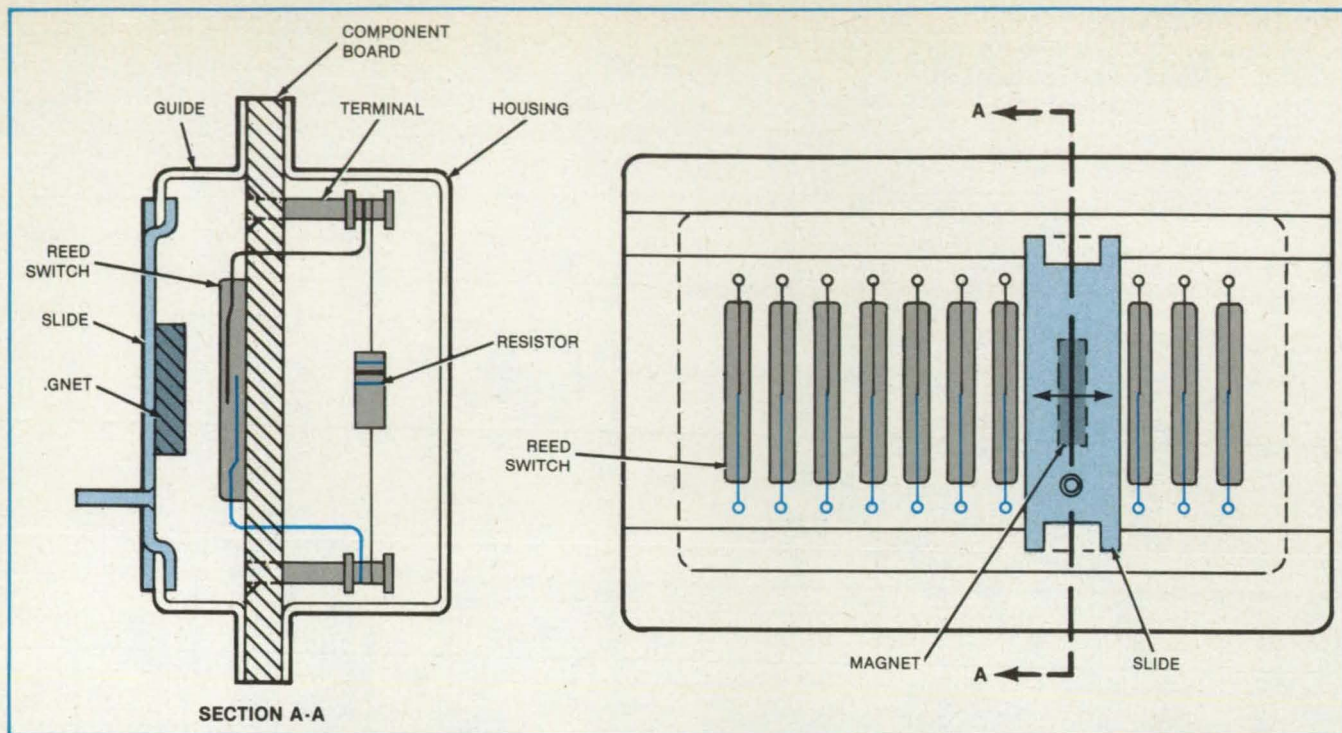
ting (see figure next page). In combination with resistors, the reed switches constitute a variable voltage-divider network, the output voltage of which changes in steps, depending on the position of the magnet.

The indicator can be used in hazardous areas that require nonexplosive electrical contacts. It has been used for controlling highly flammable fuels and can be readily adapted to oil-refining and other chemical-

processing plants.

This work was done by Frank E. Winner of Martin Marietta Corp. for **Kennedy Space Center**. No further documentation is available.

Inquiries concerning rights for the commercial use of this invention should be addressed to the Patent Counsel, Kennedy Space Center [see page 21]. Refer to KSC-11215.



Sliding Past a Row of Reed Switches, a magnet changes their state one after the other. A Voltage-Divider Network is connected to the row of magnetic reed switches to give an output voltage that varies in steps according to the position of the magnet.

Retrodirective-Optical-Transponder Concept

Pointing errors and optical imperfections would be automatically corrected.

NASA's Jet Propulsion Laboratory, Pasadena, California

A proposed retrodirective solid-state optical transponder would be based on the principle of nearly-degenerate four-wave mixing (ND4WM). Without mechanical pointing or expensive high-quality optics, the transponder would send a signal back toward the source of an incoming signal. When perfected, the concept should find important civilian and military applications in line-of-sight tracking, communication, and identification.

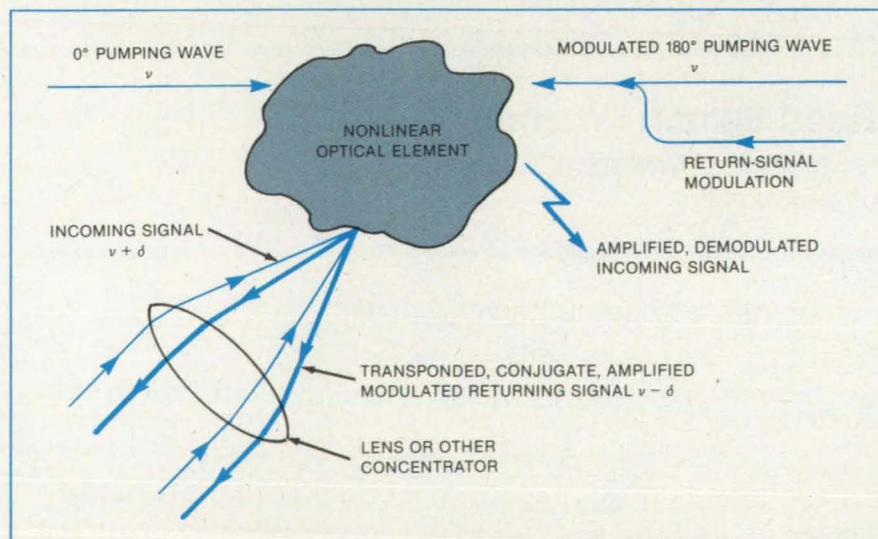
The heart of the transponder is a nonlinear optical element that performs ND4WM (see figure). The element is placed in the focal region of a reflector or other signal concentrator. An optical conjugate mirror is formed in the element as a grating generated by the nonlinear optical effect of bidirectional optical-pumping waves. The optical pump could be, for example, a solid-state laser diode operating at a frequency ν near the frequency $\nu + \delta$ of the incoming signal.

The nonlinear interaction between the two pumping waves and the weak incoming signal produces a fourth optical wave of frequency $\nu - \delta$, propagating in the direction opposite that of the incoming wave. Infor-

mation could be transmitted on the return signal by applying the appropriate modulation to the optical pump.

The phase conjugation in the element

produces a spatial duplicate of the incoming wave front, propagating in the opposite direction. Thus, the returning wave front is automatically pre-distorted to compensate



A Coherent Optical Transponder would employ nearly-degenerate four-wave mixing in a nonlinear optical element to produce a signal traveling back toward the source of an incoming signal. The return signal could be modulated for communication, navigation, data transmission, tracking, and identification.

for imperfections in the optical system: As the returning wave front passes back out through the distorting portions of the optical system, the wave front distortions are removed and the wave front emerges into free space with the same spatial character-

istics (except for the direction of propagation) as those of the incoming wave. This retrodirective ability of ND4WM thereby automatically compensates for mechanical pointing errors, thermal strains, blemishes, and aging effects in optical elements.

This work was done by Richard M. Dickinson of Caltech for NASA's Jet Propulsion Laboratory. For further information, Circle 17 on the TSP Request Card. NPO-16315

Electrically Connecting to Pressure Vessels

A proposed resilient conductive disk would eliminate the need for holes in vessel walls.

Lyndon B. Johnson Space Center, Houston, Texas

A proposed grounding disk would electrically connect a component and a pressure vessel without holes or fasteners. Ordinarily, an electrical component can be grounded to a frame by simply attaching a jumper cable to the component at one end and to a fastener, threaded to the frame, at the other end. However, if the frame is a pressure vessel, drilling holes for grounding fasteners is prohibited, since such holes would weaken the vessel or allow it to leak.

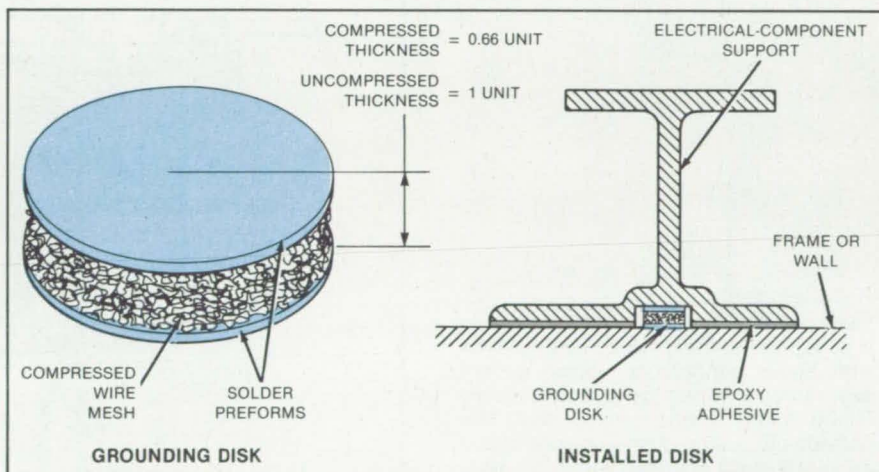
The grounding disk is made by compressing long strands of wire, forming a resilient slug of dense mesh (see figure). Round high-tin solder preforms, 1 to 2 mils (0.025 to 0.051 millimeter) thick, are melted into the flat faces of the disk. The disk fits into a slot in a flange on the electrical component support.

Emplaced in the component support, the disk can be squeezed to as little as 66 percent of its thickness. The disk conforms to the surfaces of the support and the vessel wall when the support is attached to the wall with an adhesive. The disk thus forms a reliable electrical contact from the support (and

its electrical component) to the wall.

This work was done by Peter J. Rossi of Rockwell International Corp. for Johnson Space Center. No further documentation is available.

Inquiries concerning rights for the commercial use of this invention should be addressed to the Patent Counsel, Johnson Space Center [see page 21]. Refer to MSC-20709.



The **Grounding Disk** is Made from wire and solder. It is sandwiched between the electrical-component support and the pressure-vessel wall.

Orienting Arc Lamps for Longest Life

The temperature distribution strongly affects their performance.

Lyndon B. Johnson Space Center, Houston, Texas

Tests on floodlights for the Space Shuttle payload bay show that the useful life of a metal halide dc arc lamp is prolonged by mounting it "anode down" and wiring it for maximum heat conduction away from the electrodes. Lamps that fail a 2,000 hour-life test when oriented anode up, pass when oriented anode down and rewired with copper leads (rather than nickel leads). Though the tests were done on only one type of lamp, they illustrate the importance of the thermal environment on the lifetime of high-intensity NASA Tech Briefs, Summer 1985

lamps, such as those used in streetlights, warehouses, and athletic arenas.

The tests were conducted with the reflector facing upward (see figure) as it would be in the intended application. In the first test, the lamp was unmodified, with the discharge tube oriented anode upward. For the second test, the discharge tube was oriented with the anode down. To improve the conduction of heat away from the electrodes, the nickel contact rods were replaced with stranded copper wires that

were heat-sunk to copper tabs.

Thermocouples were placed on the electrodes. Each lamp was mounted on standoff insulators in a bell jar filled with nitrogen at half atmospheric pressure. (Normally, a quartz window on the front of the lamp seals in the nitrogen, which prevents oxidation of the silver deposited on the surface of the paraboloidal reflector.)

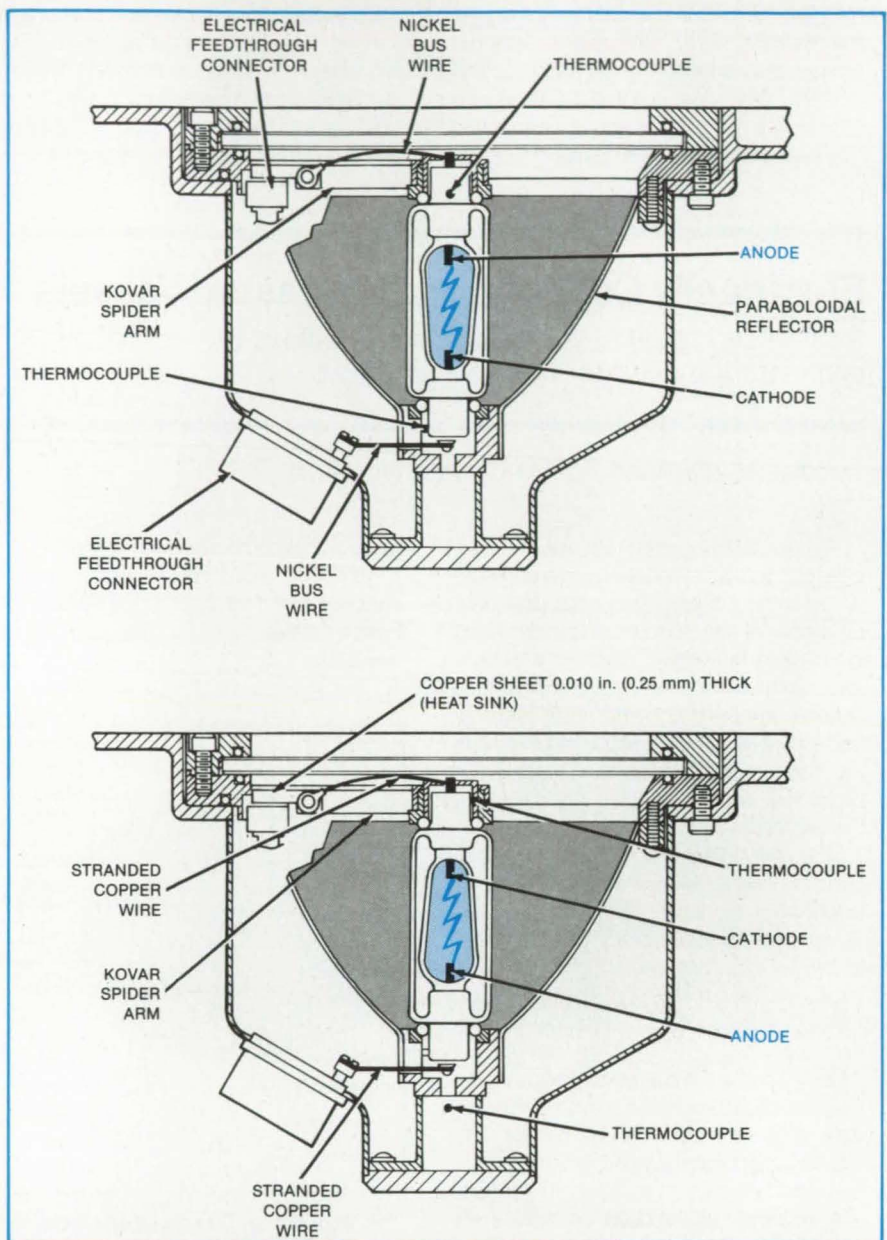
Because of electron bombardment, the anode heats more than the cathode. In the anode-up orientation, the situation is exac-

erated by convection and reflected radiation. After 1 hour of operation, the anode temperature reaches 418° C while the cathode temperature is only 269° C. Since the anode temperature exceeds the allowable maximum of 350° C, the quartz envelope cracks, causing the loss of the gas filling.

For the anode-down configuration, the anode and cathode temperatures stabilize at 333° and 313° C, respectively, after 1 hour of operation. These temperatures are both below the limit for quartz-to-metal seals, and the lamps are able to withstand a 2,000-hour life test with satisfactory light output at the end.

This work was done by John Kiss of ILC Technology, Inc., for Johnson Space Center. For further information, Circle 45 on the TSP Request Card.

MSC-20562



Two Lamp Configurations differ markedly in performance. The anode-up configuration with nickel conductors (above) suffers excessive anode heating with consequent failure of the quartz-to-metal seal. The cathode-up configuration with copper conductors (below) operates within the temperature limit and gives satisfactory light output after 2,000 hours.

Rotary Power Transformer and Inverter Circuit

Noise is lower than with sliprings.

NASA's Jet Propulsion Laboratory, Pasadena, California

A rotary transformer transfers electric power across a rotary joint. The transformer provides an alternative to the sliprings usually used to carry power between rotating bodies. Unlike sliprings, the rotary transformer does not employ sliding contacts; instead, power is transferred by induction across a gap between a primary winding and a rotating secondary winding. There are no wearing contacts, no contact noise, and no contamination from lubricants or wear debris.

A prototype model of the rotary transformer operating at 20 kHz delivered 539 W

with 580 W input (giving an efficiency of 93 percent). With more efficient transistors in the inverter circuit, efficiency could be increased even further. Power ratings of 20 to 50 kW are possible.

The design of the unit was affected by important differences between rotary and conventional transformers. First, the relatively large gap in the magnetic circuit (to allow for eccentricity and dimensional variations in the rotating parts) results in a low primary magnetizing inductance. Second, the large gap results in unusually high leakage inductance. Finally, the bore for the rotating shaft

reduces the efficiency of the core and the copper windings. This means that the rotary transformer requires more copper than does a conventional transformer for the same degree of regulation.

The windings are preferably arranged in a face-to-face configuration (see figure). Ferrite material was selected for the cores because it has low losses at high frequency and is readily machined.

A current-fed inverter supplies power to the primary. At the heart of the inverter is a pulse-width-modulation integrated circuit that controls a pair of power field-effect tran-

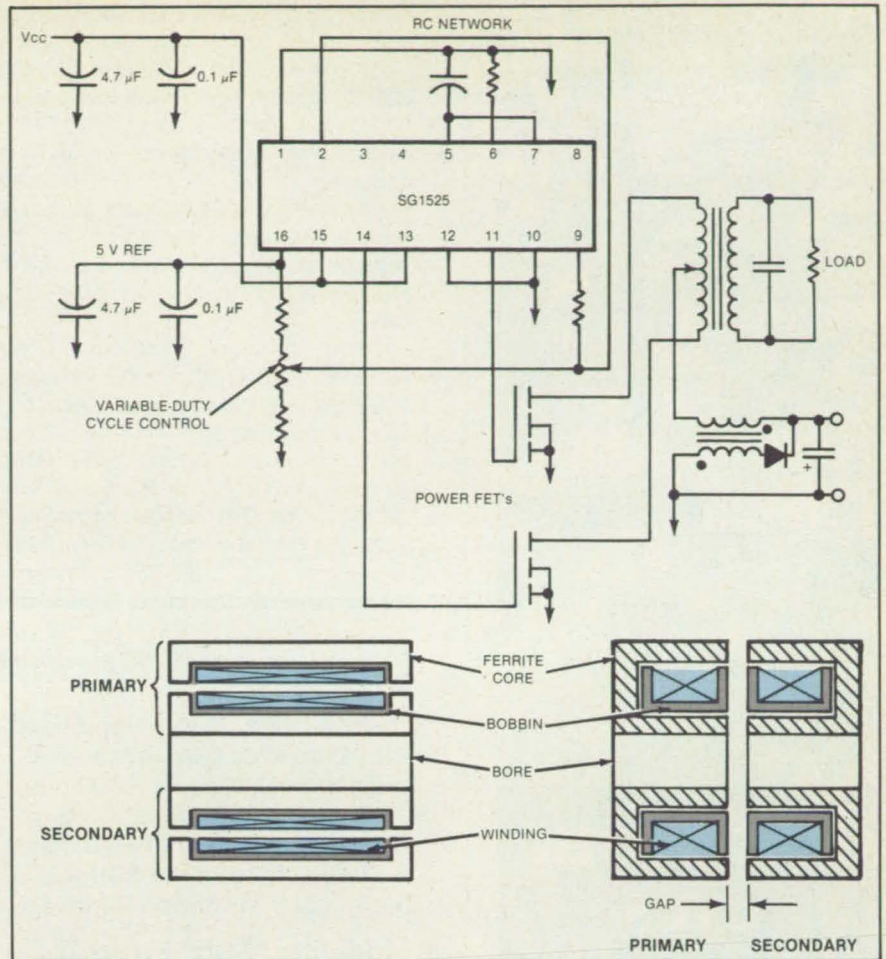
sistors (PFET's), thereby converting direct current into rectangular pulses.

The integrated-circuit output characteristics are well matched to the input capacitance of the PFET's. With an internal voltage reference, comparator, and error amplifier, the integrated circuit provides a readily-variable duty cycle. The duty cycle can thus be adjusted for minimum harmonics in the ac output. The operating frequency of the integrated circuit can be adjusted by an external resistance/capacitance network.

The inverter requires the resonant secondary tank circuit to operate properly. The tank circuit converts the alternating rectangular pulses to sinusoidal alternating current. The gap between primary and secondary of the transformer is used for the inductance of the tank circuit. Because an additional inductor is not required, the size and complexity of the circuit are thereby reduced considerably.

This work was done by Colonel W. T. McLyman and Arthur O. Bridgforth of Caltech for NASA's Jet Propulsion Laboratory. For further information, Circle 26 on the TSP Request Card. NPO-16270

An **Inverter Circuit** provides the input through the primary winding of a transformer, which is fixed. Power transferred across the transformer gap provides alternating current at the output of the secondary winding, which rotates. The insert shows the relationship of the windings for two configurations. The primary and secondary windings are concentric in the configuration at the left.



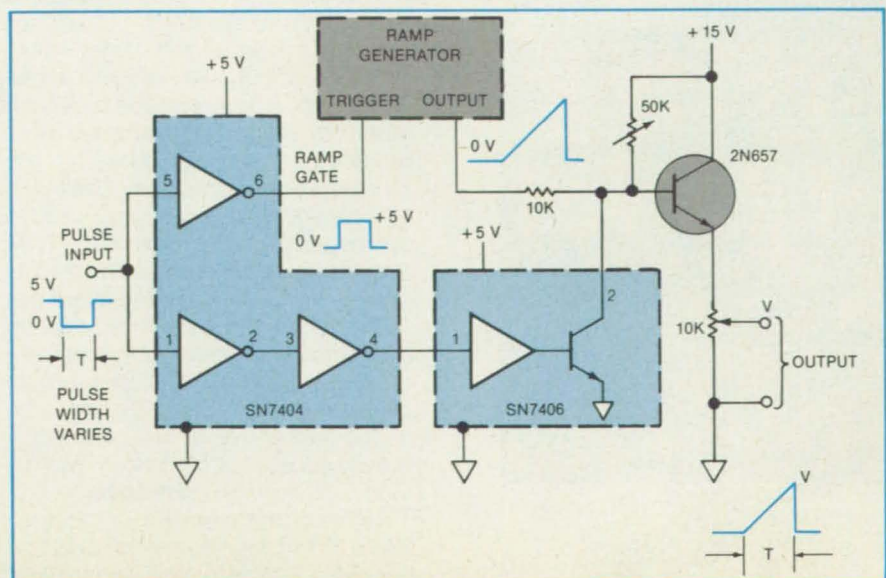
Pulse-Width-to-Analog-Voltage Converter

Peak output voltage varies linearly with input-pulse duration.

Lyndon B. Johnson Space Center, Houston, Texas

A circuit converts pulses of varying widths (as from sound-velocity instrumentation or tachometers) into analog voltages. The peak voltage increases in proportion to the pulse width. This voltage can be used, for example, to drive an x-y plotter or a storage oscilloscope.

The converter circuit (see figure) requires an external ramp generator of the type that is turned on by a positive gating



The **Pulse-Width-to-Voltage Converter** has a peak output voltage that varies with the duration of the input pulses.



With your eyes they could be seen in a different light.

As a Peace Corps volunteer working in a developing country, you could help establish the special programs that can make a big difference for the blind, the handicapped or those with learning disabilities. For further information, call toll-free 800-424-8580. And put your experience to work where it can do a world of good.

U.S. Peace Corps.
The toughest job you'll ever love.

A Public Service of This Publication



pulse and both turned off and reset to zero output when that gating pulse returns to zero. The input pulse from the instrumentation (which is actually an interruption of the otherwise-steady 5-Vdc input) is inverted by part of the SN7404 integrated circuit. The resulting positive pulse serves as the ramp gate. Since the ramp voltage rises linearly with time, the peak ramp voltage just before shutoff is proportional to the duration of the input pulse.

The ramp voltage is fed to the output terminal through an emitter follower. The input pulse is also fed through two cascaded sections of the SN7404 that serve as a noninverting buffer, then through one section of the SN7406 inverting buffer. This provides further control of the emitter-follower base by short-

ing it to ground when the input pulse is absent. This portion of the circuit could probably function without the SN7404 buffers.

The emitter-follower output voltage includes a zero-pulse-width offset voltage that is adjusted by setting a 50-k Ω variable resistor. The proportionality between the ramp rise and the pulse width is determined by setting a 10-k Ω voltage divider, a typical calibration factor being about 1 volt per 100 μ s. The converter is designed to operate with pulse widths of 10 to 250 μ s.

This work was done by Gilbert S. Sosack and Norman E. Simmons of Rockwell International Corp. for Johnson Space Center. No further documentation is available.
MSC-20006

Books and Reports

These reports, studies, and handbooks are available from NASA as Technical Support Packages (TSP's) when a Request Card number is cited; otherwise they are available from the National Technical Information Service.

Modeling "Soft" Errors in Bipolar Integrated Circuits

Mathematical models represent single-event upset in bipolar memory chips.

The physics of single-event upset in integrated circuits is discussed in a theoretical paper. A pair of companion reports present mathematical models to predict the critical charges for producing single-event upset in bipolar random-access memory (RAM) chips.

As the transistors and diodes in integrated circuit (IC) chips become smaller, they become more susceptible to bit errors caused by cosmic-ray particles or alpha particles from radioactive decay. The phenomenon, known as single-particle soft-error generation or single-event upset, occurs because, as IC geometries shrink, the amount of ionized charge that can produce an error diminishes to a single energetic ion.

The problem of how to properly divide the charge from a single-ion track is not a simple one, especially for the complex structure of bipolar transistors. This problem is ultimately part of overall charge-collection computations, which can be done rigorously only with numerical techniques.

Unlike in metal-oxide-semiconductor (MOS) RAM's, the single-event upset in bipolar RAM's has been somewhat neglected

because bipolar RAM's have been more complex. The new bipolar RAM's, as might be expected, are correspondingly complex, involving five or more current generators for a single npn transistor; nevertheless, circuit-simulation (as opposed to numerical-simulation) models for predicting single-event upsets in these RAM's can be run in a few seconds of computer time.

Bipolar transistor structures to be analyzed for single-event upset are modeled on a circuit-simulation computer program called SPICE. The devices and subcircuits in SPICE are used to construct a macromodel for an integrated bipolar transistor. Time-dependent current generators are placed inside the macromodel to simulate charge collection from an ion track.

The models are versatile. They can be adapted to more complex RAM cell structures and varied process parameters (for example, altered diffusion-doping profiles) by simple modifications of the mathematical descriptions of circuits and devices. It is easy to incorporate such features as Schottky-diode-clamped transistors, diffused or ion-implanted resistors with charge-collecting junctions, buried layers (n^+ diffusion in a p-type substrate), and transistors and diodes to aid read/write operations or to bias memory transistors.

This work was done by John Zoutendyk, Reuben Benumof, and Oldwig vonRoos of Caltech for NASA's Jet Propulsion Laboratory. To obtain copies of the reports, Circle 97 on the TSP Request Card.
NPO-16375, NPO-16384, and NPO-16293

NASA Tech Briefs, Summer 1985

Study of Contact Resistances in Integrated Circuits

Techniques are explored in the search for a rapid, reliable test.

The resistances of aluminum/silicon contacts and methods to measure them are the subjects of a NASA report. The study was undertaken to evaluate the nature and reliability of large numbers of semiconductor contacts of the type now being fabricated in integrated circuits.

The first of three main tasks of the study was to develop a yield analysis for series strings of contacts using wafer-level electrical measurements, and to identify different types of faults by visual inspection. Contact resistances were measured by the four-terminal probe technique, in which a known current is forced through two of the four terminals in a set, and the voltage is measured between the other two terminals in the set. A test chip consisting of 7,396 contacts was fabricated on a 100-mm-diameter silicon wafer. The resistances of series strings of from 172 to 2,572 contacts were measured, and each was divided by the num-

ber in the string to arrive at an average resistance per contact.

The measurement results were complicated by photolithographic and mechanical probe problems. Probe errors can be eliminated from the data set by performing resistance measurements between probe pads that are supposed to be strapped together. To characterize randomly-occurring open contacts more effectively, contact-array resistors with many more contacts will have to be used in future studies.

The second main task was to develop wafer-level tests to evaluate the reliability of contact strings. Sensitive techniques are needed to overcome the difficulty of identifying one "bad" or high-resistance contact in a long series string that has a normal value of resistance.

One promising technique is the measurement of the excess contact noise voltage (beyond the thermal noise) that is generated by the conduction process itself when a current is flowing. Another technique might be optical probing in conjunc-

tion with resistance measurements: Since metal is opaque, a metal-to-semiconductor contact resistance should be unaffected by light. Any change in resistance caused by light may reveal a diffusion error in fabrication.

The third main task was to develop a mathematical model for the current flow in contacts and to examine the contact region for evidence of microalloying. An analytical expression based on conformal mapping for one type of contact geometry predicted a contact resistance in good agreement with experimental results. However, electron-microscope pictures of some contacts showed microalloy pits. For these contacts, the interface cannot be modeled as a smooth planar surface for theoretical contact-resistance prediction.

This work was done by Martin G. Buehler, John Lambe, and Stefan F. Suszko of Caltech for NASA's Jet Propulsion Laboratory. To obtain a copy of the report, "LSI/VLSI Contact Resistance Study," Circle 113 on the TSP Request Card. NPO-16248

Scanivalve Corporation: 30 Years of Pressure Scanning Leadership

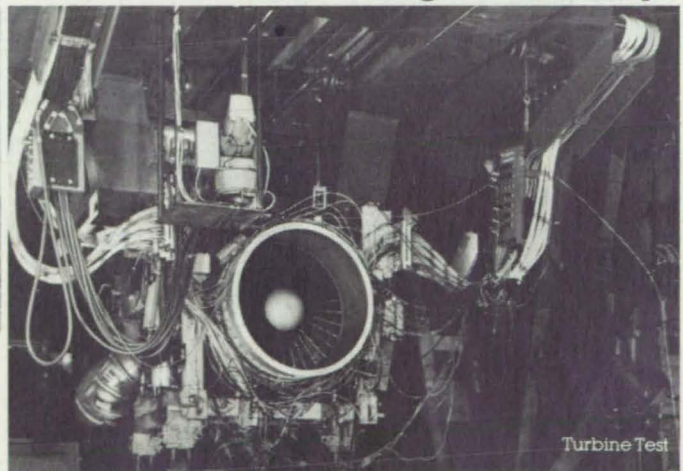


Flight Test



Wind Tunnel Test

Scanivalve Corporation has been the leading supplier of multiple point pressure scanning systems to the most advanced aerospace research facilities for nearly 30 years. Scanivalves are in use worldwide providing 0.06% accuracy while scanning 20 pressures per second for as little as \$50.00 per point. Many of our Scanivalve Systems have been in continuous operation for over 200,000 hours without failure, an outstanding record. Scanivalves are configured to automatically calibrate the transducer during each data scan. This provides the most accurate data possible, while at the same time eliminating the costly down time associated with manual recalibration of multiple dedicated transducers.



Turbine Test

For applications that require very high speed pressure data, Scanivalve Corp. pioneered the design and manufacture of electronic pressure scanners. Features unique to our electronic pressure scanners include integral valving which allows calibration data to be obtained on demand, purging of input lines, and internal leak checks. These systems are capable of scanning up to 50,000 pressures per second, allowing virtually simultaneous pressure data "snap-shots" to be taken at any time during dynamic testing.

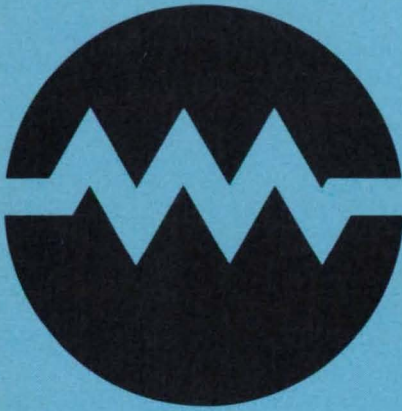
Scanivalve's pressure scanning systems have been imitated, but never equalled. For all of your pressure scanning needs, contact the originator of pressure scanning technology, SCANIVALVE CORPORATION.



Scanivalve Corporation

10222 San Diego Mission Rd / PO Box 20005 / San Diego, CA USA 92120 / (619) 283-5851 / Tlx 695023

Electronic Systems



Hardware, Techniques, and Processes

- 56 Frequency-Discriminating Acoustic-Event Counter
- 58 Online Tester for a Symbol Generator
- 60 Programmable Driver for Voltage-Controlled Oscillators
- 60 Fast Control Sequencer
- 61 Processing of Image Data by Integrated Circuits
- 62 Point Simulator for Synthetic-Aperture Radar
- 63 Airborne Cloud Detector
- 63 Communications Headgear With Protective Features
- 64 Recovering Microwave Cross-Polarization Losses

Books and Reports

- 65 Satellite Time-and Frequency-Transfer System
- 66 Latchup in CMOS Integrated Circuits
- 66 Interferometry Measures Elliptical Satellite Orbits

Computer Programs

- 67 Program Predicts Nonlinear Inverter Performance

Frequency-Discriminating Acoustic-Event Counter

Broadband events are rejected.

Lyndon B. Johnson Space Center, Houston, Texas

An acoustic-event counter discriminates against signals that simultaneously exceed preset amplitude thresholds in both the low- and high-frequency bands of its spectrum. In effect, the counter acts as a spectral analyzer for mechanical vibrations. In combination with a broadband acoustic transducer, it can discriminate between signals and noise in acoustical destructive or nondestructive testing, vibration monitoring for machinery, burglar alarms, and other monitoring/warning systems.

The figure illustrates the principle of operation. The transducer output is fed to an 80- to 160-kHz passband preamplifier. The preamplifier output is fed to a threshold detector that generates raw counting pulses when the signal exceeds the electronic noise by about 8 dB. Each such pulse is considered to denote an acoustic event.

The transducer signal is also fed to a 50- to 1,000-kHz broadband amplifier, the output of which is band-pass filtered at 80 to 160 kHz (the low-frequency band) and 325 to 650 kHz (the high-frequency band). When the low-frequency signal exceeds the noise by about 1 dB, a threshold detector generates a "lockout" pulse, the duration of which is the duration of the event plus 5 ms. The 1-dB threshold assures that there is at least one lockout pulse for every raw counting pulse. When the high-frequency signal exceeds a threshold that is adjustable from the control panel, a 1-ms high-frequency-discrimination pulse is generated.

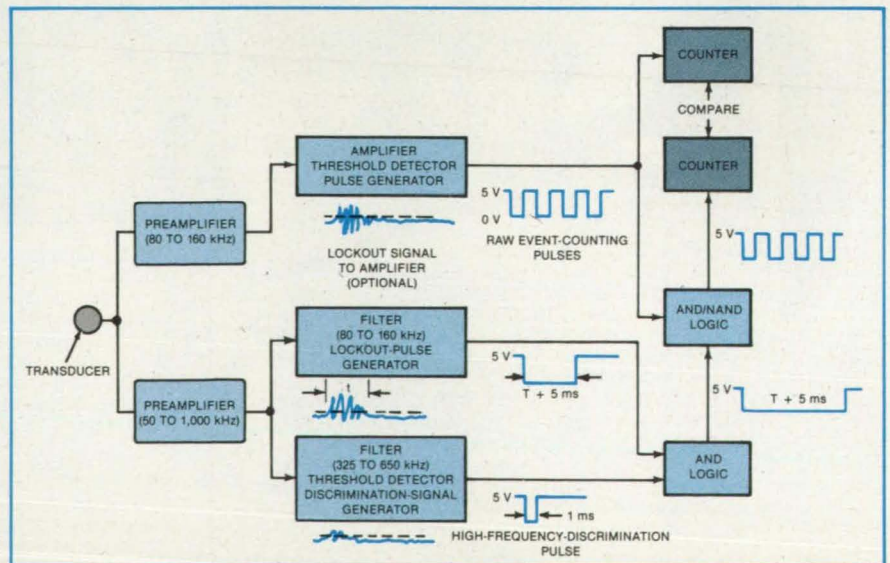
When both the lockout and discrimina-

tion pulses are present (that is, when the signal exceeds both the low- and high-frequency amplitude thresholds), an AND circuit passes the lockout pulse. This pulse is fed to a switch-selectable AND/NAND circuit along with the raw counting pulses. In the AND mode, this circuit generates counting pulses only for those events exceeding both the low- and high-frequency amplitude thresholds. In the NAND mode, it generates counting pulses only for those events that do not have high-frequency components above the threshold.

The raw event count and the AND/NAND output count are compared. In the specific situation for which the counter was designed, a "valid" acoustic event was defined as one for which a raw event pulse is not accompanied by a low- and high-frequency lockout pulse. In general, other applications will call for different passband frequencies, lockout-pulse extension periods different from 5 ms, different amplitude thresholds, and different combinations of simultaneous or sequential pulses to distinguish between "valid" and "invalid" events.

This work was done by Frank E. Sugg and Lloyd J. Graham of Rockwell International Corp. for Johnson Space Center. For further information, Circle 79 on the TSP Request Card.

Inquiries concerning rights for the commercial use of this invention should be addressed to the Patent Counsel, Johnson Space Center [see page 21]. Refer to MSC-20467.



The Frequency-Discriminating Event Counter distinguishes between signals that do and do not contain components that simultaneously exceed preset amplitude thresholds in two frequency bands.

TAKE ON TOMORROW TODAY

At General Dynamic's Convair Division, future technologies begin with the ingenuity of today's finest engineers and professionals. They work for a company that fully understands the two sides of the individual that need to be considered: the professional side and the personal side. One needs the other to satisfy the individual in mind and spirit, to satisfy the Complete Engineer. How do we do it? First, Convair offers tomorrow's most challenging assignments, today. Our team of creative specialists takes on major projects like ground-, air- and sea-launched missiles; vehicles for space launch, orbital insertion and station keeping; aircraft subsystems and energy development.

Then we combine this stimulating atmosphere with the relaxing backdrop of San Diego's sunny beaches and rolling hills. A setting that perfectly complements the fast-paced high technology environment.

We also offer competitive salaries and a highly desirable benefits package designed to help employees realize their personal goals now and for years to come.

If you have the talent to take on tomorrow's advanced technology, and the dedication to see it through, take on one of these opportunities at Convair.

ADVANCED SPACE PROGRAMS

RADAR

You should have a broad background in radar system design and analysis. Knowledge of antenna, transmitter, receiver, and signal processor technologies is essential. You will be responsible for development analysis and validation of advanced radar systems. Bistatic radar experience is desirable. The ability to develop and manage R & D contracts and to communicate complex concepts is required.

SATELLITE DESIGN

You must have experience in conceptual design, development and integration of large complex systems. You will be conducting concept feasibility studies, developing satellite design integrating subsystem equipments and preparing proposals. Experience as a design lead person and in working with subcontractor personnel is desirable. You will be required to assure that satellite designs comply with contractual and systems specifications. You will work closely with Systems Engineering, Design Engineering, Test and Operations, Manufacturing and Product Assurance personnel.

SPACE GUIDANCE & CONTROL-PERFORMANCE

You will have lead responsibility in the performance and coordination of control systems design, stability analysis of continuous and sampled data systems, dynamics analysis and simulation of non-linear systems. Requires M.S. in electrical/electronic, mechanical or aeronautical engineering with control systems major and progressive demonstrated experience in control systems design, dynamic systems modeling and FORTRAN.

SPACE GUIDANCE & CONTROL-CONTROL SYSTEMS

As a senior engineer, you will perform control system and stability analysis of continuous sampled data systems, simulation modeling of dynamic systems, and establish autopilot software requirements. Requires B.S. in electrical, mechanical or aeronautical engineering (M.S. preferred) and progressive demonstrated experience in control systems design and analysis, and software development.

SPACE GUIDANCE & CONTROL-LAUNCH VEHICLES

As a senior engineer, you will develop launch vehicle guidance equations, simulation, accuracy and error analysis, and establish software requirements. Requires B.S. in math, physics or engineering (M.S. preferred) and progressive demonstrated experience in guidance systems development, analysis and software development.

Please send your resume to: Division Vice President — Space Programs, GENERAL DYNAMICS CONVAIR DIVISION, P.O. Box 85357, MZ 11-1342-1967, San Diego, CA 92138.



GENERAL DYNAMICS

Convair Division

Equal Opportunity Employer/U.S. Citizenship Required/Principals Only

Circle Reader Action No. 360

Online Tester for a Symbol Generator

About 95 percent of faults are detected.

Lyndon B. Johnson Space Center, Houston, Texas

A programable instrument periodically checks for failures in a system that generates alphanumeric and other symbol voltages for cathode-ray-tube displays. The tester can be in plug-in modular form, temporarily wired to the generator test points, or permanently wired to these points.

The tester and symbol generator are used with each other, enabling the isolation of a fault to one of five circuit modules that can be replaced in the field. The tester exercises the generator circuits, measuring the excursions of test-point voltages from predetermined acceptable limits. Failures are detected in offset, summing accuracy, translation, rotation, overscan, scale factors, character generation, mode command, and video drive.

Three types of tests — the "zero," "non-zero," and "pulse" tests — are performed by the instrument. These tests require relatively simple circuitry. The zero test, meas-

ures offset, summing accuracy, the absence of video in checking border control, and output scale factors. During the test, the signal from the test point is gated to a pair of comparators (see figure). The comparator references are positive and negative limit voltages set by the controller. The comparator outputs are sampled during the generation of a character, vector, or conic section according to the test control signal. To pass the zero test, the signal must not exceed the positive or negative limit voltages.

The nonzero test is used primarily to verify mode commands and the generation of characters. The basic principle of operation is similar to that of the zero test except that the voltage in question must exceed the limit voltages to pass the test.

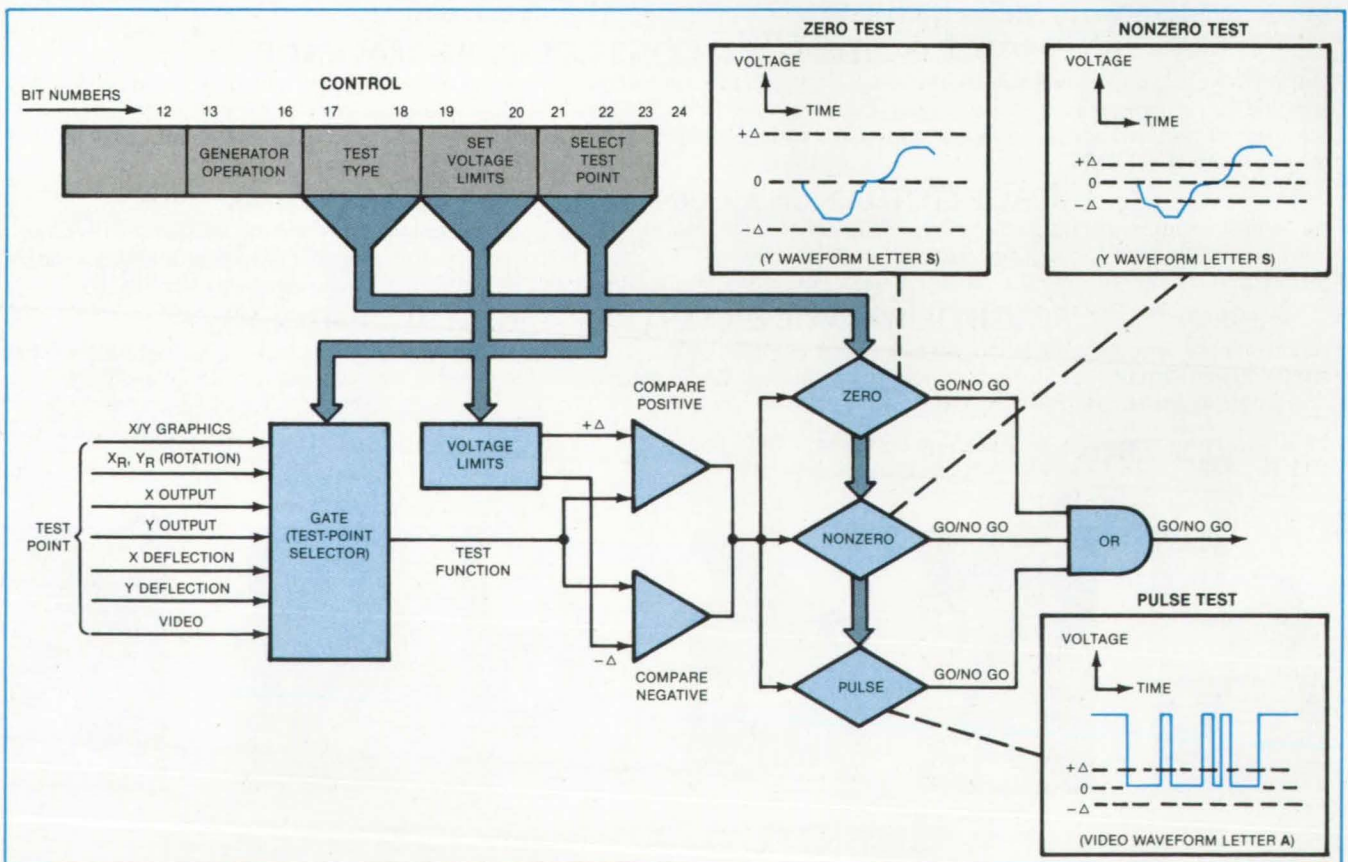
The pulse test is used to detect failures in the video channel. To pass, the tested voltage must exhibit a positive-going crossover at the positive limit voltage and no crossover

at the negative limit voltage.

The test controller is commanded by a 16-bit code-word input signal. Two bits determine the test type (no test, static zero test, static nonzero test, or pulse test). Two bits define the limit voltages, four bits select the gating control, and eight bits designate the operation that the generator is to perform while being tested.

The tester was tested by deliberately introducing faults into the symbol generator. It was able to isolate 95 percent of these faults. The only nondetectable failures occurred in the lowest order bits of the digital-to-analog converters of the symbol generator.

This work was done by Dick Juday and Kyle McConaughy of International Business Machines Corp. for Johnson Space Center. For further information, Circle 81 on the TSP Request Card. MSC-20357



The Symbol-Generator Tester compares gated test-point voltages with predetermined voltage limits while the circuit under test performs the commanded operation. A go/no-go indication is given, depending on whether a test voltage is or is not within its specification.

Engineers
and
Programmers:

INNOVATIVE SOLUTIONS THROUGH TECHNOLOGY.

When Elmer Sperry founded the Sperry Gyroscope Company in 1910 to explore new fields in technology, his achievements made history.

Sperry Corporation is still shaping the history of technology. As one of the most respected names in high technology electronics and a leading supplier of advanced electronic warfare, ship communication/navigation, automated warehousing, and flight simulation systems, we're proud of our continuing success in providing high-quality innovative solutions through technology.

We're looking for mid- and senior-level engineers and programmers skilled in the following areas who share this commitment with us:

ELECTRONIC WARFARE

- Systems Engineering
- EW Digital Systems Engineering
- EW Equipment Engineering
- Signal Processing Engineering
- Artificial Intelligence
- RF Design Engineering
- Communications Engineering
- LANs
- Multibus
- Decision Aids, Display Technology, Human Factors
- Software Design and Development Engineering:
 - Real-time Applications
 - DBMS
 - Operating Systems

- Assembler, FORTRAN, Ada, CMS-2, "C", Ultra 16, Pascal
- Mini and Microprocessor Systems

FLIGHT SIMULATION

- Systems Engineering
- Software Engineering
- R/M Engineering
- Mechanical Engineering
- Electrical Engineering
- Software Quality Assurance Analysis
- Program Management
- Engineering Management
- Program Control Administration
- Sr. Contracts Administration
- Marketing

LOGISTICS

- Provisioning Engineering
- Inventory Management Services
- Repair/Spares Procurement
- Data Base Procurement
- Data Base Administration
- Computer Systems Analysis
- TRIDENT/POSEIDON Fleet Ballistic Missile Program
- Maintenance Planning
- Automated Warehouse Systems
- COBOL/MIS Programming
- Microprocessor Software/Pascal
- Software/Hardware Documentation

SOFTWARE ENGINEERING AND SHIP SYSTEMS

- Combat Systems Integration and Design Engineering

- Shipboard Communications
- Real-time Command and Control Systems:
 - AN/UJK-20
 - AN/UJK-44
 - Unix-based HP-9020A/M-68000 Microprocessors, SEL, DEC-VAX 11/780
- CMS-2, Ultra-16, "C", and FORTRAN

We also have opportunities for professionals in various engineering disciplines, program management, technical writing, technical support and more.

Positions require a BS degree in a technical field.

Our ideal location in Reston, Virginia, is only 18 miles from downtown Washington, D.C., and a thirty-minute drive from the Blue Ridge Mountains. Here, you'll have access to both the cosmopolitan amenities of our nation's capital and the natural beauty of the Shenandoah Valley.

If you'd like to forge new solutions through technology, contact Sperry today. Please send your resume in complete confidence to:

**SPERRY CORPORATION
SYSTEMS MANAGEMENT GROUP**
12010 Sunrise Valley Drive, Dept. N700
Reston, Virginia 22091
(703) 620-7000

An equal opportunity employer, M/F/H/V.
U.S. citizenship required.



Programable Driver for Voltage-Controlled Oscillators

An electronically programmable integrated circuit allows output waveforms to be custom designed.

NASA's Jet Propulsion Laboratory, Pasadena, California

An electronically programmable read-only memory (EPROM) and a digital-to-analog converter provide a customized time-varying voltage for frequency modulation. The voltage is used to modulate an IMPATT oscillator that in turn serves as a microwave pump for a solid-state maser in a low-noise amplifier. The EPROM makes it a simple matter to tailor the voltage waveform to suit the characteristics of a given maser. The digital information for the waveform is programmed into the EPROM chip; the digital-to-analog converter reads the information and produces a corresponding analog wave. The principle can be readily adapted to other applications.

The EPROM and converter circuit (see figure) can be controlled and monitored externally by a computer through parallel ports. It can be programmed to hold a particular output or to sweep over the entire output range or any portion of it.

The circuit provides a periodic voltage ranging in amplitude from 0 to 10 V with 12-bit resolution. Its full-range output is symmetrical about one-half the total period. The symmetry is achieved by having a 12-bit up/down counter count up continuously from a low value (the low voltage limit) to a high value (the high voltage limit) and then reversing direction until the low limit is again reached. The linear digital sweep produced by the counter is used to address the

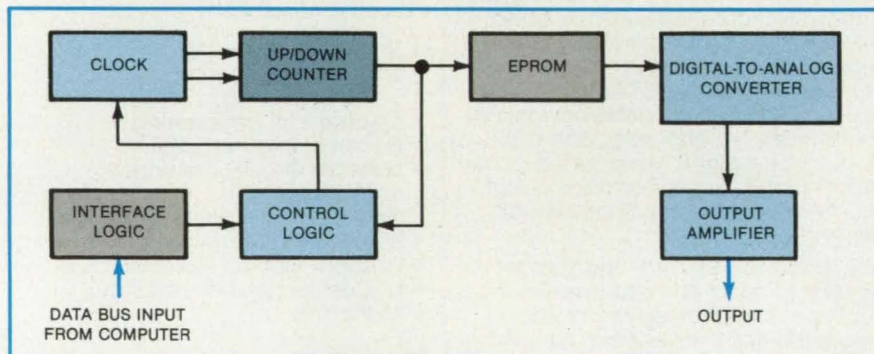
EPROM, the output of which is then presented to the digital-to-analog converter. (The output can be held constant, if required, by setting the high limit and low limit equal to each other.)

A clock signal is generated by a Schmitt-trigger oscillator and is buffered by another Schmitt trigger. This signal is steered by the counter-control logic so that it provides countup and countdown clock signals for the binary counter. The clock frequency is 2 MHz, which, at 32 points per period, yields an output frequency of 62.5 kHz.

The binary up/down counter consists of three 4-bit presettable counter chips, cascaded with the clear inputs disabled. Two

EPROM chips are addressed in parallel. The combination produces 16 bits of output data. Since the digital-to-analog converter is a 12-bit device, four of the data lines from the second EPROM chip are not used. The digital-to-analog converter has an integral sample-and-hold circuit to minimize the effects of switching transients. Two operational amplifiers serve as level shifters and buffers at the output. Two potentiometers allow adjustment of offset and gain.

This work was done by Larry E. Fowler and John A. McNeil of Caltech for NASA's Jet Propulsion Laboratory. For further information, Circle 102 on the TSP Request Card. NPO-16364



An External Computer Sends Commands via a bus to control logic, which operates a clock and up/down counter. The circuit can function as a custom driver for voltage-controlled oscillators in test instrumentation as well as in equipment for space communication.

Fast Control Sequencer

Unit is faster than conventional circuits and contains fewer integrated circuits.

NASA's Jet Propulsion Laboratory, Pasadena, California

A "nanosequencer" controller for digital logic systems is faster and simpler than conventional microprocessor-based, or "microsequencer," controllers. The new unit employs an assembly language, dedicated programs, and read-only memories (ROM's) specially designed for logic control.

Nanosequencers of any size can be built, but the prototype unit is a 32-instruction version — probably the minimum practical

size. The unit operates at a 20-MHz data rate and requires fewer than 10 medium-scale-integration chips. It has eight input status lines and eight output control lines. It is several times as fast as typical microsequencers and uses about half as many chips.

The nanosequencer lacks certain capabilities of a microsequencer. It does not have an integral repeat counter for looping, but a repeat counter can be added readily if

needed. It does not accommodate subroutines, but subroutines are not needed in most applications. Longer nanosequencer programs can be implemented: In fact, one called Stretch, capable of 256 instructions, has already been developed.

The purpose of the nanosequencer is to operate the output control lines in a systematic way based on the condition of the output status lines (see figure). The sequencer

selects the next instruction to be loaded into a pipeline register and then executed. The steps in an instruction cycle are as follows:

- Strobing an instruction into the pipeline register;
- Selecting the appropriate status line and storing its state in a status latch; and
- Selecting the next instruction from the program in memory.

During this sequence, the instruction currently in the pipeline register is being executed in the external circuitry.

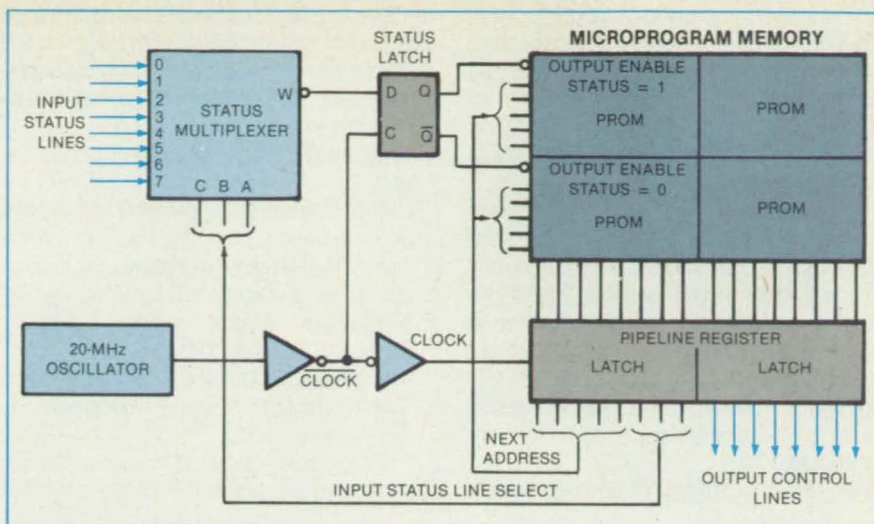
A microprogram memory stores the program to be executed. The memory consists of four bipolar programmable ROM chips. Each chip is a 32-by-8-bit memory with a 12-nanosecond access time. For fast operation, the status bit drives the output-enable pin on each chip.

The pipeline register stores a microinstruction while it is being executed. The left-most chip contains information about the next instruction to be selected. The right-most chip contains the instantaneous states of the output control lines.

A status multiplexer selects the status line, the state of which is to be sampled for conditional instructions. The eight-line multiplexer requires 3 bits of the microinstruction to select one out of eight status-line inputs.

The status latch stores the state of the sampled status input. The latch applies the state to the microprogram memory to complete the selection of the next instruction.

The first 5 bits from the pipeline register



The Fast Logic Controller accommodates three delays before the second half cycle of the clock signal strobes the status latch. First, the outputs of the pipeline register must settle. Second, the selected input status line signal must propagate through the status multiplexer and arrive at the status latch. Third, it takes 3 nanoseconds for the status latch to be set up before it is strobed. During the second half cycle, the output-enable line produces the next instruction and applies it to the pipeline register.

are used to select the next instruction from memory and are then fed back to the address lines of the memory chips. One instruction is stored in the upper-two programmable ROM's, and another quite-different instruction may be stored in the lower-two programmable ROM's. The final decision as to which one is used is based on the status bit.

This work was done by Charles R. Lahmeyer of Caltech for NASA's Jet Propulsion Laboratory. For further information, Circle 36 on the TSP Request Card.

Inquiries concerning rights for the commercial use of this invention should be addressed to the Patent Counsel, NASA Resident Office-JPL [see page 21]. Refer to NPO-16116.

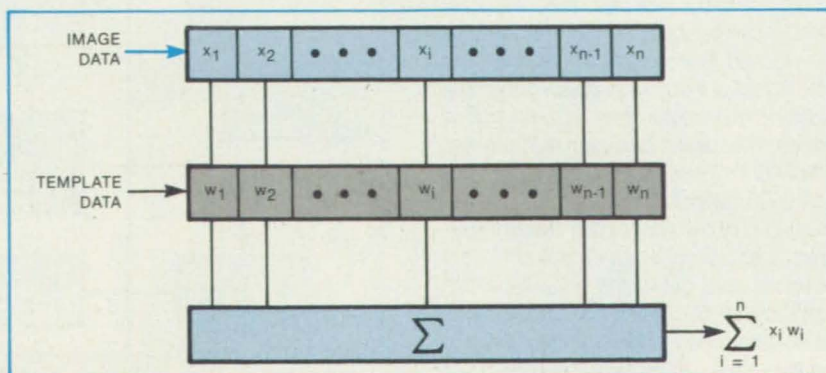
Processing of Image Data by Integrated Circuits

Sensors would be combined with logic and memory circuitry.

NASA's Jet Propulsion Laboratory, Pasadena, California

An image-processing circuit using VLSI technology would provide output signals representing the positions of objects. The circuit could be used for controlling robots, medical-image analysis, automatic vehicle guidance, and precise pointing of scientific cameras.

The circuit concept employs charge-coupled devices (CCD's) for sensing the image of an object. The video data from the CCD's are operated on to obtain a "signature" — a characteristic data pattern that identifies an object and greatly simplifies further data processing. Signatures could be produced by one or more of the known techniques of feature extraction; for example, edge detection, spatial-frequency filtering,



The Cross-Correlation of Two Inputs would be accomplished by a transversal filter like this one. For example, the position of an image would be taken to be the point where the image and template data yield the maximum value of the correlation function.

or image-area moments. The output from video processing is passed to a data processor in the circuit, which determines the position, identity, shape, or other feature of the object. The circuit may have to produce individual signatures for several objects in its field of view.

For example, signatures determined from the projections of an image along the two principal axes of a scene are particularly useful in determining location. The CCD's form a two-dimensional array of discrete elements. Taps that sense charge without destroying it are positioned under the CCD elements. The taps form both horizontal and vertical signatures in only two shift operations.

The relative position of an image within

the sensor field of view may be determined in one of several ways, depending on the complexity of the scene. In a simple scene containing only one object against a plain background, the image position may be computed by area-moment techniques. Essentially, the image intensity (in terms of the charge in each CCD element) is weighted by its distance from the midpoint of the scene. The weighted signature data in each quadrant of the scene are summed. By subtracting left-half sums from right-half sums, the horizontal position is determined. Similarly, by subtracting the bottom-half sums from top-half sums, the vertical position is determined.

Object locations in a scene containing more than one object can be done by tem-

plate matching via correlation. Image data are correlated with template data, point by point, until a maximum correlation is achieved (see figure). The template data are in the form of signatures and may be stored in the circuit or generated from the video data from the first frame of a tracking sequence. The template signatures are correlated against the scene signatures. The correlation produces an error signal that can be used to drive a control system so that the image remains at, or goes to, the desired position.

This work was done by Robert W. Armstrong of Caltech for NASA's Jet Propulsion Laboratory. For further information, Circle 9 on the TSP Request Card. NPO-15059



Point Simulator for Synthetic-Aperture Radar

Reflection from a point target is imitated electronically.

NASA's Jet Propulsion Laboratory, Pasadena, California

A signal generator simulates the synthetic-aperture-radar (SAR) return from a point target. Designed to test integrated optical SAR receivers, the simulator applies the phase modulation necessary to turn a radio-frequency pulse train into the electronic equivalent of an unfocused radar image of the target.

Approximating the range delay as a constant, the desired simulated return signal is a carrier amplitude-modulated by pulses and frequency-modulated by the relatively slow Doppler shift. The frequency modulation is linear with time, corresponding to a phase modulation that varies quadratically with time. The phase modulation is also proportional to the square of the velocity along the track and to the inverse of the range.

The simulator (see figure) includes a 10-MHz master oscillator, the output of which is divided by 2×10^4 to obtain a phase-locked pulse clock at 500 Hz. This clock signal controls the pulse generator, which generates rectangular pulses of 16.6 ns duration. The master-oscillator signal is also multiplied in frequency by 6 to obtain a 60-MHz phase-locked carrier.

A read-only memory circuit stores the required quadratic phase-shift function. This function is read out at the pulse-repetition frequency of 500 Hz and applied to a digitally-controlled phase shifter, thereby modulating the carrier with the slow quadratic phase shift (linear frequency shift).

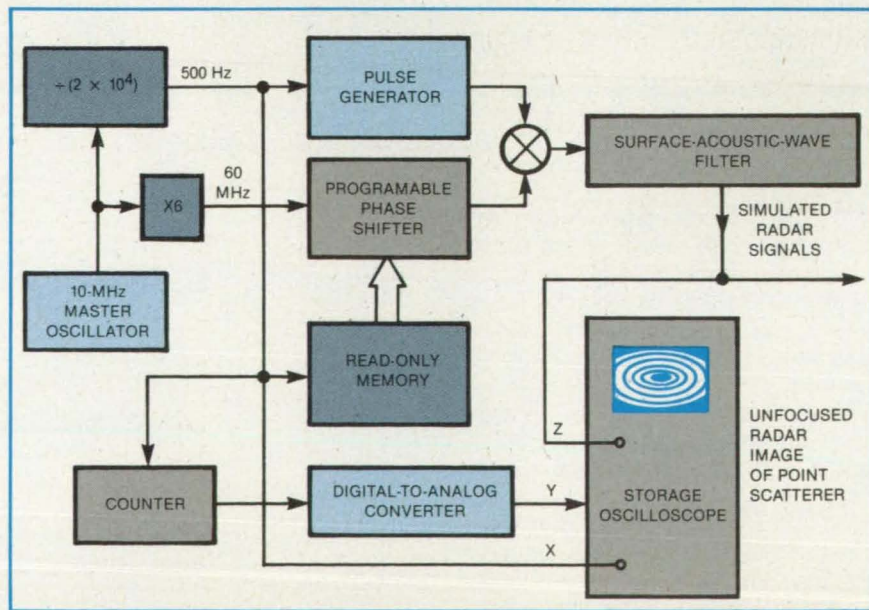
The 16.6-ns pulses are mixed with the frequency-modulated carrier. Since each

pulse has approximately the duration of only one carrier cycle, the mixer produces a wideband output that is dispersed in a surface-acoustic-wave (SAW) device: Each pulse is spread out to $6 \mu\text{s}$ in duration and to the range of 50 to 70 MHz in frequency. This SAW output is the simulated radar return.

In addition to applying the signal to the circuit under test, the signal is displayed in the simulator. It is mixed to baseband and used to modulate the intensity of an oscillo-

scope. The horizontal sweep is triggered by the pulse clock, while the vertical sweep is triggered by a slow ramp that corresponds to the slow phase shift induced by the along-track motion.

This work was done by Demetri Psaltis, Michael W. Haney, and Kelvin H. Wagner of Caltech for NASA's Jet Propulsion Laboratory. For further information, Circle 42 on the TSP Request Card. NPO-16296



This SAR Simulator produces an amplitude- and phase-modulated 60-MHz signal that resembles the SAR return of a point scatterer.

Communications Headgear With Protective Features

An uncomplicated, inexpensive intercom protects head, face, and hearing.

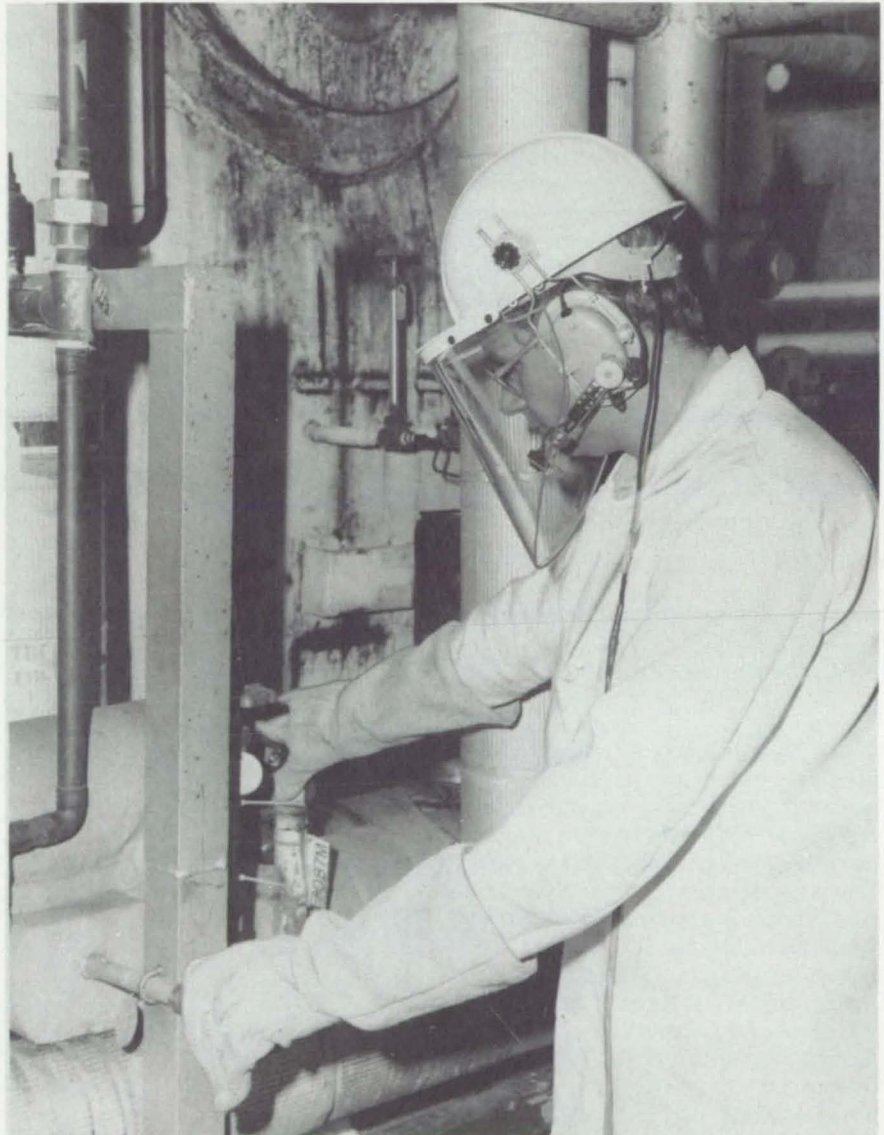
Langley Research Center, Hampton, Virginia

A need exists for a lightweight, portable device such as a sound-powered telephone or headset radio to allow communications between personnel in a central control area and those at remote working stations. This requirement is often complicated by the fact that in remote working areas (typical of many Langley Research Center facilities, for example, and many industrial situations), there may be high levels of background noise or hazardous conditions, generating additional requirements for head protection (helmet), face shield, ear protection, and sometimes even special clothing. This complex mix of requirements with use of existing equipment often renders the wearer relatively ineffective in his work.

The adaptation of a highly suitable stock helmet and face shield unit to a stock intercom headset (see figure) has provided an ideal unit, allowing the wearer total use of the hands and body while protecting the head, face, and hearing. The unit allows the wearer to work effectively, efficiently, and safely while communicating from remote areas that require special precautions.

This unit can be used at any facility for activities where both communication and protection are desired, such as wind tunnel operations, chemical handling, mining, blasting, and military uses. The possible applications are virtually limitless. The total cost of fabricating the unit shown, using stock parts and including labor, was less than \$100.

This work was done by Stanley Wade Ward of Langley Research Center. No further documentation is available.
LAR-13156



An Intercom Integrated Into Protective Headgear gives its wearer complete freedom of the hands. The unit is made from commercially available components.

Airborne Cloud Detector

Bonded to the aircraft skin, it facilitates cloud avoidance.

Langley Research Center, Hampton, Virginia

An airborne cloud detector consists of three major components: An aluminum patch durably bonded to the aircraft skin, a surge arrester, and a dual-sensitivity charge-rate amplifier. Its operation is

based on the fact that aircraft surfaces become charged when ice or water particles strike them.

The cloud detector was originally developed for use on commercial transport air-

craft that will use laminar flow control (LFC) to reduce drag and fuel consumption (by up to 25 percent). Flight tests have demonstrated that laminar flow is lost when an aircraft encounters cirrus clouds.

To realize optimal laminar flow effectiveness, it is desirable to detect cirrus clouds and to fly LFC aircraft around them. It is easy to avoid clouds when they are visible. The instrument detects subvisible clouds in daylight and all unseeable clouds at night.

The fabrication/bonding technique utilized for the new system allows the charge patch to be located on virtually any leading edge surface of an aircraft (not limited to plastic radomes, for example), and, because of the use of aircraft-quality aluminum, it is highly durable. At the input to the charge rate amplifier, the current developed by particle impingement on the patch is loaded by a combination of a 100-k Ω resistor and the input impedance of the amplifier. This load converts the charge current to voltage. In order to provide a wide input dynamic range and to allow for ranging to suit the flight environment, the amplifier has two separate gain-adjustable output channels.

The surge arrester and a bipolar Zener diode network prevent damage to the amplifier by direct lightning strikes or other electrical discharges that could result from a high potential difference between the patch and the aircraft. A similar Zener diode network in the output circuitry limits the magnitude of the signals going to the pulse code modulation (PCM) data-recording system of the test aircraft. Appropriate filtering prevents aliasing errors in the PCM system and precludes radio-frequency interference.

The detector was installed on the Langley Research Center F-106B storm-hazards research aircraft, and 13 missions were flown. Ten were thunderstorm flights, two were miscellaneous, and one was cirrus (ice-cloud) dedicated. For the first 12 missions, the amplifier gain was set for full-scale sensitivities of $\pm 25 \mu\text{A}$ (coarse sensitivity) and $\pm 1 \mu\text{A}$ (fine sensitivity).

The thunderstorm missions success-

fully demonstrated the feasibility of the device. Charge currents exceeding $25 \mu\text{A}$ were detected in heavy rain and thunderclouds, but detection of thin cirrus was more difficult. To detect light cirrus, the sensitivities of the two channels were increased to $\pm 2 \mu\text{A}$ and $\pm 0.25 \mu\text{A}$ full scale, respectively. The cirrus-dedicated mission was then flown, and excellent, well documented results were obtained, with even thin cirrus being detected.

Using the increased gain sensitivities, the cloud-particle detector is a reliable, noise-free, low-cost, high-sensitivity indicator of the type of clouds that will cause the most problems for LFC aircraft at cruise altitude.

This work was done by Richard E. Campbell and John P. McPherson of Langley Research Center. For further information, Circle 21 on the TSP Request Card.
LAR-13137



Recovering Microwave Cross-Polarization Losses

Reception is improved by adding a normally discarded portion of the signal.

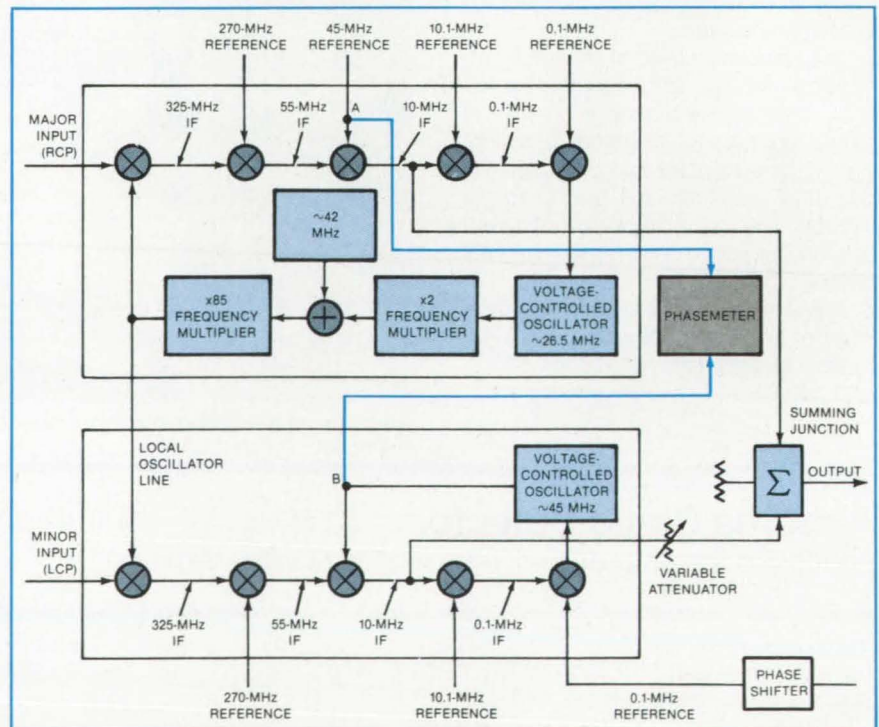
NASA's Jet Propulsion Laboratory, Pasadena, California

A signal-enhancement circuit makes it possible to recover a cross-polarized component of a radio signal and add it to the main signal. Heretofore, the cross-polarized component had to be discarded as a loss. The recovered cross-polarized signal is applied in phase to a summing junction to enhance the main signal.

In microwave communication, there is inevitably a small signal loss due to polarization conversion, primarily caused by imperfections in antenna and feed systems. For example, at a microwave station transmitting a nominally right circularly polarized (RCP) signal, there will also be a low-level left circularly polarized (LCP) signal. With the new circuit, the low-level signal can be used at the receiver to augment the main signal.

The signal coming into the receiving antenna is separated in an orthomode transducer into the primary RCP signal and the low-level LCP signal (see figure). The RCP signal is applied to a long phase-locked loop channel comprising a mixer, a phase detector, a voltage-controlled oscillator, and a frequency multiplier. The frequency multiplier provides a coherent first-local-oscillator signal for both receiver channels.

The LCP signal is applied to a channel with a short loop comprising a phase detector, a voltage-controlled oscillator, and a mixer.



For Signal Enhancement, major and minor signals are combined in slaved closed-loop receiver channels. Both receiver channels are served by a common local oscillator that is controlled by a phase-locked loop in the main channel. The 10-MHz intermediate-frequency (IF) signals of the channels are coherently summed. For polarization tracking, a phasemeter is added to measure the phase difference between points A and B.

This channel has an extremely narrow bandwidth so that it tracks the phase of the LCP component. The LCP channel can thus be kept phase coherent with the primary channel for summing in a summing junction. The signals presented to the summing junction must be adjusted in amplitude and phase to provide the optimum signal-to-noise ratio. This can be accomplished with a phase shifter in one of the 0.1-MHz reference inputs and a variable attenuator in one input to the summing junction as shown in the figure.

The signal-enhancement circuit can be adapted readily to serve as a polarimeter. It measures the phase differential between the primary RCP signal and the low-level LCP signal and thus tracks the polarization of the almost-circularly-polarized received signal. For this purpose, a phasemeter is inserted between the 45-MHz reference in the RCP channel and the narrow-band cross-polarization tracking loop (points A and B in the figure). The changes in phase at these points indicate the changes in the instantan-

eous polarization angle of the received signal. The value can be displayed on the phasemeter and read out for further processing. With appropriate calibration, the absolute value of the received polarization angle can also be determined.

This work was done by Boris L. Seidel, Charles T. Stelzried, and John E. Ohlson of Caltech for NASA's Jet Propulsion Laboratory. For further information, Circle 11 on the TSP Request Card. NPO-15353, NPO-15354, and NPO-15803.

Books and Reports

These reports, studies, and handbooks are available from NASA as Technical Support Packages (TSP's) when a Request Card number is cited; otherwise they are available from the National Technical Information Service.

Satellite Time- and Frequency-Transfer System

Time would be synchronized at distant points within a nanosecond.

A report available on request describes a satellite-borne time- and frequency-transfer system proposed for the synchronization of clocks at stations around the Earth. An orbiting hydrogen-maser clock and frequency standard would communicate by microwave links with Earth stations that use hydrogen masers as local clocks. A pulsed-laser time-transfer subsystem could also be operated concurrently, either synchronized or unsynchronized with the microwave subsystem.

The microwave and laser techniques have been proven in experiments on frequency and time shifts due to relativistic/gravitational effects. The microwave subsystem includes a two-way up/downlink and a one-way downlink at frequencies of approximately 2,118, 2,300, and 2,203 MHz, respectively. With this choice of frequencies, the combined ionospheric dispersion of the two-way link is just twice that of the one-way link and can be cancelled in subsequent frequency-difference processing at the ground terminal.

The two-way link measures the path delay between the ground and orbiting terminals and provides the reference for first-order Doppler cancellation. The 2,118-MHz uplink carrier is subjected to 90° phase modulation under the control

ATLANTIS SECURITIES CORPORATION

11100 E. BETHANY DRIVE
SUITE 4030
AURORA CO 80014
(303) 695-6890 or (800) 821-5250

offers classic investment banking services as well as a variety of other financial services.

For further information on Atlantis Securities, including ground-floor investment opportunities, simply complete the form below.

We maintain markets in emerging growth companies, such as Cellular Radio Systems Inc. and U.S. International Trading Co. Inc, who are involved in space-related activities.

Kindly indicate your investment objectives by checking the services which interest you most.

I am interested in the following:

- | | |
|--|--|
| <input type="checkbox"/> Limited Partnerships | Name _____ |
| <input type="checkbox"/> Private Placements | Address _____ |
| <input type="checkbox"/> IRA, Keough | City _____ State _____ Zip _____ |
| <input type="checkbox"/> Corporate Retirement Plan | Phone _____ |
| <input type="checkbox"/> Bonds, Mutual Funds | |
| <input type="checkbox"/> Life Insurance, Annuities | |
| <input type="checkbox"/> Income Stocks | <input type="checkbox"/> Precious Metal Stocks |
| <input type="checkbox"/> High Tech Stocks | <input type="checkbox"/> New Issues |
| <input type="checkbox"/> Oil Stocks | <input type="checkbox"/> Other (specify) _____ |

of a pseudorandom-noise (PRN) generator. At the orbiting terminal, the PRN modulation is extracted from the received uplink signal and applied to the 2,300-MHz downlink signal.

At the ground station, the digitally-delayed uplink PRN modulation is coupled in a closed-loop tracking arrangement with a time discriminator to automatically lock onto and track the delay between the uplink and downlink PRN code sequences. Divided by 2, this gives the one-way path delay used in determining the time difference between the orbiting and ground-station clocks.

The 2,203-MHz downlink is modulated by the same PRN sequence. The time difference between the orbiting and ground-station clocks plus the one-way path delay are measured at the ground station similarly to the two-way path delay by tracking the time difference between the one-way downlink received and the uplink modulating PRN sequences. The apparent time difference between the orbiting and ground clocks is calculated by subtracting half the two-way path delay from the one-way time-difference measurement, then further subtracting relativistic/gravitational effects during data reduction.

The pulsed-laser technique has been used to make time comparisons between clocks on Earth and clocks in a high-altitude aircraft. The time of arrival of the laser-light pulse at the moving station is compared with the assigned arrival time as it would be measured on the Earth-station clock. The two-way path delay of the light pulse reflected back to the Earth station (by a cube-corner reflector) is also determined. The one-way path delay, atmospheric delay, and relativistic/gravitational effects are subtracted as in the microwave subsystem.

This work was done by Robert F. C. Vessot, Hays Penfield, and Edward Mattison of the Smithsonian Institution Astrophysical Observatory for Marshall Space Flight Center. To obtain a copy of the report, Circle 108 on the TSP Request Card.

Inquires concerning rights for the commercial use of this invention should be addressed to the Patent Counsel, Marshall Space Flight Center [see page 21]. Refer to MFS-25991.

Latchup in CMOS Integrated Circuits

Sensitivity to ion beams is studied.

The latchup effect is the subject of a paper presenting the results of testing 19

types of complementary metal-oxide semiconductor (CMOS) chips from six manufacturers. The npnp structures formed by the parasitic pnp and npn transistors on a CMOS chip constitute silicon-controlled rectifiers (SCR's). Under certain bias conditions, these SCR's may be turned on by electric transients, ionizing radiation, or merely a single heavy ion and are said to be "latched" up. In this state, a chip may malfunction or burn out.

The report gives details of the sensitivity of the chips to latchup caused by argon and krypton ion beams. It identifies the parasitic npnp paths and provides a latchup cross section and a qualitative explanation of latchup sensitivity for each chip type.

The chips vary in complexity from a simple gate to read-only memories and random-access memories. They were made by many CMOS processes including metal-gate bulk, silicon-gate bulk, silicon-gate bulk with closed-circuit logic (C²L), silicon gate with silicon on sapphire, silicon-gate bulk with an epitaxial layer, and radiation hardened with a guard-banded transistor.

The circuit samples were delidded and placed in a vacuum chamber where they were exposed to the ion beam at normal operating bias and room temperature. The samples were on a board that allowed the beam to impinge on only one sample at a time. The board could be tilted to alter the angle of incidence of the beam with the chip: The angle is important because it affects the amount of charge that is deposited within the sensitive volume of the device.

With krypton ions at an energy of 120 MeV, the beam intensity was increased (up to a limit of 10⁶ ions/cm² until latchup occurred. Six of the chips latched up. One of these was a silicon-gate-bulk device with a very small geometry (gate length of 6 μm). This chip will be highly susceptible to latchup in space, but could be equipped with a supply-current sensor that would turn off the power for a few seconds to prevent damage as soon as latchup occurs. Silicon-on-sapphire chips are the least sensitive because they contain no parasitic transistors — the n islands are separated from the p islands by the sapphire substrates.

This work was done by Kamal A. Soliman and Donald K. Nichols of Caltech for NASA's Jet Propulsion Laboratory. To obtain a copy of the report, "Latchup in CMOS Devices From Heavy Ions," Circle 70 on the TSP Request Card. NPO-16304

Interferometry Measures Elliptical Satellite Orbits

Very-long-baseline interferometry offers advantages over conventional Doppler measurements.

A conference paper shows the feasibility of using data from very-long-baseline interferometry (VLBI) to locate and predict the motion of satellites in highly elliptical orbits about the Earth. The VLBI data are obtained from the Deep Space Network. The data not only improve navigation accuracy but also can be acquired with less use of the worldwide network of ground stations.

The VLBI technique uses two or more widely separated tracking stations to receive a signal broadcast by a beacon aboard the satellite. Cross-correlation of the received signals provides a precise measure of the differential time delay for wide-band signals and the rate of change of time delay for narrow-band signals. By alternate tracking of the satellite and a nearby extragalactic radio source of known location, such as a quasar, a doubly differenced one-way measurement (ΔVLBI) can be made. This measurement is insensitive to major error sources common to each downlink.

The report describes the navigation accuracy improvements possible with VLBI and ΔVLBI data. It presents preferred VLBI data-acquisition methods for achieving optimum navigation and minimizing antenna use. It examines the sensitivity of VLBI navigation accuracy to the orientation of the antenna baseline relative to the orbit plane. It also examines the effects of such major error sources as uncertainties in the mass of the Earth, gravitational harmonics, and atmospheric drag.

The report concludes that wideband ΔVLBI measurements taken near periapse yield the best results, determining the apoapse position of a scientific satellite at an altitude of 17.7 Earth radii within 285 meters. Overall, the VLBI measurements yield results at least as accurate as those of conventional Doppler measurements yet at substantially reduced time required for antenna use.

This work was done by Raymond B. Frauenholz and Jordan Ellis of Caltech for NASA's Jet Propulsion Laboratory. To obtain a copy of the conference paper, "Orbit Determination of Highly Elliptical Earth Orbiters Using VLBI and ΔVLBI Measurements," Circle 109 on the TSP Request Card. NPO-16313

Computer Programs

These programs may be obtained at a very reasonable cost from COSMIC, a facility sponsored by NASA to make raw programs available to the public. For information on program price, size, and availability, circle the reference number on the TSP and COSMIC Request Card in this issue.

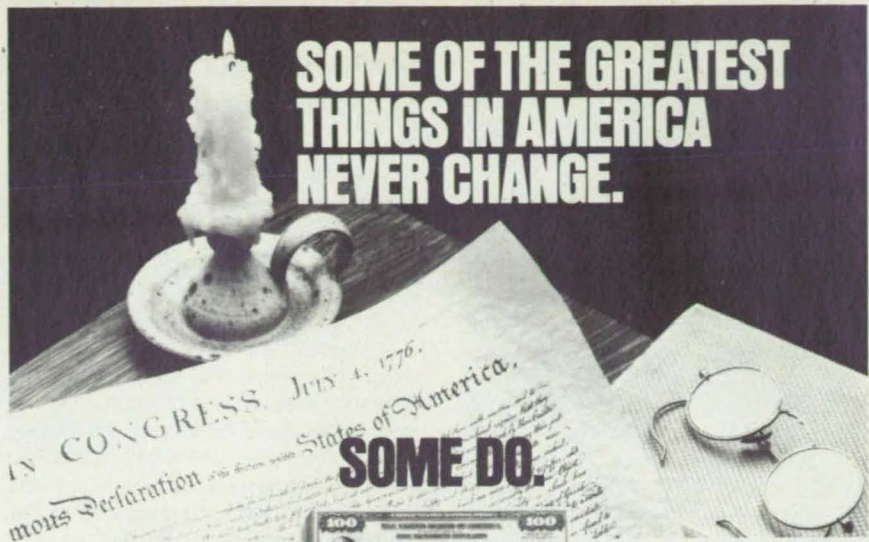
Program Predicts Nonlinear Inverter Performance

A mathematical model simulates the inverter performance at each change of state in a power distribution system.

A program developed for the ac power distribution system on the Shuttle orbiter predicts the total load on the inverters and the node voltages at each of the line replaceable units (LRU's). The program uses a mathematical model that simulates the nonlinear inverter performance at each change of state in the power distribution system to predict the node voltages at the various buses and LRU's. The model employs interpolation with an iterative technique to solve the governing network equations and could be adapted to predict inverter performance in any similarly complex ac power distribution system.

The program was written in PL/I for batch execution on an IBM 370 series computer with a central memory requirement of approximately 630k of 8-bit bytes. This program was developed in 1982.

This program was written by Rami R. Al-Ayoubi and Tedja S. Oepomo of Rockwell International Corp. for Johnson Space Center. For further information, Circle 100 on the TSP Request Card.
MSC-20769



SOME OF THE GREATEST THINGS IN AMERICA NEVER CHANGE.

SOME DO.



U.S. Savings Bonds. Now paying 10.94%.

U.S. Savings Bonds now pay higher variable interest rates—like money market accounts. At the current rate, you could double your money in less than seven years. You can buy Bonds at most financial institutions.

Now paying 10.94%.

Or easier still, through your Payroll Savings Plan.

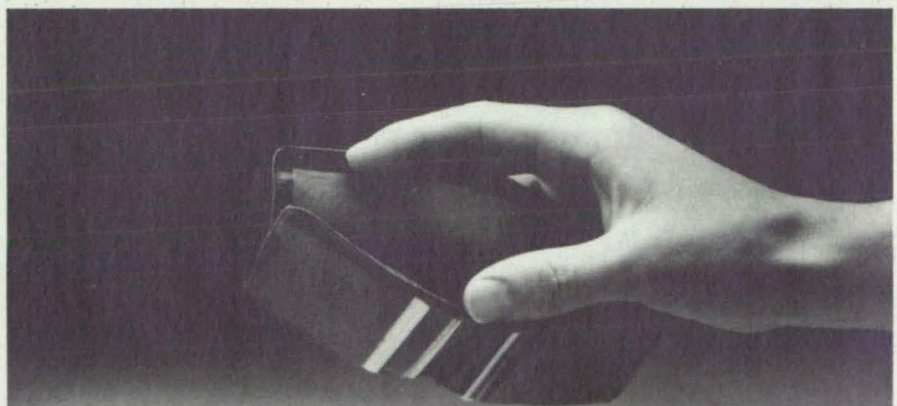
For your free booklet, write:

"50 Q&A," U.S. Savings Bonds Division, Washington, DC 20226.

U.S. SAVINGS BONDS
Paying Better Than Ever

Variable rates apply to Bonds purchased on and after 11/1/82 and held at least 5 years. Bonds purchased before 11/1/82 earn variable rates when held beyond 10/31/87. Bonds held less than 5 years earn lower interest.

A public service of this publication.



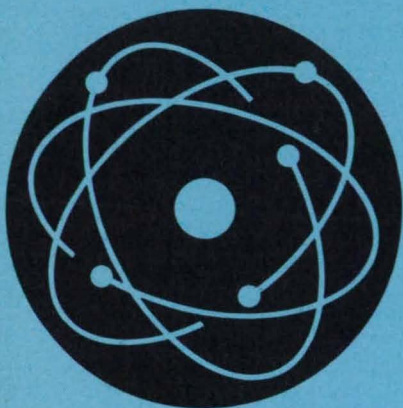
THIS IS HOW MUCH MONEY WE RECEIVE FROM THE GOVERNMENT.

Probably much to your surprise, the Red Cross receives no Federal appropriations for general operations. So it's essential that we depend on corporations such as yours for donations. Otherwise, our nation's oldest, most respected disaster relief organization could itself become a victim. And wouldn't that be a disaster.



American Red Cross

Ad Council
A Public Service of This Publication



Hardware, Techniques, and Processes

- 68 Segmented Trough Reflector
- 68 Windowless High-Pressure Solar Reactor
- 69 Monitoring Trace Gases in the Atmosphere
- 70 Measuring Soil Hydraulic Conductivity With Microwaves
- 70 High-Performance Heat Pipe
- 71 Airborne DIAL System for Remote Tropospheric Sensing
- 72 Analyzing Microchips With Dark-Field Negative Photomicrography
- 73 Optical Mounts for Cryogenic Beam Splitters
- 74 Estimating Antenna Shape From Far-Field Measurements
- 76 Improved Thermal-Diffusivity-Measuring Apparatus
- 78 Measuring Moisture in Sealed Electronic Enclosures
- 80 Lens-and-Detector Array for Spectrometer
- 80 Estimating the Performance of a Concentrating Solar Array
- 82 Crossover Concept for Optical Printed Circuits
- 83 Multiband Selector for Linear Photodetector Array

Books and Reports

- 84 Integrating Residential Photovoltaics With Power Lines
- 84 Tests of Low-Concentration-Ratio Photovoltaic Elements
- 86 Augmenting Thrust With Waste Heat

Computer Programs

- 86 Duct-Flow Analysis

Segmented Trough Reflector

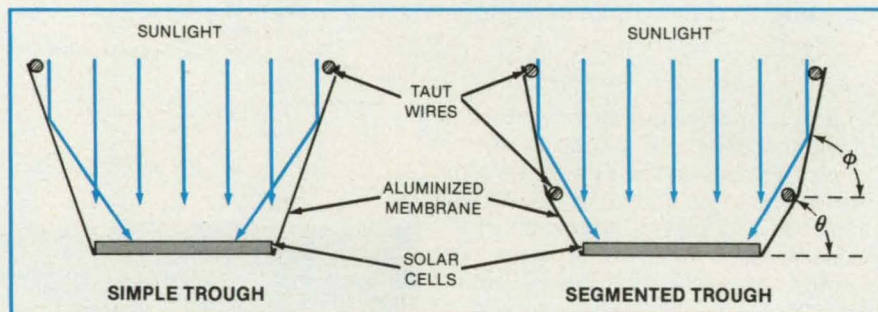
Segments at different angles direct more Sunlight to solar cells.

NASA's Jet Propulsion Laboratory, Pasadena, California

A proposed segmented troughlike reflector for solar cells would approach the concentration effectiveness of a true parabolic reflector yet would be simpler and less expensive. The walls of the segmented reflector are composed of a reflective aluminized membrane. A lengthwise guide wire applies tension to each wall, thereby dividing each into two separate planes (see figure). The planes tend to focus Sunlight on the solar cells at the center of the trough between the walls. The segmented walls provide higher Sunlight concentration ratios than do simple walls.

In cross section, the segmented trough resembles a U with the upper sides tilted at an angle Φ from the horizontal and the lower sides tilted at a somewhat smaller angle θ . The structure is light and can be deployed easily in mobile solar electric plants.

This work was done by W. R. Szmyd of Lockheed Missiles & Space Co., Inc., for NASA's Jet Propulsion Laboratory. For further information, Circle 106 on the TSP Request Card.
NPO-15026



Simple and Segmented Trough Reflectors are formed by supporting aluminized membranes on taut wires.

Windowless High-Pressure Solar Reactor

Obscuration by reaction products would be eliminated.

NASA's Jet Propulsion Laboratory, Pasadena, California

A proposed chemical reactor heated by Sunlight would employ rocket technology to maintain internal pressure. Instead of keeping the chamber tightly closed, the pressure would be maintained by the momentum balance between the incoming and outgoing materials.

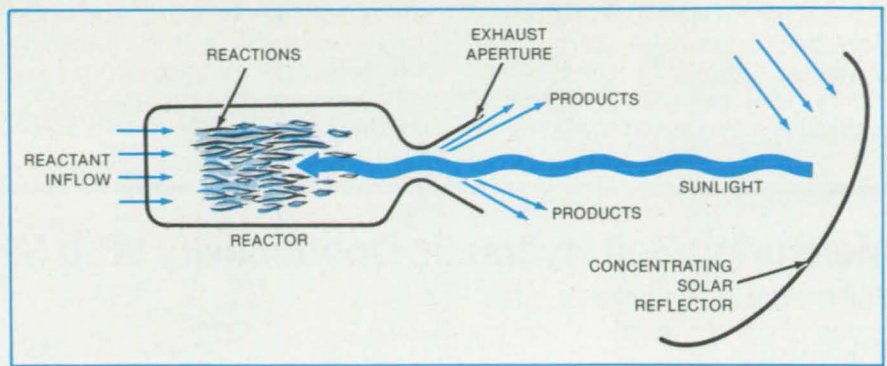
Windows in chemical and synthetic-fuel reactors that use solar heating quickly become coated with tars, glues, syrups, particulates, higher hydrocarbons, or other opaque reaction products. In the conceptual reactor, the solid window would be eliminated. Instead, Sunlight concentrated by a reflector would enter the reactor through the same hole through which the

reaction products are exhausted (see figure).

As in a rocket engine, the expansion of reaction products would cause the pressure in the reaction chamber to rise by an amount that depends on the mass flow rate, the aperture area, and the exit speed of the reaction products. Of these quantities, the input mass flow rate is easily controllable in the manner of the control of fuel flow to a rocket engine. The aperture size and solar-flux concentration may also be made adjustable, thereby giving a total of three parameters that can be adjusted independently by an automatic control system to maintain the desired reaction pressure.

The solar reflector must be placed far enough from the reactor so that it does not become coated with reaction products. A large container may have to be placed around or near the aperture to collect the products, but collection at the low pressures in the container should be relatively easy.

This work was done by Kumar N. R. Ramohalli of Caltech for NASA's Jet Propulsion Laboratory. For further information, Circle 16 on the TSP Request Card. NPO-16310



A Windowless Solar Reactor would admit concentrated Sunlight through the exhaust aperture. The pressure in the reactor would be maintained dynamically.

Monitoring Trace Gases in the Atmosphere

A tunable laser spectrometer uses reflections from ordinary objects.

NASA's Jet Propulsion Laboratory, Pasadena, California

A proposed laser spectrometer would detect trace amounts of harmful gases in the air without cube-corner reflectors or other special targets. In laboratory simulations, the spectrometer detected nitrogen dioxide in concentrations of only a few parts per million.

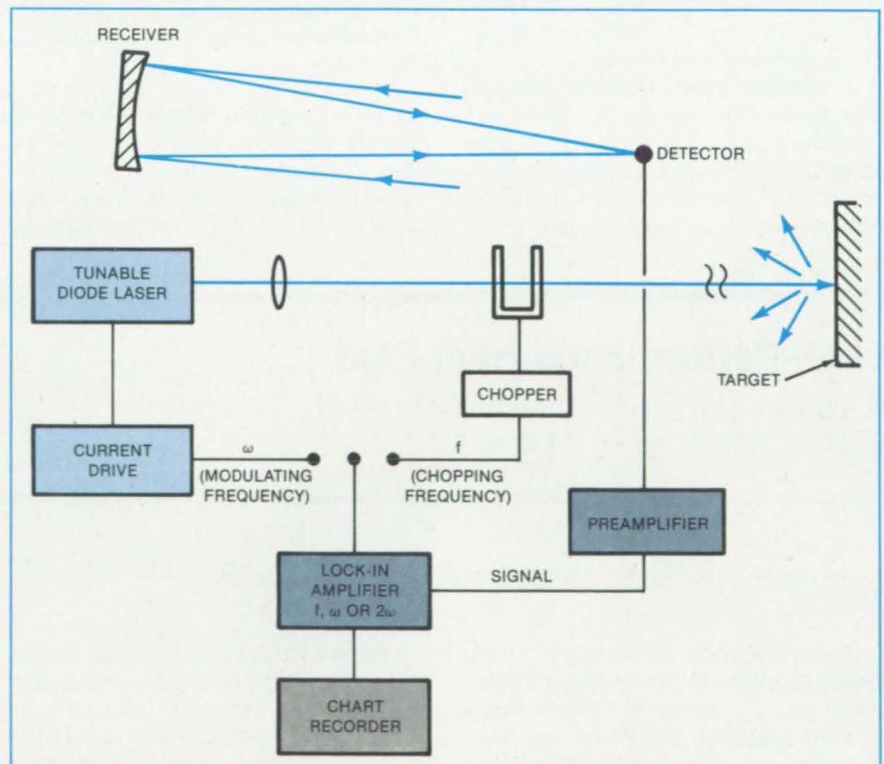
Until now, it has been necessary to use special reflectors to return the laser beams in such spectrometers. Data can be collected only in the direction of the reflectors, however, and it is therefore difficult to locate the source of a leak that does not lie along a path to a reflector. The new spectrometer would use reflections from such ordinary features of the surroundings as walls, tanks, and machinery. The proposed unit is intended primarily for searching for leaks of toxic or hazardous gases over short paths — 20 meters or less. A gas monitor of this type would be useful in refineries, waste-disposal plants, and other industrial situations where a fast response to leaks is necessary.

The spectrometer would employ a tunable semiconductor-diode laser (see figure). The collimated beam of the laser, mechanically chopped at a frequency of 400 hertz, is directed into the surrounding atmosphere. Part of the beam is reflected by an object in the surroundings and returned to a telescope receiver adjacent to the laser. The output wavelength of the laser is swept through the absorption bands of the trace gases of interest. If such a gas is in the atmosphere, it absorbs the beam at that wavelength in proportion to the gas concentration. The strong absorption ap-

pears on the plot made by the spectrometer strip-chart recorder.

The laboratory simulations showed that ordinary objects provide return signals sufficiently strong to enable the detection of absorption even though reflectance varies widely. A piece of

cardboard provides an adequate reflection, for example, and a painted wall provides twice the signal that cardboard does. An aluminum tape returns about 100 times the laser power that a cardboard target does. Interestingly, the system sensitivity does not necessarily



A Topographic Target — that is, an ordinary feature of the surroundings — can return enough energy to the receiver so that absorption by trace gases can be detected. Chopping the laser beam allows the return to be compared with the original signal. The amplifier locks in on the chopping frequency or the laser modulation frequency.

increase with an increase in the reflectance of the target. Rather, the sensitivity is limited by the background signal remaining after the gas of interest is removed and may be improved only to

the extent that the background signal may be subtracted from that containing the spectral feature being monitored.

This work was done by Christopher R. Webster and William B. Grant of Caltech

for **NASA's Jet Propulsion Laboratory**. For further information, Circle 40 on the TSP Request Card.
NPO-16278

Measuring Soil Hydraulic Conductivity With Microwaves

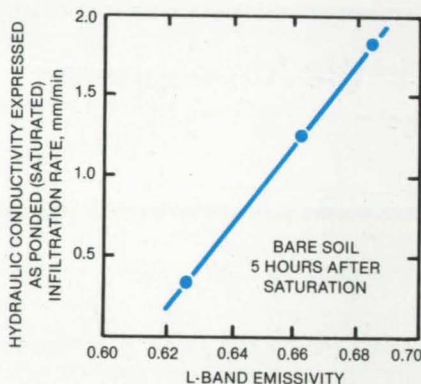
Soil mapping for large or small areas is done rapidly.

Goddard Space Flight Center, Greenbelt, Maryland

Experiments have shown that the hydraulic conductivity of soil can be calculated from passive microwave measurements taken in conjunction with temperature measurements and observations of rainfall. Hydraulic conductivity is important in the classification of soils for agricultural and engineering purposes. The microwave measurements take less time than do conventional hydraulic conductivity measurements that require sampling at many ground points. As a consequence, the hydraulic conductivities of both large and small areas can be mapped faster than before.

The technique requires simple radiometric measurements of L-band (15 to 30 cm) and thermal infrared (10 to 12 μm) emissions from the ground within 2 days after the saturation of the surface. The technique is based on the observation that a correlation exists between the L-band emissivity and the hydraulic conductivity of the soil.

A calibration curve relating the two quantities (for example, see figure) is developed from two sets of data taken from a wide range of soils in well-controlled plots. Hydraulic conductivity as measured in the soil with conventional infiltration rings is corre-



The Hydraulic Conductivity of a Soil is related to the L-band emissivity, as determined from passive measurements of the L-band radiation from the soil, and from soil-temperature measurements. The measurements must be made at a specified time within 2 days following a saturating rainfall.

lated with measurements by a microwave radiometer mounted a few meters above the ground on a truck. The use of the calibration curve is limited to 2 days after saturation because climatic conditions can cause sig-

nificant differences in the emissivity-vs.-hydraulic-conductivity relation after that interval.

Instead of (or in addition to) thermal infrared measurements, the ground temperature can be determined by thermometric probes. The microwave radiometer may be carried in the field by a truck, as in the calibration measurements, or by an aircraft or satellite, depending on the size of the desired resolution element and the extent of the area to be mapped. The occurrence of a saturating rainfall is determined by satellite photography, radar, or local ground observations.

The microwave measurements are not seriously affected by some kinds of grasses and crops, but are affected by some other crops, such as corn, and by forest canopies. The technique may also have limited applicability over urban areas, rough terrain, and coastal wetlands.

This work was done by Bruce J. Blanchard and Peggy E. O'Neill of Goddard Space Flight Center. For further information, Circle 24 on the TSP Request Card. GSC-12937

High-Performance Heat Pipe

A single vapor channel and a single liquid channel are joined by an axial slot.

Lyndon B. Johnson Space Center, Houston, Texas

A heat pipe under development for heat-rejection systems in very large space structures has a capacity of approximately 10^6 watt-inches (2.5×10^6 watt-cm) — orders of magnitude greater than the heat capacity of existing heat pipes. The new design has high radial-heat-transfer efficiency, is structurally simple, and has large liquid and vapor areas.

Present axial-groove heat-pipe technology utilizes many axial grooves as a compromise between axial heat-transport capacity (watt-meters) and radial heat-transfer efficiency (watts/ $^{\circ}\text{C}$). The heat-transport capacity could be maximized by using fewer axial grooves, with large diameters, because such a design minimizes the liquid viscous pressure losses. However, the

heat transfer is poor when only a few axial grooves are used, because evaporation takes place primarily at the liquid meniscus and hence is proportional to the number of grooves.

The new design, shown in the figure, permits high heat-transport capacity without excessively reducing heat-transfer efficiency. It contains two large axial channels, one

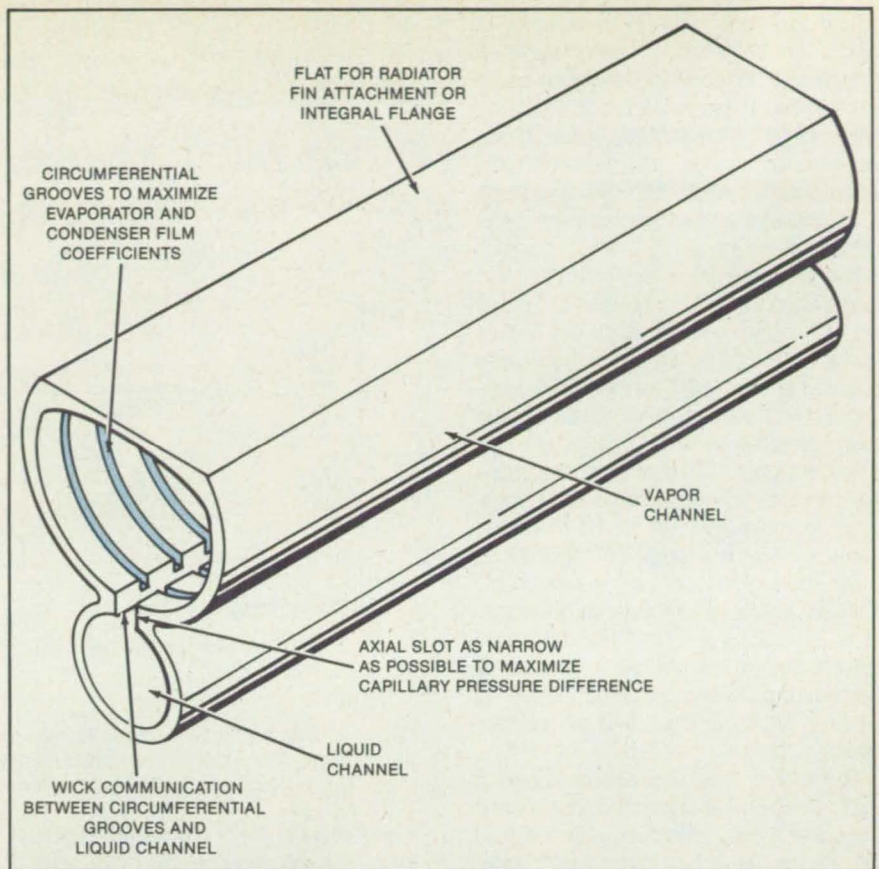
for vapor and one for liquid, which permit the axial transport and the radial heat-transfer requirements to be met independently.

The narrow slot separating the channels creates a high capillary-pressure difference. In combination with the minimized flow resistance of the two channels, this results in the high-axial-heat-transport capacity. High evaporation and condensation rates are provided separately by circumferential grooves in the walls of the vapor channel.

Initial tests of the heat pipe indicated a tendency toward premature dryout of the circumferential vapor-channel grooves, resulting in large temperature gradients (hot spots) under load. This is attributed to boiling in the liquid channel and the consequent interruption of liquid feed to the circumferential grooves. Work to eliminate these problems has been underway for some time and will be reported in an upcoming issue of *NASA Tech Briefs*.

This work was done by Joseph P. Alario, Robert Kosson, and Robert Haslett of Grumman Aerospace Corp. for Johnson Space Center.

Title to this invention has been waived under the provisions of the National Aeronautics and Space Act [42 U.S.C. 2457(f)], to the Grumman Aerospace Corp., Bethpage, N.Y. 11714.
MSC-20136



The Single-Axial-Groove High-Performance Heat Pipe can transfer heat at a much greater rate ($\sim 2.5 \times 10^6$ W-cm) than previous heat pipes.

Airborne DIAL System for Remote Tropospheric Sensing

The spatial distribution of gases and of aerosols are measured.

Langley Research Center, Hampton, Virginia

A multipurpose airborne differential absorption lidar (DIAL) system, developed at the Langley Research Center, remotely measures the profiles of various gases and aerosols in diverse atmospheric investigations. The capability to rapidly determine the spatial distribution of gases such as ozone, water vapor, sulfur dioxide, and nitrogen dioxide and to measure simultaneously the distribution of aerosols at several laser wavelengths provides the opportunity for developing an extensive data base for examining the complex interaction of atmospheric dynamics and chemistry.

Methods that employ in situ measurement techniques do not provide the coverage necessary to describe regional-scale transient phenomena adequately and, when used in global-scale studies, may miss important features that are not traversed by the aircraft. The airborne DIAL system provides gas and aerosol measurements in a broad range of atmospheric investigations,

NASA Tech Briefs, Summer 1985

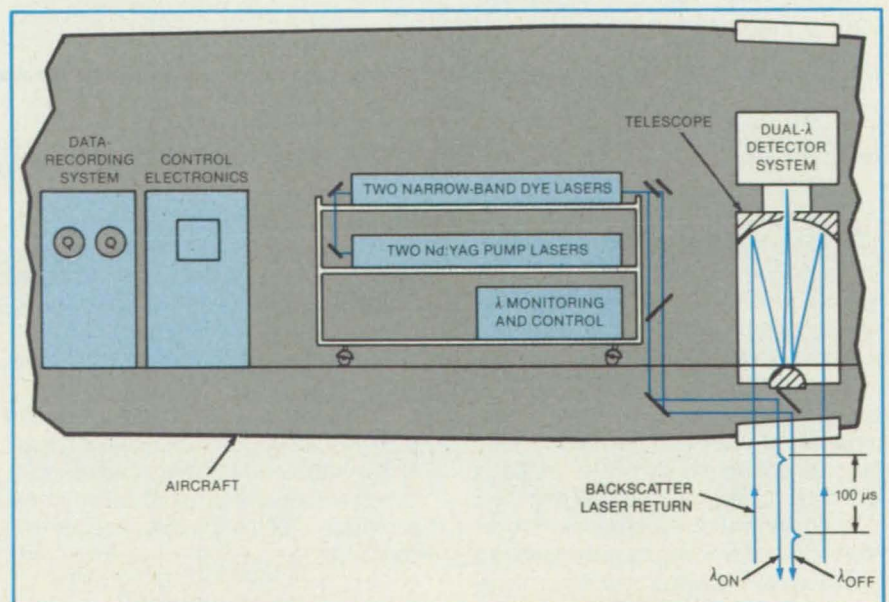


Figure 1. The Airborne DIAL System uses two frequency-doubled Nd:YAG lasers and is mounted in the NASA Wallops Electra aircraft.



including transport and photochemistry of tropospheric/stratospheric ozone, boundary-layer and tropospheric dynamics using aerosols as tracers, transport and transformation of pollutants such as sulfur dioxide and nitrogen dioxide, and meteorological applications of remote lidar measurements of water vapor and atmospheric temperature and pressure.

The airborne DIAL system uses two frequency-doubled Nd:YAG lasers to pump two high-conversion-efficiency dye lasers. Figure 1 shows a schematic of the system mounted in the NASA Wallops Electra aircraft. Some results of measurements made using the airborne DIAL system are presented in Figure 2. The results demonstrate the capability of the airborne DIAL technique to make range-resolved measurements of a broad range of tropospheric gases. The application of lidar remote sensing to investigations of atmospheric phenomena is increasing as the DIAL technique becomes more accepted as an operational method for gathering data on tropospheric gases in local, regional, and global-scale studies.

The system was originally developed to investigate several important atmospheric processes. Initial emphasis with the lidar has been on measurements of ozone, water vapor, and aerosol profiles. An understanding of the tropospheric ozone budget is essential to establishing a firm knowledge of tropospheric photochemistry and the potential impact of pollutants on the photochemical system. High-resolution remote measure-

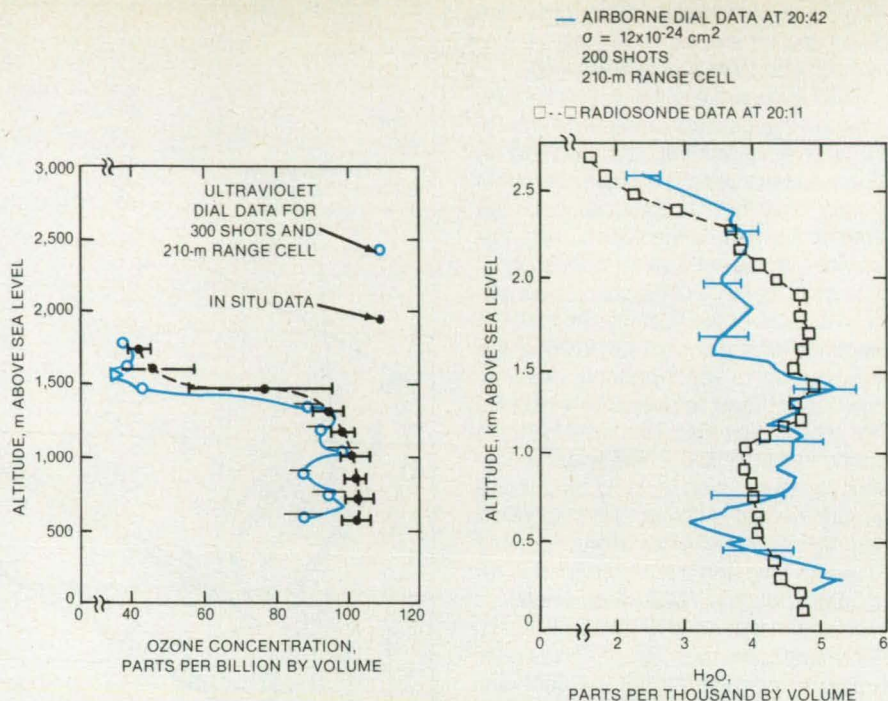


Figure 2. DIAL and In Situ Ozone Measurements above and in the boundary layer are compared at the left. Water-vapor profiles taken using DIAL are compared at the right with those taken over Langley Research Center with a radiosonde.

ments of water vapor profiles are important for such applications as the initialization of numerical weather forecast models in regions not covered by radiosonde data and in studies of latent heat flux and tropospheric/stratospheric exchange. Aerosols can be readily used to trace atmospheric dynamics, and aerosol distributions can

provide information on the boundary-layer mixing depth, condensation level, cloud-tops stable layers, and plume-dispersion parameters.

This work was done by Edward V. Browell of Langley Research Center. For further information, Circle 31 on the TSP Request Card. LAR-13002

Analyzing Microchips With Dark-Field Negative Photomicrography

Inverse development process yields fine details.

NASA's Jet Propulsion Laboratory, Pasadena, California

A photomicrographic technique produces images of integrated-circuit chips. The technique is based on dark-field illumination, in which a chip is lit with a bright central spot of light and photographed by light scattered or diffracted from the spot. It reveals more about microstructure patterns related to photoresist masking than the more conventional bright-field method, in which the chip is uniformly illuminated by bright light or by scanning electron microscopy.

Along with the dark-field illumination, the new technique employs an inverse process of photographic development. First a negative transparency is made of the chip, then a positive contact transparency is made from the negative, and finally a negative print on

paper is made from the positive transparency. The chip features appear as dark lines on a white background. The fringe-pattern effects common to bright-field photomicrography, in which oxides, nitrides, and other layers create varying shades and hues, are suppressed.

The technique is effective when used to prepare a series of views as surface material is progressively removed. Each successive exposure reveals more details of the substructure of the chip. Such sequences can be used to evaluate chip design and layout and to identify unknown structural patterns. They can also be used to determine whether a chip structure infringes on pat-

ents or to "reverse engineer" a chip — that is, determine the hidden geometry, depth, and interconnection of its features that allow it to perform the way it does.

This work was done by Stefan F. Suszko of Caltech for NASA's Jet Propulsion Laboratory. For further information, Circle 72 on the TSP Request Card.

Inquiries concerning rights for the commercial use of this invention should be addressed to the Patent Counsel, NASA Resident Office-JPL [see page 21]. Refer to NPO-16299.

Optical Mounts for Cryogenic Beam Splitters

Pellicles are held flat over a wide temperature range.

Goddard Space Flight Center, Greenbelt, Maryland

Spring-loaded optical mounts maintain the flatness and alignment of rigid, framed, or pellicle beam splitters over a wide temperature range, despite differences in thermal expansion among materials. These mounts thereby permit optical adjustments to be made at ambient temperature even though an optical system may be operated subsequently within a few degrees of absolute zero.

Figure 1 shows the version for beam splitters or other flat optical elements that are constructed integrally with frames that keep them flat. The mount includes three attachment points equally spaced about the periphery of the element. At all three points, the frame is held by springs (not shown) against the reference surface.

At one of the attachment points, the element is free to rotate in the mounting plane but not to translate. At the other points, the element is free to slide along a slot oriented radially from the rotation point. At the two translation points, the element is maintained in tension by springs that pull outward from the center of the element. This arrangement permits motion in the mounting plane to relieve stresses caused by differential thermal expansion, while maintaining a nearly constant low tension.

The second version (see Figure 2) is for pellicles that must be stretched evenly to remain flat and free of wrinkles. The pellicle is clamped between bars at six places equally spaced about the periphery. Three dividing beams are also equally spaced about the periphery. One of the beams is anchored to permit only rotation in the mounting plane, while the other two are sprung outward and are free to slide toward or away from the rotation point, as in the first version.

The spring tension is oriented to have a small component toward the reference surface so that the pellicle is pulled against it. Each beam divides the outward spring force equally between its two bars. To prevent differential stress from developing between adjacent clamps, one end of each beam is attached to permit only rotation, while the other is free to slide along the pellicle circumference.

The basic concept permits some variations: Although coil springs are shown here, leaf springs could be used. In addition, these mounts would be useful as holders for integrated-circuit master patterns,

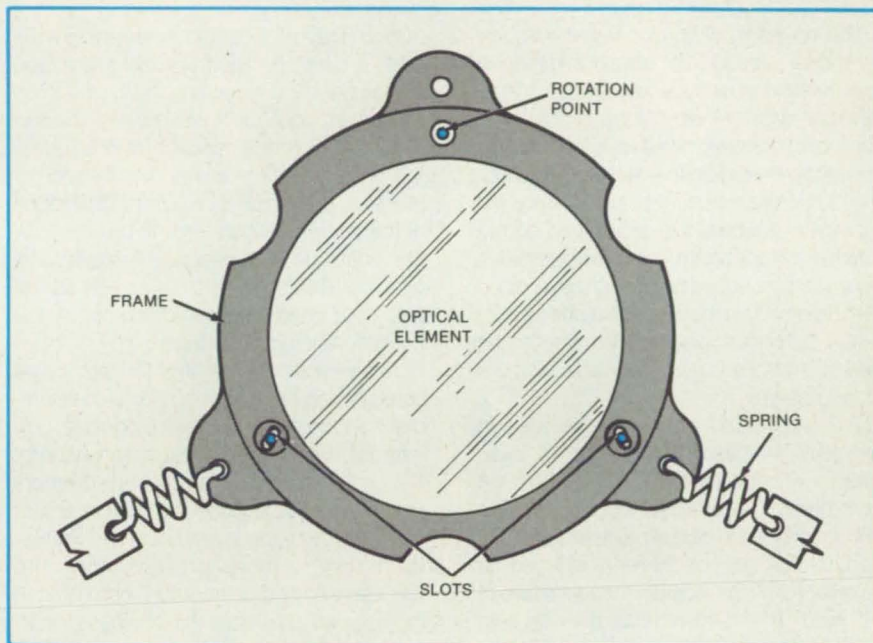


Figure 1. This **Mounting Device for Framed Optical Elements** maintains orientation in a plane while allowing for thermal expansion and contraction.

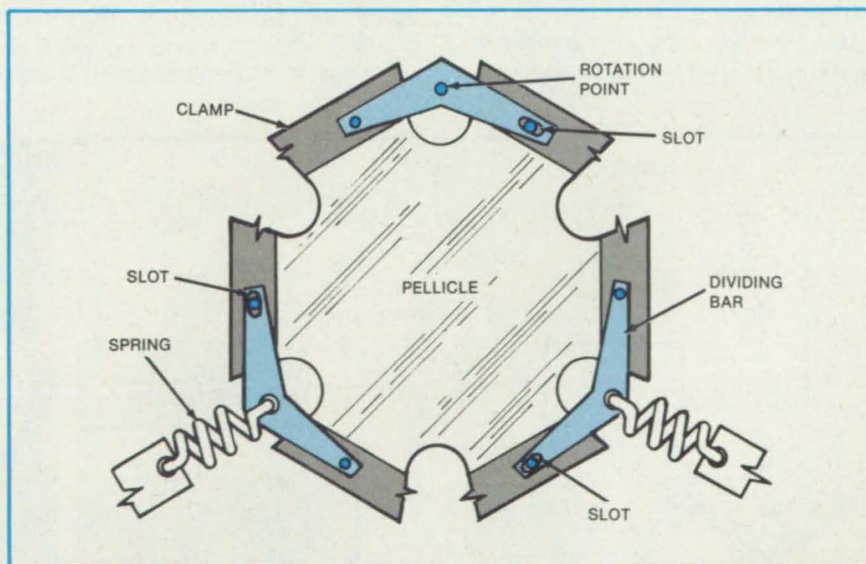


Figure 2. This **Mounting Device for Pellicles** maintains flatness and planar orientation. The spring-loading assures relatively uniform tension so that the pellicle neither breaks nor wrinkles.

survey targets, vibrating membranes, noise- or pressure-sensing membranes, osmosis filters, and fuel-cell elements.

This work was done by Arthur A.

Rudman of Goddard Space Flight Center. For further information, Circle 1 on the TSP Request Card. GSC-12923

Estimating Antenna Shape From Far-Field Measurements

Amplitude and phase measurements help characterize nearly paraboloidal reflectors.

NASA's Jet Propulsion Laboratory, Pasadena, California

The deviation of a microwave reflector from ideal paraboloidal shape is deduced from far-field amplitude and phase measurements with the help of a theoretical technique referred to as microwave holographic metrology. Based on the radiation field calculated by electromagnetic-field theory, the technique enables the estimation of the antenna-surface figure from measurements taken at a prescribed number of field points. After determining the amount of surface deviation, the performance of the antenna can then be improved by properly adjusting the surface panels.

The applicable equations have been derived for the case of a nearly paraboloidal reflector with the feed located at or near the focal point. The analysis begins with the calculation of the radiation field (far field) produced by surface currents induced on the reflector by the incident magnetic field of the feed. It is shown that the far field behaves like an infinite series of Fourier transforms of the induced surface current. For a large reflector with a narrow beam width, the series can be approximated by only the first term.

Using the first term, an expression is derived for the effect of small surface distor-

tions on the radiation field. After taking an inverse Fourier transform of the expression for the field and extracting the phase information, an equation is obtained for the surface distortion as a function of position on the antenna. While this is the desired expression, in principle it requires a knowledge of the entire radiation field. To be practical, the technique should require sampling at a finite number of field points as well as the use of a finite number of points in the Fourier-transform operation.

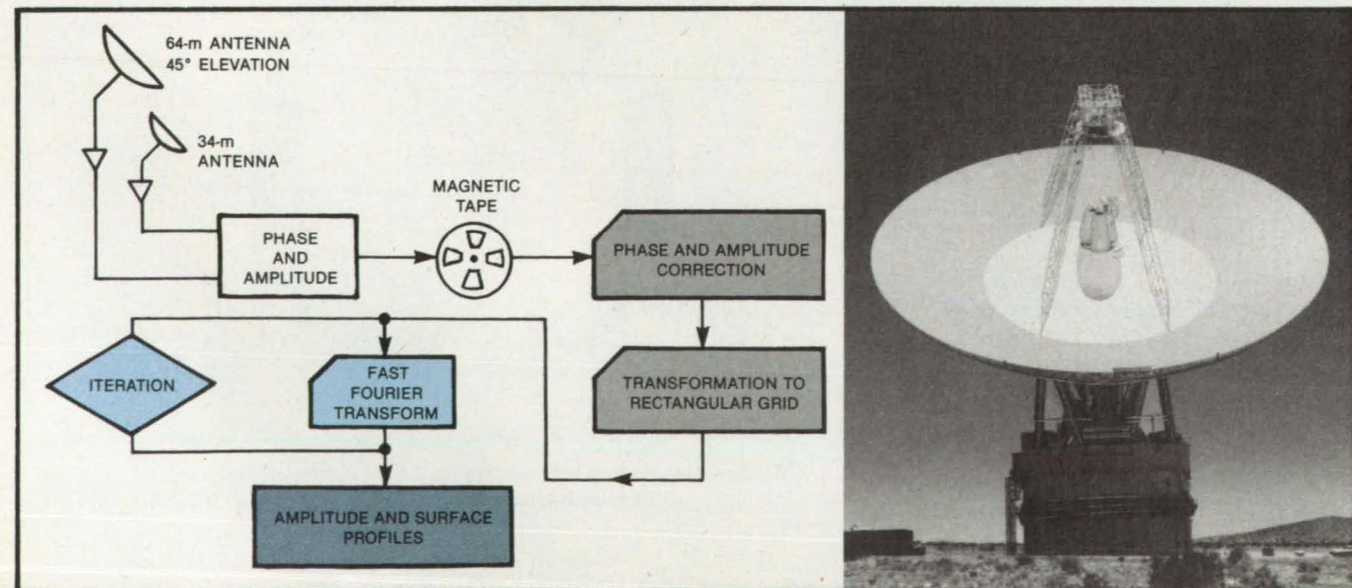
Expressions are derived for the spatial sampling intervals within the finite measurement window. An iterative technique permits the analytic/numerical continuation of the far-field pattern from the measurement points to points outside the measurement window. Thus, the inversion of the Fourier transform is more precise since the unmeasured part of the field is estimated at its likely values rather than being approximated arbitrarily by zeroes wherever it is not measured.

The technique was tested in a computer simulation of a 486.6-wavelength-diameter reflector with annular surface irregularities of 0.02 wavelength in one ring and 0.10 wavelength in another ring. Using 63 field-

sampling points and 128 transform points, the simulated-surface profile was reconstructed on a computer-generated image in a close approximation of its original form. Many other computer simulations were also performed to demonstrate the accuracy of the technique for different cases, including an error simulation study.

The technique was further tested on a 64-m-diameter astronomical dish at a wavelength of 13.15 cm in the receiving mode (see figure). The field data were taken by tracking the compact radio source 3C273 and sampling the received signal on a grid of 11 by 11 points about the centerline with 5.7-arc-minute spacings. Even with this relatively coarse grid, the reflector surface reconstructed mathematically from the field measurements shows rms distortions on the order of 1.1 mm. These distortion values are consistent with values previously estimated on the basis of reflector efficiency.

This work was done by Yahya Rahmat-Samii of Caltech for NASA's Jet Propulsion Laboratory. For further information, Circle 82 on the TSP Request Card. NPO-16425



Using the **Microwave Holographic Measurement Process** diagramed at the left, large reflector antennas are diagnosed for deviation from the ideal paraboloidal shape. The 64-m-diameter antenna shown at the right was mathematically reconstructed from electromagnetic-field measurements at only 121 points.

Announcing:
Verdix Ada Development System
for the Sun Workstation®

VERDIX ADA DEVELOPMENT SYSTEM

Why the DoD mandated Ada. When the Department of Defense mandated Ada® for embedded and mission-critical systems development, there was good reason. This reusable, high-order language can put an end to the Software Crisis. Ada decreases skyrocketing software costs, improves management and control, reduces life cycle costs, boosts productivity, dramatically reduces errors and cuts training costs. Ada is the language of the day, and Verdix speaks it. Louder and clearer than anyone.

Why others are mandating Verdix. We have the first highly portable production-quality Ada development system. The Verdix Ada Development System (VADS™) is the first production-quality Ada compiler system to meet DoD's stringent requirements for Ada language mission-critical systems development. It is now available on the DEC VAX™ series computer systems and includes:

- High performance, rehostable/retargetable Ada compiler under UNIX™ 4.2 BSD and ULTRIX™ (soon under VMS) with excellent diagnostics;
 - Symbolic Debugger;
 - Library Management Utilities;
 - Run Time System.
- Designed for large scale and embedded systems development, VADS speeds programming faster than any other Ada compiler.



VADS also helps programmers quickly learn the Ada language. The unexcelled diagnostics speed correction time and shorten development time. The Symbolic Debugger lets you watch your program execute, Ada line by Ada line or machine instruction by machine instruction, even for remote embedded systems. *And it's highly portable:* VADS will be available on a wide range of computer systems.

Fully DoD validated; available now. VADS is validated and ready to be put to work. It's not a promise. It's available now (as in "here and now") and already in use by major DoD contractors.

To find out for yourself how the Verdix Ada Development System can work for you, write, or call (703) 448-1980 and talk to Howard Nevin, Vice President of Product Planning and Corporate Development for more information.

IT'S VALIDATED. USE PROVEN. AVAILABLE NOW!

VERDIX

Ada Development System

Verdix Corporation
Westgate Research Park
7655 Old Springhouse Road
McLean, VA 22102
(703) 448-1980

© 1985, Verdix Corporation. Ada is a registered trademark of the US Government (Ada Joint Program Office). UNIX is a trademark of Bell Laboratories. Verdix and VADS are trademarks of Verdix Corporation. ULTRIX is a trademark of Digital Equipment Corporation. Sun Workstation is a registered trademark of Sun Microsystems, Inc.

Improved Thermal-Diffusivity-Measuring Apparatus

Accuracy at high temperature is improved.

NASA's Jet Propulsion Laboratory, Pasadena, California

An improved apparatus measures the thermal diffusivities of materials at temperatures as high as 1,600 K. The apparatus offers several improvements over previous versions:

- The specimen is situated inside a long furnace for uniform heating and high-temperature operation.
- The heat pulse from a flash lamp is fed to the front surface of the specimen by a fused-quartz or sapphire light pipe.
- The rear-surface temperature of the specimen is monitored by a differential thermocouple with one junction attached to the specimen and the other in juxtaposition to the first but not touching the spec-

imen. As a result, only temperature changes are recorded, and biasing with microvolt accuracy is unnecessary.

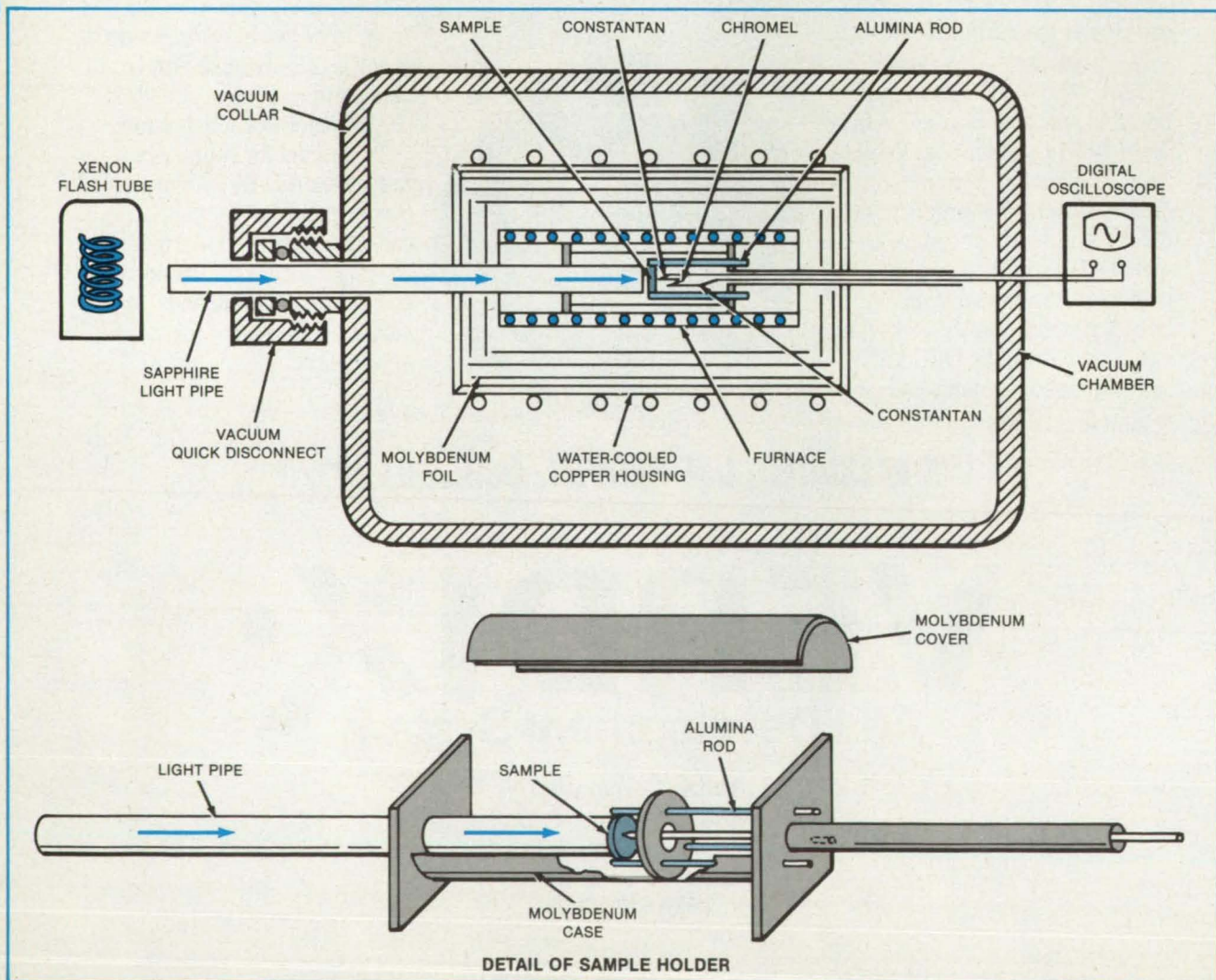
The apparatus consists of a molybdenum-wound, resistance-heated furnace in a water-cooled copper housing within an evacuated bell jar (see figure). Both the furnace and the housing are split so that they can be opened easily for loading a specimen.

The specimen holder includes a molybdenum frame that supports three thin alumina rods that in turn support the specimen. The spring tension of the rods (which the rods retain at temperatures up to 1,700 K) clamps a disk-shaped specimen at three

points on its periphery. The small contact area minimizes the conductive heat loss from the specimen.

A light pipe extends from a flash tube outside the housing, through a quick-disconnect fitting in a vacuum collar, to the specimen. For maximum light collection, the light pipe almost touches the flash tube.

If the specimen is electrically conducting, the thermocouple wires, which are 0.001 inch (0.0254 millimeter) in diameter, are attached individually to the rear surface of the specimen, about 1 millimeter or less apart, with graphite cement. The specimen thus becomes part of the first thermocouple junction. For an electrically insulating sam-



The Furnace Heats the Specimen to the experimental temperature, and a flash tube raises the specimen temperature by a small amount and for a short time so that diffusivity (a composite property of heat capacity and conductivity) can be determined. The specimen mount ensures minimum heat loss during the temperature-rise measurement.

What experts say about today's U.S. Savings Bonds:

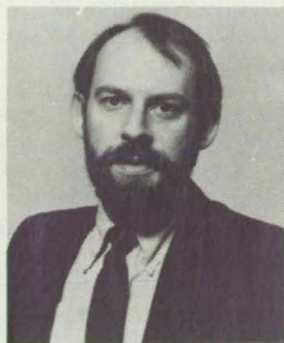


"One savings option that combines a fair return, safety and simplicity has been with us a long time—U.S. Savings Bonds. Today's Bonds have changed for the better, now offering more than adequate interest rates when held five years or more. Bonds are guaranteed safe—and easy to buy through company Payroll Savings Plans."

— **Sylvia Porter**
Journalist, economist, and editor-in-chief of
Sylvia Porter's Personal Finance Magazine.

"(Savings Bonds) pay an interest rate that is competitive with those on securities in the free market, with the rate changing every six months to reflect market conditions."

— **Carol Mathews**
"Two for the Money"
N.Y. Post, November 7, 1984



"In 1982 the Treasury Department remodeled the classic, and now it holds its own against the fast-paced investment vehicles of the '80s."

— **Jim Henderson**
USA TODAY, February 11, 1985

"One way to cut through the complexities of the bank, bond and tax-shelter markets seems almost too easy to be true: buy U.S. Savings Bonds. Americans are still laboring under the notion that savings bonds don't compare favorably with newfangled investments. But savings bonds are sound as well as safe."

— **Candace E. Trunzo**
Money Magazine, December 1984



"EE Savings Bonds require no commissions and fees, are backed by the U.S. government, pay rates of interest pegged to Treasury notes yet never less than 7½ percent, are exempt from state and local taxation, offer deferral of federal tax, are invulnerable to market loss, and may be converted to current income HH Bonds with continuing tax deferral. For an investment offering all this at a price beginning with \$25, you can't beat them."

— **Donald R. Nichols**
Director of Corporate Relations for Hartmarx Corp. and author of
Starting Small, Investing Smart and Life Cycle Investing

U.S. Savings Bonds now earn high variable interest rates
and a guaranteed return when held five years or more.

You can buy Bonds through company Payroll Savings
Plans and where you bank.

U.S. 
SAVINGS
BONDS
Paying Better Than Ever

ple, the first thermocouple junction is attached directly to the sample with graphite. The thermocouple extension leads, 0.01 inch (0.254 millimeter) in diameter, connect to a digital oscilloscope.

With the specimen heated to the requisite temperature, the light pipe carries a light pulse from the flash tube to the front surface of the specimen. The heat deposited on the front surface by the radiative pulse is con-

ducted through the specimen to the rear surface. The thermocouple senses the temperature rise at the rear surface, and the oscilloscope indicates the time for the temperature rise to reach half its maximum value. From that value and the thickness of the specimen, the diffusivity is calculated.

Chromel/Constantan thermocouples are used below 1,000° C, and platinum/platinum-rhodium or tungsten/tungsten-

rhenum thermocouples are used above 1,000° C. Measurement temperatures up to 1,000° C can be realized with a fused-quartz light pipe and up to 1,600° C with a sapphire light pipe.

This work was done by Charles Wood and Andrew Zoltan of Caltech for NASA's Jet Propulsion Laboratory. For further information, Circle 38 on the TSP Request Card.
NPO-16280

Measuring Moisture in Sealed Electronic Enclosures

Instrument checks trace amounts accurately.

Lyndon B. Johnson Space Center, Houston, Texas

The moisture in hermetically-sealed electronic equipment is measured by an instrument designed for field use. The instrument also measures pressure, volume, and contaminants of the gas in the sealed enclosure.

The major components of the instrument (see figure) are as follows:

- A valve and coupler for joining the instrument to the electronic enclosure to be tested;
- A gas-impedance device within the coupler;
- A tube for detecting water;
- A sample-collection bottle;
- A vacuum source, reference-gas supply, and pressurant-gas supply; and
- Temperature and pressure gages at critical points.

To perform a test, an operator connects the coupler to an electronics enclosure. The operator evacuates the instrument, then purges it with the reference gas. The reference gas should be a trace constituent of the atmosphere in which the electronics enclosure operates; argon is usually used. Once again, the operator evacuates the system, then opens the coupler valve.

The pressurant gas from the enclosure flows to the detector tube. The gas-impedance device in the coupler ensures that the flow is slow enough that the detector can perform its function. The detector tube contains a substance that changes color — from yellow to red — as it reacts with minute amounts of water. The amount of material that changes color is directly proportional to the amount of water reacted. Thus, by measuring the length of the red zone and comparing the value with a calibrated standard, the operator can determine the amount of moisture that was present in the enclosure.

From the detector tube, gas flows into the sample bottle. When the flow stops and the gas in the instrument is at equilibrium, the operator seals and disconnects the sample bottle. (Later, the constituents of the bottle

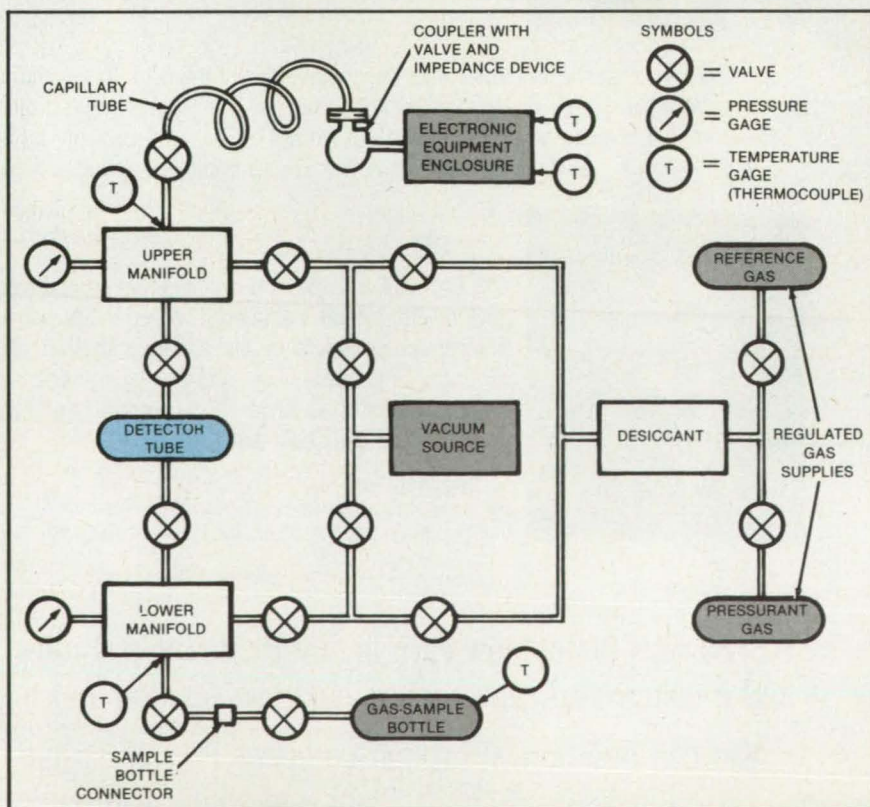
can be identified and their quantities measured by mass spectroscopy or other laboratory tests.) During the test procedure, the operator records pressures and temperatures at certain steps so that the measurements of the bottle contents can be used to calculate the conditions in the enclosure.

Finally, the operator repressurizes the enclosure with fresh, dry gas: The operator evacuates the instrument (and simultaneously the enclosure). Then the operator sends gas from the pressurant-gas supply through a desiccant, through the instru-

ment, and into the enclosure until a preset pressure is established. The enclosure is then removed from the coupler.

This work was done by Herman C. Krieg, Jr., of TRW, Inc., for Johnson Space Center. For further information, Circle 74 on the TSP Request Card.

Inquiries concerning rights for the commercial use of this invention should be addressed to the Patent Counsel, Johnson Space Center [see page 21]. Refer to MSC-18866.



The Plumbing for the Instrument uses vacuum-tight valves so that any portion of the instrument can be cleansed by opening certain valves to the vacuum source. To ensure accuracy, the manifolds are of minimal volume, each comprising only the volume within cross-shaped tubing fittings.

AFTER 35 YEARS AS HIS EMPLOYER, TELL HIM ABOUT DIRECT DEPOSIT AS A FRIEND.

Make sure the people who have given you so much through the years get everything they've got coming in the years ahead.

Direct Deposit lets your retiring employees send their Social Security straight to their checking or savings account. It's free, and it lets them enjoy the good life they deserve.

As an employer, send for a free Direct Deposit retirement planning kit today, and pass the information along...to a friend.

Write to—Direct Deposit (D1),
U.S. Treasury, Annex 1, PB-1100,
Washington, DC 20226.



DIRECT DEPOSIT



A Public Service of This Publication & The Advertising Council

United States Treasury



Lens-and-Detector Array for Spectrometer

A supporting structure aligns the lenses and serves as a light baffle.

NASA's Jet Propulsion Laboratory, Pasadena, California

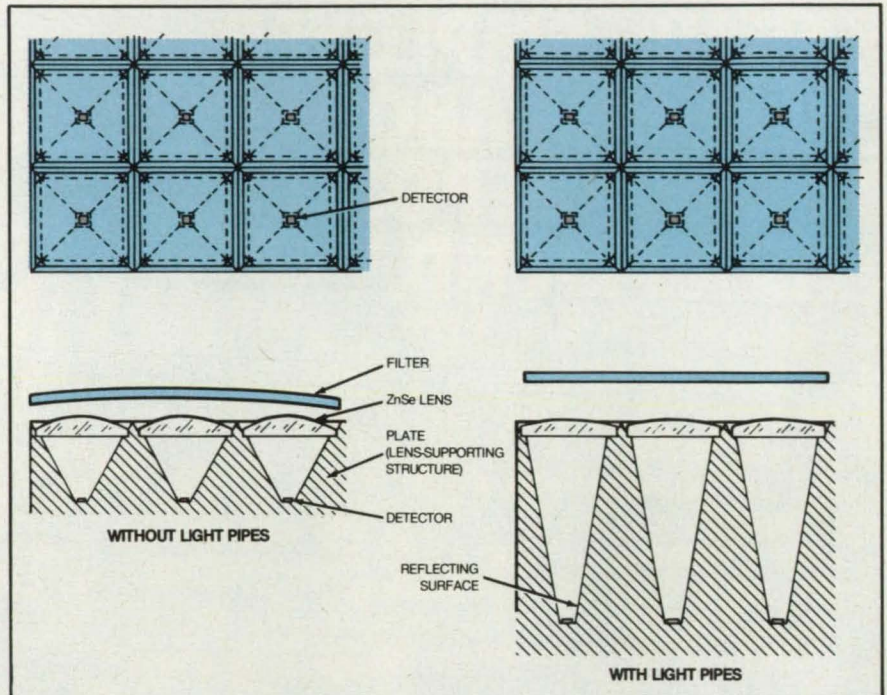
An array of lenses and photodetectors for an infrared spectrometer is mounted on a plate in a 10 by 11 array of cavities. The spectrometer includes four focal-plane sub-systems, each consisting of such an array plus a filter that passes radiation in one of four spectral bands.

Two versions have been designed; one with and one without light pipes (see figure). The cavities have a square pyramidal shape. The plate with cavities is reproduced to the required precision by electroforming.

The lenses are 4 mm square and fit into recesses around the edges of the cavities. The lens material is ZnSe, which transmits efficiently in the infrared bands of interest. Because ZnSe has a high (~ 2.4) index of refraction, the lenses can provide the required optical power with relatively low curvature. The high index does, however, dictate the use of antireflection coatings to minimize the Fresnel reflection losses at the lens surfaces. In the version without light pipes, each lens has a relative aperture of $f/0.5$ and a focal length of 2.68 mm.

The detectors, each 0.4 mm square, lie at the bottoms of the holes. The detector types and the corresponding spectral bands are: $\text{Hg}_{.814}\text{Cd}_{.186}\text{Te}$ in photoconductive mode, 14.08 to 17.67 μm ; $\text{Hg}_{.781}\text{Cd}_{.219}\text{Te}$ in photoconductive mode, 7.86 to 10.00 μm ; and InSb in photovoltaic mode, 4.93 to 5.75 μm and 3.59 to 4.38 μm . The entire module is cooled to 80 K for maximum detector responsivity and to reduce radiation by the optics and structure.

The plate maintains the lens-to-detector spacing and the optical alignment of each element. It also optically isolates each detector from the others, thereby reducing crosstalk. The rectangular grid of openings serves as a coarse alignment grid and aperture stop.



Lenses and Infrared Detectors are mounted together in cavities in an electroformed plate. The plate and cavities maintain optical alignment while serving as a light baffle and aperture stop.

The lens array at the surface of the plate is placed in the image plane of the spectrometer optics. The spectrometer-output optics and the ZnSe lenses work together to image the spectrometer system pupil onto a spot of 0.3 mm diameter on each detector. This arrangement minimizes scene-induced noise. Since the spot size is smaller than the detector size, the system can tolerate about 0.05 mm of misalignment between each ZnSe lens and its detector.

In the version with the light pipes, the cavities are longer, and lenses of smaller rela-

tive aperture ($\sim f/2$) can be used. The walls of the cavities act as reflecting surfaces to help funnel the image energy onto the detectors. The light striking the walls helps to scramble the image, thereby further reducing the scene-induced noise. This arrangement reduces efficiency, however.

This work was done by Joseph Oberheuser of Perkin-Elmer Corp. for NASA's Jet Propulsion Laboratory. For further information, Circle 98 on the TSP Request Card. NPO-16388

Estimating the Performance of a Concentrating Solar Array

An integrated approach considers optical, thermal, and electrical effects.

Marshall Space Flight Center, Alabama

A comprehensive mathematical-analysis technique has been developed for an array of solar-photovoltaic panels equipped with

truncated-pyramid concentrators. Combining existing procedures for calculating the optical, thermal, and electrical perfor-

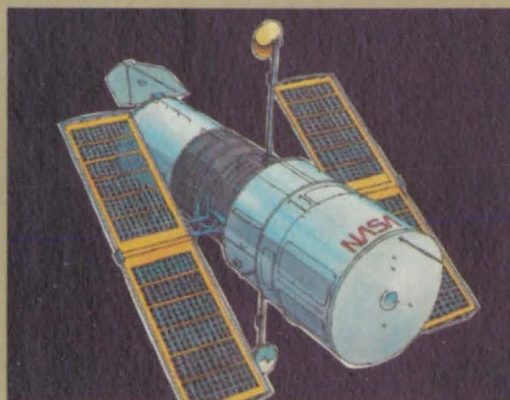
mances of the elements of the system, the analysis provides a detailed description of the interconversion of the various types of

IN 1986 OUR PHOTOELECTRONIC SENSORS WILL HELP GUIDE THE MOST POWERFUL ORBITING OBSERVATORY KNOWN TO MAN.

The NASA Hubble Space Telescope will rely on EMR matched-channel photon-counting sensors to maintain precise alignment with its targets.

EMR sensors look skyward, from Orbiting Astronomical Observatories, to map the radiant intensities of stars and nebula. And they look groundward, from Orbiting Geophysical Observatories, to measure auroral spectra and record weather conditions. They've been to the moon on Apollo 17 and past Mars on Mariner.

Since 1960, EMR has designed and built highly reliable photon detection equipment for highly demanding customers: NASA, DOD, and Schlumberger Oil Field Services. They depend on our unique capability to produce photoelectronic instruments of unequalled accuracy and durability.



When radiation sensors are designed to be rugged enough for the world's deepest oil wells—where pressures reach 20,000 psi and temperatures soar to 250 °C—they can be counted on to guide man's deepest view of space.



EMR Model 549-174, a photomultiplier electronic sensor with matched channels, was designed to generate error signals used to fine tune the Space Telescope's alignment with its "guide" stars. It operates in a photon counting mode and is sensitive to visible light in the spectral range of 466 to 700 nanometers.

For more information call or write:

SANGAMO WESTON
Schlumberger

EMR PHOTOELECTRIC

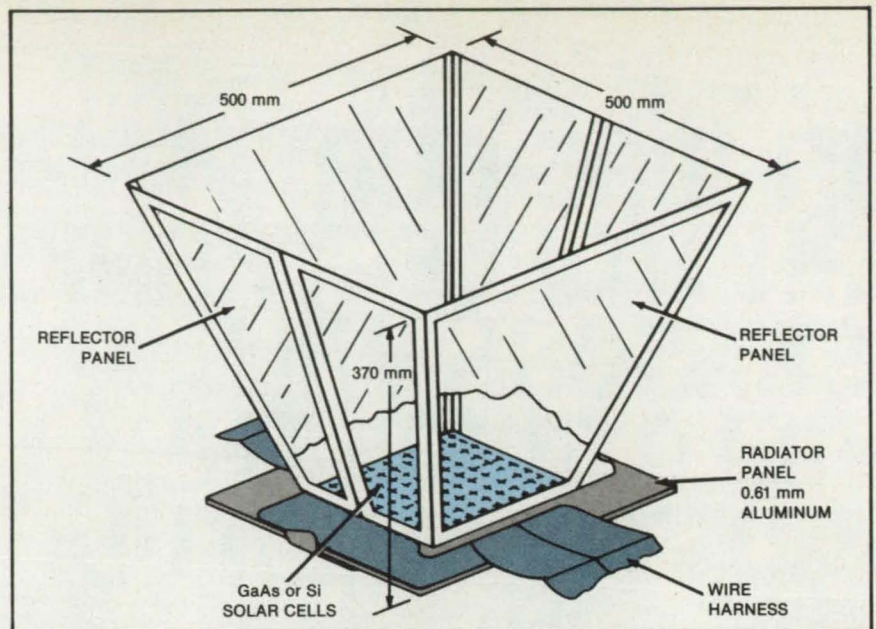
P.O. Box 44, Princeton, NJ 08542 • 609-799-1000

energy in the system. The technique is applicable, with modifications, to the analysis and design of other multiple-cell reflecting photovoltaic systems.

Each concentrator in an array (see figure) includes aluminized-polyimide-film reflectors stretched on molded-plastic frames. The solar panel at the base of the concentrator contains Si or GaAs cells 50 by 50 mm or 20 by 20 mm, respectively. In the example of the figure, the geometric concentration ratio is 6.

The optical analysis is conducted with a ray-tracing computer program that handles collimated and diffuse incoming light and both specular and diffuse reflection. The effects of diffuse illumination and reflection are modeled by Monte Carlo techniques. The program also includes the partial absorption of energy by reflecting surfaces.

The most complicated part of the thermal model is that which describes the solar-cell panel and its surroundings. The model must include the absorption of energy in each cell from direct and concentrated Sunlight, the loss of thermal energy by conversion of radiant energy to electricity, the radiation of heat from the cells back onto the reflectors and directly out into space, the nonuniform heating of the solar-cell panel and reflectors, the conduction of heat from the cells into the supporting substrate, the distribution of heat by the substrate (which extends beyond the solar panel), and radiative and other interactions between the substrate and the environment. Heat-transfer calculations must also include the exchange of radiation among concentrators in an array. A previously-developed thermal-analysis code takes advantage of the symmetry of the array and of individual concentrators to reduce the number of radiative and reflective nodes used to model the full array.



A Hollow Pyramidal Concentrator reflects Sunlight onto a panel of photovoltaic cells. A comprehensive optical, thermal, and electrical analysis is performed on an array of units like this one.

The electrical analysis considers the non-uniform heating of the solar panel, taking into account the variation of the electrical performance with the temperature of the cells. Subject to the constraints of the series/parallel connection scheme of the panel, the voltage and current of each group of parallel-connected cells are found iteratively by a Newton-Raphson calculation. The panel voltage is taken as the sum of voltages of the series-connected groups.

The ray-tracing analysis shows that the optical performance of the particular concentrator design is highly tolerant of pointing errors. The upper reflecting corners were found to be sources of reflector heating. Lower, more uniform reflector temperatures

could be obtained at a small sacrifice in optical efficiency by making these zones non-specular. The coupled thermal/electrical analysis showed that nonuniform illumination need not produce large losses due to mismatches among cells as long as the cells are connected in parallel groups across the half-panels. Experimental tests with a full-scale prototype concentrator confirmed the insensitivity to pointing errors.

This work was done by Edward P. French, Michael W. Mills, and Zdenek Backovsky of Rockwell International Corp. for Marshall Space Flight Center. For further information, Circle 7 on the TSP Request Card. MFS-28021

Crossover Concept for Optical Printed Circuits

Light traps and optimum optical path widths reduce crosstalk in planar crossovers.

NASA's Jet Propulsion Laboratory, Pasadena, California

It may be possible to reduce crosstalk between optical signals in intersecting optical conductors by taking two steps. The first is to minimize the amount of light diffracted into the wrong conductor by selecting the optimum conductor width. The second is to place light traps in each conductor.

The need for signal paths to cross arises in optical integrated circuits just as it does in conventional electronic integrated circuits. Methods have been proposed for making

multilayered "overpass" structures that keep the crossing optical conductors from intersecting. However, it would reduce fabrication complexity if single-layer crossings could be used.

The amount of light diffracted from one signal path to the other depends on both the wavelength, λ , and on the conductor width, d (see figure). With very narrow conductors ($d < \lambda$) diffraction crosstalk would be severe. On the other hand, crosstalk would be small

for very wide conductors ($d \gg \lambda$). Between these extremes the fraction of light appearing as crosstalk would have a series of maximums and minimums as a function of d , because of interference effects. The first minimum would occur near $d = \lambda$.

Diffracted light entering the wrong conductor would tend to propagate in a zigzag manner, while the desired signal light in the same conductor would proceed straight along the conductor. The zigzagging com-

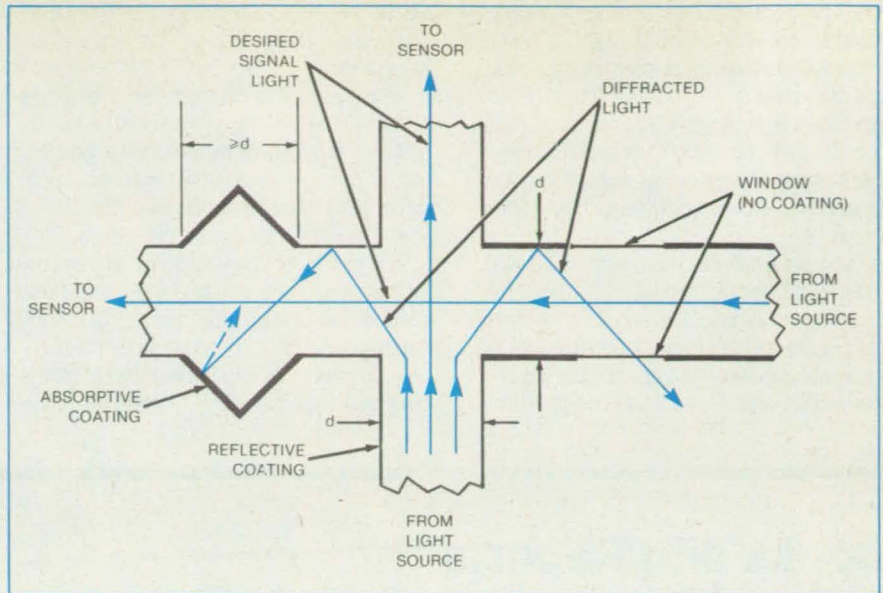
ponent can be preferentially attenuated by various traps, two of which are suggested in the figure.

The diamond-shaped trap shown at the left could be made with an absorptive coating. Alternatively, the walls of the trap could be left clear so that the trapped light would leak out. (Whether this would be desirable depends on whether the exiting light would cause trouble in some other component or be absorbed harmlessly in some other structure.) With a clear trap, ambient light would have to be excluded by a cover.

Sufficient attenuation might be achieved even more simply by merely leaving a portion of the conductor surface uncoated, as shown at the right in the figure. Normal signal light would be totally reflected internally, while a significant fraction of the zigzagging crosstalk light would escape.

How well these techniques would work depends in part on the quality of the optical conductors (particularly their surface smoothness) and on how closely the optical-signal mode of propagation approaches the ideal. The nature of the signals is also important: With digital signals, less crosstalk attenuation would be required than for analog signals.

This work was done by Robert S. Jamieson of Caltech for NASA's Jet Propulsion Laboratory. For further informa-



A Planar Optical Crossover could attenuate crosstalk light with a diamond-shaped trap, as shown in the left arm of the crossover. The clear-window attenuator shown in the right arm is simpler, but probably would be less effective than the diamond trap. In an actual crossover, there would be a trap in both legs.

tion, Circle 10 on the TSP Request Card.

Title to this invention, covered by U.S. Patent No. 4,382,655, has been waived under the provisions of the National Aeronautics and Space Act [42 U.S.C. 2457(f)], to the California Institute of Technology. For

further information regarding nonexclusive or exclusive licensing, contact Edward O. Ansell, Director of Patents and Licensing, 307 Keith Spalding Bldg., Caltech, Pasadena, CA 91125. Refer to NPO-15131.



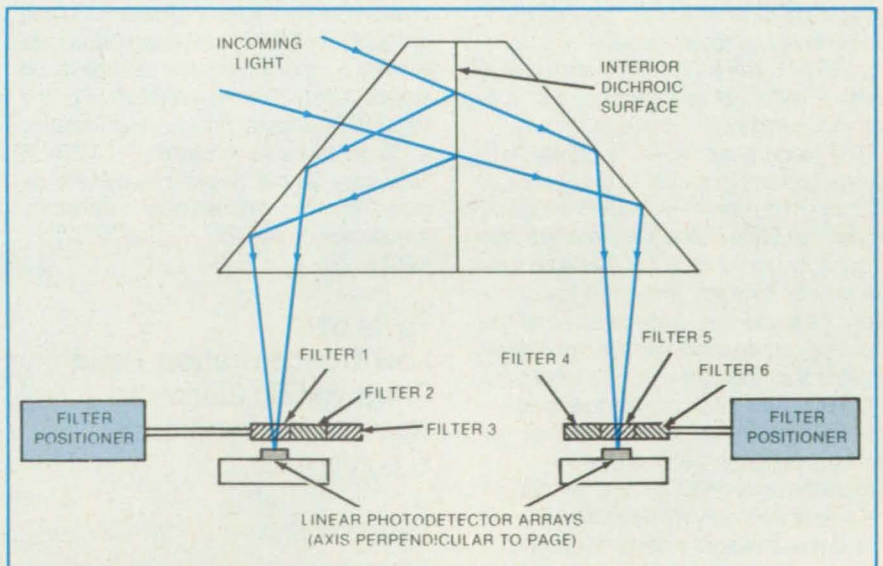
Multiband Selector for Linear Photodetector Array

A line image is observed simultaneously in two or more spectral bands.

Goddard Space Flight Center, Greenbelt, Maryland

The spectral analysis of line images (or of two-dimensional images synthesized from swept-line images) is enhanced by a multiband selector that allows simultaneous viewing of the same scene in two or more wavelength bands. Since the band impinging on each of two or more photodetector arrays is independently selectable, there is flexibility in the choice of band combinations. These capabilities are valuable in such multispectral-imaging applications as spaceborne and airborne visible and infrared observation of the Earth for geology, oil and mineral exploration, biomass distribution, forestry, agriculture, and urban and rural development.

A two-band version is shown in the figure. The focused incoming light beam enters a beam-splitting prism, wherein the light is split into two beams in different spectral regions by an interior dichroic surface. The light in each beam passes through an adjustable filter and comes to focus on a linear array of photodetectors to form a line im-



Incoming Light Is Focused Through a Beam Splitter onto two linear arrays of photodetectors to form line images. An array of band-pass filters above each detector array is positioned to select the spectral band of the line image.

age. The photodetector outputs are processed by conventional circuitry.

Each adjustable filter consists of a side-by-side array of band-pass filters. Each band-pass filter is slightly wider and longer than the detector array to assure full coverage in case of positioning error. The band-pass filters are aligned parallel to the detector arrays.

The spectral band impinging on a detector array is selected by positioning the corresponding band-pass filter above that array. The positioning could be done manually or automatically as by a motor-driven micrometer with position-feedback control that

places the filter at a commanded position corresponding to a commanded wavelength.

Many variations on the basic theme are possible. The incoming light could be initially split by a previous dichroic surface, sending part of the light to another two-band apparatus simultaneously so that the same scene could be viewed in four bands.

The number of beam splits is limited only by the available space and the energy loss at each split. The possible number of combinations of bands is determined by the number of beam splits and the number of bands in each adjustable filter. For example, if the

beam is split into four images and there are three band-pass filters in each filter array, then there are $3^4 = 81$ different spectral-band combinations available.

This work was done by Herbert L. Richard of Goddard Space Flight Center. For further information, Circle 80 on the TSP Request Card.

This invention is owned by NASA, and a patent application has been filed. Inquiries concerning nonexclusive or exclusive license for its commercial development should be addressed to the Patent Counsel, Goddard Space Flight Center [see page .21]. Refer to GSC-12911.

Books and Reports

These reports, studies, and handbooks are available from NASA as Technical Support Packages (TSP's) when a Request Card number is cited; otherwise they are available from the National Technical Information Service.



Integrating Residential Photovoltaics With Power Lines

Break-even costs and economic attractiveness are assessed for a variety of locales.

Rooftop solar-cell arrays that feed their excess power to the electric-utility grid for a fee are a potentially attractive large-scale application of photovoltaic technology, a report finds. The report presents an assessment of the break-even costs of such arrays under a variety of technological and economic assumptions.

The report gives allowable photovoltaic system costs ranging from \$1 to \$3 per peak watt for small residential systems in locales across the United States. The systems range in capacity from 2 to 10 kW. Because they are built on rooftops, they have low structural costs and can displace some of the costs of conventional roofs in new-home construction. Thus, the report calculates the value of a photovoltaic system to a prospective new-home buyer, based on savings that can be expected in the purchase of electricity from the utility grid and on revenues from the sale of electricity to the utility.

The major factors in system value differences from site to site are local weather conditions, electric generation capacity of the local utility, types of fuel used by the utility, customer power-consumption pattern, and

state taxation policy. Interestingly, locales having the highest insolation are not necessarily the most economically attractive sites; for example, Phoenix, Arizona has a lower break-even cost than Boston, Massachusetts. When residential photovoltaics are connected in parallel to the utility, high percentages of energy are sold back to the grid. Break-even costs vary widely with financing methods and tax structures.

Significant reductions in the cost of photovoltaic generation below present levels are needed before residential connection to the grid becomes practical, the report concludes. Also needed is a resolution of such institutional impediments as liability, standards, metering, and technical integration.

This work was done by Chester S. Borden of Caltech for NASA's Jet Propulsion Laboratory. Further information may be found in NASA CR-173205 [N84-16643/NSP], "The Value of Residential Photovoltaic Systems: A Comprehensive Assessment" [\$13]. A copy may be purchased [prepayment required] from the National Technical Information Service, Springfield, Virginia 22161. NPO-16331

Tests of Low-Concentration-Ratio Photovoltaic Elements

Accuracy of predictions is confirmed.

Marshall Space Flight Center, Alabama

A report describes performance measurements on elements of low-concentration-

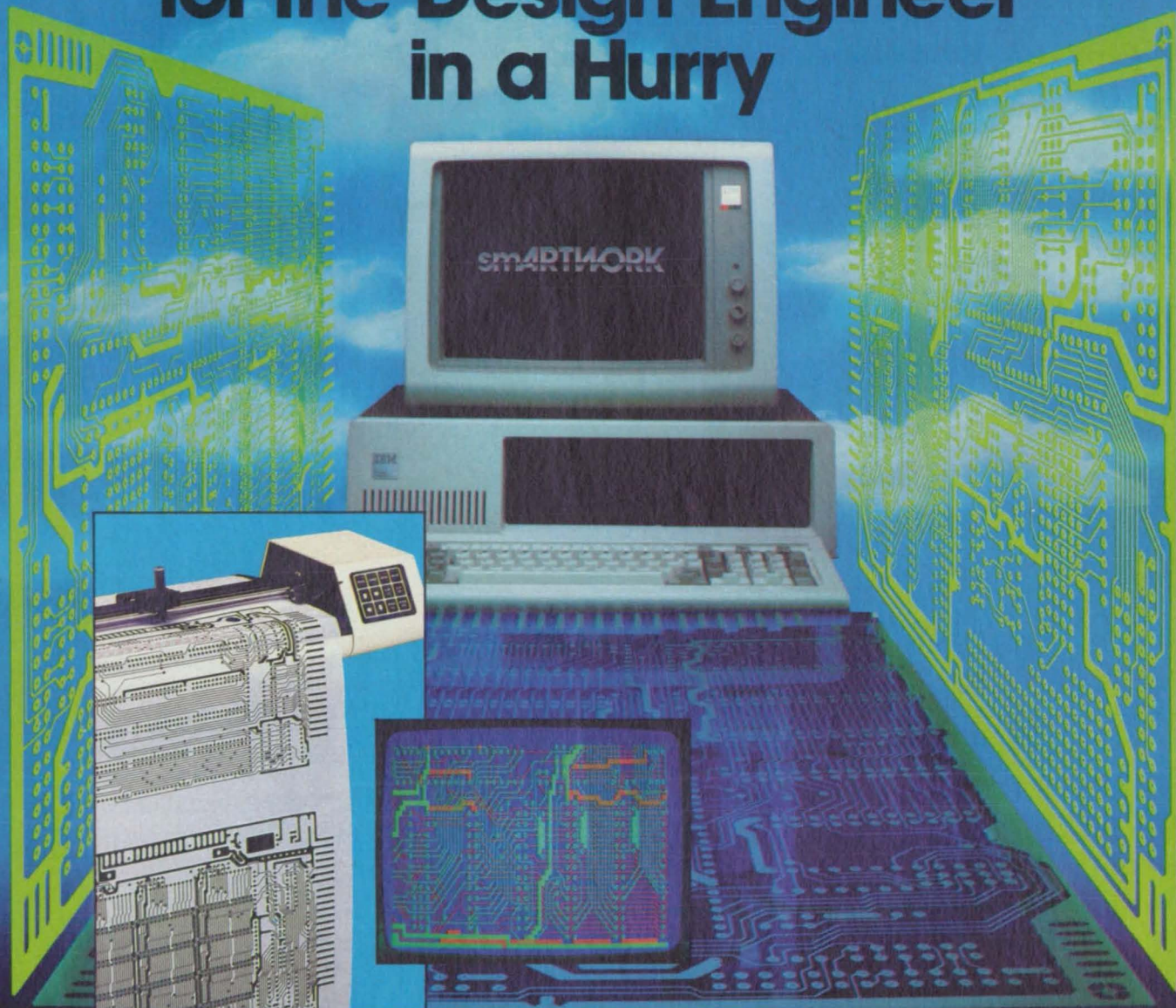
ratio solar arrays (LCRSA's) employing silicon and gallium arsenide photovoltaic cells. The measurements were intended to verify predictions of performance based on mathematical models. The measured and predicted values were found to agree closely for both normal and off-normal pointing of the array toward the Sun.

LCRSA's are designed to provide 50 to 350 kilowatts at relatively low cost for manned space stations in low Earth orbit. The low geometric concentration ratio of 6 allows the use of a design that reduces the cost, makes the array simple to deploy in space, and allows either silicon or gallium arsenide cells to be used. The array consists of thin-film reflectors stretched on rigid frames, a solar-cell panel, and a combination substrate and heat radiator for the panel.

Cells measuring 20 by 20 millimeters were used in the measurements. In the laboratory, individual solar cells were characterized under concentrated simulated Sunlight (concentration ratios of 1, 4, and 6) and at temperatures of 28°, 50°, and 70° C. Laboratory solar-simulator tests were also performed on half-panels. Natural-Sunlight tests were performed on the concentrator elements. Performance was measured as a function of off-angle pointing and various mechanical distortions. Several cells were subjected to dark reverse-bias tests, which provided data for evaluation of the need for bypass diodes.

This work was done by Michael W. Mills and Zdenek F. Backovsky of Rockwell International Corp. for Marshall Space Flight Center. For further information, Circle 50 on the TSP Request Card. MFS-28020

Circuit-Board-Artwork Software for the Design Engineer in a Hurry



For only \$895, smARTWORK® lets the design engineer create and revise printed-circuit-board artwork on the IBM Personal Computer. You keep complete control over your circuit-board artwork — from start to finish.

Forget the tedium of taping it yourself or waiting for a technician, draftsman, or the CAD department to get to your project.

smARTWORK® is the only low-cost printed-circuit-board artwork editor with all these advantages:

- Complete interactive control over placement and routing
- Quick correction and revision
- Production-quality 2X artwork from a pen-and-ink plotter
- Prototype-quality 2X artwork from a dot-matrix printer
- Easy to learn and operate, yet capable of sophisticated layouts
- Single-sided and double-sided printed circuit boards up to 10 x 16 inches
- Multicolor or black-and-white display

System Requirements:

- IBM Personal Computer, XT, or AT with 256K RAM, 2 disk drives, and DOS Version 2.0 or later
- IBM Color/Graphics Adapter with RGB color or black-and-white monitor
- IBM Graphics Printer or Epson FX/MX/RX series dot-matrix printer
- Houston Instrument DMP-41 pen-and-ink plotter
- Optional Microsoft Mouse

The Smart Buy

At \$895, smARTWORK® is proven, convenient, fast, and a sound value. Call us today. And put it to work for yourself next week.



Wintek Corporation
1801 South Street
Lafayette, IN 47904-2993
Telephone: (317) 742-8428
Telex: 70-9079 WINTEK CORP UD

In Europe contact: RIVA Terminals Limited,
Woking, Surrey GU21 5JY ENGLAND,
Telephone: 04862-71001, Telex: 859502

smARTWORK®, Wintek and the Wintek logo are registered trademarks of Wintek Corporation.

Augmenting Thrust With Waste Heat

Energy rejected by a nuclear reactor would add to rocket thrust.

According to a NASA report, waste heat from an onboard nuclear reactor could be utilized to increase the specific impulse of a rocket engine. Instead of adding energy to the rocket exhaust through electric heating wires or an arc discharge (the conventional approach),

the propellant is preheated by the thermal exhaust of the nuclear power supply. The advantage is that the heat is added at a relatively low temperature.

Waste heat from the reactor at a temperature of about 900 K would be used. While the reactor provides full power for electrical systems, 90 percent of its thermal power is available for preheating the propellant. More power and, therefore, more thrust are available than with electrical augmentation, since thermal-to-electrical conversion is only about 10 percent efficient. By varying the proportions of thermal augmenta-

tion energy and chemical reaction energy, it is possible to vary the thrust and specific impulse to obtain the best combination for a specific mission. With augmentation, the specific impulse can be increased by as much as 23 percent over that of a conventional engine.

This work was done by Robert H. Frisbee of Caltech for NASA's Jet Propulsion Laboratory. To obtain a copy of the report, "A Parametric Study of Thermally Augmented O₂/H₂ Rocket Engines," Circle 112 on the TSP Request Card. NPO-16218

Cost effective fabrics for people who can't afford failures.



Aerospace...Defense...Composites... Safety Apparel...Filtration

More than 300 fabrics engineered to exacting performance specifications are being used to insulate, dampen, seal, filter, suppress noise, retard fire, protect people and resist hostile environments. Tex-Tech Industries has the problem-solving experience and manufacturing capabilities to produce fabrics that exceed your expectations of performance.

We can help shape your ideas from concept to production with the "material difference".

Contact Tex-Tech Industries, Inc., Main Street, P.O. Box 8, North Monmouth, ME 04265. Call (207) 933-4404.



Computer Programs

These programs may be obtained at a very reasonable cost from COSMIC, a facility sponsored by NASA to make raw programs available to the public. For information on program price, size, and availability, circle the reference number on the TSP and COSMIC Request Card in this issue.

Duct-Flow Analysis

A quasi-two-dimensional velocity distribution through an annular duct is calculated.

Turbomachinery components are often connected by ducts, which are usually annular. The configurations and aerodynamic characteristics of these ducts are crucial to the optimum performance of the turbomachinery blade rows. One available method of duct-flow analysis is a finite-difference, stream-function analysis. This is a good method of analysis, but it requires a large, complex code to handle arbitrary geometries. Computer storage and execution time are fairly large. A faster and easier method of analyzing the flow through a duct with the axisymmetric swirling flow is the velocity gradient method, also known as the stream filament or streamline curvature method.

Computer program ANDUCT has been developed for calculating the velocity distribution along an arbitrary line between the inner and outer walls of an annular duct with axisymmetric swirling flow. The velocity gradient equation is used with an assumed variation of meridional streamline curvature. Upstream flow conditions can vary between the inner and outer walls, and an assumed total pressure distribution can be specified. This flow field could also be calculated by the MERIDL program, which is described in "Flow Velocities and Streamlines" (LEW-

12966), page 100, *NASA Tech Briefs*, Vol. 3, No. 1 (Spring 1978). However, ANDUCT has the advantages of much less computer time (approximately one-third the time for the given numerical example) and very much less storage. Since MERIDL is a large, general code for a finite-difference, stream-function solution including a blade row, the storage would be very much larger even with reduced array sizes. Thus, the ANDUCT program is a convenient program to use for analyzing an annular duct with modest computer time on a computer with small memory.

The objective of this analysis method is to calculate the quasi-two-dimensional velocity distribution that satisfies a specified mass flow through an annular duct. The velocity variation along a quasi-orthogonal between the inner and outer wall is determined by a momentum equation along the quasi-orthogonal. The quasi-orthogonal is a straight line between the walls of the annulus. With suitable assumptions, this leads to a velocity gradient equation. The velocity gradient equation is an ordinary differential equation that can be solved numerically. This determines the velocity distribution along the quasi-orthogonal. The analysis for one quasi-orthogonal is independent of that for other quasi-orthogonals. When the analysis is done for several lines, a velocity distribution is obtained for the entire duct.

The basic simplifying assumptions used to derive the equations and to obtain a solution along any quasi-orthogonal are the following:

1. The flow in the annulus is steady;
2. The flow is axisymmetric;
3. The fluid is a perfect gas with constant specific heat c_p ;
4. The only forces along a quasi-orthogonal are those due to momentum and pressure gradient;
5. There is linear variation of meridional streamline curvature along a quasi-orthogonal; and
6. There is a linear variation of meridional streamline angle along a quasi-orthogonal.

The flow may be axial, radial, or mixed. Whirl, stagnation pressure, and stagnation temperature must be specified but may vary between the inner and outer walls. Losses and heat transfer are not included in the analysis but may be simulated by specifying appropriate stagnation temperature and pressure distributions. ANDUCT is written in FORTRAN IV for use on an IBM 370/3033 computer.

This program was written by Theodore Katsanis of Lewis Research Center. For further information, Circle 65 on the TSP Request Card.
LEW-14000

YOU SHOULD HEAR WHAT U.S. SAVINGS BONDS ARE PAYING NOW!

Give us a call and you'll hear all about U.S. Savings Bonds' new money market rates, as well as the current rate. We'll also tell you about the guaranteed return, tax advantages, where to buy variable rate Savings Bonds and much more.

1-800-US-Bonds



U.S. SAVINGS BONDS
Paying Better Than Ever

A public service of this publication.



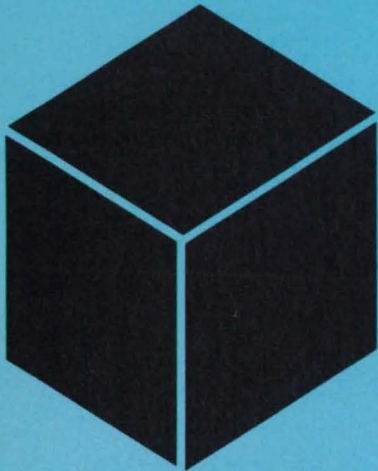
WHAT'S YOUR HIGH "Q"?

In precision electronic components, GAF Carbonyl Iron Powders show the outstanding performance characteristics necessary to the design of cores with high Q-values, excellent permeability, low loss factors and superior resistance to magnetic shock and temperature. GAF Carbonyl Iron Powders also perform well in alloy production and powder metallurgy, magnetic fluid systems, inductive heating and chemical reactions (as catalysts).

GAF is the sole domestic manufacturer of Carbonyl Iron Powders in North America. For more detailed information, contact GAF Corporation, Chemical Division, 1361 Alps Road, Wayne, NJ 07470, 201 628-3000.

GAF® CARBONYL IRON POWDERS

Circle Reader Action No. 359



Hardware, Techniques, and Processes

- 88 Filament Guides for Silicon-Ribbon Growth
- 92 Lightweight Electrical Insulation
- 92 Diffusely Reflecting Paints Containing TFE
- 94 Paramagnetic Precipitates May Raise Supercurrent
- 94 Intercalated-Carbon Low Resistivity Fibers
- 95 Ion Implantation Improves Bearing-Surface Properties
- 96 Microfissuring in Electron-Beam-Welded Nickel Alloy
- 96 Measuring Hydrogen Concentrations in Metals
- 97 Production Process for Strong, Light Ceramic Tiles
- 98 Improved Electrodes for Lithium Cells
- 98 Fluidized-Bed Particles Scavenge Silicon Fines
- 100 Magnetron-Sputtered Amorphous Metallic Coatings
- 100 Blowing Polymer Bubbles in an Acoustic Levitator
- 101 Determining Fiber Orientation in Graphite-Reinforced Composites

Books and Reports

- 102 Predicting the Fatigue Life of Structures
- 103 Corrosive Effects of Burning Fuels
- 103 Synthetic Organic Materials in Nuclear Powerplants
- 103 Degradation of Dielectrics in Space
- 104 Plasma Deposition of Doped Amorphous Silicon
- 104 Bonding Solar-Cell Modules

Computer Programs

- 104 Modeling a Transient Catalytic Combustor
- 105 Plastic and Failure Analysis of Composites
- 105 Exhaust Effluent Diffusion Model

Filament Guides for Silicon-Ribbon Growth

Contamination would be reduced in a modified growth system.

NASA's Jet Propulsion Laboratory, Pasadena, California

In a proposed silicon-ribbon-growth apparatus, capillary filament guides would be integral parts of the crucible, extending from the bottom to the top of the melt. The addition of the guides is expected to result in better thermal control of the growth process and higher silicon purity.

In the edge-supported-pulling method of silicon-ribbon growth, the ribbon edges are defined by filaments that are pulled up through the melt (see left of figure). To minimize the residual stress in the grown ribbon, the thermal-expansion coefficient of the filament material should match that of silicon as closely as possible. Typical filament materials that meet this criterion include aluminosilicates; unfortunately, these materials also contaminate the silicon melt.

In the improved apparatus (see right of figure), the filaments are drawn upward through capillary guides made of the same material as that of the rest of the crucible. The melt level is maintained at or just above the tops of the guides. Surface tension keeps the molten silicon from leaking down the guides.

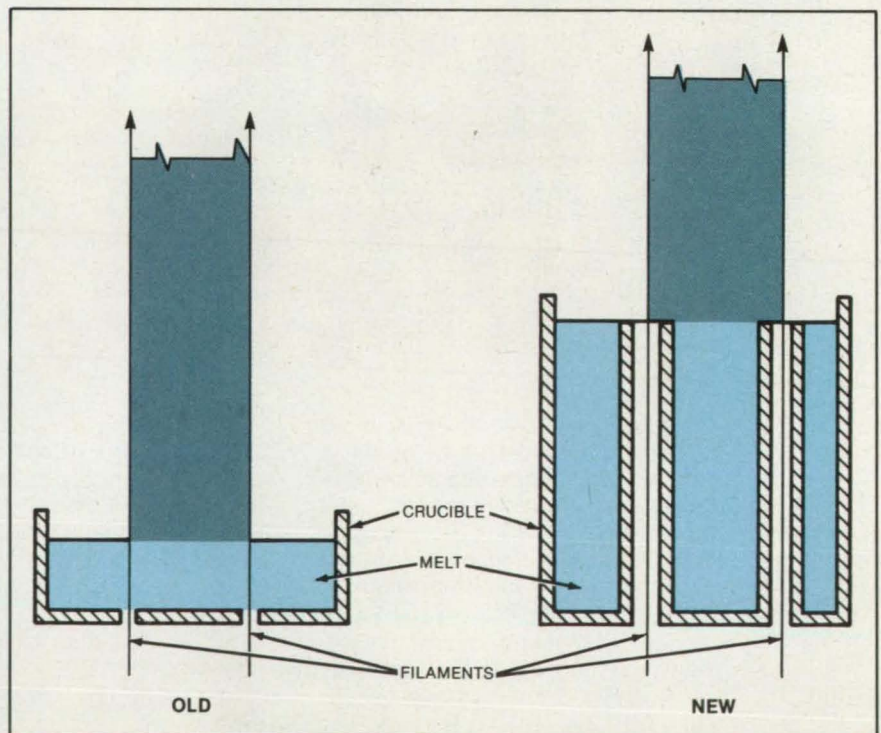
Because the filaments are in contact

with the molten silicon over a much shorter distance and for a much shorter time than they would be if pulled up through the full melt depth, the amount of impurities dissolved into the melt should be much less than before. Since it is no longer necessary to use a relatively shallow melt to minimize impurities from the filaments and to prevent silicon leakage due to head pressure, a deeper melt can be used.

The higher thermal inertia of a deeper melt reduces fluctuations in the ribbon-growth rate, thereby giving rise to ribbons of higher quality. The deeper reservoir should also enable greater dispersion of impurities from the filament, thereby increasing the ribbon purity even further.

This work was done by Andrew D. Morrison of Caltech for NASA's Jet Propulsion Laboratory. For further information, Circle 15 on the TSP Request Card.

Inquiries concerning rights for the commercial use of this invention should be addressed to the Patent Counsel, NASA Resident Office-JPL [see page 21]. Refer to NPO-16306



In the **Edge-Supported-Pulling Method** of silicon-ribbon growth, filaments pulled up through the melt define the ribbon edges. In the new version of the apparatus, the filaments would make contact with the melt over a much shorter distance than in the old version, thereby reducing the amount of impurities dissolved from the filaments.

TANSTAAFL

After the War of the Almonds, the Land of Kulumar was the richest and most powerful of all.

Its fields were bountiful and its granaries were full.

Its flocks were fat and sleek.

The Kulumese were proud and productive. They worked and they rejoiced in the highest standard of living known.

Sire The Generous surveyed all this plenty and said: "Surely a country as rich as Kulumar should provide food and housing and garments for our less fortunate. I will ask the Lawmakers to levy a tax on the workers to provide for this."

And the Lawmakers, each of whom hoped one day to become Sire, levied the taxes. They then said: "Let there also be free circuses for those who do not work. And let there be soft hassocks and free food and wines for those who watch the circuses."

And the Lawmakers levied more taxes.

When the workers of Kulumar heard of the free circuses, the soft hassocks, and the food and wines, and then figured their now monstrous taxes, they said: "This is for us."

The farmers left the fields. The shepherds abandoned their flocks. The weavers laid down their shuttles. The blacksmiths cooled their forges. All the Kulumese were watching the free circuses.

Plenty turned to scarcity. No longer was there abundant food. Garments were hard to come by. The Kulumese did not even have camel chips to heat their tents.

Prices rose and rose. And the Lawmakers raised taxes again and again. (It was the only thing they knew how to do.)

Misery and gloom replaced joy and pride.

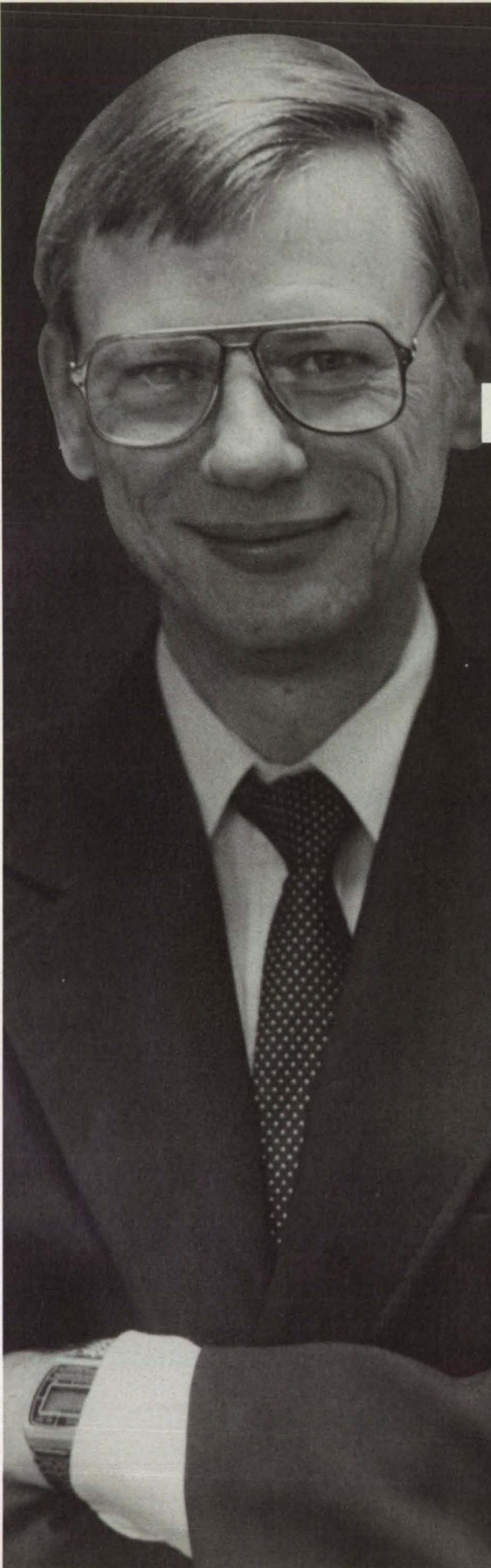
And Sire The Generous, who was well-intentioned, went to the Wise Man of the Mountain and said: "Wise One, I have tried to give the good life to my people, but they no longer want to work. Food and goods are scarce. Prices are outrageous. Taxes are even more so. Give me a solution."

And the Wise Man of the Mountain replied in Kulumese: "TANSTAAFL."

Which means: "There Ain't No Such Thing As A Free Lunch."

The above fable TANSTAAFL is reprinted with permission from *Industry Week*, April 28, 1975. Copyright ©Penton IPC, Inc., Cleveland, OH.

The term was first noted by *NTB's* editors in *The Moon Is A Harsh Mistress* by Robert A. Heinlein, ©1965, G.P. Putnam.

A black and white portrait of William L. Rasmussen, a middle-aged man with short hair and glasses, wearing a dark suit, white shirt, and patterned tie. He is smiling slightly and looking towards the camera.

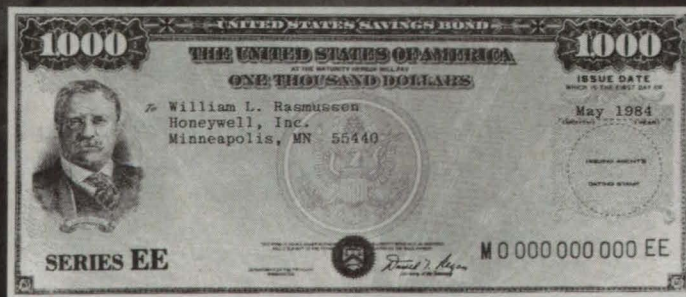
"I invest my time in high technology. I invest my money in U.S. Savings Bonds."

William L. Rasmussen
Honeywell, Inc.

William L. Rasmussen, one of the developers of the ring laser gyro, says: "I've tried many forms of investment and I'm satisfied I can't do better than U.S. Savings Bonds."

Just look at the facts. New competitive-rate U.S. Savings Bonds are the answer to sensible savings without risk. Today's Bonds pay higher market-based interest rates—the sky's the limit. And a guaranteed minimum return protects your investment. Bonds are exempt from state and local taxes, so the effective yield is even higher.

Best of all, Bonds are easy to buy—wherever you bank, or through the Payroll Savings Plan where you work. No fees or commissions. And no worries. So save time and money. Buy Bonds.



Take
stock
in America.

The logo for United States Savings Bonds, featuring a stylized eagle with wings spread, perched on a banner that reads "SAVINGS BONDS". The words "UNITED STATES" are written in a circle above the eagle.

A public service of this publication.

SCHOTT ... Precision Optical Glass Made in America and More!!!



Schott Glass Technologies is geared to work with the largest production quantities or the smallest prototype development right here in the USA. Our 300,000 square feet of manufacturing facilities, backed by our scientific knowledge and technical skills, are ready to work for you at every stage of your program.

Our in-house research and development is among the most modern of its kind

anywhere. And we have the marketing and sales know-how to assure you that products made from Schott materials or components get to your customers on time and to specification.

And, above all, Schott Glass Technologies has the widest range of precision optical glass and components available in the Western Hemisphere today.

OPTICAL DIVISION

- OVER 250 TYPES OF OPTICAL GLASSES
- FIBER OPTICS RODS
- HIGH HOMOGENEITY GLASS BLANKS FOR MASSIVE OPTICS
- ZERODUR® — LOW EXPANSION MATERIAL
- PHOSPHATE AND SILICATE LASER GLASSES
- CERENKOV COUNTERS

COMPONENTS DIVISION

- CRT FACEPLATES
- SCIENTIFIC FILTER GLASS
- INTERFERENCE FILTERS
- CRT CONTRAST ENHANCEMENT FILTERS
- FIBER OPTICS SPECIALTIES
- B-270/CLEAR SHEET GLASS
- X-RAY LEAD GLASS
- RADIATION SHIELDING GLASS AND WINDOWS

OPHTHALMIC DIVISION

- CROWN GLASS — CLEAR AND TINTS
- 1.60 LIGHTWEIGHT CROWN GLASS
- HIGH-LITE® — HIGH INDEX LOW DENSITY GLASS
- SUN MAGIC® PHOTOCROMICS — FOR SUNWEAR
- PHOTOCROMICS — FOR PRESCRIPTION
- INDUSTRIAL SAFETY GLASS
- UV FILTERING CROWN
- SPECIALTY GLASS

TECHNICAL SERVICES

- CONTRACT RESEARCH AND DEVELOPMENT
- CUSTOM MELTING
- ANALYTICAL/PHYSICAL/OPTICAL MEASUREMENTS

— and the list goes on . . .

Our commitment . . .

**Research & Development, Manufacturing, Sales, Service — Total Capability
. . . your advantage.**



400 York Ave., Duryea, Pennsylvania 18642
(717) 457-7485 TWX 510-671-4535
Telefax (717) 457-6960

Circle Reader Action No. 383

Lightweight Electrical Insulation

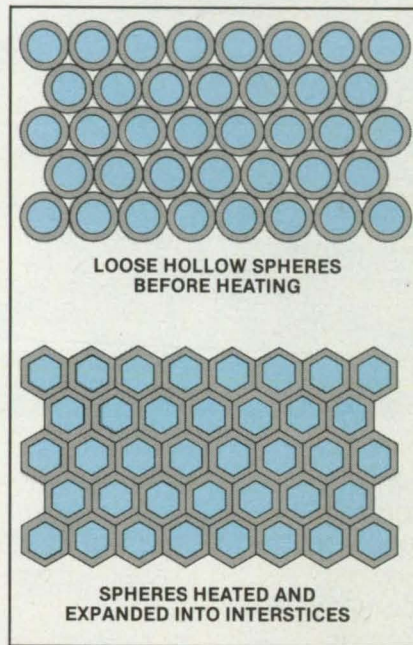
Hollow plastic spheres would be expanded and fused together.

NASA's Jet Propulsion Laboratory, Pasadena, California

A conceptual manufacturing process would make a high-quality foam with a nearly uniform and approximately hexagonal close-packed structure (see figure). Such a foam could be used as lightweight, electrically insulating material in place of solid ceramic, glass, or polymer. Padding to protect against mechanical shocks might be another application for such a dense, regular foam.

The raw material for the foam is a mass of loose, gas-filled polymer spheres, perhaps manufactured by the process described in the preceding article. The spheres are placed in a mold along with the object(s) to be covered. The mold is evacuated to remove the air from the spaces around the spheres.

The mold and its contents are then heated to soften the walls of the spheres. The gas in the spheres forces the walls of the spheres outward, expanding to fill up the interstices. The walls are forced together and become bonded by fusion (or by conventional adhesive bonding if an adhesive is included). The mold is then cooled, leaving a rigid foam with a high strength-to-weight ratio.



Hollow, Gas-Filled Plastic Spheres are piled in a mold (above). Heating in a vacuum softens and expands the spheres, forcing them together into nearly regular hexagonal close packing (below).

It is estimated that the density of such a foam could be as low as 5 to 10 percent of that of ceramic insulation. Suitable insulating plastics for use as spheres include chlorinated polystyrene, polycarbonate, and polyacrylate. The gas filling is preferably sulfur hexafluoride or another electro-negative species. By changing the ratio of spherical-shell thickness to diameter, the strength and dielectric properties of the foam can be modified.

This work was done by James E. Schroeder of Caltech for NASA's Jet Propulsion Laboratory. For further information, Circle 13 on the TSP Request Card.

Inquiries concerning rights for the commercial use of this invention should be addressed to the Patent Counsel, NASA Resident Office-JPL [see page 21]. Refer to NPO-16165.

Diffusely Reflecting Paints Containing TFE

Paints are washable and usable as optical reference surfaces.

Goddard Space Flight Center, Greenbelt, Maryland

Highly reflective, diffused coatings have been developed by incorporating polytetrafluoroethylene (TFE) pigment with alcohol-soluble binders. These coatings are useful on reflectance-standard surfaces for calibrating radiometric instruments in both the laboratory and the field.

Any alcohol-soluble binder can be used, though silicone-based binders work best. Optionally, a nonionic wetting agent can be added to facilitate the coating of the TFE particles by the binder/alcohol mixture. The wetting agent also inhibits the agglomeration of the TFE particles once they are dispersed in the mixture.

The alcohol and binder are mixed together in a blender before adding the TFE. The TFE is preferably outgassed in a mechanical-pump vacuum for a typical interval of 4 hours before adding it to the liquid. Like the wetting agent, the vacuum treatment helps to prevent clumping of the TFE and eases its dispersion throughout the mixture. The mixture should be blended for 3 to 5 minutes before it is used.

The paints have typical shelf lives of at least 4 weeks if refrigerated. The refrigeration reduces the rate of reaction of the binder with itself. Before reusing the coatings, they should be mixed in a blender for several minutes.

These paints can be used on many substrates including metals, plastics, and ceramics. Aluminum is the preferred metal. In preparation for painting, the surface should first be degreased; for example, by a vapor-solvent bath or by washing with a liquid detergent in hot water. After degreasing, the surface should be roughened by sand blasting or abrading.

The roughened surface should be primed before painting. The preferred primer is one part of N-(2-aminoethyl)-3-aminopropyltrimethoxysilane dissolved in 99 parts of isopropyl alcohol and applied by spraying or brushing. The paint is applied to the primed surface by spraying. A

A REPAIR SHOP LIKE NO PLACE ON EARTH.

In low orbits around the Earth, satellites gather, analyze and transmit critical information—for scientists, for corporations, for countries.

Because of the high cost of getting them up there in the first place, some of these satellites are designed to be repaired where they are if something goes wrong.

A manned space station could act as the neighborhood garage—the local spare parts and repair facility for these valuable satellites. That's one reason why

McDonnell Douglas is working to put a space station in orbit by the 1990s.

Since 1960, when we did the first Manned Orbiting Research Laboratory studies, we've been a world leader in space systems. We built the original space station—Skylab. And we've been a pioneer in space systems operations, from launches to payload integration.

Now we're devoting our space experience, systems expertise, and technological ingenuity to taking America the next step into

space—with a manned station.

Such a station could lower the cost of technological upkeep—for science, for industry. We think that's a very good reason to build a repair shop like no place on Earth.



**MCDONNELL
DOUGLAS**

Circle Reader Action No. 374

recommended minimum dry thickness is 30 mils (0.8 mm), which can be achieved by multiple applications.

In most cases, air drying at ambient temperature is sufficient. The coating may be dry to the touch in as little as 1 hour. But since some binders cure slowly (3 to 4 weeks for a full cure), it may be preferable to hasten the process by heating the coated part in an oven. Typical oven-curing temperatures are 85° to 150° C.

The cured paint has a matte finish. Its

reflection characteristic is more nearly lambertian (like an ideal diffuse reflector) than that of other optical-reference paints. The exact reflection or transmission characteristic depends on the coating thickness and the nature of the substrate. Typically, the paint exhibits about 90 percent reflective efficiency in ultraviolet light and 95 percent in visible light.

The paint is stable in the presence of heat and light. Although it is soft, the paint can be washed repeatedly by water

spraying or immersion.

This work was done by Michael C. Shai and John B. Schutt of **Goddard Space Flight Center**. For further information, Circle 19 on the TSP Request Card.

This invention is owned by NASA, and a patent application has been filed. Inquiries concerning nonexclusive or exclusive license for its commercial development should be addressed to the Patent Counsel, Goddard Space Flight Center [see page 21]. Refer to GSC-12883.

Paramagnetic Precipitates May Raise Supercurrent

Higher critical currents are anticipated for Ti/Nb alloys.

Marshall Space Flight Center, Alabama

The addition of Mn to Ti/Nb superconducting alloy has been suggested as a way to increase the critical current (the current beyond which a superconductor reverts to normal conductivity). The improvement is expected to result from differences among the magnetic properties of the crystalline phases present in the Mn/Ti/Nb alloy system.

For a superconductor to carry a large current in a strong magnetic field (as in an electromagnet), the current and its associated magnetic field must be locked in place by "flux pinning." Flux pinning sites may be metallurgical defects of various kinds. Among them are nonsuperconduct-

ing hexagonally-close-packed precipitates, known as the α phase. These anchor the flux by virtue of the magnetic-energy difference between them and the surrounding superconducting body-centered cubic Ti/Nb alloy matrix (the β phase). If the α precipitates are paramagnetic, then the magnetic-energy difference is even more favorable to flux pinning.

It happens that α -phase Ti/Mn alloys are strongly paramagnetic at superconducting temperatures, while β -phase Ti/Mn is no more paramagnetic than β -phase Ti/Nb. Thus, adding Mn to a Ti/Nb alloy should have little effect on the major superconducting β phase, but should con-

fer a strong paramagnetic susceptibility on the α -phase particles. The α -phase particles should therefore become stronger flux pinners, resulting in an increase in critical current.

This work was done by E. W. Collings of **Batelle Columbus Laboratories for Marshall Space Flight Center**. For further information, Circle 32 on the TSP Request Card.

Inquiries concerning rights for the commercial use of this invention should be addressed to the Patent Counsel, Marshall Space Flight Center [see page 21]. Refer to MFS-25925.

Intercalated-Carbon Low-Resistivity Fibers

Uses may include electronic-equipment enclosures.

NASA's Jet Propulsion Laboratory, Pasadena, California

Experiments have shown the feasibility of making lightweight, electrically conductive fibers from graphite intercalation compounds. The fibers are thermally stable in air up to 100° C. These materials might be used as ingredients in composite enclosures for electronic equipment, especially where such equipment must be both light in weight and electrically conductive for electrostatic drainage or radio-frequency suppression.

The conductivity of the fibers is increased by intercalation with CuCl_2 or other compounds. While CuCl_2 intercalation is not new, lower resistivity was obtained in these

Intercalant	Fiber	Resistivity in $\mu\Omega\text{-cm}$
None	P100-4	200 \pm 30
ICl	P100-4	42 \pm 7
Br_2	P100-4	30 \pm 5
CuCl_2	P100-4	15 \pm 3
CuCl_2	P100-3	22 \pm 4
CuCl_2	HTT 3,000	12.9

NOTE: Fibers in the P-100 series have the radial structure.

Electrical Resistivities were measured on commercial carbon fibers treated with the compounds shown at the left.

experiments by the use of improved starting fibers and attention to process details.

Commercial pitch-based fibers were used in the experiments. They were first heat-treated above 3,000° C. Individual fibers were suspended vertically and intercalated with CuCl_2 by sublimation and vapor transport at 480° C, using N_2 and Cl_2 as transporting gases. Runs were also conducted with Br_2/HNO_3 , ICl, ICl/ Br_2 , and Br_2 as intercalants.

For one type of fiber, the treatment with CuCl_2 resulted in a resistivity of 12.9 $\mu\Omega\text{-cm}$, representing a reduction of almost 14 times below the starting value (see table). The im-

provement is believed to be due, in part, to the radial orientation of the graphite-molecule layers in this type of fiber: This geometry is more favorable to the reaction with the vapor. One disadvantage of the radial geometry is that it also exposes more edges for reaction with air and may thereby

decrease thermal stability.

Intercalants other than CuCl_2 may reduce fiber resistivity further, but may not be stable in air. Since pure single-crystal graphite has a room-temperature resistivity of $40 \mu\Omega\text{-cm}$ (as compared with typical starting fiber resistivities of 110 to $390 \mu\Omega\text{-cm}$),

further improvements may be obtained by using fibers of higher initial graphite content.

This work was done by Andre H. Yavrouian and John A. Woollam of Caltech for NASA's Jet Propulsion Laboratory. For further information, Circle 27 on the TSP Request Card. NPO-16307

Ion Implantation Improves Bearing-Surface Properties

Selected ions are fired into rolling elements to increase resistance to rolling-contact fatigue.

Marshall Space Flight Center, Alabama

Implanting nitrogen or titanium ions in metals improves their resistance to fatigue, corrosion, and wear — without altering the bulk properties. Unlike such surface treatments as conventional nitriding, conventional carburizing, and coating, ion implantation is a low-temperature process, requires no finishing operations, and produces a highly-alloyed surface layer. The implantation process can also help to conserve such strategic materials as chromium and cobalt by using them only where they are needed.

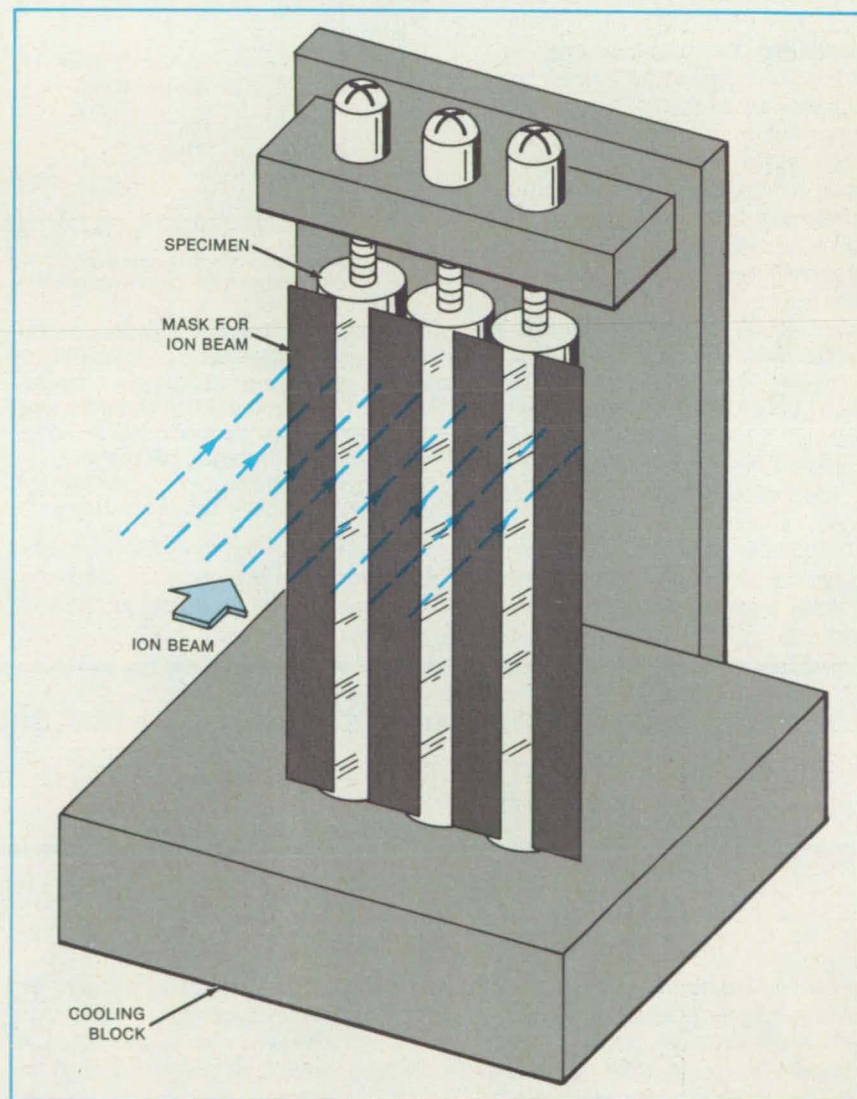
Cylindrical specimens of 440C stainless steel were each implanted in four overlapping increments of 105° of circumference (see figure). The ion beam was masked to prevent sputtering of the implanted ions, and the nitrogen-ion flux was $2 \times 10^{17} \text{ cm}^{-2}$. These provisions resulted in a nitrogen concentration of 24 atomic percent in the surface layer, with a penetration depth of $0.15 \mu\text{m}$.

The process substantially improved the rolling-contact fatigue resistance of the specimens. A 40-percent improvement in fatigue life expectancy was observed after nitrogen implantation and 17 percent after titanium implantation.

The ion-implantation process can be extended to improve such surface properties as corrosion, fatigue, and resistance to oxidation. For example, it can be used to reduce wear in gears and bearings in fine-positioning mechanisms. Once the property to be improved has been identified, the implanted-ion species and substrate can be selected, and the necessary concentration-vs.-depth profile can be determined.

This work was done by M. S. Misra and F. M. Kustas of Martin Marietta Corp. for Marshall Space Flight Center. No further documentation is available.

Inquiries concerning rights for the commercial use of this invention should be addressed to the Patent Counsel, Marshall Space Flight Center [see page 21]. Refer to MFS-25995.



Mask Strips Confine Implantation to 105° arcs on the cylindrical surfaces. After implantation, the specimens are rotated to expose fresh surfaces. The specimens are kept cool by a copper block through which a refrigerant is circulated.

Microfissuring in Electron-Beam-Welded Nickel Alloy

A model predicts powers and speeds that will produce microfissures.

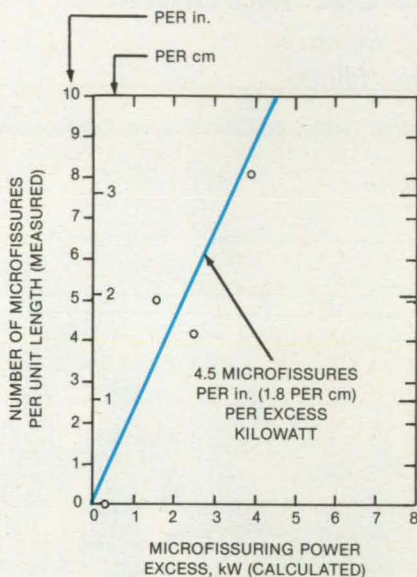
Marshall Space Flight Center, Alabama

A mathematical model has been developed for microfissuring of a commercial nickel alloy during electron-beam welding. The model agrees well with experimental data, although further studies, particularly on thicker plates at higher welding powers, are needed for a more substantial data base and further evaluation of the model.

Microfissures appear to be associated with grain-boundary liquation, or partial melting, below the solidus temperature. Microfissuring does not necessarily occur with grain-boundary liquation alone, however; there must also be sufficient mechanical strain before microfissures form. Under this combination of conditions, cracks tend to open up in a direction perpendicular to the maximum tensile strain. Large grains produced above 1,820° F (993° C) also appear to promote microfissuring by diminishing the number of grain boundaries: Strain concentrated at liquated grain boundaries becomes more potent as the grain boundaries available to absorb it become fewer.

The mathematical model is based on this explanation of microfissure formation. It comprises:

- A model of the temperature field in the vicinity of the weld;
- A computation of the stress/strain state in the vicinity of the weld due to the thermal stresses produced by the temperature field; and



The Number of Measured Microfissures Per Unit Length of Weld was plotted against the excess power calculated by the computer model. Excess power is that above the level likely to produce microfissures. In agreement with the model, measured microfissures increase at the rate of 4.5 per inch (1.8 per centimeter) per excess kilowatt.

- A criterion for the formation of microfissures under the stress/strain conditions prevailing in the heat-affected zones of the weld.

The model takes into account weld power and speed, weld loss (efficiency) characteristics, thermal and mechanical properties of the material, temperature, grain size, and strain. The model predicts the power level that produces microfissuring at a given welding speed. Reducing power below this level should eliminate microfissuring. The model can be adapted to other metals subject to microfissuring by altering the material characteristics.

To verify the accuracy of the model, alloy specimens 0.25-inch (6.4-millimeters) thick were electron-beam welded under a variety of combinations of power and speed. Although it was expected that some adjustment of the model would be necessary, theory and experiment agreed well from the outset (see figure).

This work was done by A. C. Nunes, Jr., of Marshall Space Flight Center. Further information may be found in NASA TM-82531 [N83-29356/NSP], "Interim Report on Microfissuring of Inconel 718" [\$8.50]. A copy may be purchased [prepayment required] from the National Technical Information Service, Springfield, Virginia 22161. The report is also available on microfiche at no charge. To obtain a microfiche copy, Circle 5 on the TSP Request Card. MFS-27041

Measuring Hydrogen Concentrations in Metals

An electrochemical method aids the study of hydrogen embrittlement.

Marshall Space Flight Center, Alabama

A commercial corrosion-measurement system has been adapted to the electrochemical determination of hydrogen concentrations in metals. The system has been used to study hydrogen uptake, hydrogen elimination by baking, the effect of heat treatment, and the effect of electroplating on high-strength steels.

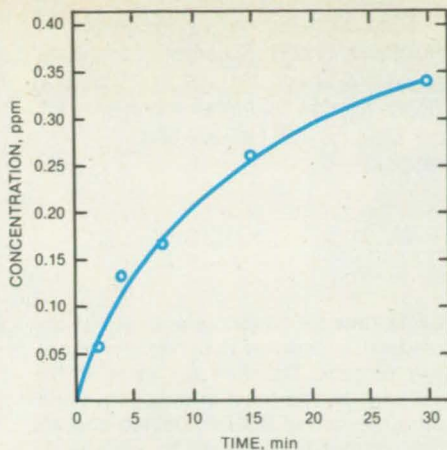
When high-strength steel parts such as aircraft landing gear fail catastrophically, the cause is often hydrogen embrittlement — a condition of low ductility

resulting from absorption of hydrogen. The source of the hydrogen may be corrosion, but can also be a pretreatment such as pickling, welding, or plating. Although the role of hydrogen in such failures has long been recognized, it has been difficult to study because hydrogen concentrations are low and not easily measured.

The new measuring technique is based on the diffusion of hydrogen through a foil specimen of the metal. In a sample holder, hydrogen is produced on one side of the

foil, either by a corrosion reaction or by a cathodic current. Hydrogen diffused through the foil is removed on the other side by a constant anode potential, which leads to oxidation of the hydrogen to water. The anode current is a measure of the concentration of hydrogen diffusing through the foil.

For hydrogen-uptake studies, heat-treated AISI 4340 steel was electrolyzed for various lengths of time in dilute sulfuric acid. As expected, the curve of hydrogen



The Uptake of Hydrogen by AISI 4340 steel is asymptotic; the hydrogen concentration approaches a limiting value with time.

concentration versus time followed an asymptotic approach to a saturation value (see figure). The peak concentration is 100 times that which would prevail if the hydrogen were only on the surface of the specimen in a single layer of atoms. The excess hydrogen, therefore, must be retained in the interior of the metal.

For hydrogen-elimination studies, samples of several high-strength steels were electrolyzed at the same current density for 30 minutes to establish an initial hydrogen concentration. The samples were then baked at 65.6° C for different lengths of time. With the exception of one sample, the effect of the heat treatment was to increase the retention time for hydrogen. This may be a result of a change in metal structure during heat treatment.

For the electroplating experiments, samples were plated with bright and dull cadmium. The cadmium plating was then completely stripped by an ammonium nitrate solution before the hydrogen concentration measurements. The hydrogen concentration for the dull cadmium plating was

Power tower of Kapton®

Lightweight KAPTON helps make solar array experiment possible

Du Pont KAPTON polyimide film insulated the individual cells of the ten-story solar array deployed by the space shuttle "Discovery."

Why was KAPTON the engineering material of choice? It's lightweight, flexible, bondable, transparent, and it retains its structural strength in temperatures from -269° to 240°C.

Explore the down-to-earth advantages of KAPTON, made only by Du Pont. For free sample and literature, write Du Pont Co., KAPTON, Room X 40804, Wilmington, DE 19898.



Circle Reader Action No. 401

found to be 0.07 ppm, while that for the bright cadmium was 0.02 ppm. Although these values are lower than expected, they nevertheless reflect the greater tendency toward hydrogen embrittlement with dull cadmium plating.

This work was done by Merlin D. Danford of Marshall Space Flight Center. Further information may be found in NASA Technical Paper 2113 [N83-16491/NSP], "An Electrochemical Method for

Determining Hydrogen Concentrations in Metal and Some Applications" [\$7]. A paper copy may be purchased [prepayment required] from the National Technical Information Service, Springfield, Virginia 22161. The report is also available on microfiche at no charge. To obtain a microfiche copy, Circle 4 on the TSP Request Card. MFS-27020

Production Process for Strong, Light Ceramic Tiles

Proportions of ingredients and sintering time/temperature schedule are changed.

Lyndon B. Johnson Space Center, Houston, Texas

A production process for lightweight, high-strength ceramic insulating tiles for the Space Shuttle is more than just a scaled-up version of the laboratory process for making small tiles. Instead, the laboratory process has been modified to meet the special requirements of large tiles.

The tiles, which are composed of silica fibers and aluminum borosilicate fibers [known as fibrous refractory composite in-

sulation (FRCI)], are stronger than all-silica tiles previously used. The boron in the aluminum borosilicate fibers allows fusion at points where fibers contact each other during sintering, thereby greatly strengthening the tile structure.

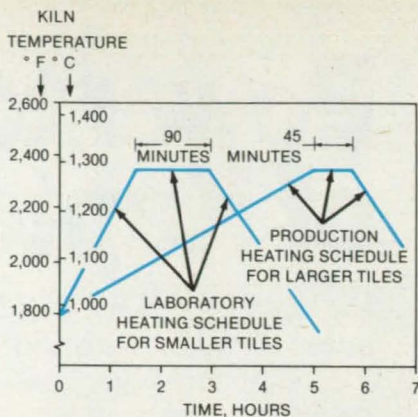
The specific tile material, FRCI-12, has a density of 12 lb/ft³ (192 kg/m³). It has approximately the same tensile strength and insulating properties as those of the all-silica

counterpart, LI-2200, which has a density of 22 lb/ft³ (352 kg/m³).

The new process produces billets measuring 16.2 by 16.2 by 7.9 inches (41.2 by 41.2 by 20.1 centimeters); the laboratory process, in contrast, made billets measuring only 8.5 by 8.5 by 4.5 inches (21.6 by 21.6 by 11.4 centimeters). A higher proportion of

both silica and aluminum borosilicate are used to form the slurry from which the billets are cast and a modified sintering cycle is employed so that the fibers fuse adequately but billet shrinkage is kept to a minimum. These provisions ensure that the larger tiles not only have the strength but also have the low thermal conductivity of the smaller tiles.

One of the large billets requires 9.35 lb (4.24 kg) of silica fibers, 2.64 lb (1.19 kg) of aluminum borosilicate, and 0.24 lb (0.11 kg) of silicon carbide powder. The dry density is 10 lb/ft³ (160 kg/m³) — higher than that of the laboratory method. However, after slowly rising to the sintering temperature of 2,400° F (1,315° C) and dwelling there for only 45 minutes (see figure), the finished



large tile has the same low density as the smaller laboratory tile.

This work was done by E. R. Cordia, G. R. Holmquist, and R. S. Tomer of Lockheed Missiles & Space Co., Inc., for Johnson Space Center. For further information, Circle 33 on the TSP Request Card. MSC-20602

Cycle Time for Sintering is longer for the production process than for the laboratory process. The tiles are raised to the sintering temperature at only about one-third the rate of the lab method and are held at that temperature for only about half the time.

Improved Electrodes for Lithium Cells

A chlorinated elastomeric binder improves the cell mechanical and electrical characteristics.

NASA's Jet Propulsion Laboratory, Pasadena, California

A rubber-based binder for carbon electrodes improves the performance of lithium electrochemical cells. When substituted for PTFE binder, chlorinated polyethylene rubber allows high cell-discharge rates and higher stored energy per unit volume. In addition, it costs about one-eighth as much as PTFE.

The initial step in preparation of the electrode is dissolution of chlorinated polyethylene rubber in an organic solvent such as chloroform. The cathode material, such as carbon black, is blended in the solution to give a mixture of 10 percent by weight of binder. The mixture is applied to a current-collector screen of nickel, aluminum, or carbon, the solvent is evaporated, and the screen is rolled into sheet form.

PTFE is not an elastomer at room temperature (at which lithium cells are assembled and operated). The cathode formed with a PTFE binder cannot tolerate electrode expansion, which occurs during cell discharge. It therefore has poor mechanical properties, tending to be brittle. Chlorinated polyethylene rubber, in contrast, is an elastomer. It can be rolled without cracking in cell fabrication and readily accommodates electrode dimensional changes.

A more polar material than PTFE, chlorinated polyethylene rubber is more readily wet by the electrolyte, such as sulfur oxyhalide. It thus enhances ion and electron exchanges between the electrode and the electrolyte, increasing the discharge rate efficiency and energy density. Moreover,

chlorinated polyethylene rubber swells when wet, bringing more of the cathode material in contact with the electrolyte and further improving the discharge and density characteristics.

This work was done by Shiao-Ping Siao Yen, Subbarao Surampudi, Boyd J. Carter, and Robert B. Somoano of Caltech for NASA's Jet Propulsion Laboratory. For further information, Circle 103 on the TSP Request Card.

Inquiries concerning rights for the commercial use of this invention should be addressed to the Patent Counsel, NASA Resident Office-JPL [see page 21]. Refer to NPO-16397.

Fluidized-Bed Particles Scavenge Silicon Fines

Waste is reduced, and the silicon production rate is improved.

NASA's Jet Propulsion Laboratory, Pasadena, California

A fluidized-bed reactor for producing high-purity silicon from the thermal decomposition of silane (SiH₄) has been made

technically feasible by adjustments to the design and operating conditions. Experiments have shown that very efficient con-

version of silane to product silicon can be achieved at previously unattainable concentrations of silane without excessive loss

of silicon as fine powder. These data indicate that this fluidized-bed process, recognized as having the potential for the most economical high-purity silicon process, can be made practical when additional data suitable for design are made available.

In the process, silicon is formed by the thermal decomposition of SiH_4 . Part of the silicon is formed on silicon seed particles as a result of a surface chemical reaction. However, silicon that is formed by a homogeneous reaction in the gas phase tends to form aggregates of the silicon atoms, which appear as fine particles (like a dust). It is believed that a scavenging action of the seed particles enables a large fraction of the fines to be incorporated onto the seed surface. This mode of growth seems to be confirmed by electron microscopy photographs (see figure).

To take advantage of the scavenging mechanisms, it is necessary to design the gas-distributor and heaters to maximize heat transfer at the bottom of the reactor. The distributor must form tiny bubbles of gas to facilitate the transfer of heat from the silicon particles to the gas, thereby promoting gas decomposition on the particles and the capture of smaller particles by larger ones at the reactor entrance zone. It is also necessary that the temperature for the pyrolysis reaction (about 700°C) be reached very close to the distributor, thus reducing fines formation in the upper portion of the bed where the opportunity for capture is lower. Thus, the fluidized bed is made to act somewhat like a filtration column.

Before these improvements, it was necessary to operate at SiH_4 concentrations (the other gas is H_2) as low as 1 to 20 percent in order to keep down the production of silicon fines. In experiments with an im-

proved reactor, fines production was below 10 percent, even with SiH_4 concentration in the feed gas as high as 65 volume percent.

Experiments indicate a deposition rate of about $8\ \mu\text{m}/\text{min}$ at 700°C and 50 percent SiH_4 . Under these conditions, a fluidized bed of 2 in. (5.08 cm) diameter would pro-

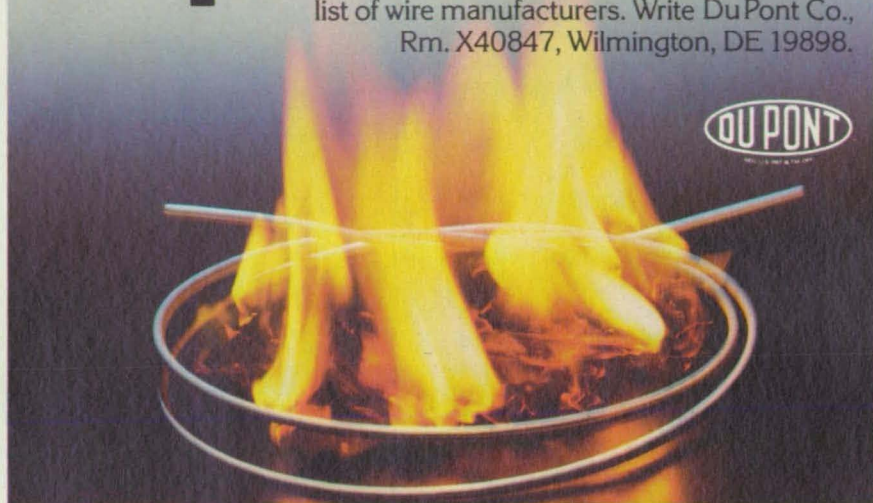
#1 in wire insulation for aerospace.

DuPont KAPTON polyimide film.

A high-performance wire and cable insulation rated for 200°C continuously and up to 400°C for short periods. Won't melt, drip or propagate flame. Practically no smoke in a fire.

Send for more information and a list of wire manufacturers. Write DuPont Co., Rm. X40847, Wilmington, DE 19898.

Heat resistant Kapton[®]



Circle Reader Action No. 399

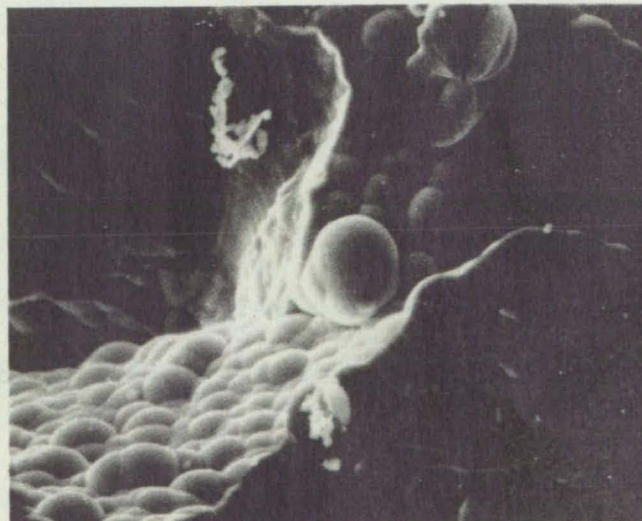
duce about 0.5 kg/h of polysilicon.

This work was done by George C. Hsu, Naresh Rohatgi, Ralph Lutwack, and Richard Hogle of Caltech for NASA's Jet Propulsion Laboratory. For further information, Circle 104 on the TSP Request Card. NPO-16034



FEED

50 μ



PRODUCT

A Silicon Feed Particle (left) becomes coated with nodules of silicon by a combination of chemical vapor deposition and aggregation with smaller particles. The resulting surface of a product particle is shown at the right.

Blowing Polymer Bubbles in an Acoustic Levitator

Gas would be injected into levitated drops.

NASA's Jet Propulsion Laboratory, Pasadena, California

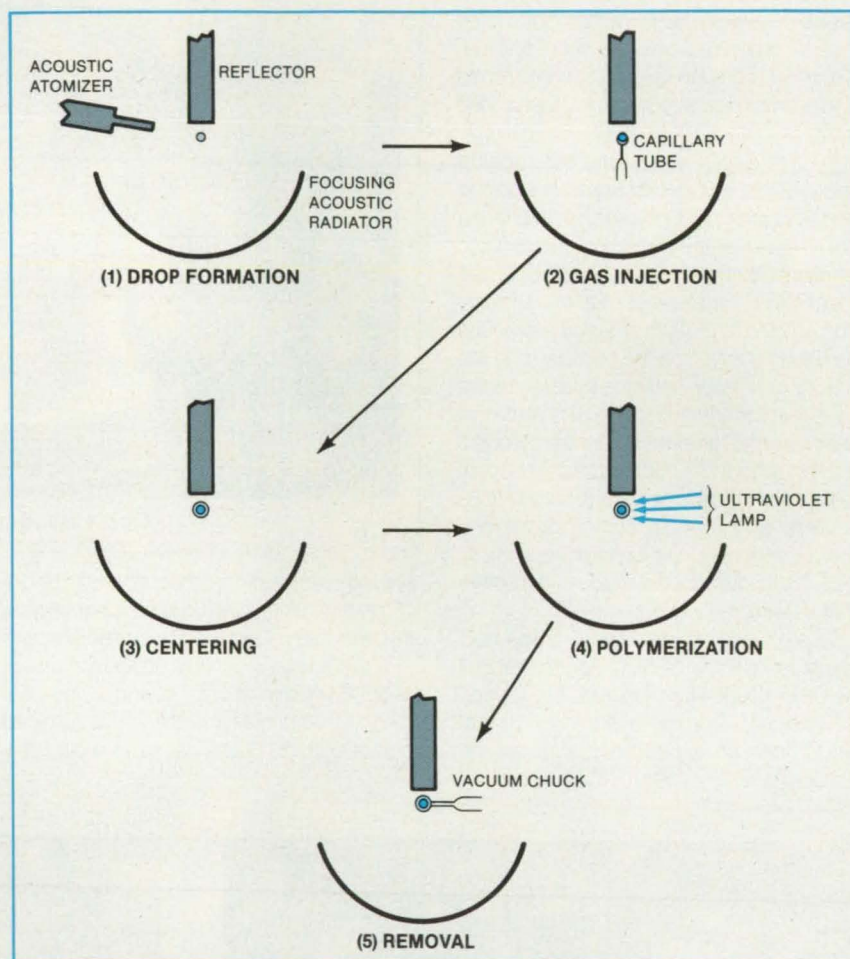
In a proposed manufacturing process, small gas-filled polymer shells would be made by injecting gas directly into acoustically levitated prepolymer drops. In contrast to free-fall methods that allow only a few seconds for bubble formation, the new process would allow sufficient time for the precise control of the shell geometry. Applications are foreseen in the fabrication of deuterium/tritium-filled fusion targets and in pharmaceutical coatings. The new process may also be useful in glass blowing and blow molding.

The steps of the process are as follows (see figure):

1. A graduated acoustic atomizer injects a measured volume of prepolymer liquid into the focal region under the reflector of an acoustic levitator.
2. The reflector is moved to bring the prepolymer drop to a second station, where a capillary tube is micromanipulated to pierce the prepolymer drop. A measured volume of gas is injected into the drop near the center.
3. The reflector is moved to bring the gas-filled drop to a third station, where it is vibrated for several seconds to allow the centering of the gas filling in the drop.
4. The reflector is moved to bring the gas-filled drop to a fourth station for irradiation to polymerize the liquid.
5. The reflector is moved to bring the completed bubble to a fifth station, from which it is removed by a vacuum chuck.

This work was done by Mark C. Lee of Caltech for NASA's Jet Propulsion Laboratory. For further information, Circle 28 on the TSP Request Card.

Inquiries concerning rights for the commercial use of this invention should be addressed to the Patent Counsel, NASA Resident Office-JPL [see page 21]. Refer to NPO-16212.



In a **Focusing Acoustic Levitator**, a precisely sized drop of prepolymer liquid is filled with a precise amount of gas, vibrated in place to improve sphericity, then polymerized under ultraviolet or other suitable radiation. A trough-shaped focusing acoustic radiator would be particularly useful here, since the work stations could be located sequentially along its length.

Magnetron-Sputtered Amorphous Metallic Coatings

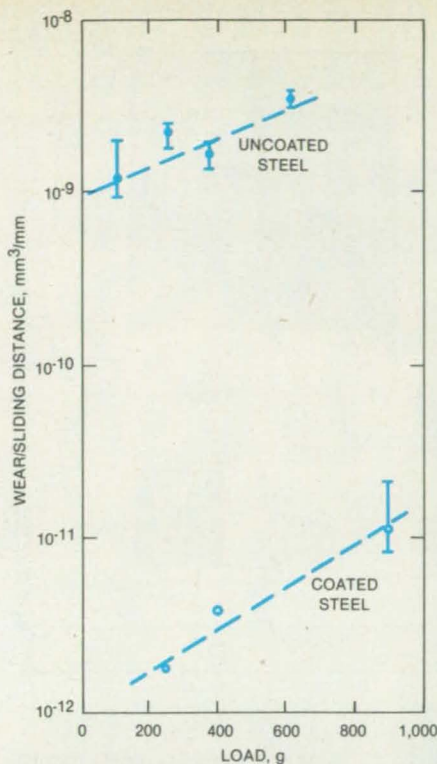
Refractory metal/metalloid-based amorphous deposits are extremely hard and wear resistant.

NASA's Jet Propulsion Laboratory, Pasadena, California

Amorphous coatings of refractory metal/metalloid-based alloys deposited by

magnetron sputtering provide extraordinary hardness and wear resistance. The unusual

protective properties of these coatings are primarily due to their amorphous structure,



A Pin-On-Disc Wear Test shows that wear is less for tungsten-rhenium-boron coated steel than for uncoated steel. Wear is measured in terms of the ratio of volume of worn-away material to pin sliding distance, plotted as a function of load.

which is thermally stable at temperatures up to 1,000° C. These coatings are dense, pinhole-free, extremely smooth, and significantly resistant to chemical corrosion in acidic and neutral aqueous environments.

Magnetron sputtering creates highly adherent coatings at reasonably high deposition rates. A variety of multicomponent materials can be deposited by magnetron sputtering with a close control over their chemical composition. A major advantage of magnetron sputtering is that the substrate need not be as hot as in reactive deposition techniques, some of which require as much as 800° C. For magnetron sputtering, 350° C

is adequate to obtain high adhesion strength with low internal stress.

Magnetron sputtering has been used to deposit tungsten/rhenium/boron ($W_{0.6}Re_{0.4}B_{24}$) coatings on 52100 steel. A sputtering target was fabricated by thoroughly mixing powders of tungsten, rhenium, and boron in the stated proportions and pressing at 1,200° C and 3,000 lb/in.² (21 MPa). The substrate was lightly etched by sputtering before deposition, then maintained at a bias of -500 V during the initial stages of film growth while the target material was sputtered onto it.

#1 in wire insulation for aerospace

The 707, 727, 737, 757, 767 and now the 747. Boeing relies on KAPTON polyimide film to meet their high-temperature wire insulation requirements. The reasons: KAPTON saves weight and space. It won't melt, drip or propagate flame. And even in a current overload condition, it emits practically no smoke.

Learn why Boeing and other leading aerospace manufacturers rely on KAPTON, made only by DuPont. For a new booklet on why nearly all high-performance aircraft use KAPTON, write DuPont Company, KAPTON, Room X40786, Wilmington, DE 19898.

Boeing 747s now use Kapton®



Circle Reader Action No. 400

Argon gas at the pressure of ~10 torr or Hg (~1.3 Pa) was used as a carrier gas for the sputter deposition. In wear tests, a substrate coated with 4 μm of the amorphous alloy exhibited three orders of magnitude superior wear resistance over that of the uncoated substrate (see figure).

This work was done by Anilkumar P. Thakoor, Madhav Mehra, and Satish K. Khanna of Caltech for NASA's Jet Propulsion Laboratory. For further information, Circle 23 on the TSP Request Card. NPO-16221

Determining Fiber Orientation in Graphite-Reinforced Composites

A simple electrical method aids in testing materials.

Marshall Space Flight Center, Alabama

The orientation of fibers in graphite-fiber-reinforced plastics is easily determined with a new method. Materials scientists can thus ensure that fibers, which are usually not visible after the graphite/plastic composite has been cured, are properly oriented in test specimens and that the test results accurately

represent the characteristics of the composite.

The method is based on the fact that continuous graphite fibers embedded in a cured polymer matrix are actually parallel conductors. Thus, the resistance measured across a laminate is at a minimum when the probes

of the ohmmeter are connected to the opposite ends of the fibers.

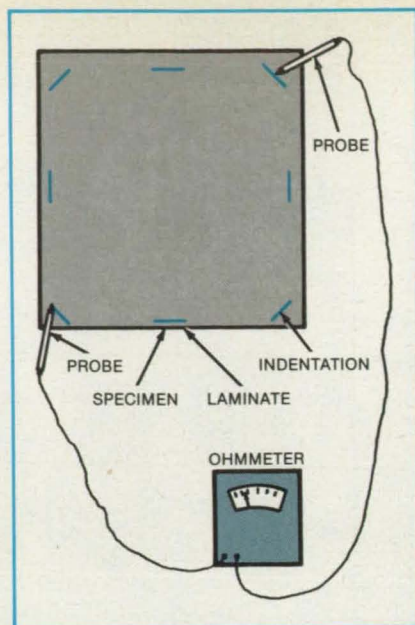
Small, parallel indentations extending below the laminate surface are made in a specimen with a small, flat jeweler's file (see figure). The technician selects a pair of opposing indentations and holds one ohm-

meter probe in a fixed position in one of the indentations while moving the other probe along the opposite member of the pair. The user observes the resistance value on the instrument and notes the position of the moving probe at which the value is least. With a nonindenting machinist's pencil, the user draws a line between this minimum-value point and the position of the fixed probe. This line indicates the orientation of the fibers in the specimen.

This work was done by Julie G. Daniels, Frank E. Ledbetter III, Johnny M. Clemon, Benjamin G. Penn, and William T. White of Marshall Space Flight Center. No further documentation is available.

Inquiries concerning rights for the commercial use of this invention should be addressed to the Patent Counsel, Marshall Space Flight Center [see page 21]. Refer to MFS-28032.

A Line Drawn Between Minimum-Resistance Points indicates the fiber orientation in a ply of a laminate. This specimen measures 12 by 12 inches (30.5 by 30.5 centimeters).



Books and Reports

These reports, studies, and handbooks are available from NASA as Technical Support Packages (TSP's) when a Request Card number is cited; otherwise they are available from the National Technical Information Service.

Predicting the Fatigue Life of Structures

Linear elastic fracture mechanics provides accurate predictions for many situations.

A report reviews fracture-mechanics technology for predicting the life expectancy of structural components subjected to cyclic loads. The report covers analytical tools for modeling and forecasting subcritical fatigue-crack growth in structures. It emphasizes use of the tools in practical, day-to-day problems of engineering design, development, and decisionmaking.

The recently introduced linear elastic fracture mechanics (LEFM) approach is favored in the analyses over the traditional alternating-stress-vs.-cycles technique. The LEFM approach offers three major advantages over the traditional approach:

- It accounts for initial cracklike defects and growing cracks.
- It allows a family of stress-vs.-cycle curves to be generated from a single specimen and thus greatly reduces specimen costs and testing time.

- It allows the life expectancies for other components and crack geometries to be predicted from the single specimen; that is, it eliminates geometry as a test variable, again with considerable savings.

The fracture-mechanics equations link three parameters; the defect size, the intrinsic fracture toughness or subcritical crack-growth rate, and the applied stress. If any two of these parameters are known, the third can be quantified.

A section of the report is devoted to a review of the current state of elastic stress analysis of cracked bodies. When bodies can be idealized as two-dimensional, a wide variety of stress-intensity solutions is available. However, solutions for three-dimensional bodies are not nearly as numerous and comprehensive. Since cracks occupying only a portion of the thickness of such structures as plates and shells must be treated three-dimensionally, this is a serious gap. The report notes that efforts to fill the gap are making good progress.

The largest section deals with the response of a cracked material to applied forces. Even for the simple case of constant-amplitude cycling, many factors influence the crack-growth rate, including the ratio of minimum to maximum load, the environment, the cyclic-loading frequency, and the temperature. Matters become increasingly complex in the more realistic case of variable-amplitude cyclic loading. The crack growth per cycle is influenced by loading history. Although much work remains to be done in this area, several computer programs provide adequate accuracy for many applications. However, none of the programs is comprehensive, and consolidation of all available predictive proce-

dures into one general-purpose program has yet to be accomplished.

Plasticity effects can be important for accurate life prediction. The few tools available to address crack-growth problems in which plasticity is a factor are described in a section on nonlinear fracture mechanics.

Numerous topics of peripheral interest are reviewed. One of growing importance is probabilistic fracture mechanics. With probabilistic calculations, the effects on lifetime calculations caused by scatter in material properties, the stochastic nature of imposed loads, and uncertainties in the sizes of cracks can be quantified and assessed. Another such topic is proof testing. The tradeoffs between damaging good components in a proof test and allowing unsafe components to go into service are discussed. The report concludes with a discussion of weld cracks, an important topic because many life-limiting defects originate in welds and because the study of many cracked-weld problems combines the technologies of fracture mechanics and material behavior.

This work was done by P. M. Besuner, D. O. Harris, J. M. Thomas, D. E. Allison, J. M. Bannantine, S. B. Brown, C. S. Davis, G. A. Derbalian, J. W. Eischen, G. F. Fowler, J. D. Osteraas, J. N. Robinson, R. A. Sire, and G. A. Vroman of Failure Analysis Associates for Marshall Space Flight Center. Further information may be found in NASA CR-170903 [N84-17622/NSP], "A Review of Fracture Mechanics Life Technology" [\$31]. A paper copy may be purchased [prepayment required] from the National Technical Information Service, Springfield, Virginia 22161. The report is also available on microfiche at no charge. To obtain a microfiche copy, Circle 6 on the TSP Request Card. MFS-27049

Corrosive Effects of Burning Fuels

Literature is synthesized to develop corrosion predictions for unconventional fuels.

A report presents studies of the probable corrosive effects of such unconventional fuels as liquefied coal. The report was prepared by analyzing the probable composition of the fuels when they come into wide use, identifying the important compounds, and searching the literature for information about corrosion problems associated with the compounds in environments like those in industrial and commercial boilers and furnaces.

The main fuel constituents that cause corrosion are sulfur, alkali metals, vanadium, carbon, carbon monoxide, iron, and chlorine. Sometimes one of these substances acts as a catalyst in corrosive reactions initiated by another compound, and sometimes a corrosive agent inhibits the action of another corrosive material. The report recommends that such situations be studied further to determine whether corrosive compounds can be combined in concentrations that will minimize damage to metals.

Also recommended is a theoretical and experimental study of oil-spray combustion, the formation of cenospheres (the porous carbonaceous particles that form while oil droplets burn), and cenosphere combustion in a cloud of cenospheres. Further research on cenospheres is important because traces of corrosive agents in the liquid fuel can become highly concentrated in the solid particles.

The report is divided into two main parts: Deposits and corrosion. In the discussion of deposits, the compounds that deposit on boiler surfaces are identified and theories of deposition and research in progress are summarized. In the section on corrosion, the chemical composition of the deposits is described in detail so that the several paths that lead to corrosion can be traced. In addition, the relationships of chemical composition, additives, and boiler operating conditions are discussed. A final section makes recommendations on ways to mitigate high-temperature corrosion in furnaces and boilers using broad-specification fuels.

This work was done by Josette Bellan and Said Elghobashi of Caltech for NASA's Jet Propulsion Laboratory. To obtain a copy of the report, "Impact of Fuel Composition on Deposits and on High Temperature Corrosion in Industrial/Commercial Boilers and Furnaces," Circle 96 on the TSP Request Card.
NPO-16345

Synthetic Organic Materials in Nuclear Powerplants

Materials are evaluated for suitability in safety-related equipment.

A report aids plant designers and qualification engineers in ensuring that organic materials in nuclear powerplants will perform satisfactorily in such safety-related equipment as insulation on motor windings, pump diaphragms, motor and pump lubricants, and pump seals and gaskets. The report provides information for service that may include both mild and harsh nuclear environments.

Synthetic organic materials in nuclear power-generating stations are exposed to low-level radiation for long periods, perhaps punctuated by one or more brief exposures to high-level radiation. Critical electrical and mechanical components, which must perform their functions during or after accidental radiation surges, frequently contain such materials.

The report first discusses general radiation effects on synthetic organic materials in terms of types of particles in the radiation environment, radiation thresholds, and combined effects of radiation and such other stresses as heat, chemicals, steam, and seismic vibration. A general scarcity of such combined-environment data is noted. It then gives specific radiation data for materials in five categories: Solid electrical insulators, elastomeric seals and gaskets, lubricants, adhesives, and protective coatings. Definitions and methods used for tabulation of the data are explained in detail. Cautions are given against extending existing data to environments different from those under which they were observed.

Of the five categories, the elastomeric seals and gaskets have the lowest thresholds of radiation damage. Frequently, the threshold varies widely, depending on curing agents, fillers, and additives. Usually, such agents increase the threshold.

Extensive references are provided. Appendixes contain tables of radiation conversion factors, a list of trade names for synthetic organic polymers, and a brief glossary.

This work was done by Frank L. Bouquet and John W. Winslow of Caltech for NASA's Jet Propulsion Laboratory. To obtain a copy of the report, "Techniques To Forecast the Responses of Synthetic Organic Materials to Space Radiation and to Nuclear Reactor Radiation," Circle 107 on the TSP Request Card.
NPO-16424

Degradation of Dielectrics in Space

Effects of electron and proton irradiation are presented.

The effects of radiation (principally, electrons and protons) on dielectric materials are summarized in a report. The report is based on radiation tests of optical coatings, temperature-control coatings, adhesives, radomes, thermal insulators, and light-control surfaces. The materials are primarily polymers and metal/organic coatings.

Fifteen materials were subjected to proton irradiation. Four were subjected to electron radiation.

Various criteria were established for evaluating the response of a material to radiation, depending on the function of the material and its location in a spacecraft. Often, the limiting criterion was surface erosion that could generate dust. By collecting on scientific instruments and navigation and guidance sensors, the dust could interfere with their operation. Other criteria include changes in the Sunlight reflectance and absorptance of surface coatings, changes in antireflective coatings on lenses, and loss of strength in adhesives.

Before and after exposure of specimens to radiation, the following tests were performed:

- Weight was measured.
- Surface reflectance and absorptance were measured at several wavelengths.
- Surfaces were examined by a scanning electron microscope.
- Surface particles were collected on adhesive tape and examined for quantity and size to determine erosion.

Most of the materials were not significantly damaged by the radiation. A few materials changed color at the highest radiation levels. The most significant change was the graying of zinc orthotitanate paint at the highest proton radiation levels. The emissivity of the paint increased by 9.22 percent and the white absorptance increased by 249 percent.

This work was done by Frank L. Bouquet of Caltech for NASA's Jet Propulsion Laboratory. For further information, Circle 111 on the TSP Request Card.
NPO-16003

Plasma Deposition of Doped Amorphous Silicon

Films are deposited on aluminum.

A pair of reports present further experimental details of an investigation of the plasma deposition of films of phosphorous-doped amorphous silicon. The process was described in "Plasma Deposition of Amorphous Silicon" (NPO-14954), page 42, *NASA Tech Briefs*, Vol. 6, No. 1 (Spring, 1981).

In the nonequilibrium plasma-jet process, the reactant gas containing silicon (SiCl_4 , SiHC1_3 , or SiH_4) and the reactant gas containing phosphorus (a mixture of H_2 , PH_3 , and Ar) are introduced downstream of an electrode assembly in a hydrogen plasma. The phosphorous-doped-silicon reaction product is deposited on the substrate, which is an electrode heated to 550 K.

In the earlier article, it was stated that strongly adhering films had been deposited on aluminum and on Pyrex and Vycor (or equivalents). As stated in the present reports, deposition tests on Pyrex and Vycor were unsuccessful. Probe measurements of the electrical resistance of the deposited films indicated that the films were not uniform. In general, it appeared that the resistance decreased with film thickness.

This work was done by Hartwell F. Calcote for **NASA's Jet Propulsion Labor-**

atory. To obtain a copy of the reports, "A Means of Doping Films Prepared from SiH_4 with P To Increase the Electrical Conductivity" and "A Means of Preparing Strongly Adhering Amorphous Silicon Films on Aluminum from SiH_4 ," Circle 71 on the TSP Request Card.

NPO-14955 and NPO-14956

Bonding Solar-Cell Modules

Theories, materials, and processing are reviewed.

The status of a research program on chemical bonding for solar-cell arrays is the subject of a 57-page report. The program is aimed at identifying, developing, and validating weather-stable chemical bonding promoters. These materials are a key to ensuring long life in encapsulated photovoltaic modules for electric-power generation. To be cost-effective, modules must hold together for at least 20 years, reliably resisting delamination and separation of the component materials.

The report tabulates data on a variety of bonding agents, including adhesives, potting compounds, and adhesion promoters. Bonding agents were qualified by measuring the dry bond strength, or peel strength, of control specimens, then measuring the

bond strength of identical specimens that were immersed in water for various periods. A bonding agent was rejected if its control or wet value was zero. The bonding agents were evaluated on the basis of their bond strength between various combinations of materials likely to be found in photovoltaic modules; for example, ethylene vinyl acetate to glass, polyurethane to polyvinyl fluoride plastic film, and ethylene methyl acrylate to steel.

The report goes on to consider theories of the chemically bonded interface with particular attention to the bonding of organic polymers to such inorganic substrates as glasses and metals. Included is a discussion of different models of the interphase — the region between the coupling agent/substrate interface and the bulk organic adhesive.

Finally, the report considers processing techniques for strong, durable bonds. Topics include surface preparation, application, and curing.

This work was done by Daniel R. Coulter, Edward F. Cuddihy, and Edwin F. Plueddemann of Caltech for **NASA's Jet Propulsion Laboratory.** Further information may be found in NASA CR-173460 [N84-22008/NSP], "Chemical Bonding Technology for Terrestrial Photovoltaic Modules" [\$10]. A copy may be purchased [prepayment required] from the National Technical Information Service, Springfield, Virginia 22161. NPO-16399

Computer Programs

These programs may be obtained at a very reasonable cost from COSMIC, a facility sponsored by NASA to make raw programs available to the public. For information on program price, size, and availability, circle the reference number on the TSP and COSMIC Request Card in this issue.

Modeling a Transient Catalytic Combustor

The model assumes a quasi-steady gas phase and a thermally "thin" solid.

Catalytic combustors are becoming more important in advanced power-generating systems. The design and operation of these combustors are limited by the high-temperature capability of the catalysts and by the low-temperature emission levels of CO and unburnt hydrocarbons. Catalytic combustor modeling can contribute to environmental and efficiency improvements by providing a greater understanding of the processes occurring in the reactor and by serving as a design guide, thus minimizing the number of experimental tests needed.

A transient model of a monolith catalytic combustor is presented in a report done under NASA/DOE contract. The model assumes a quasi-steady gas phase and a thermally thin solid with the substrate thermal in-

ertia responsible for the combustor response-time delay. In the gas-phase treatment, several quasi-global chemical reactions are assumed that are capable of describing CO and unburnt hydrocarbon emissions in fuel-lean operations. By neglecting heat conduction along the flow direction in the gas and the solid in high-speed approaching flows, the system of differential equations describing the combustor transient is simplified, and a Runge-Kutta integration scheme is applicable. The resulting computation scheme is highly efficient in computational time and is suitable for parametric calculation for both steady states and transients.

In the steady-state computation presented, the influence of selected operating

and design parameters on the minimum combustor length is studied. Special attention is given to the effect of after-bed gas-phase reaction space. Comparison with reported data indicates that the model is able to describe the salient features found in experiments, including the appearance of a CO peak and the efficiency reversal phenomena at high inlet temperature and pressure. Quantitative agreement with CO emission data is possible if a certain degree of rate-constants adjustment is made.

In the transient analysis, a quasi-steady gas phase and a thermally thin substrate are assumed. The combustor-response delay is due to the substrate thermal inertia. Fast response is found to be favored by thin substrate, short catalytic bed length, high-combustor inlet and final temperatures and, in most cases, small gas-channel diameters. The calculated gas and substrate temperature/time history at different axial positions provide an understanding of how the catalytic combustor responds to an upstream condition change. The computed results also suggest that the gas residence times in the catalytic bed and in the after-bed space are correlatable with the nondimensional combustor response time. When fast transient responses are required, both steady and unsteady studies have to be made to achieve a meaningful compromise in design.

This program was written by James S. T'ien of the Case Western Reserve University for Lewis Research Center. For further information, Circle 2 on the TSP Request Card.

LEW-13723

Plastic and Failure Analysis of Composites

The program is particularly suited for analyzing laminated metal-matrix composites.

The increasing number of applications of fiber-reinforced composites in industry demands a detailed understanding of their material properties and behavior. A three-dimensional finite-element computer program called PAFAC (Plastic and Failure Analysis of Composites) has been developed for the elastic/plastic analysis of fiber-reinforced composite materials and structures. The evaluation of stresses and deformations at edges, cutouts, and joints is essential in understanding the strength and failure of composites. In addition, elastic/plastic analysis is crucial for metal-matrix composites since the onset of plastic yielding starts very early in the loading process as compared to the ultimate strength of the composite. Such comprehensive analysis

can only be achieved by a finite-element program like PAFAC.

PAFAC is particularly suited for the analysis of laminated metal-matrix composites. It can model the elastic/plastic behavior of the matrix phase while the fibers remain elastic. Since the PAFAC program uses a three-dimensional element, the program can also model the individual layers of the laminate to account for thickness effects.

In PAFAC, the composite is modeled as a continuum reinforced by cylindrical fibers of vanishingly small diameter, which occupy a finite volume fraction of the composite. In this way, the essential axial constraint of the phases is retained. Furthermore, the local stress fields and strain fields are uniform.

The PAFAC finite-element solution is obtained using the displacement method. Solution of the nonlinear equilibrium equations is obtained with a Newton-Raphson iteration technique. The elastic/plastic behavior of composites consisting of aligned, continuous elastic filaments and an elastic/plastic matrix is described in terms of the constituent properties, their volume fractions, and mutual constraints between phases indicated by the geometry of the microstructure. The program uses an iterative procedure to determine the overall response of the laminate. From the overall response, the program determines the stress state in each phase of the composite material. Failure of the fibers or matrix within an element can also be modeled by PAFAC.

PAFAC is written in FORTRAN IV for batch execution and has been implemented on a CDC CYBER 170 series computer with a segmented memory requirement of approximately 66k (octal) of 60-bit words. PAFAC was developed in 1982.

This program was written by C. A. Bigelow and W. S. Johnson of Langley Research Center and Y. A. Bahei-El-Din, consultant. For further information, Circle 62 on the TSP Request Card.
LAR-13183

Exhaust Effluent Diffusion Model

It predicts the environmental impact of materials injected into the troposphere.

The burning of rocket engines during the first few seconds before and immediately following a vehicle launch results in the formation of a large cloud of hot, buoyant, exhaust products near ground level. The rocket engines also leave an exhaust trail that extends through the depth of the troposphere and beyond. The Rocket Exhaust Effluent Diffusion Model (REEDM) predicts concentrations, dosages, and depositions downwind from normal and abnormal launches of

rocket vehicles at NASA's Kennedy Space Center. REEDM calculations are used by NASA for the following purposes: (a) Mission planning activities and environmental assessment, (b) prelaunch forecasts of the environmental effects of launch operations, and (c) postlaunch environmental analysis. REEDM offers the user a transport and dispersion model that may be useful in predicting the environmental impact of any type of material injected into the troposphere. REEDM predictions should also assist in the implementation of environmental monitoring plans and in the review of monitoring data.

REEDM is controlled by operator response to plain language inquiries and by internal management routines. Inputs to REEDM include meteorological data and effluent source information such as release rates of materials and heat. Once the operator has elected to perform calculations for a launch or launch abort of a particular vehicle, the program calculates the spatial position and dimensions of the cloud during cloud rise at the point of display of the vertical profiles of wind and temperature data and the cloud dimensions at stabilization.

After the final selection of input parameters has been made and the user given the opportunity to alter program-calculated parameters, the program computes the desired dosage/concentration or deposition calculations. If the dosage/concentration calculation option is elected, the print output includes peak concentration at 1 km intervals downwind from the launch pad as well as the total dosage and time mean concentration for the period of interest at these distances.

The print output for gravitational deposition shows maximum ground-level deposition as a function of distance from the launch pad. If the option to calculate deposition due to precipitation scavenging is selected, either maximum deposition or maximum surface-water pH is printed. The user also has the option to plot isopleth (dosage, concentration, or deposition) levels of interest on a base map of Kennedy Space Center.

REEDM is written in FORTRAN IV for interactive execution and has been implemented on an HP 1000 computer operating under RTE4 with a segmented central memory requirement of 32k of 16-bit words. REEDM is designed to be used with a CRT or TTY terminal and an X-Y plotter. REEDM was developed in 1982.

This program was written by J. R. Bjorklund, R. K. Dumbauld, C. S. Cheney, and H. V. Geary of H. E. Cramer Co., Inc., for Marshall Space Flight Center. For further information, Circle 68 on the TSP Request Card.
MFS-25940





Books and Reports

106 Multispectral Analysis of NMR Imagery

Books and Reports

These reports, studies, and handbooks are available from NASA as Technical Support Packages (TSP's) when a Request Card number is cited; otherwise they are available from the National Technical Information Service.

Multispectral Analysis of NMR Imagery

Earth-mapping techniques are applied to medical imaging.

A conference paper discusses initial efforts to adapt multispectral satellite-image analysis to nuclear magnetic resonance (NMR) scans of the human body. The flexibility of these techniques makes it possible to present NMR data in a variety of formats, including pseudocolor composite images of pathological internal features. The techniques do not have to be greatly modified from the form in which they are used to produce satellite maps of such Earth features as water, rock, or foliage.

The NMR spin echo signal from a volume element (a small region of the human body) contains information on proton density, proton flow, and proton-spin relaxation time. These, in turn, depend on the type of tissue in which the protons are located. The information is extracted by computer processing of the responses to various NMR pulse sequences, which is analogous to the processing of raw satellite imagery in various spectral bands. Different NMR pulse sequences enable the production of several NMR images of the same body section, each with different contrasts.

Each pulse sequence used by an NMR scanner results in images with 256 or more gray levels. If a feature space with a three-dimensional histogram is formed by plotting the gray levels of many picture elements of three NMR images of the same scene taken with different pulse sequences, clusters of data points are observed. Different kinds of tissue are identifiable through such clustering, and algorithms to identify clusters are therefore included in the image-processing program.

The separation of scene components from a multispectral data set is performed in both satellite and NMR imaging by either of two techniques:

- Unsupervised (that is, automatic) classification, in which the computer analyzes the data without operator intervention, and in which likenesses among picture elements are usually determined by the proximity of those elements in feature space; and
- Supervised classification, in which an operator intervenes to train the computer on scene components that are known and which is analogous to training on known land features in satellite imagery.

In supervised classification, the operator locates an interactive cursor over a region of interest containing a known structure such as bone. The computer flags each point in the region of interest that lies nearby in feature space. The operator adjusts the feature-space histogram limits so that similar features are identified elsewhere in the NMR image by their feature-space characteristics. If features are subsequently found to be incorrectly identified by the computer, the operator trains on another region of interest or readjusts the histogram limits.

Both supervised and unsupervised classification have been applied to NMR imagery of human-body sections. Body tissues including cerebrospinal fluid, white and gray brain matter, subcutaneous fat, muscle, and bone have been identified.

This work was done by Robert L. Butterfield of Kennedy Space Center, Michael W. Vannier and associates of the Washington University School of Medicine, and Douglas Jordan of the University of Florida. To obtain a copy of the paper, Circle 25 on the TSP Request Card.

KSC-11301

Capture the Glory!

Now you can own this collector's print, commemorating Columbia's exploits, at an exceptional introductory price.

Noted aviation artist Ken Kotik has captured *Columbia* in all its glory to commemorate the completion of four test flights and the first operational mission, STS-5. This fine print—truly a collector's item—depicts the orbiter in full color, side view, with every feature crisply detailed.

Arranged beneath the ship, also in full color, are the five distinctive mission patches. But what makes Ken Kotik's work most unique is his method of creating a 'historical panorama' via individual vignettes surrounding the side view of *Columbia*.

Educational as well as eye-appealing, these scenes, which are expertly rendered in a wash technique, include such subjects as the orbiter under construction at Rockwell, on the launch pad, at touch-down and during transit on its 747 carrier. Concise copy, hand-written by the artist, accompanies each vignette. (Important: The greatly reduced print reproduced here is intended only to show style—at the full 32" by 24" size, all copy is clearly readable.)

About the artist.

Ken Kotik, a 37-year old Colorado native, has been a professional commercial artist for the past 14 years. In his own words, he "eats, drinks and sleeps flying." It shows in the obvious care and attention he brings to each print or mural. When not at his drawing board creating artworks for such prestigious institutions as the Air Force Academy, Ken can be found at the controls of his Schweitzer sailplane, in which he competes nationally. A self-taught artist, he specializes in airbrush-applied acrylic techniques. *Space Shuttle Columbia: The Pathfinder* is his first work on the space program, and the original art has been accepted by the Smithsonian Air and Space Museum for its permanent collection.

About the artwork.

Space Shuttle Columbia: The Pathfinder was printed in five colors, after individual press proving, on exhibit-quality 80 lb text 'Hopper Feltweave' textured paper. The feltweave texture yields properties most desirable for framing and display.

About ordering.

Each *Columbia* print comes packed in a sturdy mailing tube and will be shipped upon receipt of your order at the introductory price of \$9.95. Please allow two to three weeks for delivery. There is a one-time first class postage and handling charge of \$2.50 for each order. (If you order

three prints, for example, you still include only \$2.50 for postage and handling to cover the entire order.) To ensure that you receive your prints without delay, fill out and mail the coupon today, including check or money order only and local tax where applicable. If coupon has been clipped, mail your order to: NASA Tech Briefs, Columbia Print Offer, 41 E. 42nd St., New York, N.Y. 10017.

Actual size: 32" wide by 24" high—In full color!



(\$17.95 for two; \$26.95 for three; \$7.95 each additional plus postage and handling.)

ONLY \$9⁹⁵ EACH

MONEY BACK GUARANTEE

If not completely satisfied, return undamaged print, in wrapper, within 10 days for a full refund of print purchase price.

Mail to: NASA Tech Briefs
Columbia Print Offer
41 East 42nd St.
New York, N.Y. 10017



Note: One print \$9.95; two \$17.95; three \$26.95; each additional \$7.95, plus \$2.50 postage and handling per order.

Please rush _____ Columbia prints.
I have enclosed \$ _____ plus \$2.50
for first class postage and handling.
Total enclosed: \$ _____.

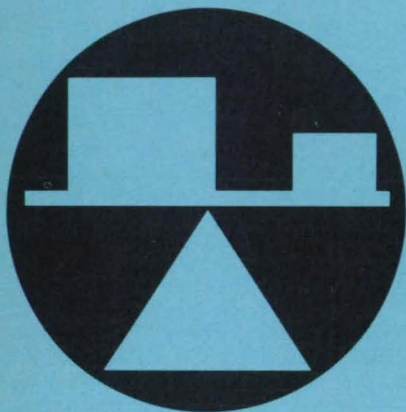
Name _____

Address _____

City _____ State _____ Zip _____

New York State residents add 7% sales tax.
New York City residents add 8.75% sales tax.

Please add my name to your mailing list
for future print offerings. SS-1



Hardware, Techniques, and Processes

- 108 Retractable End Plates for Aircraft Lifting Surfaces
- 109 Aerodynamic Rear Cone for Trucks
- 109 End Restraints for Impact-Energy-Absorbing Tube Specimens
- 110 Accurate Airborne Particle Sampler
- 111 Testing Machine for Biaxial Loading
- 112 Combination Heat-Flux and Temperature Gage
- 113 Sequentially-Deployable Tetrahedral Beam
- 114 Hand-Held Electronic Gap-Measuring Tools
- 115 Fixture for Linearly Variable Displacement Transducers
- 116 Inexpensive Eddy-Current Standard
- 116 Force Sensor for Large Robot Arms
- 117 Tabs Reduce Helicopter-Blade Vibrations
- 117 Flowmeter for Clear and Translucent Fluids
- 118 Low-Temperature Seal for Actuator Rod
- 119 Detecting Cracks in Rough Metal Surfaces

Computer Programs

- 120 Statistical Energy Analysis Program
- 127 Analyses of Multishaft Rotor-Bearing Response

Retractable End Plates for Aircraft Lifting Surfaces

Telescopic and fanlike end plates can be used with movable lifting surfaces.

Langley Research Center, Hampton, Virginia

End plates and winglets improve the aerodynamic characteristics of aircraft wings and other fixed lifting surfaces, thereby reducing fuel consumption. However, these devices are not suitable for use with movable lifting surfaces, such as flaps, elevators, ailerons and rudders, since these surfaces operate only during certain maneuvers and remain neutral the rest of the time.

Retractable end plates can improve the aerodynamic characteristics of movable lifting surfaces without paying a heavy drag penalty. Two types of retractable end plates, telescopic and fanlike, have been developed.

The telescopic end plate [see Figure 1(a)] consists of an upper and lower set of snugly fitting concentric shells that take the shape of the lifting surface in their fully folded position. The inner shells of each set are interconnected by flexible wires, whereas the outermost upper and lower shells are held together by a spring dashpot system. In Figure 1, only the outermost upper and lower shells are shown for clarity.

The end plates are mounted between the fixed lifting surface (wing or tail) and either side of the moving surface (plain flap, aileron, elevator, rudder). They are free to

rotate about the pivot and have a cutout around the shaft about which the lifting surface is deflected. Two disks are mounted freely on the shaft [see Figure 1(b)]. In the range of practical interest, the shaft engages disk 1 only in the clockwise direction and disk 2 only in the counterclockwise direction [see Figure 1(c)]. Rigid links AB and CD couple disk 1 to the outermost upper and lower shells, and rigid links EF and GH connect disk 2 to the outermost upper and lower shells, respectively.

When the shaft rotates clockwise; that is, when the lifting surface is deflected downward, disk 1 is engaged by the shaft, and rigid links AB and CD push the shells outward. The outer shells in their turn pull the inner shells by means of the flexible wires. Anticlockwise rotation of the shaft (surface deflected upward) results in the extension of the shells through links EF and GH, respectively. The extent of the spread depends on the design parameters and the angle of deflection and can be determined for any particular application. When the shaft is brought back to its neutral position, links AB and CD or EF and GH, along with the dashpot system, bring the outermost shells to the retracted position, and the in-

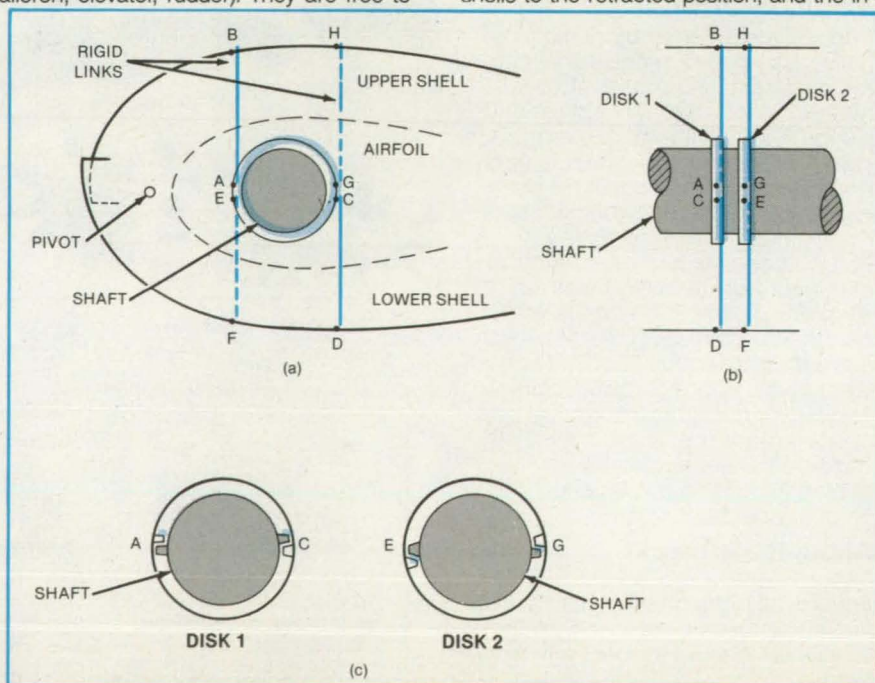


Figure 1. The **Telescopic End Plate** consists of upper and lower concentric shells that are linked to an extension mechanism.

ner shells just fold up within.

As shown in Figure 2, the fanlike end plate is very similar in construction. The only difference is that the inner shells are replaced by leaves of thin flat plates interconnected by flexible wires as in an oriental fan. The operation is similar to that of the telescopic end plate, but the telescopic end plate is structurally more rigid, and its shells offer more resistance to crossflow. However, the fanlike end plate is simpler, less expensive, and has less overall thickness.

It is well known that gaps between the fixed lifting surface and the deflected surface can have an adverse effect on aerodynamic characteristics. The retractable end plates effectively seal these gaps and not only increase the effective span of the deflected lifting surface, but, by providing an efficient barrier against the crossflow between the fixed and deflected surfaces, they improve the flow quality in the entire neighborhood. For example, when the lifting sur-

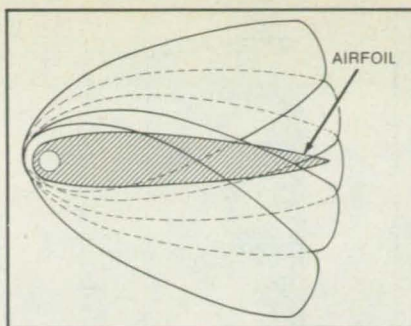


Figure 2. The **Fanlike End Plate**, shown in extended position, operates like an oriental fan.

face is deflected downward, there is a strong tendency for a crossflow to exist between the undersurface of the fixed wing and the upper surface of the deflected body. In the absence of an end plate, this crossflow destroys considerable lift both on the fixed and the deflected surfaces. By sealing this gap, the retractable end plates appreci-

ably improve the effectiveness of the lifting surfaces. Comparative tests indicate also an improvement in vortex wake attenuation.

The retractable end plates are automatically actuated by the same shaft that deflects the lifting surface and require little or no extra power and absolutely no control input from the cockpit. Besides being modular in construction, they are easily fitted to any existing aircraft design with only minor modifications.

This work was done by William D. Harvey of Langley Research Center and Sivaramakrishnan M. Mangalam of the National Academy of Sciences. No further documentation is available.

This invention is owned by NASA, and a patent application has been filed. Inquiries concerning nonexclusive or exclusive license for its commercial development should be addressed to the Patent Counsel, Langley Research Center [see page 21]. Refer to LAR-12946 and 12947.

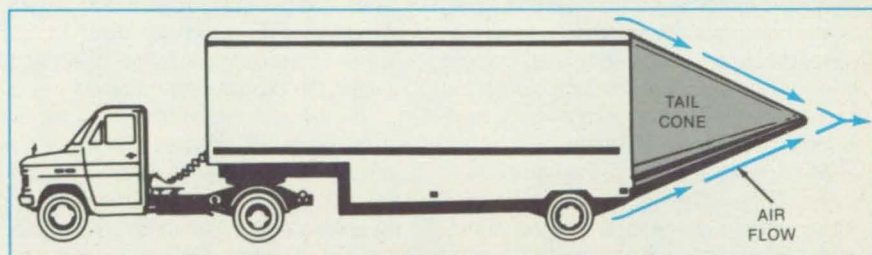
Aerodynamic Rear Cone for Trucks

A wind-inflated airfoil may improve fuel efficiency.

Marshall Space Flight Center, Alabama

A proposed windstream-inflated airfoil would create a tail cone at the rear of a truck (see figure). The cone would guide air over the truck body so that it flows in a more nearly laminar mode. Energy lost to air turbulence would be greatly reduced, and fuel consumed by the truck would be reduced accordingly. In addition, less air turbulence would mean less disturbance to nearby vehicles on a highway.

The cone would be made of a flexible material. With the truck at rest, the cone would fold against the rear of the vehicle. As the truck picks up speed, air would enter inlets at the rear of the truck and puff out the cone until it is fully deployed. The cone would then reduce aerodynam-



A **Wind-Inflated Cone** may reduce the turbulence that ordinarily occurs in air just behind a square-back truck traveling at high speed. Wind around the truck would enter slits in the folded cone and automatically deploy it.

ic drag at normal highway speeds. A model has been tested successfully on a toy truck.

This work was done by Jack Bullman of Marshall Space Flight Center. No further documentation is available. MFS-28007

End Restraints for Impact-Energy-Absorbing Tube Specimens

The radial expansion of a rubber insert prevents tipping of the tube specimen.

Langley Research Center, Hampton, Virginia

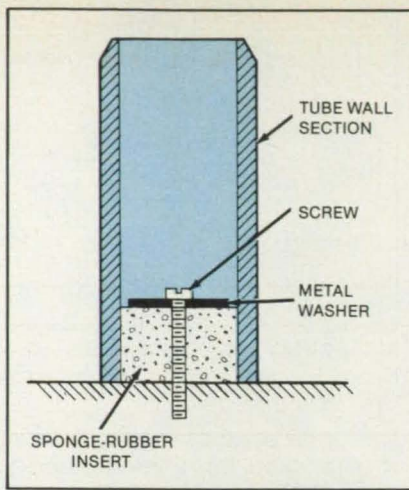
Tube specimens approximately 4 inches (10 centimeters) in length are impacted at Langley Research Center to NASA Tech Briefs, Summer 1985

measure the energy absorption capability of composite materials. A weighted table slides down guide rails and impacts the

specimen. The crushing force is determined by the deceleration of the table as the specimen is crushed. As a result of the

dimensional tolerances between the table guides and the rails, the table can impact the tubes in a nonlevel condition. This can result in tipping over and damaging the specimen. Depending on the geometry of the tubes, invalid test results can occur in as many as 30 percent of the tests. Typical composite tube specimens cost between \$75 and \$400 each.

An inexpensive device was developed that eliminates the tipping problem without affecting the crushing process. The device (see figure) consists of a soft sponge-rubber insert approximately 0.5 inches (1.3 centimeters) thick, cut to the same diameter as the internal diameter of the tube specimen. A metal washer, slightly smaller than the internal diameter of the tube, is placed on top of the rubber insert. A screw is passed through the washer and rubber insert and threaded into the base of the test machine. As the screw is



The Free End of the Tube Is Chamfered so that crushing always initiates at the non-supported end.

tightened against the washer, the rubber insert is compressed and expands radially. The radial expansion applies pressure against the internal wall of the tube specimen, which provides sufficient support to the tube to prevent tipping.

To preclude initiation of crushing at the supported end, thus yielding erroneous results due to the support provided by the device, the free end of the tube is chamfered. Crushing always starts at the chamfered end and is progressive. The device has virtually eliminated tipping and damage to the test specimen as a result of nonlevel conditions.

This work was done by Gary L. Farley of Structures Laboratory, U.S. Army Research and Technology Laboratories, AVSCOM and John T. Modlin of Langley Research Center. No further documentation is available.
LAR-13179

Accurate Airborne Particle Sampler

Air is inducted isokinetically into a centrifugal collector.

Langley Research Center, Hampton, Virginia

A new airborne particle sampler collects a representative sample of cloud-water droplets that are combined to form one bulk liquid sample, making it possible to chemically analyze the liquid content of clouds for trace constituents.

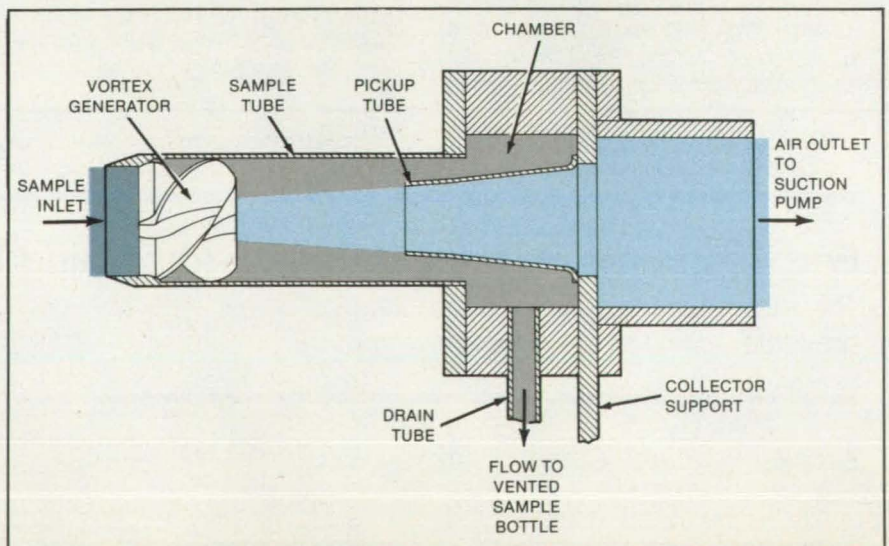
As shown in the figure, the component parts of the sampler include a sample tube, vortex generator, pickup tube, chamber, and drain tube. The vortex generator consists of a set of fixed vanes or airfoils that are set at an angle within the sample tube near the tube inlet.

The airborne device is flown through a cloud causing particle-laden air to enter the sample tube and to be rotated by the vortex generator. This rotation acts as a centrifuge to drive the particles in the airstream toward the wall of the sample tube. The airstream at the wall, containing the larger particles, flows through an annular opening at the rear of the sample tube. The airstream in the center of the sample tube flows through a smaller concentric tube called the pickup tube. The design of this assembly (sample tube, vortex generator, and pickup tube) and the airstream parameters (axial velocity, temperature, and particle density) determine the minimum size of particles to enter the annular opening and be captured; particles below this size are discharged through the pickup tube.

Thus, it is possible to capture all the liquid droplets in a cloud but discharge the smaller aerosol particles present between the droplets in that cloud.

Inside the collector, the captured airstream, called the scavenger airstream, enters the chamber where droplet impaction occurs. This impaction causes a stream of water to form. Both the water and the air flow down the drain

tube to a sample container that collects the water and vents the air. The airstream in the center of the sample tube, called the lean airstream, flows through the pickup tube. A suction pressure is applied to both the lean and scavenger airstreams by an amount that produces an axial velocity in the sample tube equal to the velocity of air approaching the tube. This is an isokinetic condition that is ob-



A Cloud Drop Collector can accurately and efficiently sample droplets and reject aerosol particles.

tained when the static pressure in the sample tube equals the static pressure of the free stream surrounding the tube. This condition, together with a thin wall or sharp edge at the sample tube inlet, results in a representative sampling of any airborne particle-size distribution. Scavenger airflow is regulated to obtain

maximum collection efficiency and is usually about 10 percent of the total flow in the sample tube.

A number of these collectors can be connected in series, each so designed that the largest size fraction of droplets is captured in the first one and successively smaller size fractions captured in the

others. By analyzing each size fraction, the chemical composition of cloud droplets can be related to drop size.

This work was done by Irvin M. Miller of Langley Research Center. For further information, Circle 39 on the TSP Request Card.
LAR-13080

Testing Machine for Biaxial Loading

A standard tensile-testing machine applies bending and tension simultaneously.

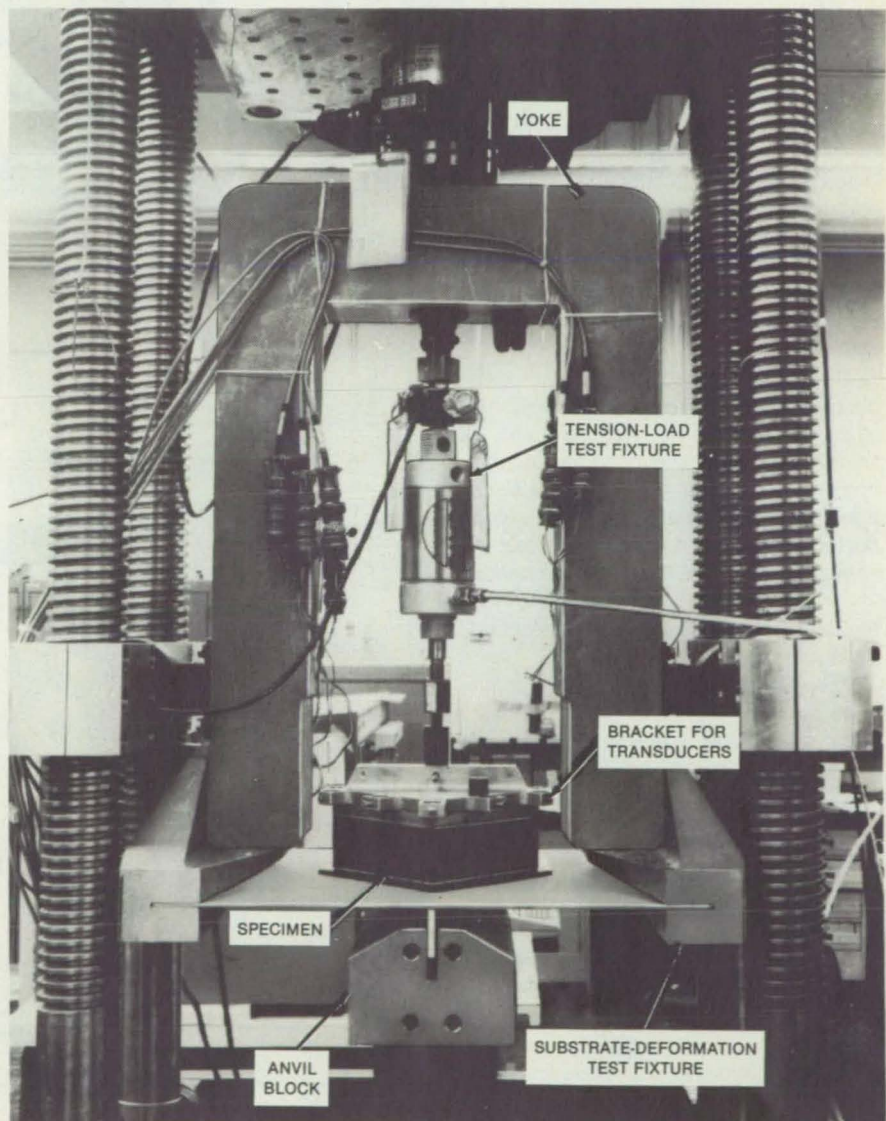
Lyndon B. Johnson Space Center, Houston, Texas

Special fixtures added to a commercial tensile-testing machine apply bending loads to a test sample that is also under tensile stress. In many cases such biaxial loading can simulate conditions of actual use more accurately than can simple tensile testing alone. Multiaxial load testing can be particularly important for composite structures. The modified test apparatus was originally developed to load-test Space Shuttle surface-insulation tiles.

The bottom surface of the specimen is bonded to a relatively thin metal substrate. The top surface of the specimen is bonded to a thicker metal plate, to which is attached a bracket that holds 10 transducers around its periphery (see figure). A downward-projecting tab forms a "T" at the middle of the plate and enables a vertical tensile stress to be applied through the metal plate to the specimen.

The substrate-deformation fixture has two parts. The upper part is a fixed, inverted U-shaped yoke that attaches to the tensile-testing machine at the top and grips the two ends of the horizontal substrate plate at the bottom to keep the ends from rotating. The substrate deformation is thereby forced to approximate a sine wave. In the lower part of the fixture, an anvil block grips the tab extending downward from the substrate. The anvil mounts on a servo-controlled hydraulic actuator which moves the anvil block up or down to control the curvature of the substrate. The 10 transducers measure the substrate deflection.

The tension-loading fixture pulls upward on the test sample. A pneumatic cylinder attached to the yoke and to the bracket on top of the specimen applies the tension. A load cell in mechanical series with the pneumatic cylinder measures the tension. The operator controls the loading rate with a needle valve in the cylinder supply line and controls the peakload by adjusting the supply pressure.



A Biaxial-Loading Test Machine has been created by adding two test fixtures to a commercial tensile-testing machine. The bending moment is applied by the substrate-deformation fixture comprising the yoke and the anvil block. The pneumatic tension-load fixture pulls up on a bracket attached to the top surface of the specimen. Tension and deflection are measured with transducers.

This work was done by Robert J. Demonet and Richard D. Reeves of Rockwell International Corp. for Johnson

Space Center. For further information, Circle 36 on the TSP Request Card.
MSC-20477

Combination Heat-Flux and Temperature Gage

Instrument measures both temperature and temperature gradient in confined areas.

Lyndon B. Johnson Space Center, Houston, Texas

A new gage combines the functions of temperature measurement and heat-flux measurement in a miniature package. Its small size makes the instrument suitable for testing scale models of aircraft and monitoring thermal effects in automobile engines, turbines, and heat exchangers.

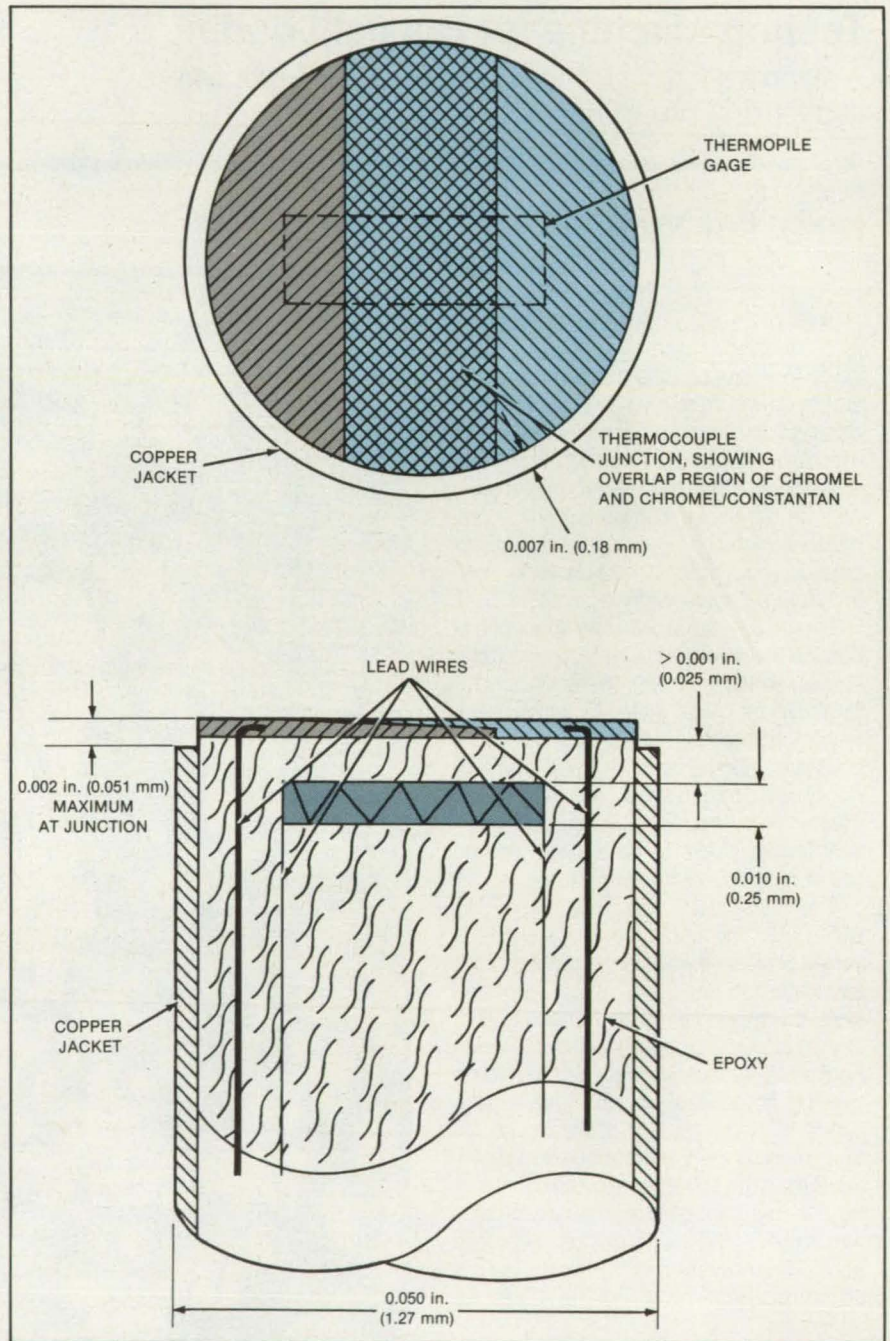
As shown in the figure, a thermopile heat-flux gage and two thermocouple lead wires are cast with an epoxy filling in a copper sleeve of outside diameter 0.050 inch (1.27 millimeters). The thermocouple is then formed on the epoxy surface by vapor-depositing a film of Chromel (an alloy of Ni, Cr, and Fe), or equivalent, and a film of Chromel/constantan (constantan is an alloy of Cu and Ni), or equivalent. Each of the films is 0.001 inch (25 micrometers) thick, and each occupies two-thirds of the top surface, overlapping at the center. A mask may be used to delineate the film areas during vapor deposition.

The unit is installed so that the thermocouple is flush with the surface of the object to be measured. Heat from an external source increases the surface temperature of the unit, generating an electrical signal from the thermocouple junction. Heat conducted into the unit produces a temperature difference across the thermopile heat gage. The difference is proportional to the heat flux, and the gage produces a corresponding electrical signal.

Previously, it was necessary to mount a separate thermocouple and a heat-flux gage side by side. This was difficult when the object to be measured was small or the section to be measured was restricted. In addition, large errors could result because the thermal conditions at the thermocouple were not necessarily those at the heat gage. Alternatively, a calorimeter was used: This device, which consisted of a heat-flux gage with a companion thermocouple embedded in its base, was unsatisfactory because the temperature gradient between the surface and the thermocouple precluded accurate computation of surface heat-transfer coefficients.

This work was done by Eugene C. Knox of Rockwell International Corp. for Johnson Space Center. No further documentation is available.

MSC-20706



With a Thermopile Embedded in epoxy close to a thermocouple, a single unit measures both temperature and heat flow. The epoxy is selected for low thermal conductivity and compatibility with the test environment.

Sequentially-Deployable Tetrahedral Beam

Beam geometry can be varied three-dimensionally after the beam is deployed.

Langley Research Center, Hampton, Virginia

The sequentially-deployable tetrahedral beam can become a crane, a manipulator arm, an antenna feed support, or other type of lineal structural member. The beam is completely packageable, automatically deployable, and capable of having its geometry varied during use.

A stick model of the deployed tetrahedral beam is shown in Figure 1. The beam is a tandem series of interconnected tetrahedra. Common sides, or battens, of adjacent tetrahedra form equilateral triangles, or batten frames. Each tetrahedron of the beam is thus composed of two such equilateral triangular frames that have a common batten for their bases. Apexes of the two frames are held apart by a longeron member. The length of the longeron member can be different from that of the batten mem-

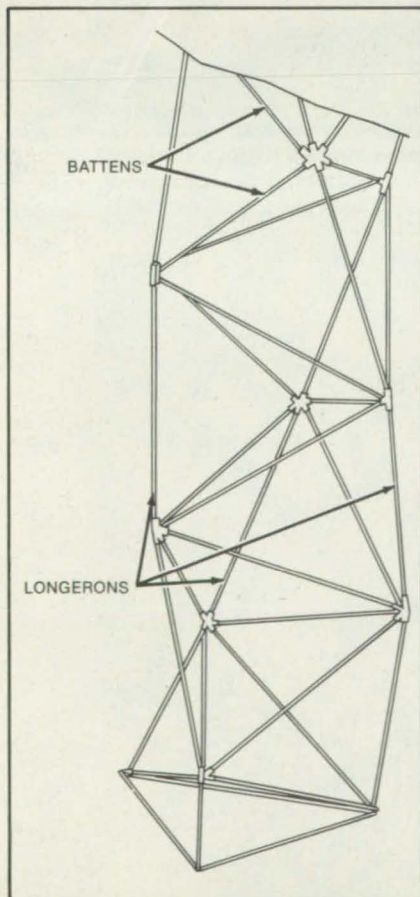


Figure 1. A Series of Interconnected Tetrahedra comprises the tetrahedral beam that folds into a compact package. The beam readily unfolds as a structural support member or an extension arm.

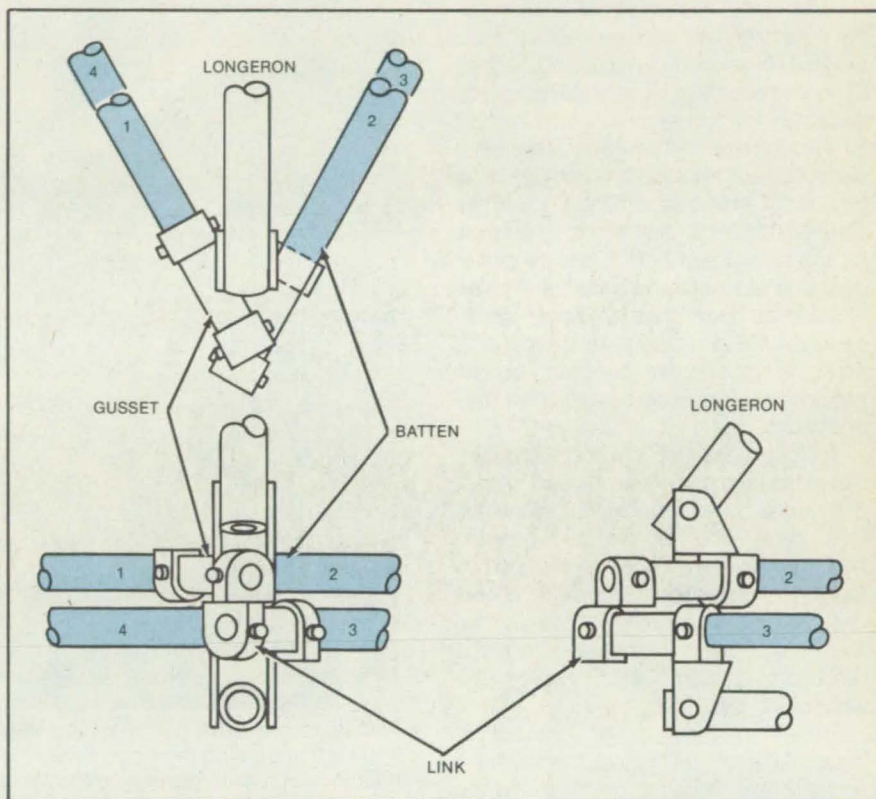


Figure 2. Specially-Designed Corner Joints allow compact folding of the beam. The battens shown here fold one against the other.

bers. Thus, the tetrahedral beam is composed of any desired number of tetrahedra in series, with adjacent common faces being equilateral triangular-batten frames.

When the tetrahedral beam is completely retracted, each longeron is shortened indefinitely so that frames at each end of the longeron are folded together to lie one against the other. Each tetrahedron of the beam can be so retracted to achieve compact packaging of the entire beam. Each longeron can be shortened by folding it at its midlength and ends, by telescoping it, or by other means. Thus the beam has a variable geometry capability (e.g. bendable) by varying the length of one or more of the longeron members.

Adjacent batten frames are folded one against the other by joining them at their corners by gussets and links that swivel. A typical corner is shown in Figure 2. Batten members 1 and 2 are connected into an upper gusset, battens 3 and 4 and into a lower gusset, and these assemblies are interconnected by a link that is attached to the ends of battens 1 and 3, the ends of which pro-

trude through their respective gussets. In folding and deployment, batten 1 swivels in the upper gusset, and the link that is fixed to batten 1 swivels on the end of batten 3. Battens 2, 3 and 4 are fixed to their respective gussets. This arrangement allows the two rotational degrees of freedom at each corner so that the batten frames fold together one against the other. Compression and tension loads applied to the longeron member of the model demonstrate that this corner-joint design constitutes a stable linkage system in any phase of partial or complete deployment.

This work was done by Martin M. Mikulas, Jr., of Langley Research Center and Robert F. Crawford of General Research Corp. For further information, Circle 47 on the TSP Request Card.

This invention is owned by NASA, and a patent application has been filed. Inquiries concerning nonexclusive or exclusive license for its commercial development should be addressed to the Patent Counsel, Langley Research Center [see page 21]. Refer to LAR-13098.

Hand-Held Electronic Gap-Measuring Tools

Repetitive measurements are simplified by a tool based on LVDT operation.

Lyndon B. Johnson Space Center, Houston, Texas

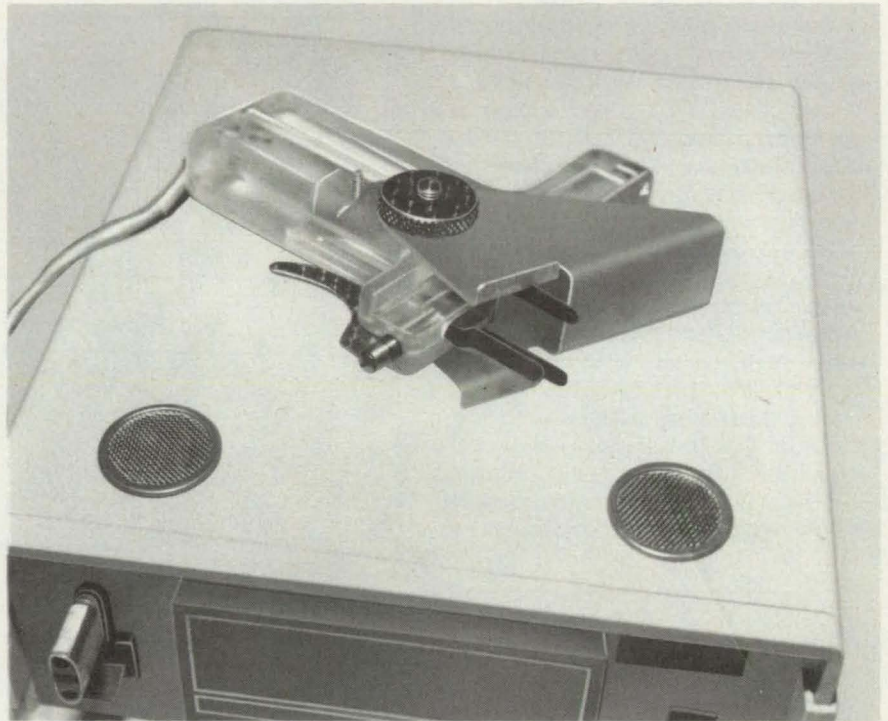
A hand-held tool accurately measures the separation between adjacent surfaces. Originally developed for measuring the gaps between the surface tiles of the Space Shuttle orbiter, the tool reduces measurement time from 20 minutes per tile to 2 minutes. It also reduces the possibility of damage to the tiles during the measurement. The tool has potential applications in mass production; for example, it can help to ensure proper gap dimensions in the assembly of refrigerator and car doors. It could also be used to measure the dimensions of components and to verify the positional accuracy of components during progressive assembly operations.

The gap-measuring tool contains fingers that extend from the cores of linear variable-differential transformer (LVDT) windings (see figure). When inserted in a gap, the fingers press lightly on the opposite gap surfaces. The separation between the fingers changes the inductance of the transformer. The transformer is connected to a digital readout instrument, which displays the width of the gap.

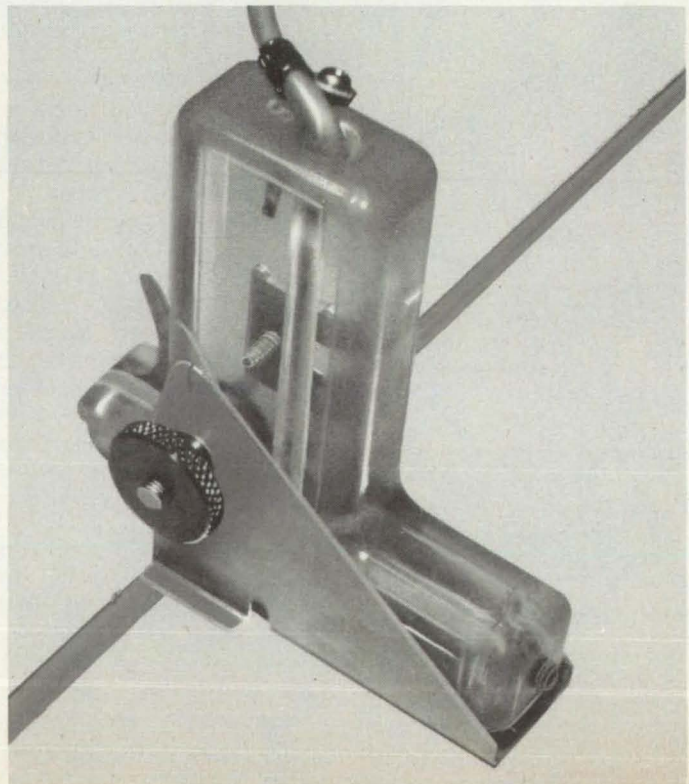
To insert the fingers in a gap, the user depresses a trigger on the tool, thereby lining up the fingers. Once the tool is inserted, the user releases the trigger, thereby allowing the central finger to expand and make contact with the gap surface opposite the two stationary fingers. The user can then read the gap spacing on the digital display.

The previous method of measurement used plastic feeler gages. The user selected two gages according to the minimum and maximum allowable gap spacing and slid them along the gap to perform a go/no-go test. The method was not only time consuming but also could result in erroneous readings or tile damage if an oversize gage was moved between the tiles.

This work was done by Frank E. Sugg, Fredrick W. Thompson, Lino A. Aragon, and Douglas B. Harrington of Rockwell International Corp. for Johnson Space Center. For further information, including specification and drawings, Circle 73 on the TSP Request Card.
MSC-20176



With its fingers in the open position, the **Gap-Measuring Tool** rests on a digital readout instrument (top). With the fingers inserted in a gap (bottom), gap separation alters the inductance of a linear variable-differential transformer in the plastic handle.



Fixture for Linearly Variable Displacement Transducers

The original point of interest on a shear panel is tracked throughout loading.

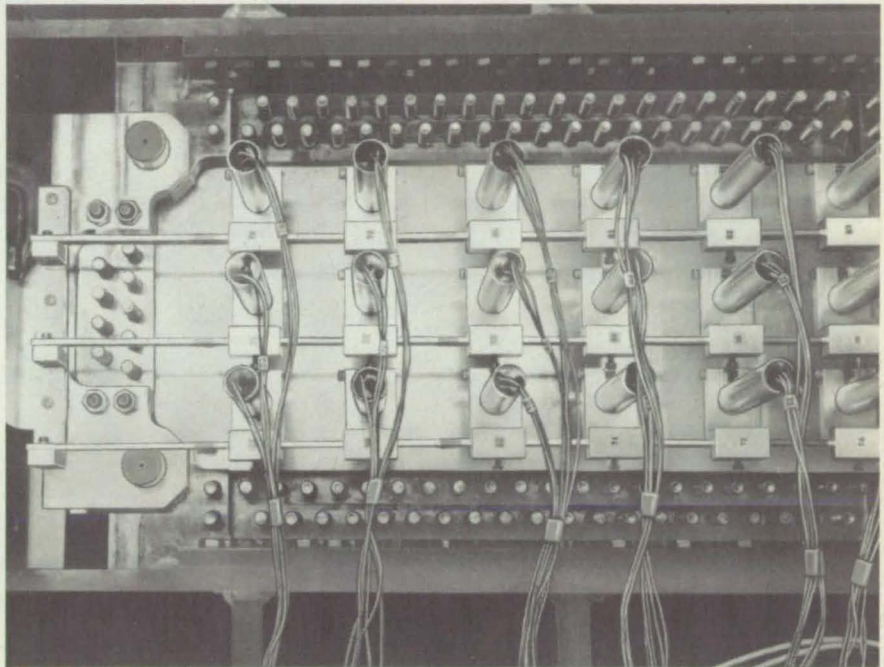
Langley Research Center, Hampton, Virginia

A technique and fixture measure the out-of-plane displacements on a shear panel using linearly variable displacement transducers (LVDT's) while tracking the original panel location. The technique is adaptable to any size shear panel.

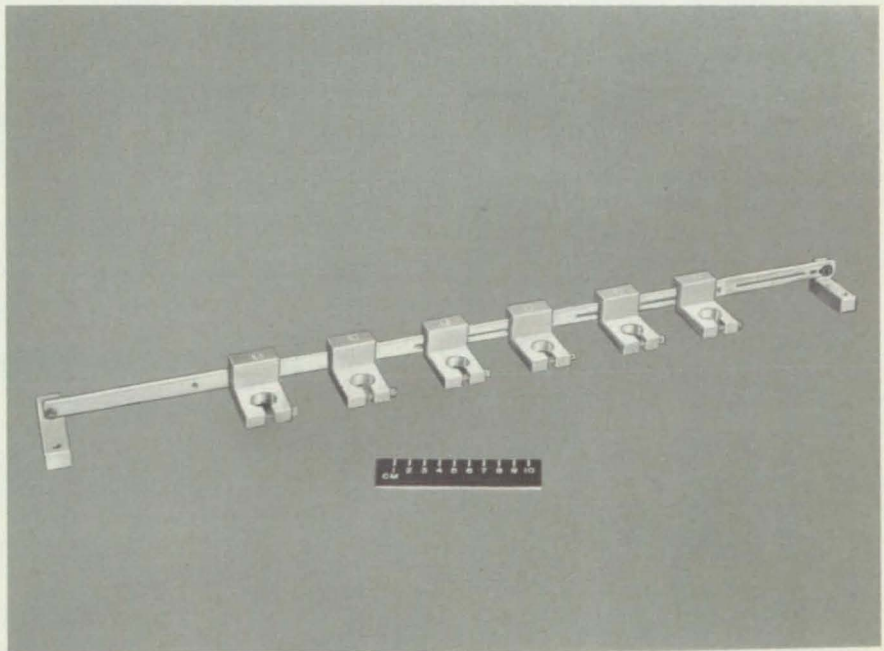
The figure depicts the fixture with (top) and without (bottom) the LVDT's. During shear tests, the horizontal rails of the shear fixture may rotate about their axes; by use of a pivot between the mounting pad of the LVDT bracket (which fastens to the horizontal rail) and the long vertical fixture bar component to which the LVDT's are fastened, the gridwork remains planar independent of the deformation of the panel. Therefore, the reference frame of the transducers remains unbiased for measurement of out-of-plane deformation.

At the top of the figure, three rows of LVDT fixtures are shown attached to a shear-panel fixture. Up to six LVDT's are currently used on each LVDT fixture at Langley Research Center, though this number is not a limitation for other applications. As the shear fixture deforms, the small L-brackets rotate relative to the horizontal rails of the shear fixture. This rotation keeps the fixture bar parallel to the vertical rails of the shear fixture and ensures the tracking of the original point on the panel.

This work was done by Gary L. Farley and Donald J. Baker of the Structures Laboratory, U.S. Army Research and Technology Laboratories — AVSCOM for Langley Research Center. For further information, Circle 20 on the TSP Request Card.
LAR-12937



The LVDT Fixture is shown with (top) and without (bottom) the LVDT's attached. The fixture permits measurement of shear-panel out-of-plane displacement while tracking the original panel location.



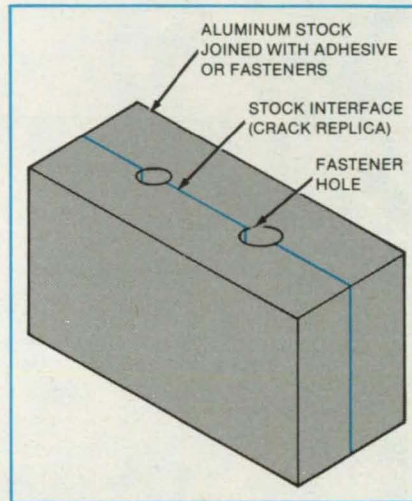
Inexpensive Eddy-Current Standard

Radial crack replicas serve as evaluation standards.

Langley Research Center, Hampton, Virginia

The nondestructive evaluation of aircraft and other metal structures often entails the utilization of eddy-current inspection techniques. Eddy-current inspections are designed to detect metal defects, one type of which consists of radially propagated cracks from or through fastener holes. Proper implementation of these inspections necessitates technique setup and verification utilizing accurate defect replicas or standards.

A simple technique facilitates the fabrication of radial fastener hole crack replica standards. As shown in the figure, this technique entails intimately joining two pieces of appropriate aluminum alloy stock and centering a drilled hole through and along the interface. The bore surface of this hole presents two vertical stock in-



terface lines 180° apart. These lines serve as radial crack defect replicas during the eddy-current technique setup and verification.

This standard fabrication technique affords an inexpensive and rapid means of manufacturing radial crack standards. Furthermore, it is versatile because multiple fastener holes of varied diameters may be placed within the same standard.

This work was done by Robert F. Berry, Jr., of Langley Research Center. No further documentation is available.
LAR-13154

Drilled Holes along the interface simulate radial fastener hole defects.

Force Sensor for Large Robot Arms

A modified Maltese-cross force sensor allows claw drives to be mounted inside large robot arms.

NASA's Jet Propulsion Laboratory, Pasadena, California

A modified Maltese-cross force sensor is larger and more sensitive than earlier designs. It can measure inertial forces and torques exerted on large robot arms during free movement as well as those exerted by the claw on manipulated objects. The large central hole of the sensor allows the claw drive to be mounted inside the arm instead of perpendicular to its axis, eliminating a potentially hazardous projection. Originally developed for the Space Shuttle, the sensor may find applications in large industrial robots.

The figure shows the wrist, claw, and sensor in cross section. The "Maltese cross" consists of four deflection bars. They are twisted and/or bent by forces between the outer shell and the claw support. Two strain gages are bonded to each side of each deflection bar. Opposing pairs of gages are quad-wired in a full bridge circuit to reduce imbalances from thermal drift. The bridge readings are then resolved into signals proportional to the three orthogonal forces and three torques acting on the sensor assembly.

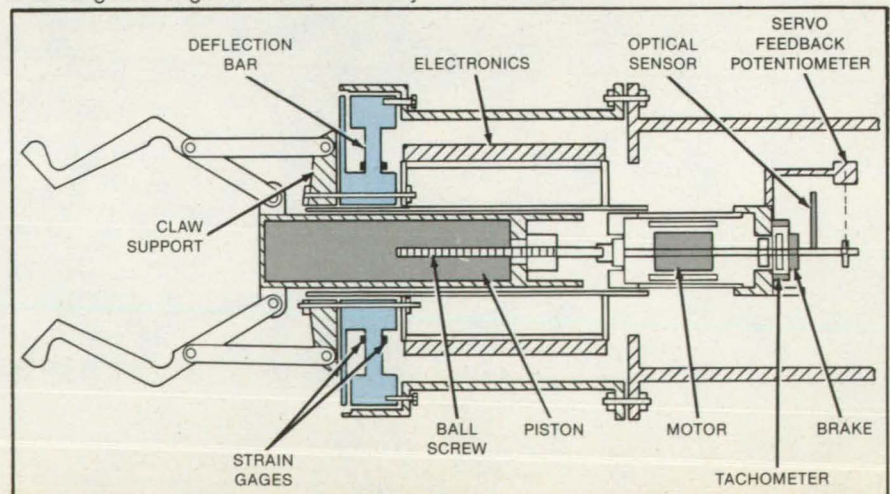
The claws open and close according to

extension and retraction of the piston, which is driven by a brushless motor. A servo feedback potentiometer, tachometer, a brake, and an optical sensor control claw position and speed.

The force sensor was fabricated in 45-kg and 90-kg size ranges. It was successfully

tested with a simulated Space Shuttle arm.

This work was done by Antal K. Bejczy, Howard C. Primus, and Victor D. Scheinman of Caltech for NASA's Jet Propulsion Laboratory. For further information, Circle 29 on the TSP Request Card.
NPO-16097



The **Maltese-Cross Sensor** measures forces and torques on a robot arm with semiconductor strain gages.

Tabs Reduce Helicopter-Blade Vibrations

Sprung and hinged passive control surfaces interact with harmonic airloads.

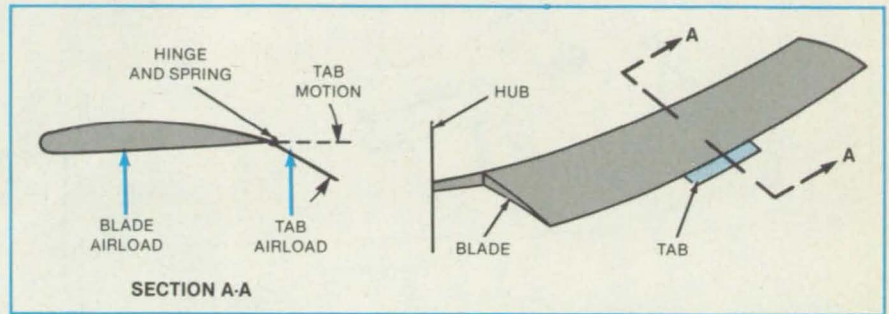
Ames Research Center, Moffett Field, California

A tuned flaplike tab on the trailing edge of a helicopter rotor blade reduces blade vibration. When properly designed, the tab should have little effect on the handling characteristics of the helicopter.

When the spring-loaded tab deflects, it changes both the lift and pitching moment characteristics of the rotor blade (see figure). The additional airload results from a camber-induced shift of the lift coefficient for a fixed blade angle-of-attack. This shift also induces a shift in the blade-pitching moment coefficient, which creates yet more airload because the blade becomes twisted, changing its angle-of-attack. If the tab deflects in harmonic motion, the additional airload and pitching moment created by tab motion are also harmonic and can add or, preferably, subtract from vibration caused by harmonic airloads, depending on the amplitude and phase of tab motion.

The force driving the tab is the combination of its own inertia and the airflow as the blade flaps and twists. By offsetting the tab center-of-gravity from the hinge line, the inertial forcing can be increased. The dynamic response of the tab to the inertial forcing can be altered by tuning the natural frequency of the tab: This is done by changing the stiffness of the tab-hinge spring.

Thus, there is a direct relationship between the motion that inertially forces the tab to deflect and the vibration that results from that same motion. The success of exploiting the relationship depends on correctly sizing and placing the tab along the rotor-blade span and choosing the tab mass and



A Flapping Tab on a Rotor Blade produces aerodynamic loads that oppose vibrational aerodynamic loads. With the proper choice of tab parameters, the tab can be made to cancel much of the blade vibration over a wide range of rotor speeds and airspeeds.

natural frequency. When this is done, the airload created by the tab has the right amplitude and phase to cancel a portion of the inherent harmonic component of the airload that induces the vibration in the rotor.

Placement of the tab along the blade is critical. In an analysis of a Black Hawk helicopter traveling at 175 knots (90 m/s), it was found that the best position for a tab was at 60 percent of the radius from the rotor hub to the blade tip. The most effective resonant frequency consistent with vibration-amplitude design constraints was 10 tab-deflection cycles per revolution of the rotor.

Another important design parameter is the length of the tab. An increase in length increases the control surface area, which augments the control authority of the tab. If tab length increases beyond 15 percent of the blade length, however, such mechanical

difficulties as tab bending and hinge binding arise, and benefits tend to diminish.

Increasing the tab chord also increases control authority, although not nearly as strongly as increasing tab length. However, a greater chord does help to reduce the amplitude of tab motion. A 4.2-inch (10.7-cm) chord was selected because it gives rise to an angular motion of only 4.5° in contrast to 8° for a 2.1-inch (5.3-cm) chord.

This work was done by Thomas G. Campbell of United Technologies Corp. for Ames Research Center. For further information, Circle 76 on the TSP Request Card.

Inquiries concerning rights for the commercial use of this invention should be addressed to the Patent Counsel, Ames Research Center [see page 21]. Refer to ARC-11444.

Flowmeter for Clear and Translucent Fluids

Displacement of a diaphragm is measured electro-optically.

Marshall Space Flight Center, Alabama

A transducer with only three moving parts senses the flow of a clear or translucent fluid. The displacement of a diaphragm by the force of the flow is detected electro-optically and displayed by a panel meter or other device. Such a transducer might be used, for example, to measure the flow of gasoline to an automobile engine.

In the absence of flow, two slightly-compressed opposing coil springs hold a diaphragm at the midplane of a small chamber (see figure). A round hole at the center of the diaphragm is encircled by spring-centering washers on the upper and lower faces. The conical tip of a set screw protrudes through the hole from the upstream

side.

When the fluid flows, it must pass through the hole in the diaphragm. The flow pushes on the diaphragm, thereby lifting the diaphragm away from the cone. The opening between the edge of the hole and the cone widens until the cross section is sufficient to satisfy the flow requirement. The hole size

[typically 1/4 in. (6.35 mm)] is chosen so that the pressure drop across the transducer is negligible at maximum flow. The volumes above and below the diaphragm help to reduce turbulence in the flow.

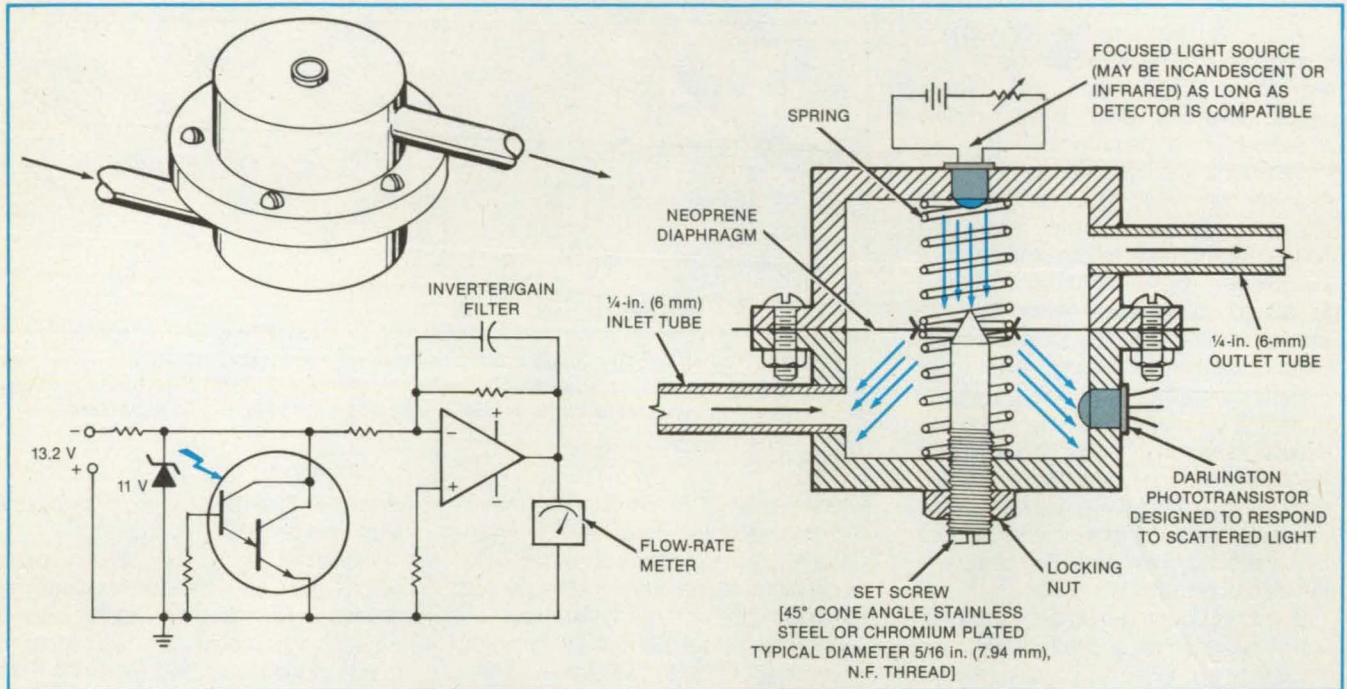
An incandescent lamp or other light source illuminates the opening from the upstream side. (An optical fiber can be used to extend the light source to a point near the cone tip.) A photodetector on the down-

stream side senses the scattered light that passes through the opening, thereby effectively measuring the size of the opening and the amount of flow. At zero flow, the set screw is adjusted so that it just barely makes contact with the cone, as indicated by a scattered-light reading with an incipient rise from zero.

The transducer is operated with external circuitry that amplifies, filters, or otherwise

processes the detector output to give a reading calibrated in terms of the flow rate. The materials in the transducer must, of course, be chemically compatible with the fluid.

This work was done by Paul R. White of Marshall Space Flight Center. No further documentation is available.
MFS-28030



The Fluid Flows Along the Cone Toward the Tip, displacing the diaphragm and enlarging the opening around the cone. The size of the opening is measured in terms of the scattered light that passes through.



Low-Temperature Seal for Actuator Rod

Seal redesign eliminates cracking at low temperatures.

Lyndon B. Johnson Space Center, Houston, Texas

A combination bearing and seal used on the Space Shuttle functions reliably at temperatures as low as -160°F (-107°C) and as high as $+130^{\circ}\text{F}$ (54°C). Shown in Figure 1, the assembly seals a reciprocating actuator rod against leakage of helium pressurized to as much as 780 psig (5.4 MN/m^2). In its open position, the rod allows fuel to replenish a tank. In its closed position, the rod blocks the flow of fuel.

The new design replaces a version that was subject to cracking of the seal lip at low

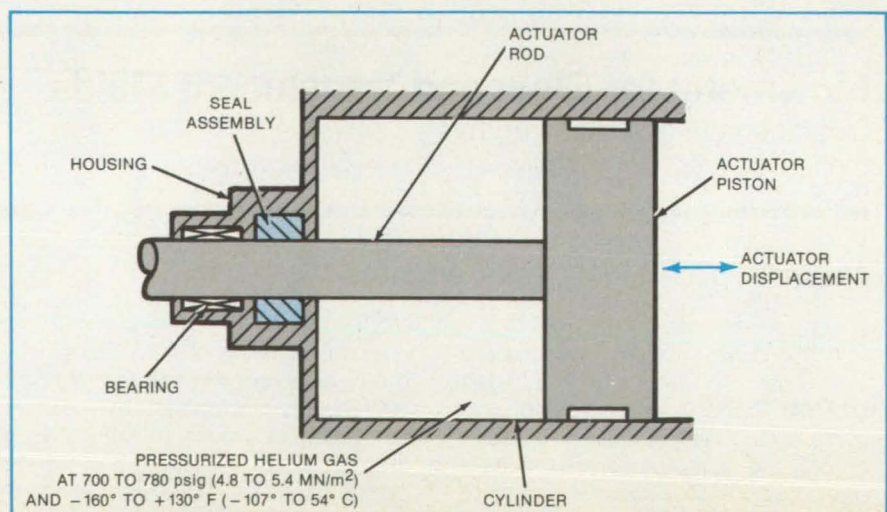


Figure 1. The Seal Assembly is shown in relation to the other parts of the actuator system.

temperatures (see Figure 2). In the new seal, the bearing surface is separated by a bridge from a flexible sealing lip in both the primary and secondary seals. As a result,

the seals can be axially preloaded to prevent leakage without unduly stressing a bearing located elsewhere along the rod.

This work was done by Robert J. Lindfors

of Consolidated Controls Corp. for Johnson Space Center. No further documentation is available.
MSC-20744

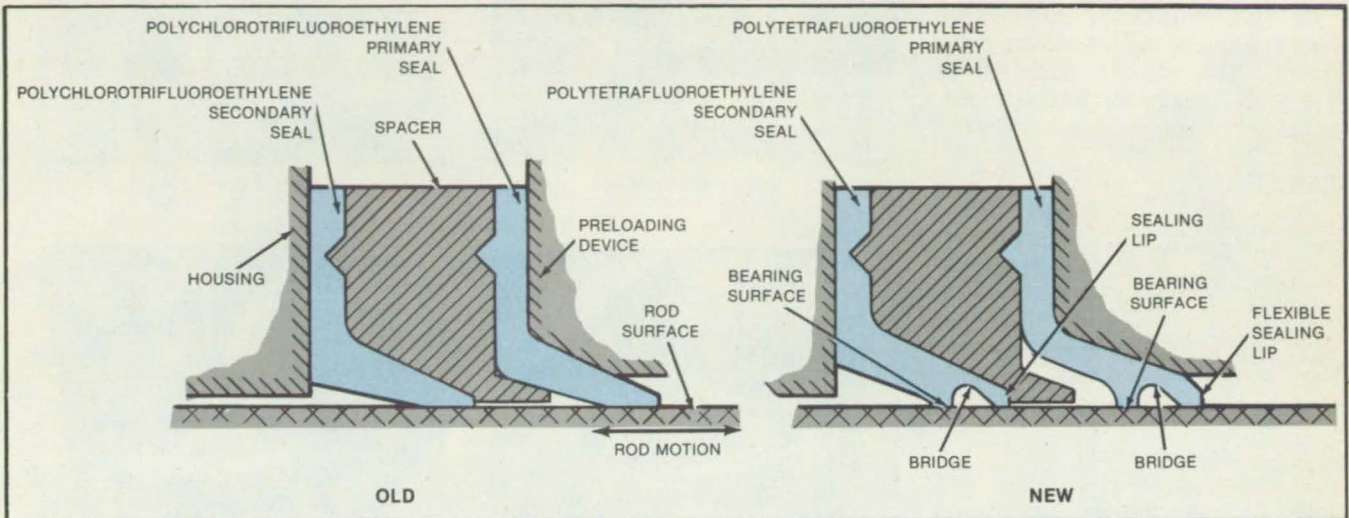


Figure 2. A Corrosion-Resistant Stainless-Steel Spacer separates secondary and primary seals in both the old and the new versions of the seal assembly. In the new version, however, the combination of the flexible sealing lip and bridge is less susceptible to cracking at low temperatures.

Detecting Cracks in Rough Metal Surfaces

An eddy-current test succeeds where visual inspection fails.

Lyndon B. Johnson Space Center, Houston, Texas

A test based on the eddy-current probe technique identifies cracks in swaged metals. By visual inspection alone, cracks are often difficult or impossible to distinguish from folds, swaging displacements, tool marks, or other features of the rough swaged surface. The method is suitable for many kinds of metal parts, including swaged fittings, tubing, and pipes. It can be used for rapid crack/no-crack determinations in suspect parts already installed.

As shown in Figure 1, the eddy-current probe coil is mounted on an adjustable slide on a collar that fits around the swaged fitting or other part to be tested. The probe position relative to the collar and the tested part is varied by unlocking and adjusting the slide. The collar is made of a nonconducting material so as not to disturb the probe reading. A spring-loaded latch helps to keep the collar in position, yet allows it to flex to accommodate surface roughness.

As in other eddy-current techniques, the probe coil is placed near, or in contact with, the part to be tested. The coil is excited at one or more frequencies (in this case, 500

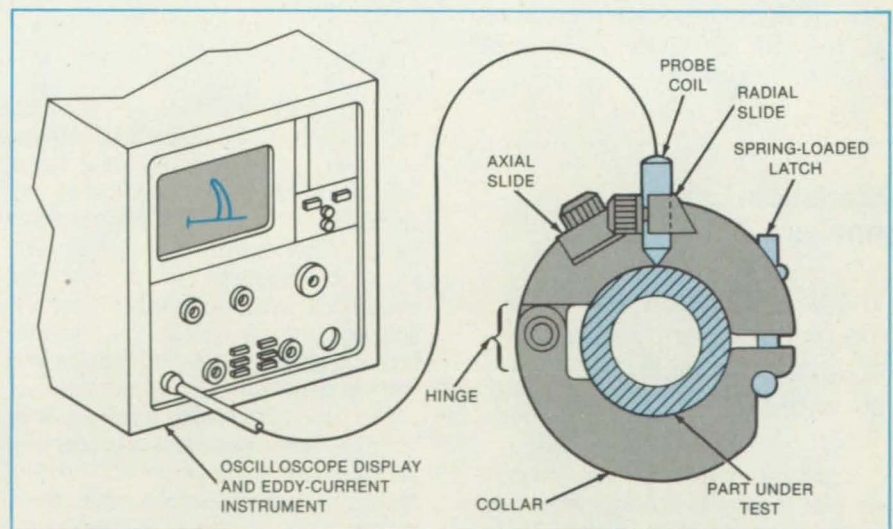
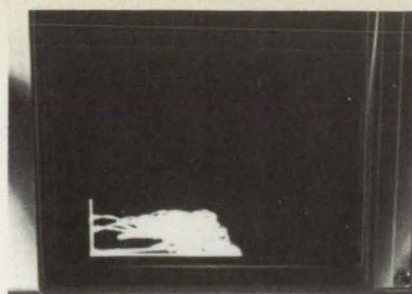


Figure 1. A Hinged Collar with a spring-loaded latch holds the probe in place on the part to be tested. For repeated measurements on the same or similar parts, the collar is loosened and moved to the various measuring positions.

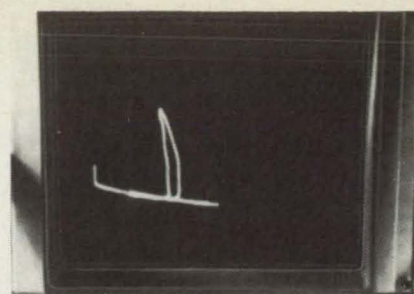
kHz), and an analog of the complex coil impedance is displayed on an oscilloscope. A crack or discontinuity affects the impedance, resulting in a displacement of the oscilloscope trace (see Figure 2).

This work was done by Nelson T. Zuver, Frank E. Sugg, Fred H. Stuckenberg, and Edward T. Morrissey of Rockwell International Corp. for **Johnson Space Center**. For further information, Circle 35 on the TSP Request Card.

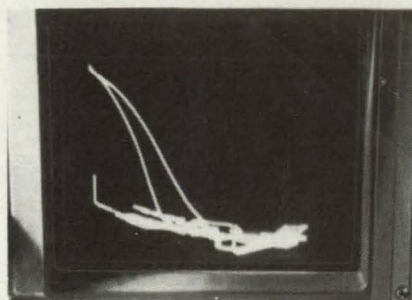
MSC-20734



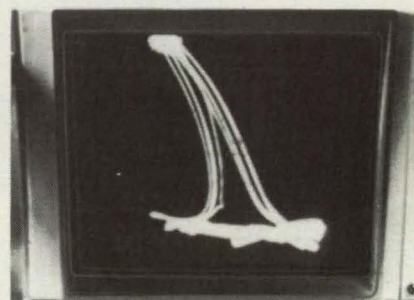
TYPICAL RESPONSE OVER GOOD SWAGE



RESPONSE FROM SMALL-TO-MEDIUM CRACK



RESPONSE FROM MEDIUM CRACK



RESPONSE FROM LARGE CRACK (SEVERAL PASSES)

Figure 2. These **Sample Oscilloscope Traces** were taken by eddy-current probe measurements on "good" and "bad" swaged fittings.

Computer Programs

These programs may be obtained at a very reasonable cost from **COSMIC**, a facility sponsored by **NASA** to make raw programs available to the public. For information on program price, size, and availability, circle the reference number on the TSP and COSMIC Request Card in this issue.

Statistical Energy Analysis Program

The SEA program estimates the high-frequency vibration spectra of complex structures.

Significant high-frequency random-vibration environments are generated during the operation of aerospace vehicles within the atmosphere. To achieve optimum vehicle design, vibration and acoustic criteria are constructed early in the vehicle development program and are updated periodically as the design matures. Statistical Energy Analysis (SEA) is a powerful tool for estimating the high-frequency vibration spectra of complex structural systems and has been incorporated into a computer program. The SEA analysis method is based on

the estimation of the power flow between idealized gross elements of a vibrating system. The method is statistical in that averaging assumptions are made with regard to the distribution of energy within an element, the distribution of resonant modes, and the coupling between elements. These assumptions greatly simplify the computational complexity associated with the normal mode method.

The basic SEA analysis procedure is divided into three steps: Idealization, parameter generation, and problem solution. The idealization step consists of the user modeling the physical structure in terms of the available SEA program elements. The SEA program can analyze systems with up to 20 elements, with each element being made up of one or more subelements. The subelement system provides a convenient way to compute and include the modal density and mass properties of the individual structural pieces. The types of subelements available are beams, plates, cylinders, membranes, and reverberant rooms.

Once a suitable model has been developed, the parameter generation step consists of selecting those parameters that specify the analysis to be performed. Random acoustic or mechanical excitation can be applied in $\frac{1}{3}$ octave bands to any arbitrary number of elements in the model. The problem solution step is performed by the SEA computer program. The program output includes the calculated modal densities and the power spectral density for each element for each analysis frequency.

The SEA computer program is written in FORTRAN V for batch execution and has been implemented on a UNIVAC 1100 series computer with a central memory requirement of approximately 15k of 36-bit words. The program was developed in 1981.

This program was written by Robin C. Ferebee, R. W. Trudell, L. I. Yano, and S. I. Nygaard of McDonnell Douglas Astronautics Co. for **Marshall Space Flight Center**. For further information, Circle 64 on the TSP Request Card.
MFS-27035

Multiple Pages Missing from Available
Version

Analyses of Multishaft Rotor-Bearing Response

The method works for linear and nonlinear systems.

A finite-element-based computer program has been developed to analyze the free and forced response of multishaft rotor-bearing systems. The acronym, ARDS, denotes Analysis of Rotor Dynamic Systems. Systems with nonlinear interconnection or support bearings or both are analyzed by numerically integrating a reduced set of coupled-system equations. Linear systems are analyzed in closed form for steady excitations and are treated as equivalent to nonlinear systems for transient excitation.

The primary method of analysis used in ARDS is based on the concept of component mode synthesis (CMS) or substructuring. It is possible with linear systems, however, to bypass CMS and analyze the system by a direct method. The user may specify on input whether he wishes to use the ARDS-DM (-Direct Analysis of Multiple Shaft Systems) option or the ARDS-CM (-Component Mode Synthesis Analysis of Multiple Shaft Systems) option.

Both the direct and CMS methods of analysis utilize a fixed reference frame to describe the system motion and can, therefore, accommodate nonsymmetric interconnection, support damping, and stiffness properties. With the CMS option, the interconnection and support bearings may also be nonlinear. The rotating assemblies are considered to be composed of a number of finite elements, each of which may possess several subelements, thereby allowing for reasonable flexibility in modeling systems with several geometric discontinuities. The rotating assemblies are considered to be mounted on a rigid foundation except for the case of steady unbalance response using CMS. In this case, a rigid foundation may be used, or dynamic flexibility properties of the foundation support points may be included.

The CMS and direct options of the program both possess the capability to perform the following functions and analyses for systems supported on rigid foundations:

1. Accept user input data in a "koded" format essentially independent of order, process the data for optional output as a check of input, and prepare it for use in requested analyses;
2. Analyze the stability of system whirl modes;
3. Determine the steady unbalance response of the system for a specified unbalance distribution and specified ranges of spin speed;

4. Determine the steady response of the rotating assemblies relative to the rigid foundation due to the specified base motions:
 - a. Constant translational acceleration and
 - b. Constant turn rate;
5. Determine the static response of the rotating assemblies relative to the rigid base due to specified external fixed reference forces or moments or both. The CMS option of the program includes two additional analysis subroutines that:
6. Determine the steady unbalance response of the system for a specified unbalance distribution and specified ranges of spin speed, including the effect of foundation flexibility;
7. Determine the transient response of the rotating assemblies relative to a rigid foundation due to the following excitations:
 - a. Step change in unbalance distribution,
 - b. Arbitrary external forces,
 - c. Base step turn rate, and
 - d. Arbitrary base translational acceleration.

ARDS is a FORTRAN program that was developed on an Amdahl 470 (similar to an IBM 370). ARDS is written in double precision (Real*8, Complex*16) and uses the appropriate double precision FORTRAN Library functions. It makes use of several subroutines from the IMSL (International Mathematical and Statistical Library).

This program was written by H. D. Nelson and W. L. Meacham of the Arizona State University for Lewis Research Center. For further information, Circle 67 on the TSP Request Card.
LEW-13925

Are you reading someone else's copy of NASA Tech Briefs?

Qualified engineers and other new product development personnel can receive their own personal copy of NASA Tech Briefs by checking the subscription box and filling in one of the bound-in cards.

1	Exxon
2	General Motors
3	Mobil
4	Ford Motor
5	IBM
6	Texaco
7	E.I. du Pont
8	Standard Oil (Ind.)
9	Standard Oil of Cal.
10	General Electric
11	Gulf Oil
12	Atlantic Richfield
13	Shell Oil
14	Occidental Petroleum
15	U.S. Steel
16	Phillips Petroleum
17	Sun

27 million Americans can't read. And guess who pays the price.

Every year, functional illiteracy costs American business billions.

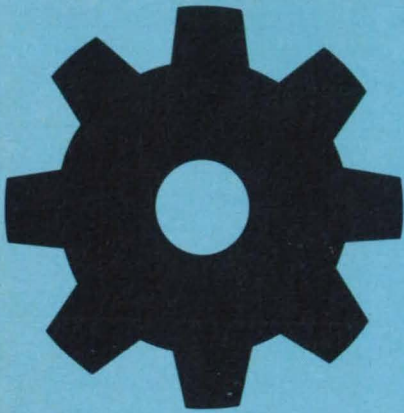
But your company can fight back...by joining your local community's fight against illiteracy. Call the Coalition for Literacy at toll-free **1-800-228-8813** and find out how.

You may find it's the greatest cost-saving measure your company has ever taken.

A literate America is a good investment.



Coalition for Literacy



Hardware, Techniques, and Processes

- 128 Automated Coal-Mining System
- 129 Pointable Auger
- 130 Modular Pick-and-Bucket Mining Machine
- 131 Reducing Coal Dust With Water Jets
- 132 Slurry-Mixing Chamber
- 133 All-Water-Jet Coal Excavator
- 134 Coal-Sizing Auger
- 134 Service Modules for Coal Extraction
- 135 Side Shield for Wall Support
- 136 Roof Shield for Advance and Retreat Mining
- 136 Compact Hydraulic Excavator and Support Unit
- 137 Curtain Wall Creates Ventilation Channel
- 138 Holder for Ultrasonic Evaluation of Small-Diameter Tubes
- 138 Improved Highway Pads for Tracked Vehicles
- 140 Low-Friction Joint for Robot Fingers
- 140 Blind-Side, High-Temperature Fastener Lock
- 141 Insulating Cryogenic Pipes With Frost
- 142 Precise Electrochemical Drilling of Repeated Deep Holes
- 143 Adapter Helps To Align Plasma Torch
- 143 Thermal Shock-Resistant Composite Crucible
- 144 Miniature Rocket Motor for Aircraft Stall/Spin Recovery
- 145 Shaft Seal Compensates for Cold Flow
- 146 Improved Exhaust Diffuser for Jet-Engine Testing
- 147 Gradually Acting Shaft Stop
- 147 Hand-Held Power Clamp
- 148 Anvil for Flaring PCB Guide Pins

Books and Reports

- 148 Effects of Bearing Clearance on Turbopump Stability
- 149 Optimizing Load Spectra for Gears
- 149 Predicting Leakage in Labyrinth Seals
- 149 Experiments With a Manipulator Sensor System

Computer Programs

- 150 Hybrid and Electric Advanced Vehicle Systems Simulation
- 151 Automatically-Programed Machine Tools
- 151 Analysis of Spiral Bevel Gearing

Automated Coal-Mining System

A proposed system offers safety and large return on investment.

NASA's Jet Propulsion Laboratory, Pasadena, California

A concept for a highly automated coal-mining system would increase productivity, make mining safer, and protect the health of mine workers. The system, which could be operating by the year 2000, would employ machines and processes that are based on proven principles. It encompasses operations ranging from extraction of the raw mineral to delivery of purified fuel to power stations. This article describes the overall

proposed system. Several of the subcomponents are described in more detail in the articles that follow, and others will be described in future issues of *NASA Tech Briefs*.

According to the concept, a line of parallel machines, connected in groups of four to service modules, attacks the face of a coal seam (Figure 1). High-pressure water jets and a central auger on each machine break

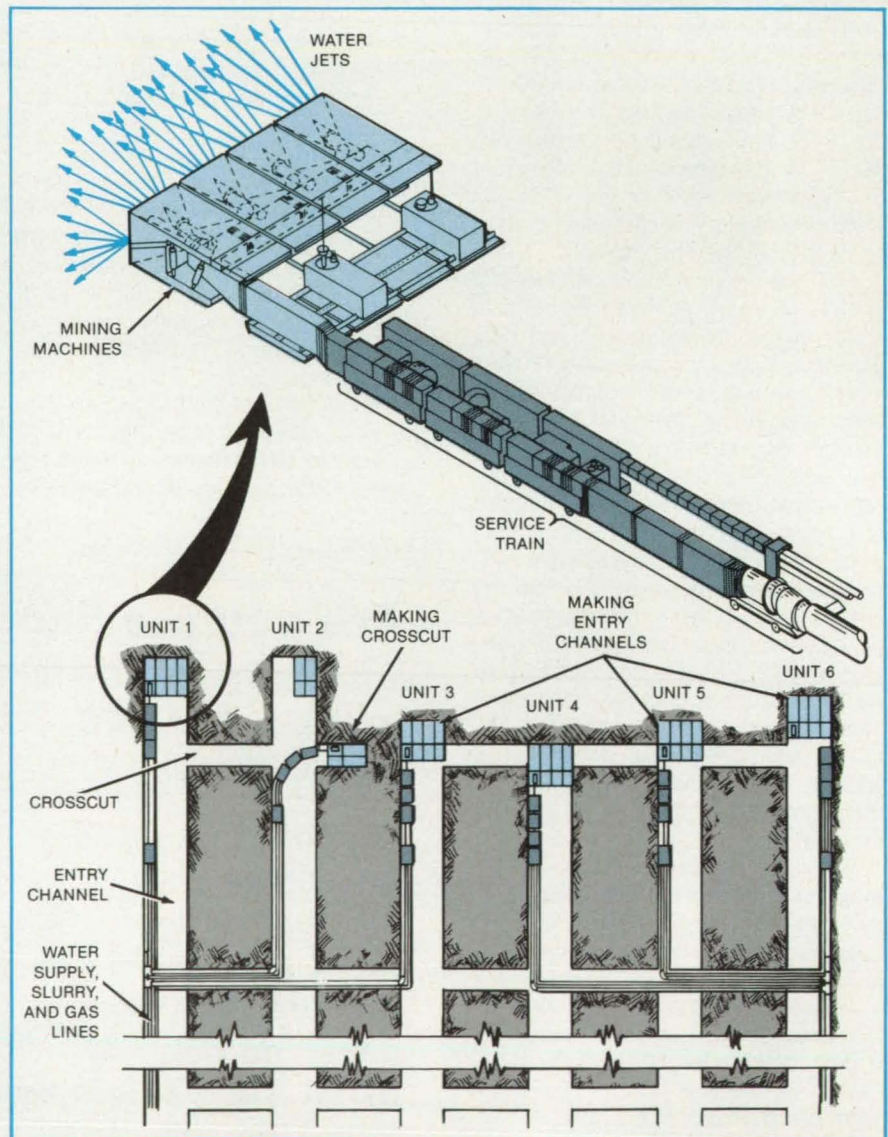


Figure 1. Groups of Four mining machines work independently to excavate channels and crosscuts. Each machine is 5 feet (1.5 meters) wide; thus, the channels are 20 feet (6.1 meters) wide. The crosscuts may be 5, 10, 15, or 20 feet wide, depending on whether one, two, three, or four machines are used. A service train follows a four-machine unit to provide water, electricity, gas exhaust, and slurry removal facilities.

the face. Jaws scoop up the coal chunks, and the auger grinds them and forces the fragments into a slurry-transport system. The slurry is pumped through a pipeline to the point of use.

The hydrojet-jaw mining machines advance as a group of four on hydraulic legs, inserting bolts to support the newly excavated roof as they proceed. After the group has driven an entry, it is reoriented to drive a crosscut that joins with a neighboring entry. (The crosscuts may be filled with dirt, waste, or low-grade coal/concrete mix, rather than braced with roof plates, to prevent them from collapsing.) When a grid of channels has been cut, the group of machines assembles in a line at the far end of the mine chamber and retreats together to the end from which it started, excavating the remaining coal mass and concrete fill as it goes. Another, more conventional retreat technique labeled "pillar punching" is illustrated in Figure 2. In this configuration, entry filling is unnecessary.

The water, electrical, and exhaust utilities for a group of mining machines are provided by the train of service modules that trails behind the machines. A group of machines and its service train advance at a rate of 3 to 4 in./min (7.6 to 10.2 cm/min.) For a cut 4 ft (1.2 m) high and 20 ft (6.1 m) wide, production of clean coal by a single machine would amount to 223 to 297 tons (202 to 269 metric tons) per shift. Six to eight groups of machines working in parallel would produce up to 1,200 tons (1,089 metric tons) per shift. Since a small crew operates these six to eight groups of machines, the productivity is very high.

An in-mine coal-processing unit would be part of the slurry-transport system. The unit would contain hydrocyclones to remove dirt and would process the coal chemically to form a stable 70 percent coal/30 percent water mixture of low sulfur and ash content. This mixture can be transported to the user without further process-

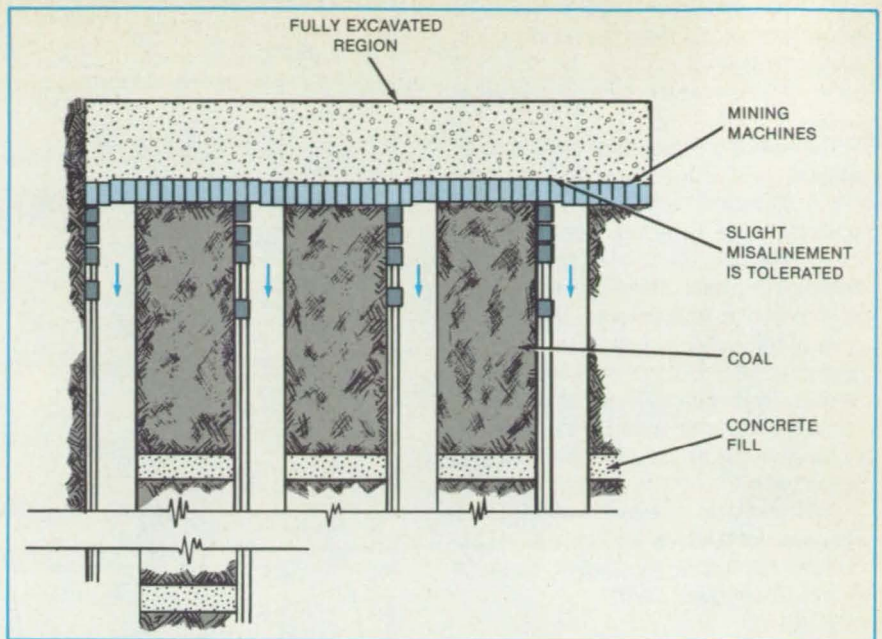


Figure 2. A Pillar Punching method can use the machines without ganging them, and thus providing more reliable operation. This method is closer to conventional retreat techniques and is therefore more suitable than that shown in Figure 1.

ing on the surface.

The waste would be dried and used as backfill in the mine. With 25 percent waste, areas of the mine under important surface structures can be filled to prevent the surface from subsiding. Since waste will be disposed underground, surface dumps and tailing ponds will not be needed.

The mining system will use a large number of sensors. Lasers will provide horizontal guidance. The machines will be guided vertically by coal/rock-interface sensors; radar and nucleonic devices are under consideration for this purpose. A charge-coupled-device camera on each miner will give the operator a picture of the unit during operation. (One operator will handle a number of machines from a console.) Methane, carbon monoxide, and infrared sensors will be

positioned at the seam face and at critical points in the system. Unusual conditions will prompt warning signals, and, if the rates of change warrant it, the system will be shut down and emergency procedures will be started. Optical dust gages will measure respirable dust concentrations at key locations. Waterflow and pressure, slurry flow and pressure, airflow, voltage, current, power, and other parameters will be measured and transmitted to control stations.

This work was done by Mukund D. Gangal, Lionel Isenberg, and Edward V. Lewis of Caltech for NASA's Jet Propulsion Laboratory. For further information, Circle 85 on the TSP Request Card. NPO-16177

Pointable Auger

Machine drills, crushes, and feeds coal — and seeks out extra-hard inclusions.

NASA's Jet Propulsion Laboratory, Pasadena, California

The central auger on the hydrojet-jaw mining machine performs several functions. Its diamond teeth break up the coal seam, it crushes the coal fed to it by the mining machine jaws, and its screw action pushes the crushed coal into the slurry-forming chamber.

The auger is mounted on a gimbal so that it can be swung to almost any point on the seam face within the perimeter of the jaws (see figure). This feature allows the auger to be positioned to break up hard rock inclusions that resist cutting by the hydrojets on the jaws. The pointable auger thus prevents

the machine from falling behind when it encounters extra-hard material as it moves with other machines in a group.

The pointable auger also assists the hydrojets in breaking away jet-cut coal. In themselves, the hydrojets merely cut kerfs in the seam. The coal thus cut would other-

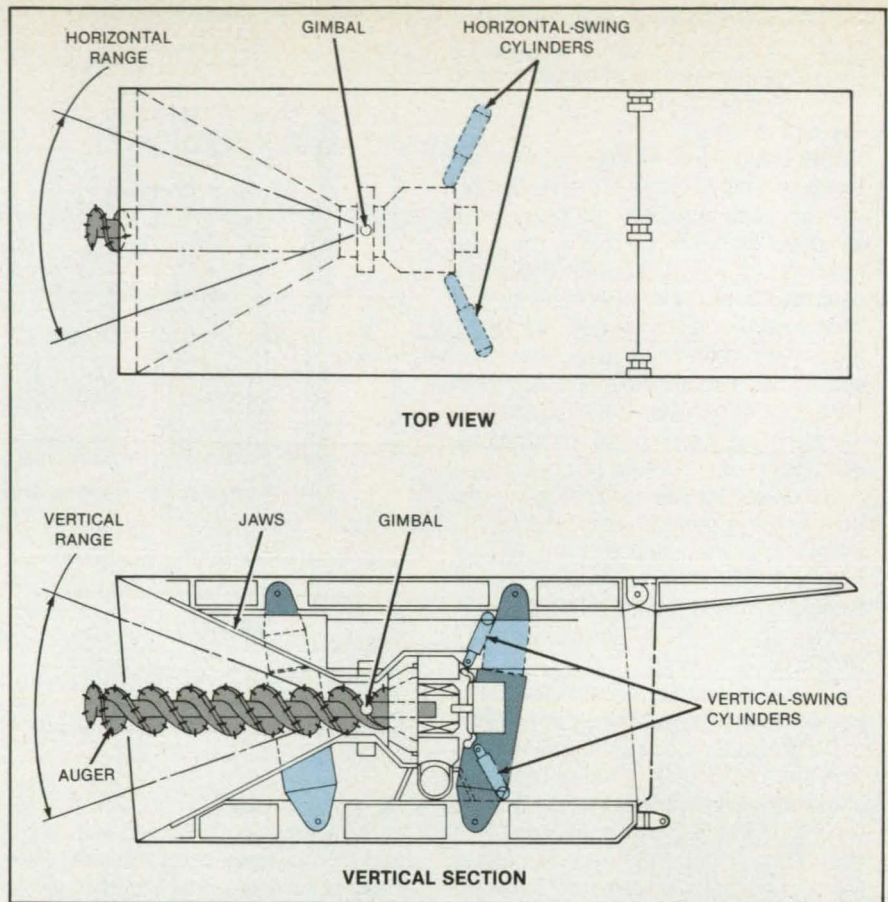


wise remain cantilevered until torn away by its own weight. By periodically drilling into such cantilevered material, the pointable auger causes smaller, more manageable pieces to break away.

The swinging of the auger is effected by opposing pairs of hydraulic cylinders — one pair in the vertical plane and one pair in the horizontal plane. A microprocessor controls the cylinders, thereby pointing the auger according to a preset drilling pattern or, when an inclusion is encountered, bringing the point of the auger to bear directly on the hard material. Inclusions may be detected by a variety of means: By sensing a reduction in the rotational speed of the auger, an increase in the auger motor current, or a slowdown in the advance of the machine.

This work was done by Edward V. Lewis of Caltech for NASA's Jet Propulsion Laboratory. For further information, Circle 54 on the TSP Request Card.
NPO-16178

The **Auger is Mounted on a Gimbal**, located at its center of gravity for ease of maneuvering. Opposing hydraulic cylinders cooperate to point the auger under control of a microprocessor.



Modular Pick-and-Bucket Mining Machine

Modules can be added to machine to increase its cutting width.

NASA's Jet Propulsion Laboratory, Pasadena, California

A concept for an improved conventional pick-and-bucket mining machine has been offered as a backup for the proposed hydrojet-jaw mining machine. The new pick-and-bucket machine would be a modification of a commercially available machine; it could be developed more quickly and offers an alternative in case of unforeseen difficulties with the hydrojet miner. (The hydrojet machine is preferable, however, because it generates less dust.)

Conventional pick-and-bucket miners come in fixed cutting widths. To bore greater widths, they must make two or more passes. The proposed modified machine is modular. It can be expanded to excavate large channels in a single pass. Moreover, unlike conventional machines, the new version can tilt its cutters vertically and skew them horizontally to changing floor slopes and seam heights.

The proposal calls for two end modules between which incremental modules are placed to adjust the cutting width (see

figure). A continuous chain encircles the combined modules. The chains carry picks on blocks between buckets. The picks dislodge chunks of coal, and the buckets scoop them up. The buckets dump their contents into a hopper as they pass over it. The chunks are then crushed, the particles mixed with water, and the resulting slurry pumped away as in the hydrojet-machine system. In the modified pick-and-bucket machine, the buckets are lined with diamond cutters that break off relatively fine particles from the seam; these particles are small enough to be used directly in the slurry, and the load on the crusher is thereby reduced.

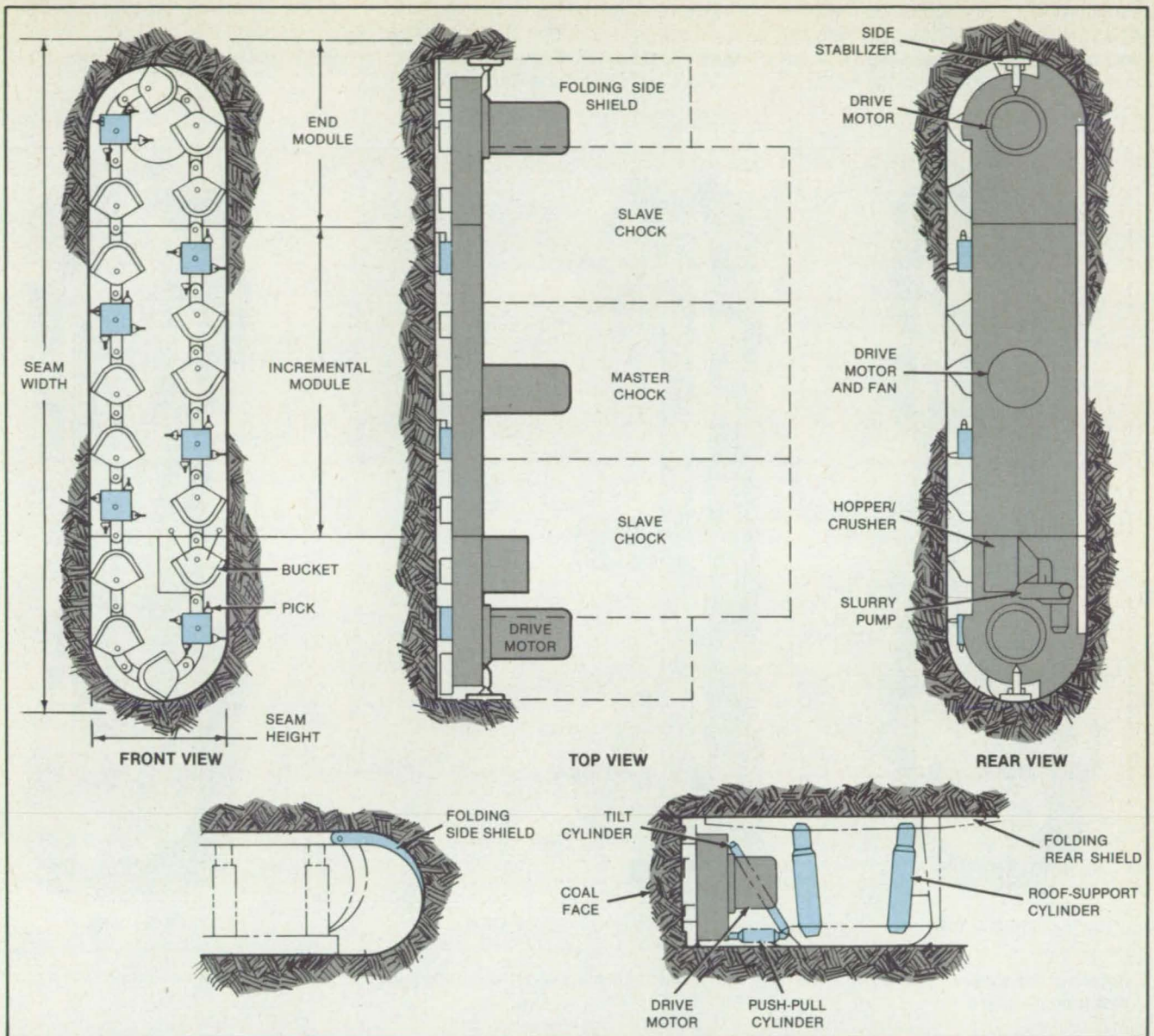
As modules are added or removed, corresponding picks, buckets, and lengths of chain are added or taken out. Each module contains its own drive motor to provide the power needed by its chain, picks, and buckets. In addition, the incremental modules carry exhaust fans to ventilate the seam face.

Like the hydrojet machine, the pick-and-bucket miner is mounted on walking roof-support chocks. Large hydraulic cylinders extend to support the roof and retract to allow advance; when the support cylinders are retracted, they are pushed forward by horizontal cylinders connected to neighboring, momentarily fixed chocks.

Similar hydraulic cylinders tilt the machine to adjust to a changing seam height. Other cylinders skew the miner horizontally to allow for a small change in seam width or to change the direction of entry.

Folding curved shields protect the sides of the miner from falling coal and rock. Two side stabilizers — extendable hydraulic members — anchor the miner against lateral drift.

This work was done by Mukund D. Gangal and Edward V. Lewis of Caltech for NASA's Jet Propulsion Laboratory. For further information, Circle 86 on the TSP Request Card.
NPO-16179



Picks on a Chain dislodge coal and buckets on the chain scoop it up. Depending on the width to be cut, the unit may be composed of only the two end modules or of the end modules plus one, two, or three incremental modules.

Reducing Coal Dust With Water Jets

Jets also cool and clean cutting equipment.

NASA's Jet Propulsion Laboratory, Pasadena, California

The modular pick-and-bucket miner proposed as an alternative to the hydrojet-jaw machine suffers from the disadvantage that it would create large quantities of potentially explosive coal dust, as do all mechanical mining machines. Often, the dust clogs the

drive chain and other parts and must be removed by hand. In addition, the picks and bucket lips become overheated by friction and have to be resharpened or replaced frequently.

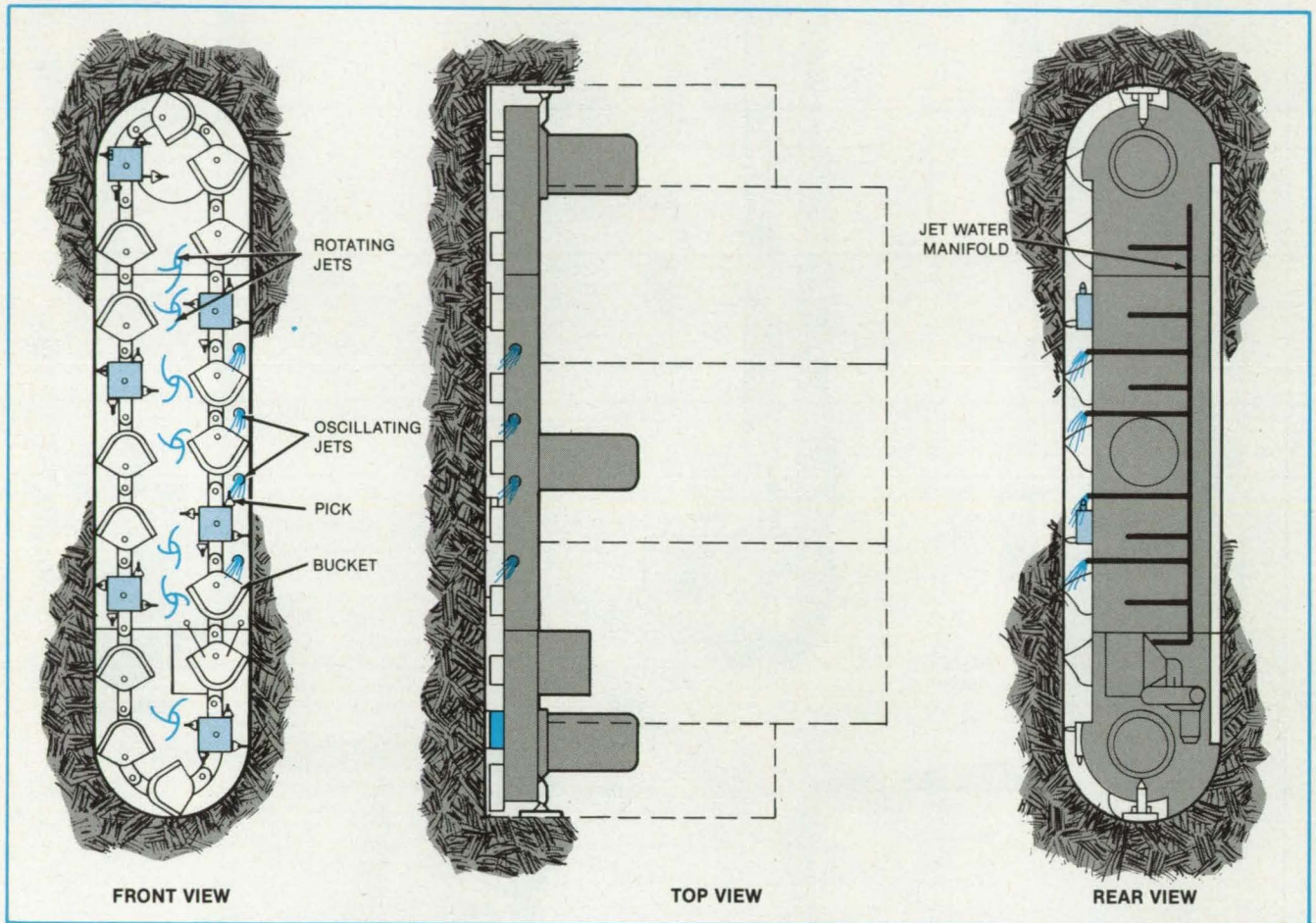
The addition of oscillating and rotating

water jets to the pick-and-bucket machine will keep down dust, cool the cutting edges, and flush the machine. The jets operate at moderately high pressure — about 20,000 lb/in² (138 MPa). Rotating jets on the face of the machine spray the chain (see figure).

Oscillating jets at the top of the machine face spray the picks and buckets from behind as they pass by. The jets are fed water from a manifold at the rear of the machine.

The wet coal dust settles to the mine floor. This work was done by Mukund D. Gangal and Edward V. Lewis of Caltech for NASA's Jet Propulsion Laboratory. For

further information, Circle 87 on the TSP Request Card. NPO-16180



Rotating Jets wash dust away from the drive chain. Oscillating jets cool the cutting surfaces. Both types of jet wet airborne coal dust so that it precipitates.

Slurry-Mixing Chamber

Paddles and water jets create a uniform, continuous flow.

NASA's Jet Propulsion Laboratory, Pasadena, California

A slurry-mixing chamber on the hydrojet-jaw mining machine ensures a uniform, continuously flowing slurry of coal particles in water. By mixing the coal and water at high speed and keeping the resulting slurry in constant motion, the chamber prevents the slurry from becoming a dry semisolid that blocks flow. It also prevents coal particles from settling and caking in bends, corners, and other locations where flow

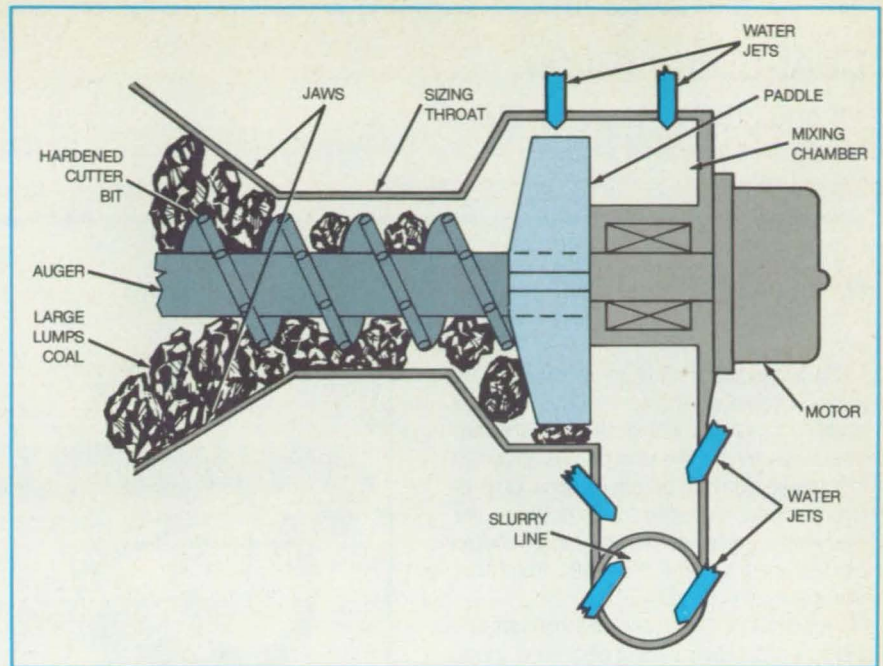
changes in direction or speed.

As coal particles leave the sizing throat where they are broken up by the auger, they enter the mixing chamber (see figure). There, paddles mix the coal with the water and impart a swirling motion to the mixture. The water is added at a high tangential velocity that creates a vortex, sweeping out corners and agitating the coal particles continuously. The jets continuously scrub the

walls of the chamber. The coal/water mixture thus flows to the slurry pump at constant speed and composition.

This work was done by Edward V. Lewis of Caltech for NASA's Jet Propulsion Laboratory. For further information, Circle 90 on the TSP Request Card. NPO-16182

Arranged on the Periphery of the Mixing Chamber, jets of water provide a medium for moving coal out of the mining machine and scrub the chamber to prevent caking. Paddles help to keep the mixture in motion.



All-Water-Jet Coal Excavator

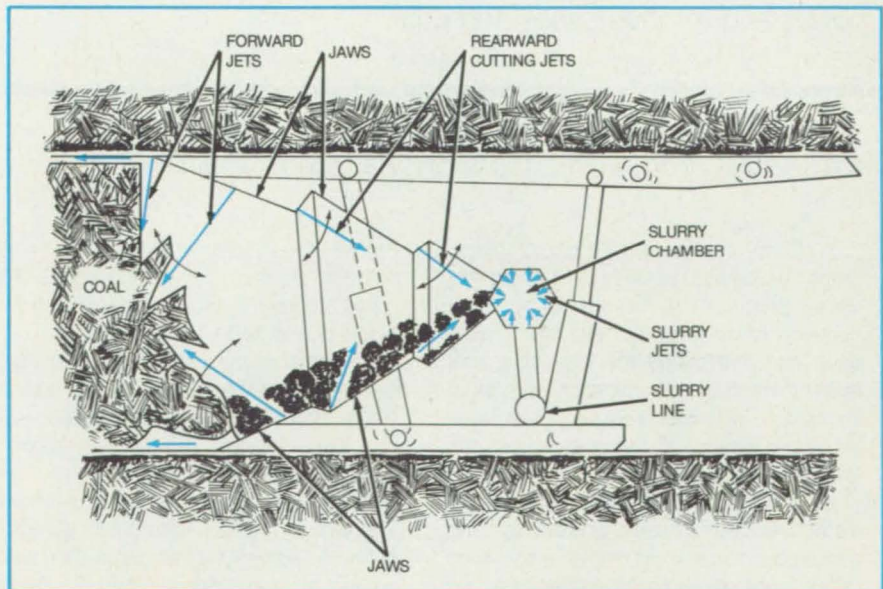
A version of the jaw miner operates without mechanical cutting and crushing.

NASA's Jet Propulsion Laboratory, Pasadena, California

An alternative to the auger that cuts, sizes, and feeds coal in the hydrojet-jaw mining machine uses oscillating water jets to break up coal and feed the particles to the slurry-mixing machine. Since the alternative has few moving parts and does not rely on mechanical crushing, it has the advantages of long life and low maintenance. Moreover, although the auger generates little dust, the all-jet machine generates even less; it therefore poses a lesser explosion or health hazard.

At the front of the jaws, cutting into the coal face from the roof to the floor, forward-pointing water jets are aimed at the coal (see figure). As the side jets oscillate in a vertical plane, they define the side boundaries of the cut. Simultaneously, transversely oscillating jets sever the coal at the roof and floor. Additional transverse jets farther up the throat of the jaws cut up the coal broken off the face. Rearward-pointing jets push coal up the lower jaw to the mouth of the slurry chamber, breaking the coal into smaller pieces in the process.

This work was done by Mukund D. Gangal of Caltech for NASA's Jet Propulsion Laboratory. For further information, Circle 92 on the TSP Request Card. NPO-16183



Forward-Pointing Jets of water dislodge and break up coal. Rearward-pointing jets further break up the coal and force the particles into the slurry chamber. The oscillating-jet mechanism itself stays within the "jaw" structure and is thus protected from the wear and tear associated with coal handling.

Coal-Sizing Auger

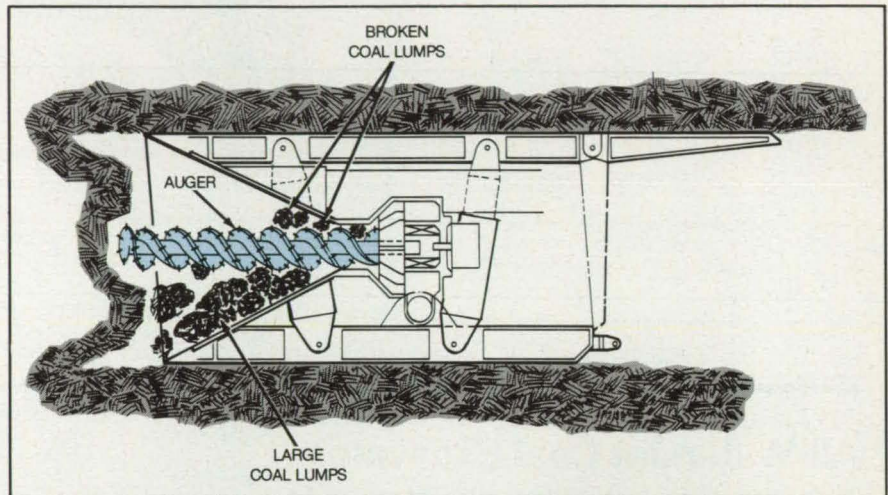
Aft end crushes material broken off by the forward end.

NASA's Jet Propulsion Laboratory, Pasadena, California

Since the auger and hydrojets on the jaw miner break coal into relatively large chunks, further crushing and grinding are necessary so that the coal can be removed in a water slurry. In no case can a lump of coal exceed the internal diameter of the slurry tube, and preferably the lumps should be reduced to less than one-third that diameter.

Accordingly, the aft end of the auger, like the forward, face-piercing end, is equipped with hard cutting bits such as diamonds. As the auger breaks the face, it pulls the broken coal lumps into the jaws and forces them into a hardened throat section (see figure). There, the cutting bits chew up the lumps: The clearance between the throat and the auger shaft sets the maximum size for coal particles that pass through. The auger motion pushes the coal particles into the mixing chamber, where paddles combine them with water.

This work was done by Edward V. Lewis of Caltech for NASA's Jet Propulsion Laboratory. For further information, Circle 91



The Aft Portion of the Auger crushes coal lumps broken from the coal face. The crushing prepares the coal for transportation in a slurry.

on the TSP Request Card.

Inquiries concerning rights for the commercial use of this invention should be ad-

dressed to the Patent Counsel, NASA Resident Office-JPL [see page 21]. Refer to NPO-16184.

Service Modules for Coal Extraction

Service cars supply water and electric power and remove gases and coal.

NASA's Jet Propulsion Laboratory, Pasadena, California

A service train follows a group of mining machines, paying out utility lines as the machines progress into the coal face. Unlike conventional mining machines, which work back and forth along the face of a coal seam, the hydrojet-jaw miner bores straight into a face. High coal production is attained by arraying a row of machines across the face, working side by side.

As the machines move forward, their water and slurry hoses, powerlines, and ventilation ducts must move along with them. Since each machine needs its own hoses, cables, and ducts, a chaotic situation would result if the service connections were allowed to lie on the floor in disarray. A considerable expenditure of worker time and

machine resources would have to be devoted to managing the connections. Frequent stoppages and occasional disasters would be inevitable.

The service train (see figure) will bring order to chaos by confining service connections to articulated, detachable, self-propelled modules. The train will supply a group of four mining machines with connections for water, slurry, power, and ventilation. The cars of the train will contain pumps, a hydraulic power unit, electrical distribution equipment, and a ventilating fan. The cables and hoses are protected by flexible armored carriers. Initially, the carriers are coiled; as the miners progress, they are uncoiled. The ventilation duct consists of flexible bellows-

like sections; as the miners move, the sections expand.

With the service train contracted to its minimum length, the fourth and last car in the train is connected to fixed supply lines. The last car is then detached from the other cars to allow the flexible lines to pay out between cars. As the miners move forward, the remaining three cars keep pace until the connections to the detached car are fully stretched out. At this time, the third car is detached from the first two, connections are allowed to stretch out, and then the second car is detached. When all the service connections are fully extended, mining is stopped, and the service train is fully recontracted and connected to fixed supply lines

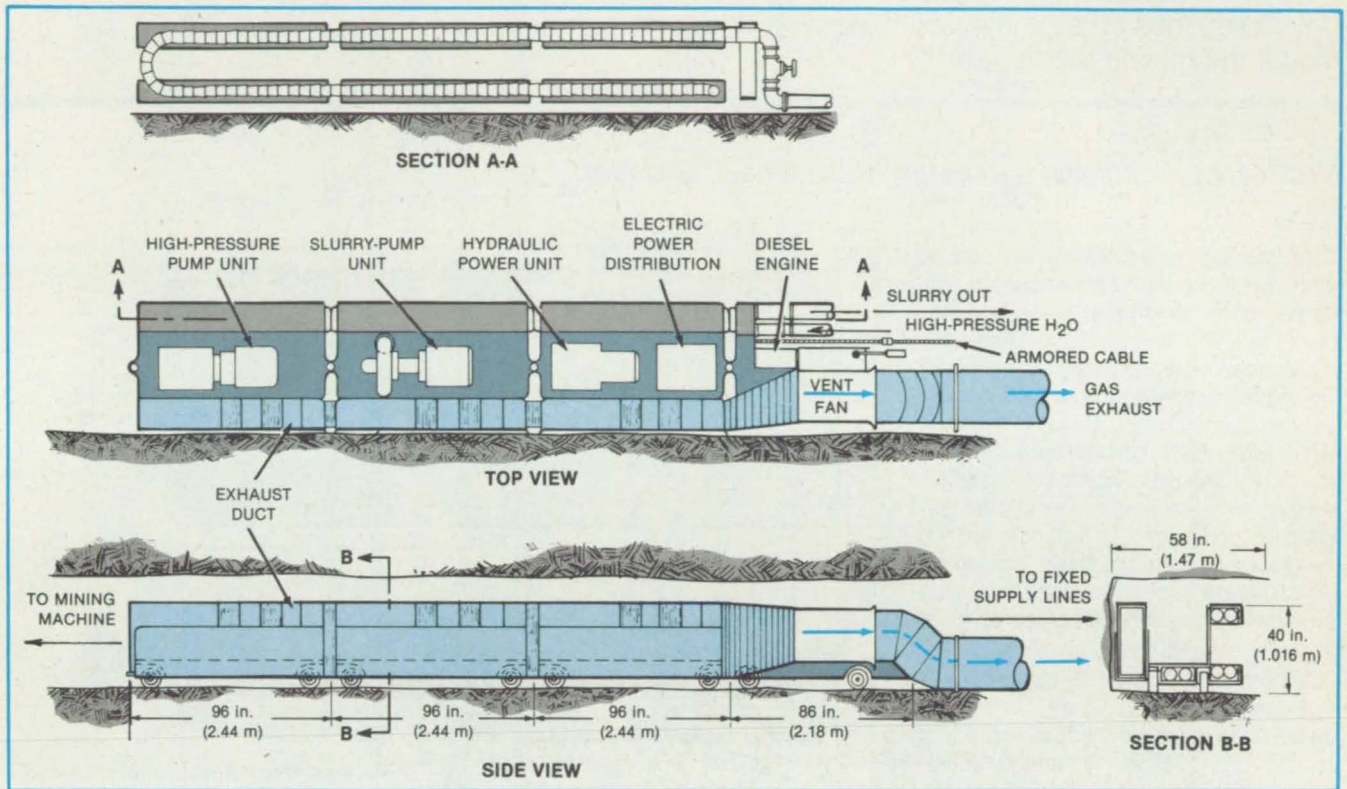
at a new forward position. The expansion procedure is then repeated. Since the full extension of the supply train is about 40 ft (12 m) and miners advance 80 to 120 ft (24 to 37 m) in an 8-hour period, there will be only two or three interruptions per shift. Reconnection of the service train takes only a

few minutes.

The first car is self-propelled so that it can tow the other cars as the miners advance. Self-propulsion is not essential for the other cars, but is an advantage in maneuvering in and out of crosscuts and around corners.

This work was done by Mukund D.

Gangal and Edward V. Lewis of Caltech for NASA's Jet Propulsion Laboratory. For further information, Circle 88 on the TSP Request Card. NPO-16185



A **Service Train** for four mining machines removes gases and coal and provides water and electricity. Flexible, coiling armored carriers protect cables and hoses.

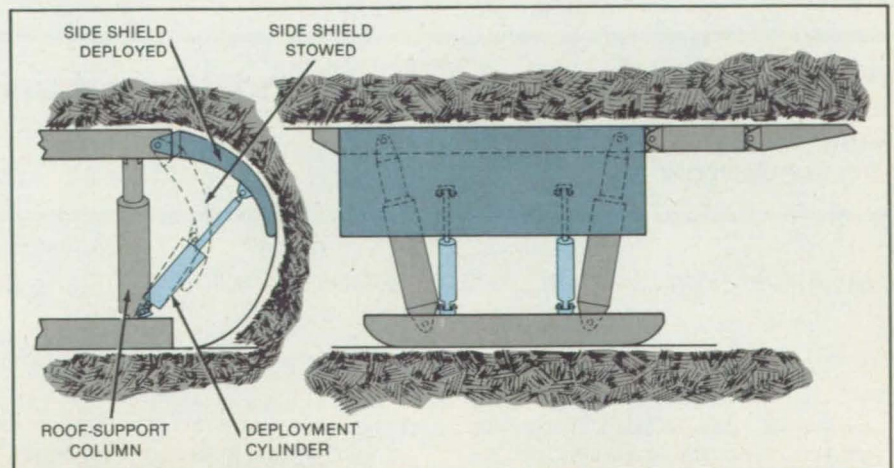
Side Shield for Wall Support

Curved plates prevent side cave-ins.

NASA's Jet Propulsion Laboratory, Pasadena, California

A curved shield is proposed for preventing collapse of sidewalls in channel mining. Such collapse is a common and dangerous occurrence and can immobilize the mining machine. Pick-and-bucket miners, even with roof supports, are particularly prone to sidewall falls. This type of miner is an alternative to the advanced hydrojet-jaw miner for the automated mining system.

The method employs a curved shield on each side of the mining machine (see figure). In its stowed position, a shield is



A **Retractable Side Shield** supports a sidewall. The shield may be curved as shown, or it may be flat to conform to straight ribs.

folded against the roof-support columns on one side. In its deployed position, the shield is raised and braced against a coal-seam wall by a hydraulic cylinder. The shield sup-

ports the wall until the roof and wall are properly secured by bolting and cement coating.

This work was done by Edward V. Lewis

of Caltech for NASA's Jet Propulsion Laboratory. For further information, Circle 59 on the TSP Request Card. NPO-16188

Roof Shield for Advance and Retreat Mining

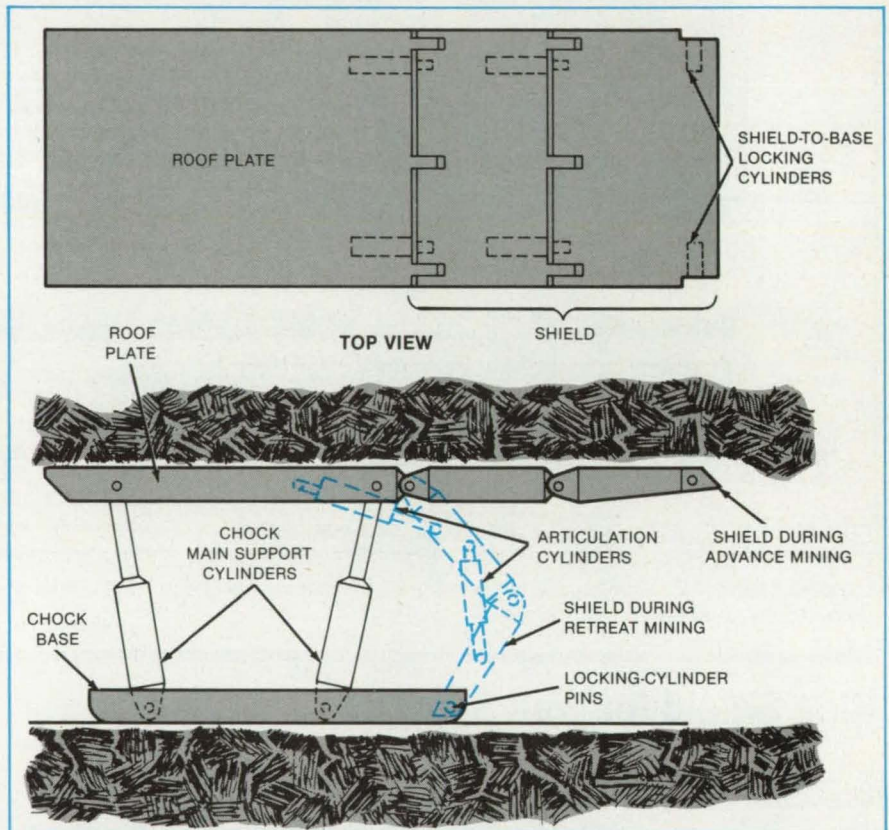
Shield sections change their configuration to suit the mining mode.

NASA's Jet Propulsion Laboratory, Pasadena, California

An articulated shield would adapt a set of roof-support chocks to both advance and retreat modes of mining. In the advance mode, in which the hydrojet-jaw miner excavates channels and crosscuts, the shield would provide an extended area of protection immediately behind the chocks to shelter equipment until roof bolts are inserted. In the retreat mode, in which the miner removes the remaining material between channels and crosscuts, roof bolts are not used; for this mode, the shield folds downward to enclose the rear of the chocks and prevent engulfment by falling debris.

The proposed shield consists of two plates connected to the trailing edge of the roof-support plate (see figure). For the advance mode, the shield projects rearward in the same plane as that of the roof plate. For the retreat mode, the shield is dropped and bent so that it covers the back end of the chock structure. Hydraulic articulation cylinders move the shield from one position to the other. Hydraulic locking cylinders brace the shield in the advance position. The shield can accommodate roof heights ranging from 36 to 60 inches (0.9 to 1.52 meters).

This work was done by Edward V. Lewis of Caltech for NASA's Jet Propulsion Laboratory. For further information, Circle 89 on the TSP Request Card. NPO-16189



Articulation Cylinders raise the rear shield to the advance position (solid lines), and locking cylinders hold it there. To change to the retreat position (dashed lines), the articulation cylinders lower the shield. Locking pins at the edge of the outermost shield plate latch the shield to the chock base.

Compact Hydraulic Excavator and Support Unit

Continuous-coal-mining machine is maneuverable.

NASA's Jet Propulsion Laboratory, Pasadena, California

A hydraulic coal excavator is combined with a chock, or roof-support structure, in a self-contained unit that can move itself forward as it removes coal from a seam. Unlike

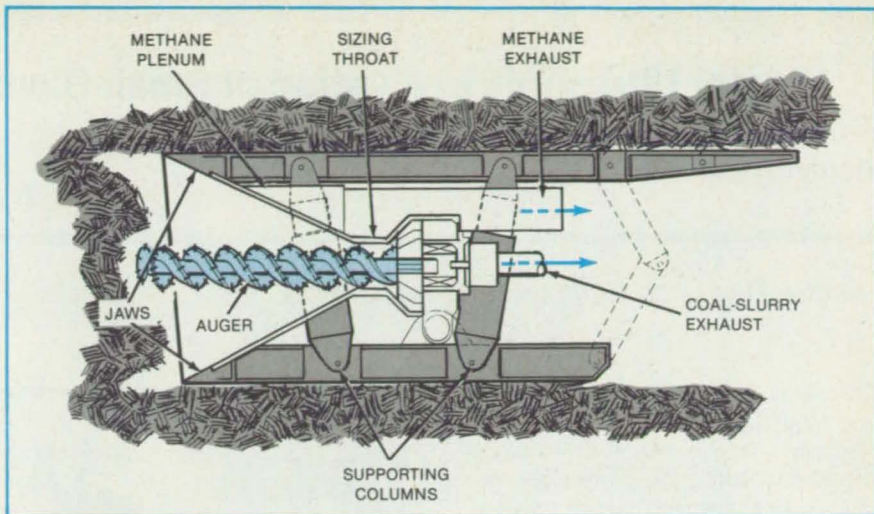
previous such units, the new machine is compact enough to be easily maneuverable; it can even make small-radius right-angle turns.

The unit is compact because many of its functional components are mounted between the supporting columns of the chock rather than fore or aft of them (see figure).

The auger and jaws of the hydraulic excavator project forward from the leading column so that the auger can make a central bore, and the jaws can direct a stream of high-pressure water to loosen the coal above and below the bore. The loose coal is scooped up by the jaws, further ground by the auger, fed to a slurry chamber, and pumped out through a slurry exhaust line. A plenum on the upper jaw removes methane from the excavated region.

The telescoping columns are alternately retracted and extended so that the chock walks forward to expose the auger to new material continually. The chock may be stripped of its functional elements so that it can serve as a simple supporting structure for the mine roof.

This work was done by Edward V. Lewis of Caltech for NASA's Jet Propulsion Laboratory. For further information, Circle 55 on the TSP Request Card. NPO-16190



Major Functional Components of the excavator chock are located in the space between the supporting columns. These components include the methane plenum, the exhaust duct, and the sizing throat around the auger.

Curtain Wall Creates Ventilation Channel

Explosive gas and dust are removed through an extending corridor.

NASA's Jet Propulsion Laboratory, Pasadena, California

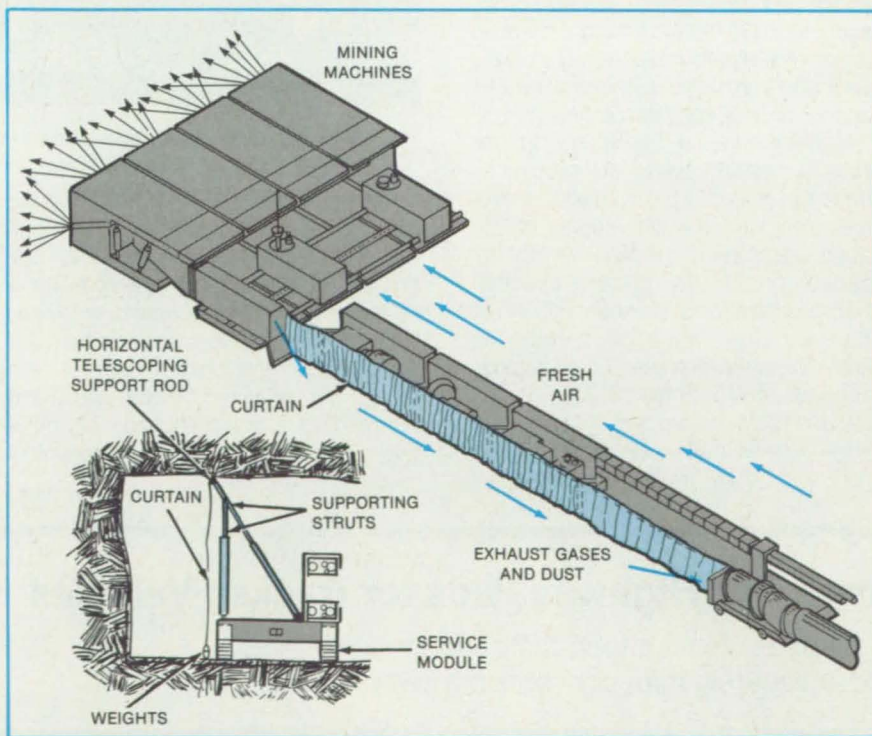
A curtain-wall structure is proposed for removing methane and airborne coal dust from hydrojet-jaw mining machines. The channel between the curtain wall and the mine wall forms a closed exhaust passage. Through it, gas and dust would be continuously removed so that high concentrations of these explosive materials would not build up.

A rolled curtain of nonporous material extends from the exhaust-fan module in the service train to a mining machine. The mining machine unfurls the curtain as it moves forward into the channel it is cutting (see figure). The machine simultaneously extends a telescoping rod at the top of the unfurling curtain to provide support. A human operator on the service train periodically inserts struts under the rod as it is extended to brace it against the roof. Weights at the bottom of the curtain press it against the floor. Thus sealed at the top and bottom, the curtain prevents the exhaust flow from mingling with incoming air.

A plenum at the mining-machine group carries the exhaust to the channel defined by the curtain wall. At the rear end of the curtain wall, the exhaust fan directs the gas and dust into an exhaust duct.

This work was done by Edward V. Lewis of Caltech for NASA's Jet Propulsion Laboratory. For further information, Circle 93 on the TSP Request Card.

Inquiries concerning rights for the com-



The Curtain Wall Unfurls and its telescoping support rod extends when both elements are pulled by an advancing mining machine. An operator inserts self-adjusting supporting struts manually.

mercial use of this invention should be addressed to the Patent Counsel, NASA Resi-

dent Office-JPL [see page 21]. Refer to NPO-16194.

Holder for Ultrasonic Evaluation of Small-Diameter Tubes

A simple holder eliminates the requirement for an expensive turntable.

Langley Research Center, Hampton, Virginia

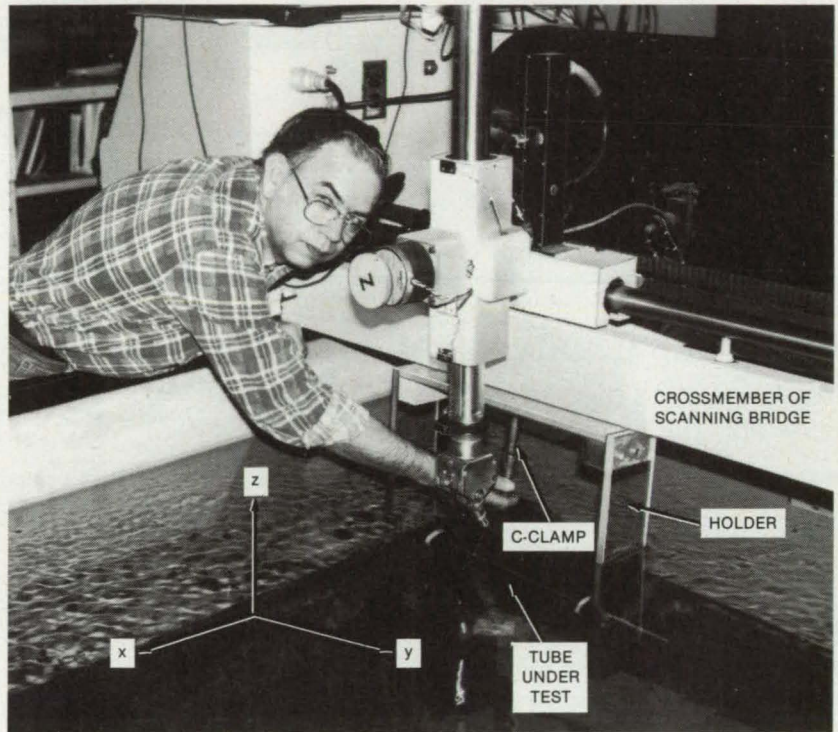
A simple but effective device holds and rotates a cylindrical specimen and sonically reflective mirror in the proper relationship during the ultrasonic testing of cylindrical specimens such as small-diameter polymeric tubes. The holder was designed for use with a commercially available electromechanical drum-type ultrasonic immersion testing device used for the nondestructive evaluation of a variety of materials.

The commercial system tests both flat and cylindrical specimens; however, testing of cylindrical specimens requires the installation of a turntable to rotate the specimen. When an appropriate turntable is installed, movement of the transducer is automatically synchronized with the rotation of the specimen about the z-axis to produce accurate results.

This synchronized movement is essential when testing cylindrical objects. A turntable for this system costs approximately \$18,000 (1983 dollars). However, a holding device to replace the turntable was made from in-house materials with a material cost of approximately \$30.

As shown in the figure, the holder works by rotating cylindrical specimens about the y-axis. This rotation is synchronized with the movement of the transducer to permit testing without the use of a turntable. The holder is attached to a crossmember of the scanning bridge with a C-clamp. The holder permits the testing of small-diameter tubes rapidly, accurately, and economically.

As the test is conducted, the scanning bridge indexes in the x direction. Friction



The Holder Synchronously Rotates the cylindrical specimen for ultrasonic testing.

between the wheels of the holding device and the table in the water tank causes the specimen to rotate. This rotation is synchronized with the movement of the testing device. Sound is pulsed from the transducer, passed through the specimen at the point closest to the transducer, reflected by the glass, and returned to the transducer. The ultrasonic instrument detects the amount of

sound loss in the specimen and forwards the information to the storage display scope where the test results are recorded. Use of the holding device does not require any physical alteration of the commercially available system.

*This work was done by Edward C. Taylor of Langley Research Center. For further information, Circle 43 on the TSP Request Card.
LAR-13152*

Improved Highway Pads for Tracked Vehicles

New pads would attach faster and hold more securely than conventional pads.

NASA's Jet Propulsion Laboratory, Pasadena, California

Three new designs would ease the installation of rubber pads on the treads of tracked vehicles to prevent damage to highways. The designs could apply to bulldozers,

cranes, and excavating machines.

The new designs speed installation and make retightening of bolts unnecessary. In one design (see Figure 1), the steel shell

bonded to the pad includes a lip on one side and a T-shaped tab on the other side. The lip engages a recess on one side of the tread, and the tab is bent into a T-shaped locking

Figure 1. The **Rubber Pad is Held** on a tread by the bent locking tab and by the lip that engages a recess in the tread. The tab is hammered in during installation and pried out during removal.

recess on the other side of the tread.

The tab is forced into the recess by hitting it with a sledge hammer or by prying. The tab and recess have an interference fit, causing the tab to curve. The interference fit, spring action, and curvature of the tab wings combine to hold the tab in place during the vibration and stress of travel. Since the pad is confined by the box-shaped recess in the road-contacting surface of the tread, the squirming of the pad exerts little force on the tab and lip.

To remove the pad, a crowbar is inserted in the pry-out groove to bend the tab out of place. Since the tab can withstand only a limited amount of bending, the pad is intended to be used only once. But since the steel shell with the lip and tab is formed by stamping, the cost is lower than that of a conventional pad with threaded fasteners, and the cost of labor to retighten is eliminated.

In another design (see Figure 2), the pad is retained by split, round hardened-steel collets that grip smooth, soft iron pins attached to the steel shell. (In the third design, which is similar in principle to this one, flat tabs are retained by flat collet plates.) The split collets are sprung together and held by rubber cast into the tread. The resilient rubber mounting permits the pins to enter despite misalignments and resists damage from stresses during travel.

Hardened teeth on the gripping surfaces of the collets are slanted like buttress threads to facilitate the insertion and resist the withdrawal of the pins. The pad is installed by inserting the pins in the collet holes, then hammering or kicking it in. Every time the tread passes underneath, the weight of the vehicle helps to seat the pad even more firmly. Thus, the pad remains firmly attached during travel, automatically retightening with each revolution of the tread.

To remove the pad, a tapered cam rod is inserted from the side and hammered, pried, or bolted to force the tapers against the collets. This pries the collets apart, thereby releasing the pins.

This work was done by Earl R. Collins, Jr., of Caltech for NASA's Jet Propulsion Laboratory. For further information, Circle 56 on the TSP Request Card. NPO-16318

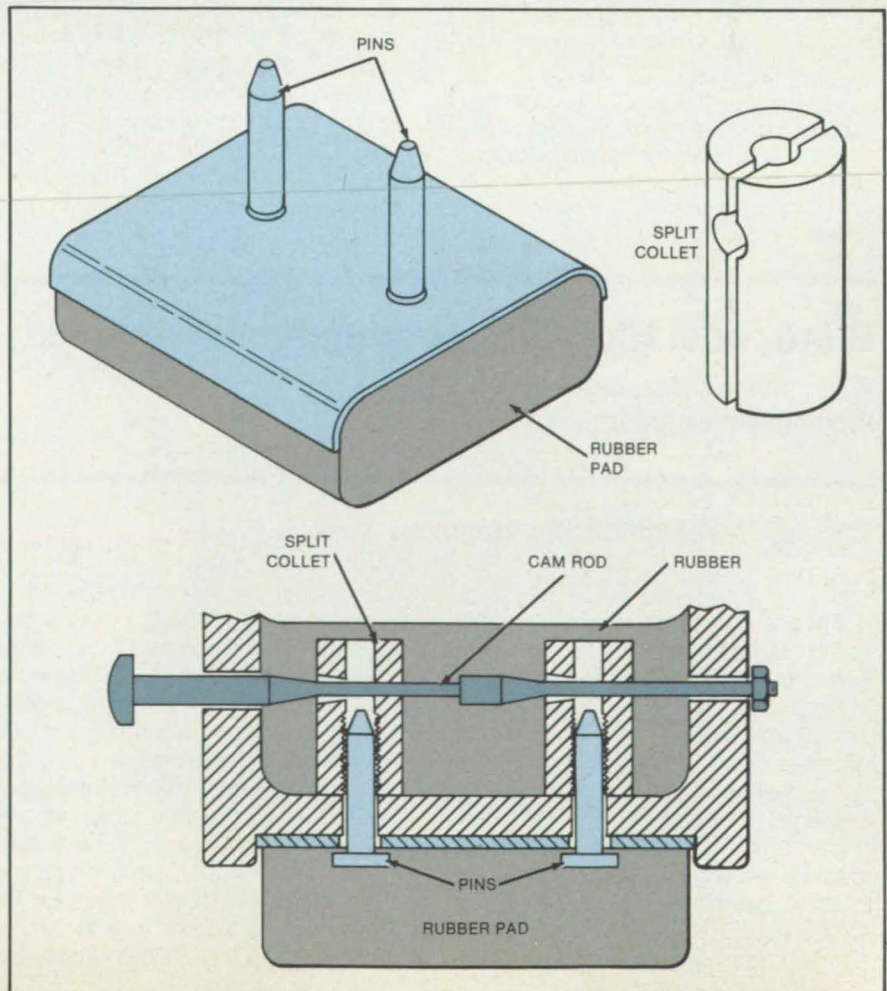
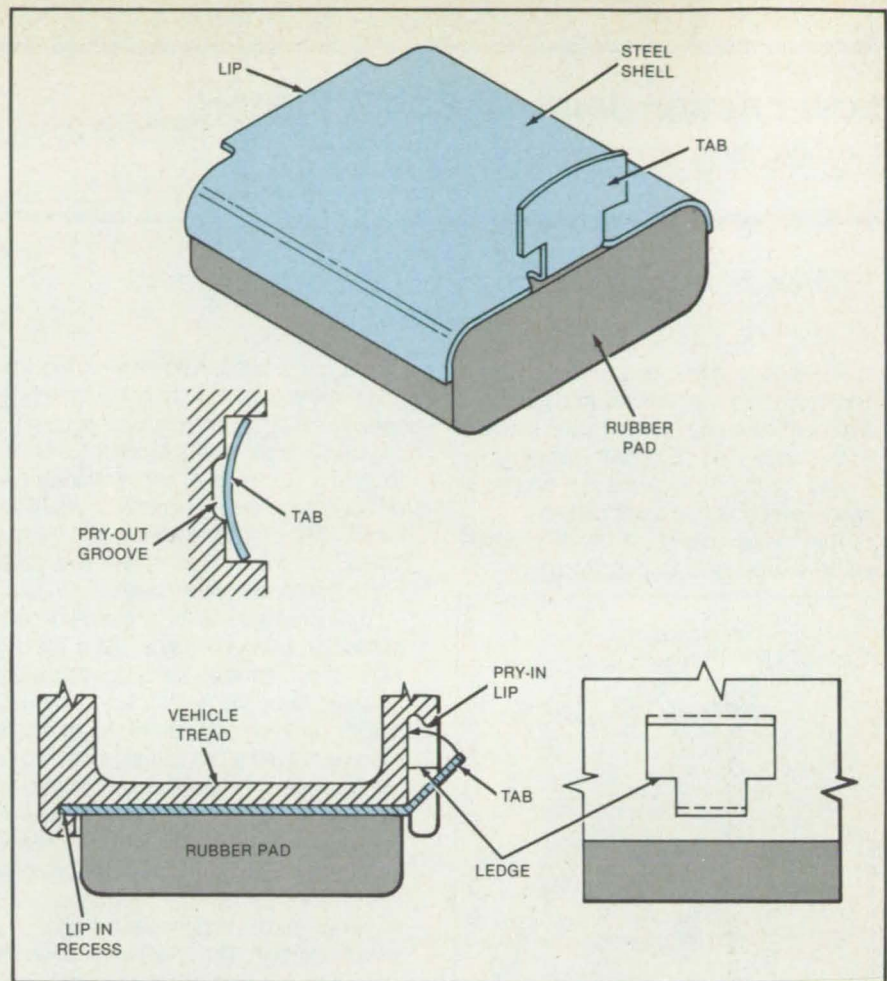


Figure 2. **Split Collets** grip pins to hold the pad in place. To release the pins, the collets are pried apart with the help of a cam rod.

Low-Friction Joint for Robot Fingers

Linkage concept employs opposing bands.

NASA's Jet Propulsion Laboratory, Pasadena, California

A mechanical linkage would allow adjacent parts to move relative to each other with low friction and with no chatter, slipping, or backlash. The proposed linkage is intended for the finger joints in mechanical hands for robots and manipulators.

The linkage consists of bands wrapped partially around the adjacent parts (see

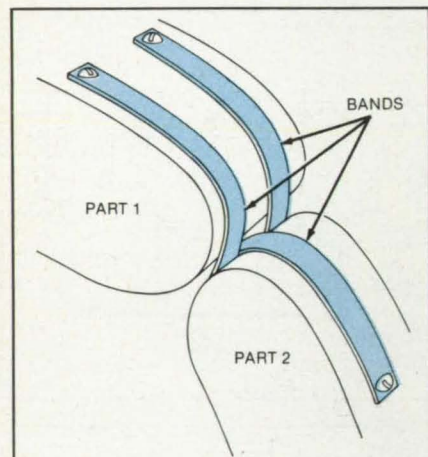


Figure 1. A **Low-Friction Joint** of the new type has two surfaces in rolling contact, held in alignment by taut flexible bands. There is no sliding friction or "stick-slip" motion: There is only the rolling-contact friction and the bending friction within the bands.

Figure 1). The bands hold the parts together and allow only rotation of one part with respect to the other. The rotation is carried out as one part rolls on the other. If the bands and parts are made of hard materials that do not deform greatly under load, there will be very little contact friction. In fact, the major friction will be that of the molecules within the bands as they bend.

The contact surfaces of the parts need not be circularly cylindrical. As a band is paid out during rolling, the opposing band is taken up. Thus, the parts need not be identical or symmetrical. One of the parts can even be flat. As a part rotates by rolling on the other part, the point of contact moves along the other part by a distance equal to that paid out and taken up by the bands: Thus, there is no mismatch in the positions of the bands.

Motion can be imparted to the parts by a sheathed cable. The sheath would be anchored to one part, and the internal cable would be anchored to the other part. If the cable is a stiff wire that can act in a push-pull fashion, then it will serve in some applications to impart both opening and closing motions. In some cases, however, the wire motion, when it is pushing, will be too imprecise, especially under load. Then a pair of cables, each pulling in the opposite direc-

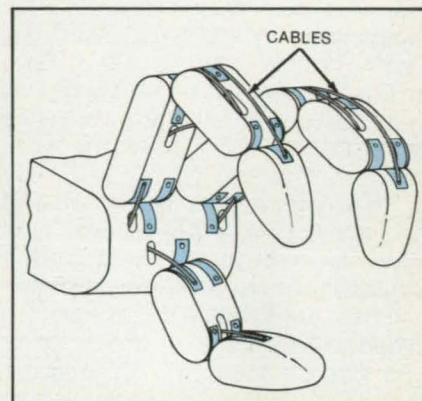


Figure 2. A **Robot Hand** includes fingers made with the new joints. Two adjacent parts are turned around a joint by pulling on a cable.

tion, can be used (see Figure 2). The second cable would be placed on the opposite side of the parts from the first.

This work was done by Carl F. Ruoff of Caltech for NASA's Jet Propulsion Laboratory. For further information, Circle 53 on the TSP Request Card.

Inquiries concerning rights for the commercial use of this invention should be addressed to the Patent Counsel, NASA Resident Office-JPL [see page 21]. Refer to NPO-15914.

Blind-Side, High-Temperature Fastener Lock

A formed-in-place staple provides a positive mechanical lock.

Langley Research Center, Hampton, Virginia

For post-supported, advanced carbon/carbon standoff panels, currently under consideration as an alternate thermal protection system for the Shuttle orbiter, there is a possible need to lock the post and its grommet to prevent relative rotation. The locking feature must be applicable to temperatures of 1,600° F (870° C) and higher and must be employable after the panel is installed, resulting in a blind application.

A blind-side locking technique developed for this application employs a wire staple (see figure) that, when inserted into grooves

in the post, is formed in place by the ramped portion of the post grooves. This splays out the wire ends that move into the castellated end of the grommet, mechanically locking the post and grommet against relative rotation. The splayed ends provide a mechanical lock to prevent the wire from falling out. This technique, therefore, does not rely upon friction for either locking or retention.

The wire is removed by prying it up and pulling it out. For modest antitorque requirements, only the post is grooved. For higher locking torque, both the post and

grommet are grooved to provide continuous locking along the length of the threads, in which case the castellated feature is not required. For ODS alloys, a wire staple made from Chromel (or equivalent) material may be used, while coated refractory metals would employ a smaller diameter pure iridium wire.

This technique eliminates concerns about creep-loosening of deformed friction lock approaches and replaces mechanical staking, which involves destructive drilling out of the stake for removal. More impor-

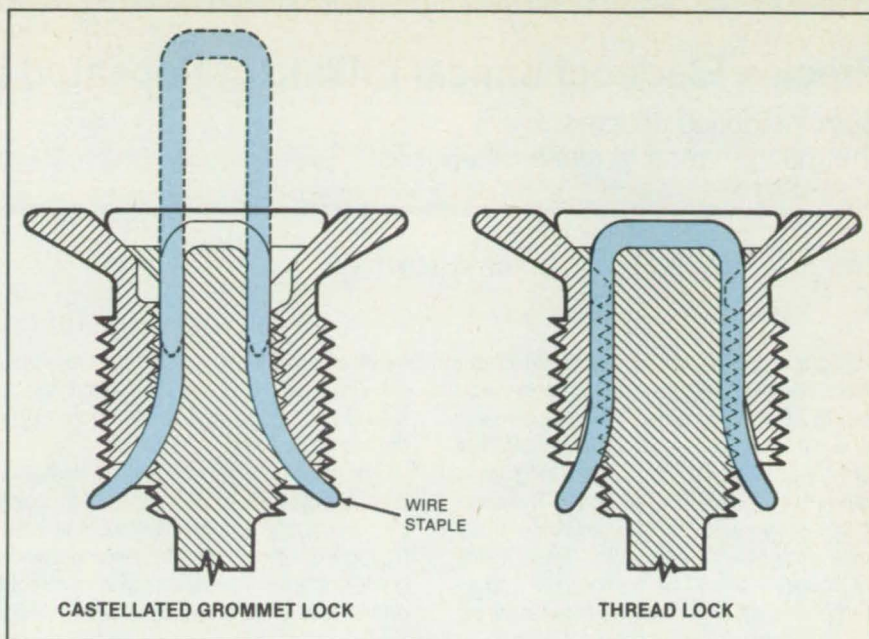
tantly, it provides a means of locking coated refractory metal fasteners where coatings may be damaged by standard locking techniques. The technique is applicable to any blind-side fastener application where frequent fastener removal may ultimately destroy friction lock features. It is also applicable to high-temperature installations that are above current temperature limits for friction locks.

This work was done by E. C. Matza and D. M. While of Vought Corp. for **Langley Research Center**. No further documentation is available.

Title to this invention has been waived under the provisions of the National Aeronautics and Space Act [42 U.S.C. 2457(f)], to the Vought Corporation, Dallas, TX 75265.

LAR-13037

A Wire Staple is used to lock the post and grommet in both the castellated grommet and thread lock systems.



Insulating Cryogenic Pipes With Frost

Crystallized water vapor fills voids in pipe insulation.

Lyndon B. Johnson Space Center, Houston, Texas

The frost that usually constitutes a nuisance on pipes carrying cold liquids could be exploited to enhance the insulation of such pipes in selected applications. The frost impedes the transfer of heat into bare pipes or through cracks in the insulation material of covered pipes. Possible industrial applications include large refrigeration plants or facilities that use cryogenic liquids.

For best insulating properties, the frost should be formed under controlled atmospheric conditions that must be determined for each situation. An example is given by the situation for which the frost-insulation technique was developed — namely, the liquid-oxygen and liquid-hydrogen pipes in the aft fuselage section of the Space Shuttle orbiter. This section is continuously flushed with inert gaseous nitrogen before a launch. However, the nitrogen penetrates cracks in the insulation and condenses on the bare pipes, adding heat to the cryogenic liquids flowing through them. Even worse, the condensed nitrogen drips out of the cracks and falls on the metal structure below. The drops vaporize instantly, thereby rapidly cooling the structure as well as the adhesive that bonds the external thermal-protection tiles to the structure. The

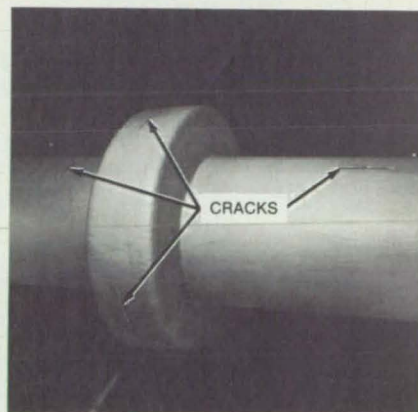
thermal shock endangers the bond and could result in the loss of tiles during lift-off.

A small, carefully controlled amount of water vapor is introduced into the dry nitrogen gas before it enters the aft fuselage. The vapor freezes on the pipes, filling cracks in the insulation (see figure). The ice prevents gaseous nitrogen from condensing on the pipes and dripping on the structure, in addition to helping to insulate all parts.

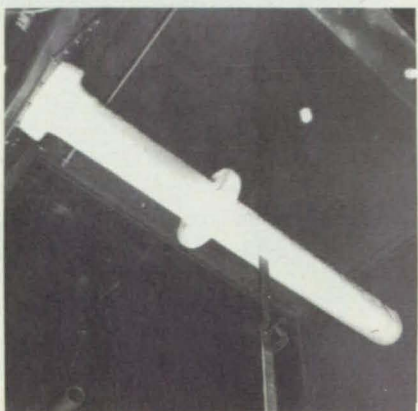
A ratio of 25 grains of water per pound (weight ratio of 1:280) of dry nitrogen gas will ensure a dewpoint of 30° to 32° F (-1.1° to 0° C) at sea level. Frost formed under these conditions has the best insulating properties. The adjustment of water content for a dewpoint of 18° F (-7.8° C) yields the greatest reduction in heat transfer per unit weight of frost.

The conditions for preventing nitrogen condensation must prevail before cryogenic liquids start flowing through the pipes. Once liquid-nitrogen condensation and dripping begin, a humid purge will not stop them.

This work was done by James G. Stephenson and Joseph A. Bova of Rockwell International Corp. for **Johnson Space Center**. For further information, Circle 8 on the TSP Request Card. MSC-20426



Cracks in Pipe Insulation (top) permit heat gain by cryogenic liquids in the pipe and create condensates that may harm other parts. A coating of frost (bottom) — if properly controlled — reduces heat transfer and eliminates dripping.



Precise Electrochemical Drilling of Repeated Deep Holes

Special tooling enables the maintenance of close tolerances.

Marshall Space Flight Center, Alabama

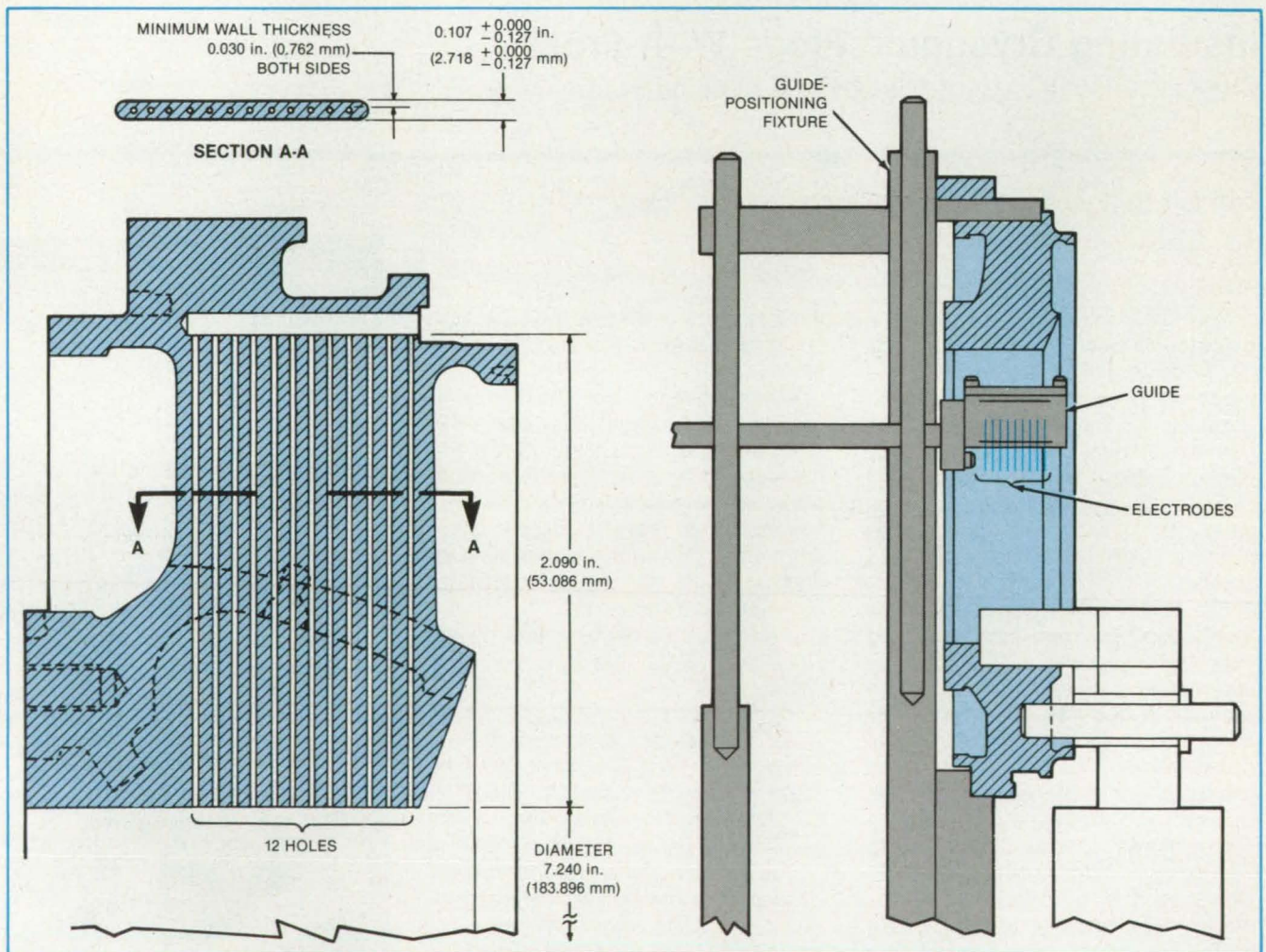
Special tooling made it possible to drill long, narrow through holes in the 41 radial struts of a complicated ring-shaped part. The job specification called for 12 holes per strut, each about 2.1 in. (53 mm) long with a diameter of 0.025 in. (0.635 mm). The holes had to be located precisely and have a precise center-to-center spacing (see left side of figure). It would be cumbersome to attempt this job with a conventional indexing

machine tool (milling machine, for example) and difficult or impossible to maintain the required tolerances with such machinery in this configuration.

The special tooling devised for this situation (see right side of figure) includes a guide that holds electrochemical drilling electrodes in the proper relative alignment and a guide-positioning fixture that clamps directly on the reference surfaces of a strut. High

precision was achieved by positioning the tooling anew on each strut before drilling: Tolerances of ± 0.0003 in. (0.008 mm) were maintained in some details.

This work was done by Joseph P. Kincheloe of Rockwell International Corp. for **Marshall Space Flight Center**. No further documentation is available. MFS-19767



The Part Shown in Cross Section on the left had to be drilled with 12 precise holes. The special tooling shown on the right was used to electrochemically drill the part to close tolerances in hole location and diameter.

Adapter Helps To Aline Plasma Torch

A fitting acts as a crude collimator.

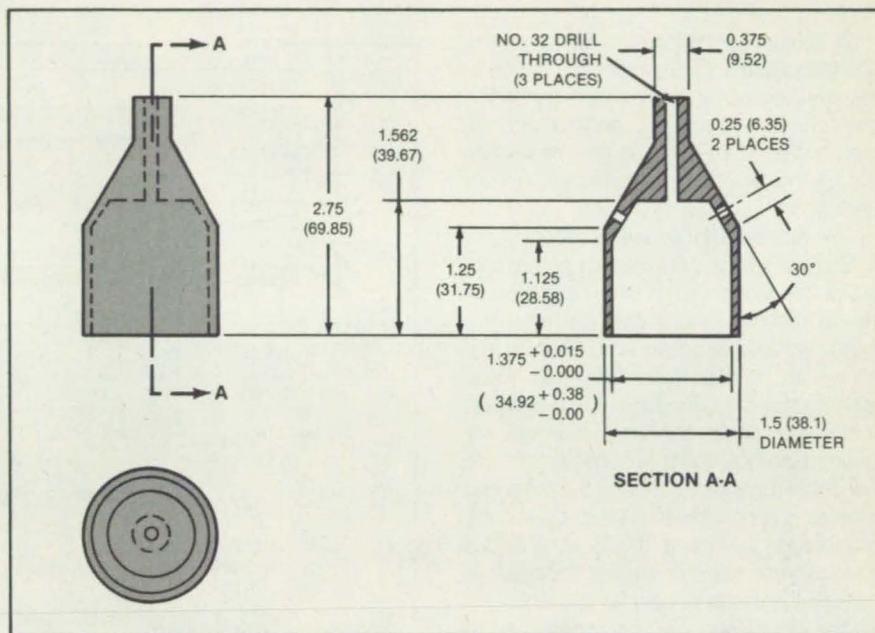
Marshall Space Flight Center, Alabar

A simple adapter allows a plasma welding torch to be alined accurately on a weld seam. The adapter confines a beam of light to a small spot on the seam to be welded. Previously, it was necessary to estimate the torch position before it was turned on by comparing the location of the torch pilot arc with the location of the seam.

The adapter fits over the nozzle of the torch. Light from the pilot arc inside the torch passes through a central orifice in a cone (see figure). The light emerges from the cone as a beam that creates a spot of light at the point where the torch will impinge on the workpiece. When the torch has been alined with the work, the adapter is removed, the plasma arc is struck, and welding proceeds.

This work was done by Charles A. Brosemer of Denver Aerospace for Marshall Space Flight Center. No further documentation is available.

Inquiries concerning rights for the commercial use of this invention should be addressed to the Patent Counsel, Marshall Space Flight Center [see page 21]. Refer to MFS-28024.



A Narrow Bore connects the interior of the adapter to the outside. Slipped over the nozzle of a plasma-welding torch, the adapter beams light through the bore to the workpiece. Dimensions are in inches (millimeters).

Thermal Shock-Resistant Composite Crucible

Heating rates of 350° F per minute have not caused cracking.

Lewis Research Center, Cleveland, Ohio

Only a limited number of suitable refractory materials may be used for high-temperature crucibles. Crucible properties can vary significantly due to the types, purities, and mixture ratios of refractory components. Induction heating of charged crucibles can result in rapid heating and cooling rates and result in thermal stresses on the crucible. These stresses can induce anything from fine cracks in the crucible wall to complete failure of the crucible. In either event, the result is loss of crucible integrity and termination of the operation.

This problem has been overcome using a composite crucible developed at Lewis Research Center. Originally intended for use in a Chill Block Melt Spinning

(CBMS) apparatus, the crucible is adaptable to other operations involving rapid self-induction heating of metallic charges.

The crucible consists of an inner dense alumina (Al_2O_3) crucible for containment of the metallic charge. Alumina is used because of its high melting temperature [about 3,600° F (1,980° C)] and chemical inertness. It is also low in porosity and nearly impervious to most gases.

Surrounding the inner crucible is an annulus of loosely packed alumina powder, which serves as a compressible insulating material. A second annulus consisting of a section of fused-quartz tubing surrounds and retains the alumina powder. The quartz tube is held in place by refrac-

tory cement, which helps to contain the alumina powder. Small holes in the upper ring of cement allow the alumina powder to outgas during operation in vacuum.

Composite crucibles of this type have been used to contain nickel superalloys at temperatures to 2,500° F (1,370° C) and intermetallic compounds to 3,100° F (1,700° C). Heating rates of 350° F (180° C) per minute have not caused cracking. Composite crucibles have had repeated use as many as seven times without cracking.

This work was done by H. J. Geringer and R. W. Jeck of Lewis Research Center. No further documentation is available.

LEW-14105

Miniature Rocket Motor for Aircraft Stall/Spin Recovery

The design accommodates different thrust levels and burn times with minimum weight.

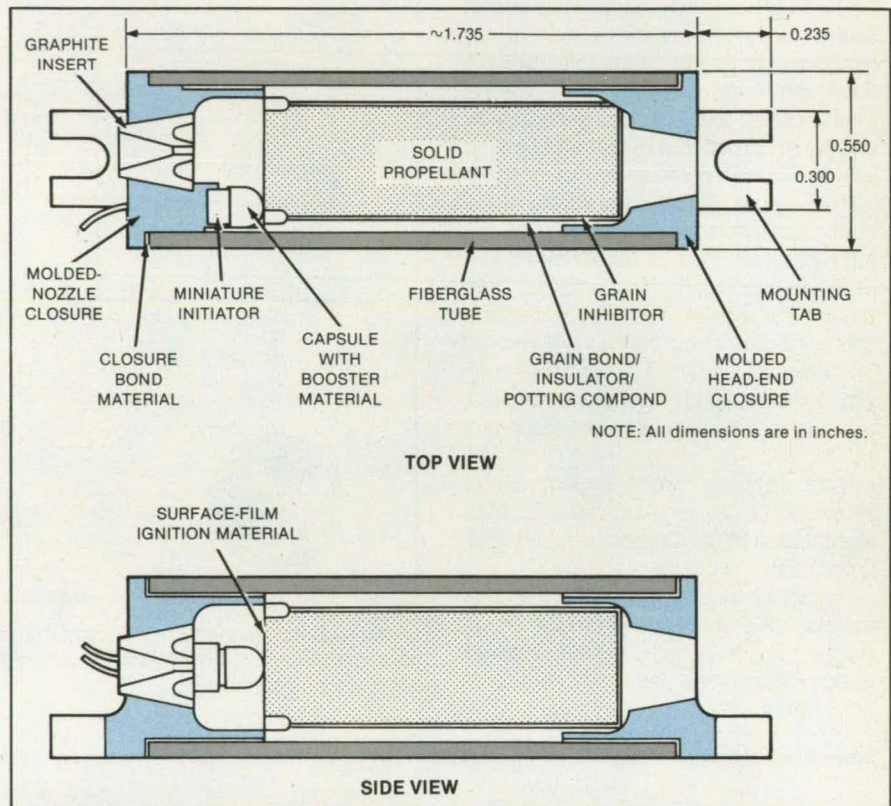
Langley Research Center, Hampton, Virginia

A lightweight, miniature all-composite solid propellant rocket motor can be used to identify the energy requirements for an aircraft stall/spin recovery positive propulsion system. The motor is electrically initiated, is a neutral burner, and has predictable performance.

The rocket motor (see figure) consists of a fiberglass tube with molded plastic closures bonded into each end. Each closure has a mounting tab molded in situ. The head-end closure possesses a feature that allows an inhibited propellant grain to be easily bonded into the tube. It also contains features to center the grain automatically during assembly and to ensure the optimum bond-line thickness between the tube and closure. It is possible to witness grain burn-out through the hole in this closure, as it is filled with transparent material. The material acts as the pressure seal for the motor.

The nozzle-end closure contains an in situ molded-graphite throat insert and mounting provisions for a miniature electrical initiator. The graphite insert has a special surface configuration to ensure a good mechanical bond with the plastic and to act as a seal. The insert is machined later (as shown) to produce a partially submerged nozzle with the proper throat diameter and exit geometry. The initiator mounting-seat provision actually holds the miniature squib in position, has two very small tapered holes for the electrical leads, and during assembly is filled with a small amount of RTV (or equivalent) silicon rubber compound to provide a motor seal. The miniature squib is an improved version of a standard device with increased output. A molded plastic capsule bonded onto the squib has been added to contain additional powder. A film of ignition material is placed on the end of the propellant grain, and loose ignition powder is contained in the free volume.

The double base propellant is an end-burning design, and it produces little or no smoke. It is inhibited on the outside to prevent unwanted burning. A groove is cut on the end of the grain at its maximum diameter to enhance ignition and to make the initial portion of the thrust history neutral. The forward end of the grain can possess a small, colored-smoke powder charge to help visually detect motor burnout. Motor burning is readily apparent through the translucent inhibitor/bond material/tube



The Longest, Solid-Propellant Motor of this design weighs 12 ounces (340 g) and produces a 5-ounce (1.4-N) thrust for 4 seconds.

wall, and ignition is also obvious.

Different thrust levels are achieved by substituting other propellants of different diameter and burn-rate characteristics. Different burn times are achieved by simply changing the length of the grain/tube assembly. The grain bond material also acts as an insulator for the fiberglass tube. The rocket motor is attached to an aircraft model and ignited from a radio-controlled 4.8-volt power source.

An early problem of nonuniform grain burning was solved by providing controlled separation between the grain bond material and the tube wall to account for material shrinkage.

When power is applied to the squib, the burning of the bridge wire sets off the powder in the capsule, which in turn ignites the loose powder, the surface film, and then the propellant grain. The device provides more than twice the energy available in previous

designs at only 60 percent of the weight. It also achieves 90 percent of theoretical performance. Since the motor features all-composite construction, there is virtually no postfire heating; therefore, no additional protection of the model is required. The motor can sustain internal pressures in the order of 13 ksi (9×10^7 N/m²).

This work was done by Melvin H. Lucy of Langley Research Center. No further documentation is available.

LAR-13199

Shaft Seal Compensates for Cold Flow

Seal components are easy to install.

Marshall Space Flight Center, Alabama

A ring seal for rotating or reciprocating shafts is spring-loaded to compensate for the slow yielding (cold flow) of the sealing material. The new seal is relatively easy to install because the components can be preassembled, then installed in one piece.

Older seals of the same general type had to be assembled in place from separate parts.

The seal assembly fits in an annular recess in the housing about the shaft (see Figure 1). The resilient part of the seal is an elastomeric or soft metallic ring cup. A

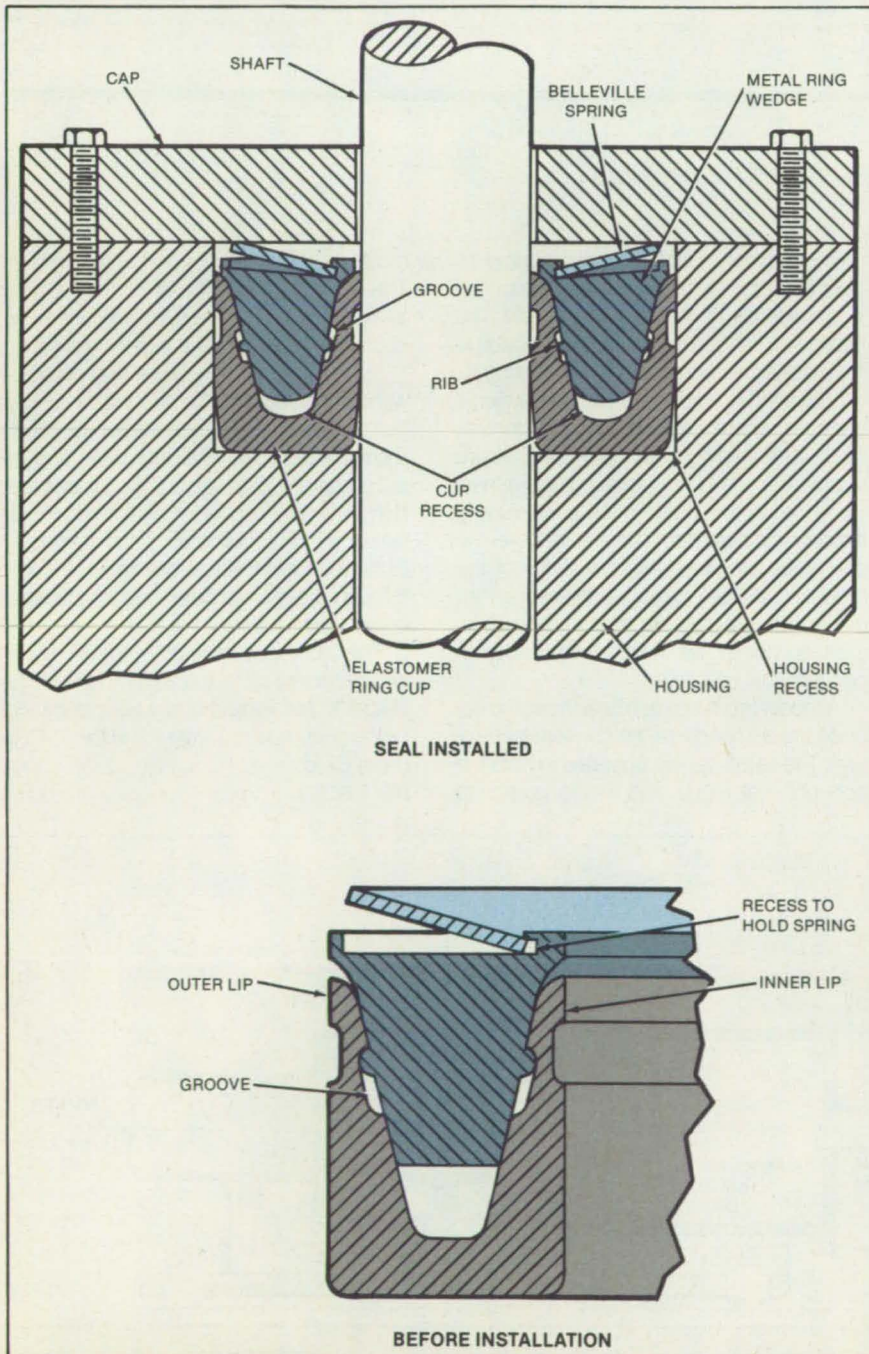


Figure 1. The **Shaft Seal** includes an elastomeric ring cup that is held against the shaft and housing by a sprung ring wedge.

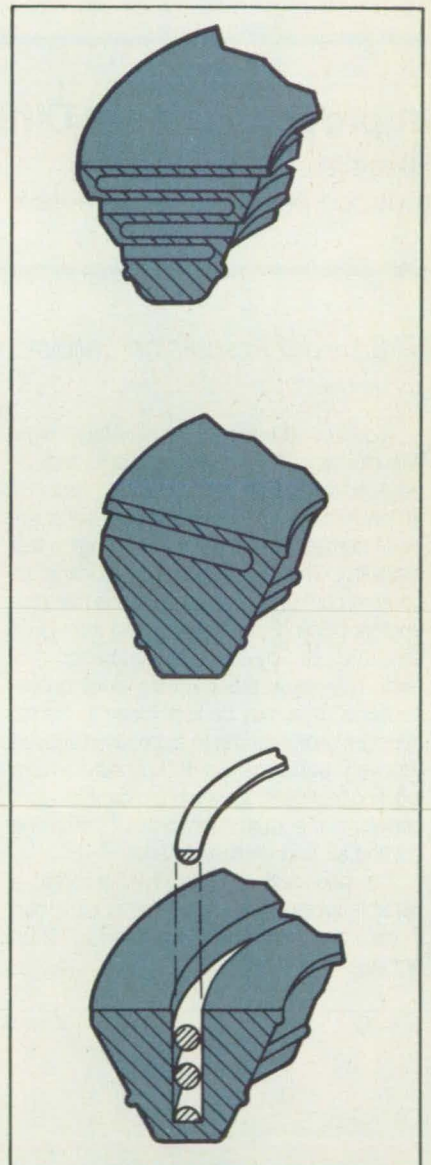


Figure 2. These **Springs for the Ring Wedge** may be used instead of the Belleville spring washer of Figure 1.

metal ring wedge fits into a wedge recess in the ring cup. A Belleville spring washer is held in a recess on top of the ring wedge.

Ribs on the metal ring wedge fit into elongated grooves in the walls of the cup recess. Before installation in the housing recess, the ring wedge is pressed into the cup recess so that the ribs snap into place in the grooves. As shown in the lower part of Figure 1, the spring action of the resilient ring cup pushes the ribs to the upper ends of the grooves. In this configuration, the in-

ner and outer walls of the ring cup are roughly parallel: The cup-and-ring-wedge assembly fits loosely in the housing recess and can slide in and out.

After insertion of the assembly into the housing recess, the cap is bolted onto the housing. As the cap pushes against the Belleville spring, the spring pushes the ring wedge farther into the cup recess. This forces the inner and outer lips of the cup apart, pressing them against the shaft and housing, respectively. As the inner and

outer lips gradually yield under the sealing pressure or as the inner lip wears away from the shaft motion, the spring pushes the ring wedge against the walls of the cup recess to maintain sealing pressure.

Other springs may be used in place of the Belleville spring washer. A sinuous spring top may be fabricated as an integral part of the ring wedge (Figure 2, top). A Belleville spring could be formed integrally with the wedge. (Figure 2, middle). A coil spring could protrude from a

narrow slot (Figure 2, bottom).

This work was done by William N. Myers and Leopold A. Hein of Marshall Space Flight Center. For further information, Circle 3 on the TSP Request Card.

This invention is owned by NASA, and a patent application has been filed. Inquiries concerning nonexclusive or exclusive license for its commercial development should be addressed to the Patent Counsel, Marshall Space Flight Center [see page 21].
Refer to MFS-25678.

Improved Exhaust Diffuser for Jet-Engine Testing

High-altitude simulator has reduced power requirements.

NASA's Jet Propulsion Laboratory, Pasadena, California

A proposed concept for simulated high-altitude tests of jet engines would reduce peak power consumption during tests by 48 percent and reduce overall power costs by 41 percent for a typical TF-30 engine test program. The test cell uses its exhaust-capture duct only to remove gases from the engine; cooling air is evacuated through a separate path by an auxiliary suction system. This way, the capture duct cross-sectional area may be kept close to the exhaust jet area, leading to a greatly improved recovery performance. It thus differs from existing test cells, in which the capture duct performs the dual functions of removing cooling air and engine exhaust.

The new test cell would incorporate a variable-cross-section capture duct. It can therefore accommodate engines of different sizes.

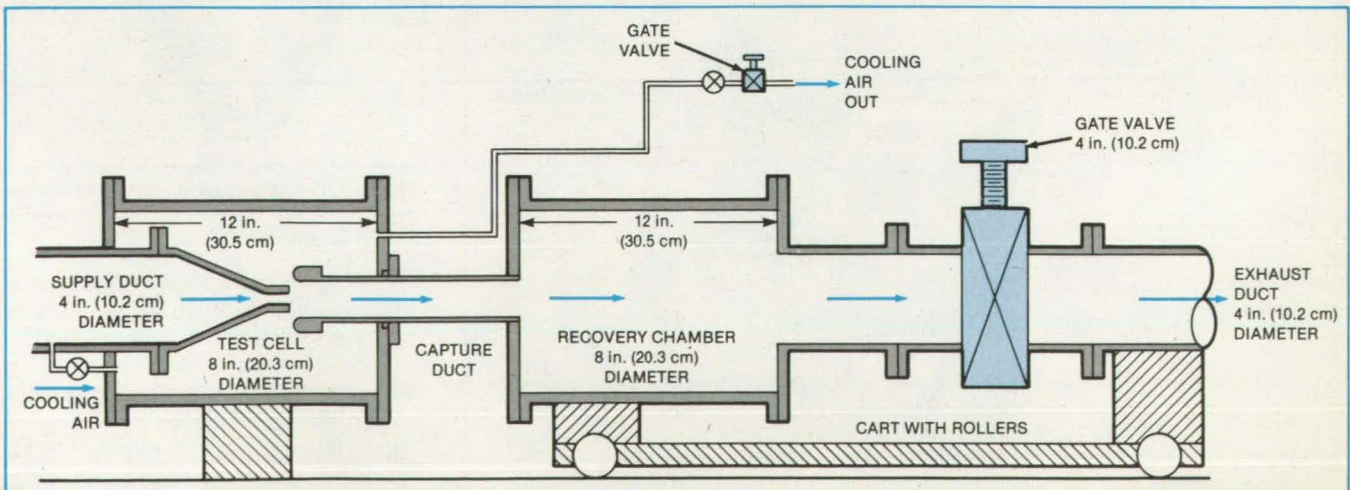
The auxiliary cooling-air evacuation allows the test-cell pressure to be controlled independently of the cooling-air flow. The maximum altitude that can be simulated is limited only by the capacity of the cooling-air exhauster. This is in contrast to conventional test cells, where the maximum simulated altitude is limited by choking of the capture duct as the cooling-air fraction is increased. Once the capture duct is choked, increasing the duct-exhauster suction will not lower the cell pressure. Moreover, the ability of the proposed test cell to recover pressure from the jet exhaust does not deteriorate with increased cooling-air fraction, as it does in conventional test cells.

A model test setup has been built and operated to demonstrate the concept (see figure). The setup can be operated in both the conventional mode and in the proposed

mode of separate cooling-air removal. Three nozzles, with throat and exit diameters chosen to simulate common types of jet engines, were used in the demonstration.

Performance data were first obtained without cooling air. The secondary air was then turned on. By simultaneous adjustments of the main exit gate valve and the secondary air gate valve, it was possible to duplicate the recovery performance obtained without cooling air. Thus cooling air, introduced into the test cell and evacuated through a separate path, had no influence on performance.

This work was done by Pradip G. Parikh and Virendra S. Sarohia of Caltech for NASA's Jet Propulsion Laboratory. For further information, Circle 77 on the TSP Request Card.
NPO-16328



This **Demonstration Model of the Test Apparatus** can be used with or without separate cooling-air exhaust. The recovery chamber and its gate valve are mounted on a cart on a track. The cart allows quick withdrawal of the recovery chamber for changing nozzles and capture ducts.

Gradually Acting Shaft Stop

This mechanism brakes rotation with minimal shock.

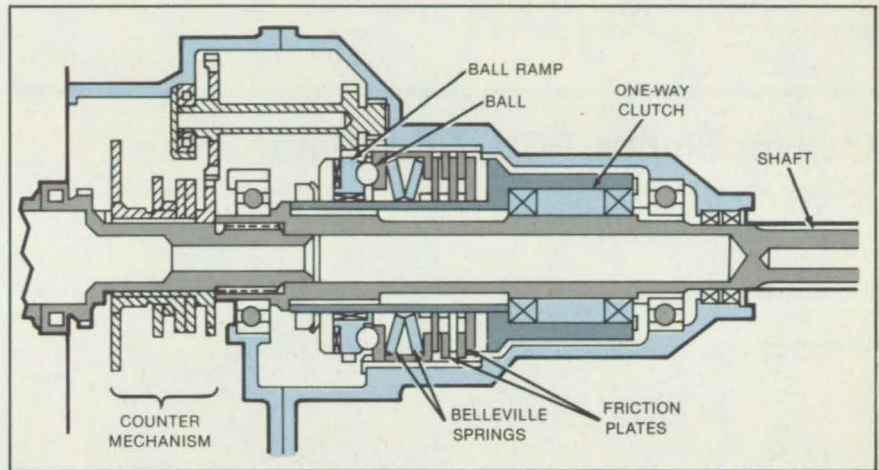
Lyndon B. Johnson Space Center, Houston, Texas

A brake stops a shaft gradually, with minimal shock load, at a predetermined limit of rotation. Because the brake absorbs energy from the shaft over a brief period of time rather than instantaneously, it can be made smaller than brakes that allow only hard stops.

The brake can be used to automatically stop control mechanisms on aircraft and ships. It can serve as a spindle brake on a machine tool. On a robot, it can prevent overtravel of an arm or hold it in a fixed position. It can be adapted as a handbrake that provides powerful, but not-too-sudden stopping forces on a rotating shaft, independent of shaft position.

A counter similar to a car odometer measures the shaft rotational position. As the shaft approaches its preset limit, the counter actuates a ball-ramp mechanism (see figure), which converts a low torque applied at a small angle into large axial forces on the brake friction plates. Belleville springs between the ball ramp and the plates ensure that the forces are applied gradually. Once the ball-ramp mechanism is actuated, the brake torque increases linearly with shaft rotation.

When the shaft has been completely



Balls Rising on a Spiral Ramp generate a large axial force on brake friction plates, thereby generating a large braking torque. A counter triggers the rise of the ball.

stopped, the brake friction plates apply just enough torque to hold the shaft in its final position. A one-way clutch enables the brake to be disengaged simply by rotating the shaft in the opposite direction.

This work was done by David J. Lang of Sundstrand Energy Systems for Johnson Space Center. No further documentation is

available.

Title to this invention has been waived under the provisions of the National Aeronautics and Space Act [42 U.S.C. 2457(f)], to Sundstrand Energy Systems, Rockford, IL 61125. MSC-20729

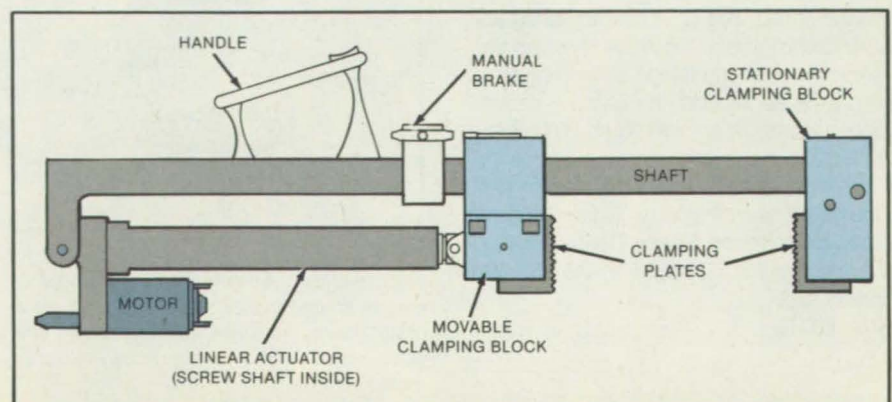
Hand-Held Power Clamp

Tool furnishes large pushing or pulling forces.

Lyndon B. Johnson Space Center, Houston, Texas

A new power clamp, originally designed to secure a payload aboard the Space Shuttle, can be operated with one hand to apply an opening or closing force of up to 1,000 lb (4,400 N). The clamp has potential applications as an end effector for industrial robots and in rescue work to push or pull wreckage with great force.

The device includes two clamping blocks, two clamping plates, and a motor-driven linear actuator with a self-locking screw shaft (see figure). In addition, the clamp has a redundant manual lock and a handcrank for use if the actuator motor fails.



The Power Clamp exerts an opening or closing force at the push of a switch. The tool is approximately 1 m long. Smaller, less forceful versions can be designed on the same principle.

The user controls the clamp by depressing a rocker-arm switch on the handle. Rocking the switch to the "close" position causes the linear actuator to move one of the blocks along the shaft so that it presses an object against the other block. With the switch in the "open" position, the shaft rotation is reversed, and the clamping blocks are separated.

The clamping blocks retain the clamping plates. The clamping plates may be changed to suit the particular task. A plate is released from a block by pressing a detent button on that block. A new plate may

then be inserted. The stationary clamping block can be tilted about 30° so that the tool can be used on objects with skewed surfaces.

This work was done by John P. Clancy of McDonnell Douglas Corp. for Johnson Space Center. For further information, Circle 22 on the TSP Request Card.

Inquiries concerning rights for the commercial use of this invention should be addressed to the Patent Counsel, Johnson Space Center [see page 21]. Refer to MSC-20549.

Anvil for Flaring PCB Guide Pins

Spring-loaded anvil results in fewer fractured pins.

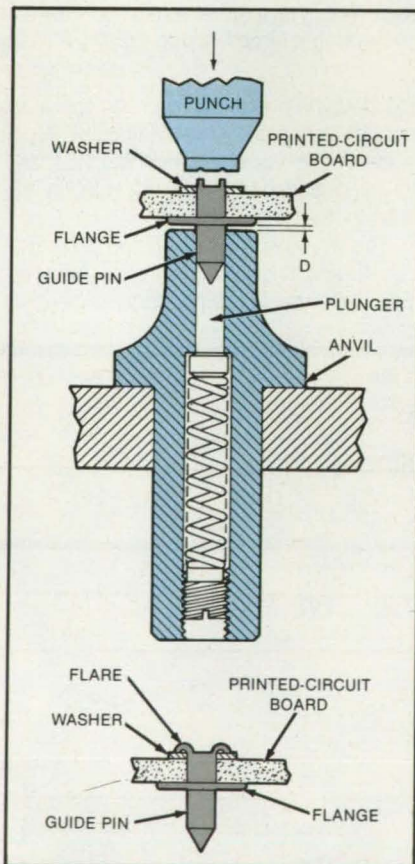
Lyndon B. Johnson Space Center, Houston, Texas

A pneumatic-press anvil for flaring hardened-aluminum and stainless-steel guide pins in printed-circuit boards (PCB's) includes a load-absorbing spring. Previously, the pin flange had to withstand the full press force, often fracturing and causing the boards to be rejected. The fractured pins had to be removed by grinding down the flares and replaced with new ones, a time-consuming and costly operation. In contrast, the new anvil distributes the load of the flaring force to portions of the pin that are better able to support the load, resulting in fewer damaged pins and increased work output of the flaring press.

In the improved anvil shown in the figure, a plunger and load-absorbing spring are inside the anvil. A screwplug adjusts the spring compression.

When the press is operated, the press punch contacts the tubular end of the pins, closing a small gap of dimension D between the anvil and the pin flange and compressing the spring. The compressed spring absorbs part of the press force, reducing the stress between the flange and pin body. In the NASA application, the spring is dimensioned to absorb approximately 80 percent of the total press force.

This work was done by Edward Winn and Robert Turner of Sperry Flight Systems Corp. for Johnson Space Center. For further information, Circle 34 on the TSP Request Card.
MSC-20345



The New Anvil for Flaring Guide Pins in printed-circuit boards absorbs approximately 80 percent of the press force. As a result fewer pins are damaged, and the work output of the flaring press is greatly increased.

Books and Reports

These reports, studies, and handbooks are available from NASA as Technical Support Packages (TSP's) when a Request Card number is cited; otherwise they are available from the National Technical Information Service.

Effects of Bearing Clearance on Turbopump Stability

A realistic mathematical model is presented.

The effects of bearing clearances, or "dead bands," on bearing loads and rotor stability in turbopumps are examined in a 194-page report. A relatively simple mathematical force model for analyzing the effects is highlighted. The report shows that the nonlinear characteristics resulting from bearing dead bands have a significant effect on the dynamics of turbomachinery and cannot be ignored as they have in the past.

High-performance turbopumps rotate at very high speeds and move large amounts of fluid at high rates. As a result, bearing loads can be high, and potentially damaging subsynchronous orbiting, or "whirling," of rotors can occur. Until now, linear models for analyzing such behavior have included many degrees of freedom and have provided limited insight into the phenomena involved. These models ignore the nonlinear effects that arise from precise balance of the rotor. Because a typical rotor is so well balanced, its eccentricity (the distance between its center of mass and its geometric axis) is about the same as or less than the bearing clearance of 0.0005 to 0.0025 inch (13 to 64 micrometers). Thus, dead bands can have pronounced nonlinear effects. However, if they were taken into account, the already complex models would become even more difficult to deal with.

The report presents a model that retains the important driving forces, but readily lends itself to analysis. The model is an adaptation of a relatively simple, older one known as the Jeffcott model. It has been modified by the addition of dead-band effects and fluid-seal forces. In addition, the equations of motion have been rewritten in polar coordinates; this form is more naturally suited to the problem because whirling paths tend to be circular. A number of computer programs to implement the model are listed toward the end of the report.

Another addition to the model is a constant side force to account for misalign-

ments between bearings and seals and for hydrodynamic forces created by pumped fluids. The model shows that the combination of side force and dead-band effects influences stability in a peculiar way: In the proper combination, they enhance stability — but only locally; it is still possible for impulsive disturbances or large rotor imbalances to drive the system into instability.

The model, despite its simplicity, gives realistic results. It is only a planar model, but can readily describe rotor whirling motion. Thus, values of effective mass, stiffness, dead band, and seal coefficients predicted by the model are close to those of more complex models. Although exact critical speeds and stability boundaries cannot be inferred, qualitative behavior can be.

This work was done by Control Dynamics Co. for Marshall Space Flight Center. Further information may be found in NASA CR-170986 [N84-19814/NSP], "Effects of Bearing Deadbands on Bearing Loads and Rotor Stability" [\$17.50]. A paper copy may be purchased [prepayment required] from the National Technical Information Service, Springfield, Virginia, 22161. The report is also available on microfiche at no charge. To obtain a microfiche copy, Circle 48 on the TSP Request Card. MFS-27063

Optimizing Load Spectra for Gears

Life expectancy of gear systems can be extended.

A NASA document presents an algorithm for gear-load-spectrum synthesis (GLSS) as an aid in choosing the best load spectrum for a machine containing gears. The objective of GLSS is to determine the best schedule or combination of load elements — one that will yield the longest possible fatigue life for the machine.

The fatigue life of a machine is determined by the spectrum of loads applied to it. A load spectrum is not necessarily fixed: Factors such as the load magnitude, the amplitude of load alternation, and the number of load cycles can be varied among individual load blocks. For a machine in which a gear is a critical component, the load spectrum should be chosen with particular care; otherwise, heavy fatigue damage may be imposed on a few gear teeth. Machine life can be greatly increased if fatigue damage is uniformly distributed among all teeth.

The GLSS algorithm has been used to modify the load spectrum of the Space Shuttle rudder-and-speed-brake-actuation subsystem. The lifetime of one of the four rotary actuators in the subsystem was increased 211 percent as a result.

The document presents equations for curves of stress vs. number (S-N) of fatigue cycles and for constant-life curves. It describes a semigraphic method for generating S-N curves of arbitrary ratios and adapts the semigraphical method to curve generation by digital computer.

The document defines a quantity, "damage factor," to reflect the fatigue damage imposed on a machine part by each load block in a load spectrum. The document describes an exhaustive search technique involving the comparison of all flexible load spectra to determine which one offers the longest fatigue life. Although the search technique is effective, it can become very time consuming, and the document therefore provides a couple of data-reduction methods. By applying these methods before a search is started, the problem can be simplified, and the computation effort can be greatly reduced.

The program for performing the complete GLSS by computer is described in detail. Illustrative examples of the use of the program are also furnished.

This work was done by Shio-ping P. Oyoung of Sundstrand Energy Systems and William L. Carson of the University of Missouri for Johnson Space Center. To obtain a copy of the report, "Fatigue Life Optimization for Gear Critical Actuation Systems by Load Spectrum Synthesis and an Algorithm for S-N-R Curve Generation," Circle 95 on the TSP Request Card. MSC-20487

Predicting Leakage in Labyrinth Seals

Analytical and empirical methods are evaluated.

A 264-page report presents comprehensive information on leakage in labyrinth seals. Such seals are widely used in rotating machines, such as pumps, compressors, and turbines.

The report summarizes previous analyses of leakage. It reviews leakage tests conducted by the authors and evaluates the various analytical and experimental methods of determining leakage and discusses leakage prediction techniques.

In preparation of the report, the open literature pertaining to incompressible flow in straight-through, staggered, stepped, and radial labyrinth seals was surveyed. For straight-through labyrinth seals, an analytical leakage prediction developed by L. Dodge was found to produce the best results. By adding empirical corrections to leakage rates

predicted by Dodge's technique, a more-accurate and general leakage-prediction technique was produced. For straight-through labyrinth seals, the agreement between predictions and data was reasonable.

For stepped labyrinth seals, the empirical technique for straight-through seals was modified. Because of the lack of published data, experiments were performed to gather data for a leakage model of stepped seals. The experimental leakage rates were found to be highly dependent on the axial locations of seal teeth with respect to seal steps: The rate in a given seal is least when the tooth is centered on the step. The model developed from the experimental data is accurate for stepped seals with more than four throttles.

It was not possible to develop a generalized leakage-prediction method for radial and staggered labyrinth seals. Too few data were available; an extensive testing program would be required.

A computer program was developed to calculate the turbulent flow in a cavity of a labyrinth seal using the Navier-Stokes equations. Two different cavity geometries were investigated. The calculated flows showed how the interaction between turbulence and the mean flow affects the overall pressure drop in a seal cavity. For a given mass-flow rate, changing the cavity shape can greatly influence the pressure drop through the cavity.

This work was done by Gerald L. Morrison, David L. Rhode, Kevin C. Cogan, Daesung Chi, and Jonathan Demko of Texas A & M University for Marshall Space Flight Center. To obtain a copy of the report, "Labyrinth Seals for Incompressible Flow," Circle 110 on the TSP Request Card. MFS-27051

Experiments With a Manipulator Sensor System

Force and torque data aid the operator.

A report describes experiments with a system that displays data on forces and torques acting on the end effector of a remote manipulator. [The system was previously described in "Displaying Force and Torque of a Manipulator" (NPO-15942), *NASA Tech Briefs*, Vol. 8, No. 2, page 186.] The experiments demonstrated the use-

fulness of the display in manipulation tasks with narrow geometric and dynamic tolerances. Such tasks are encountered in manufacturing and in operations requiring the use of tools.

The system displays the three orthogonal forces and the three orthogonal torques acting at the base of the end effector of a 16-meter-long arm. The experimental system contained the following components:

- Two force/torque sensors, one for the 0-to-100-pound (0-to-445-N) range and the other for the 0-to-200-pound (0-to-890-N) range;
- A servocontrolled end effector;
- Interchangeable three-claw and four-claw

end effectors;

- A graphics terminal that displays the forces and torques (the operator has a selection of scales and formats, activated either manually or by voice command);
- A network of microcomputers for data processing, control of the end effector, operation of the display, and voice-command recognition; and
- An eight-channel analog chart recorder for sensor data and end-effector status.


Two sets of experiments were performed. In the first set, operators used the end effector to remove a keyed cylinder and a box from a task board and then reinserted the objects. The removal and insertion of the box required the use of a screw-

driver and a box wrench. In the second set, operators maneuvered a simulated payload into a latching mechanism. Four test operators performed a total of 110 tests. All operators consistently performed the final phase of the payload insertion without any visual feedback, relying only on the display of forces and torques.

This work was done by Antal K. Bejczy and Ronald S. Dotson of Caltech and Jeri W. Brown and James L. Lewis of Johnson Space Center for NASA's Jet Propulsion Laboratory. To obtain a copy of the report, "Force-Torque Experiments with Simulated Space Shuttle Manipulator," Circle 12 on the TSP Request Card. NPO-16094

Computer Programs

These programs may be obtained at a very reasonable cost from COSMIC, a facility sponsored by NASA to make raw programs available to the public. For information on program price, size, and availability, circle the reference number on the TSP and COSMIC Request Card in this issue.



Hybrid and Electric Advanced Vehicle Systems Simulation

Predefined components are connected to represent a wide variety of propulsion systems.

The Hybrid and Electric Advanced Vehicle System (HEAVY) computer program is a flexible tool for evaluating the performance and cost of electric and hybrid vehicle propulsion systems. It allows the designer to quickly, conveniently, and economically predict the performance of a proposed drive train. It provides the capability to configure and test a proposed vehicle propulsion system at a preliminary level of detail without requiring the user to be a simulation expert. Instead, the user defines the system to be simulated using a library of predefined component models that may be connected to represent a wide variety of propulsion

systems.

Moreover, HEAVY places these capabilities in the hands of propulsion systems analysts and designers who are not necessarily simulation or computer programming experts. Components of the HEAVY library may be assembled into propulsion systems using a special-purpose computer language that requires little or no knowledge of computer programming. However, a user who desires may enhance his HEAVY model by adding standard FORTRAN statements when needed. Furthermore, HEAVY is not limited by the existing component library. New components may be added, and existing components may be modified to add more detail or to reflect improved mathematical models.

HEAVY is a tool that is intended for use early in the design process/concept evaluation, alternative comparison, preliminary design, control and management strategy development, component sizing, and sensitivity studies. The models in the standard component library contain sufficient detail to be useful in predicting the performance of an electric or hybrid vehicle. They are not intended to be used as detailed design tools for a specific device, but instead to represent generic devices.

The HEAVY standard component library is a collection of predefined, pretested, and compiled subroutines intended to free the

HEAVY user from the necessity of building models of individual vehicle components. It is important to recognize that the capabilities of HEAVY are defined by the contents of this library and not by constraints either in the model generation or simulation programs. If it is necessary to simulate a new propulsion system component, then the only modification needed to HEAVY is the addition of a new component to the library.

Only those characteristics that have a significant impact upon the vehicle's general performance are modeled by HEAVY. Propulsion systems components are modeled by their steady-state performance, either by algebraic equations or by performance maps. Differential equations in the model represent long-term dynamics-vehicle speed and position and drive train shaft speed, etc., rather than transients such as drive-shaft flexing. This type of simulation consists of a sequence of closely spaced steady-state conditions rather than a true dynamic simulation. Transients are modeled in terms of duration, energy loss, and energy transfer.

This program was written by Raymond F. Beach of Lewis Research Center and Ronald A. Hammond and Richard K. McGehee of Boeing Computer Services Co. For further information, Circle 83 on the TSP Request Card. LEW-13927

Automatically-Programmed Machine Tools

Software produces cutter location files for numerically-controlled machine tools.

APT, which is an acronym for Automatically Programmed Tools, is one of the most widely used software systems for computerized machine tools. Such machine tools, whose motions and functions are specified by computer-generated data, are frequently called numerically controlled, or NC, machine tools.

APT was developed for the explicit purpose of providing an effective software system for programming NC machine tools. The APT system includes the specification of the APT programming language and a language processor, which executes APT statements and generates the NC machine-tool motions specified by the APT statements.

The syntax of the APT language has similarities to that of FORTRAN. However, APT also includes extensions to represent geometries and describe the tool paths needed to machine specified geometries. The APT geometry definitions and machine-tool instructions that constitute a typical machining operation are called a part program.

The APT language is statement oriented and sequence dependent. With the exception of such programming techniques as looping and macros, statements in an APT program are executed in a strict first-to-last sequence. To provide programming capability for the broadest possible range of parts and machine tools, the APT input (and output) is generalized, as represented by three-dimensional geometry and tools, and arbitrarily uniform, as represented by the moving-tool concept and output data in absolute coordinates.

The APT part program is processed by the APT execution software and results in a cutter location (CL) file. The CL file is processed by a user-specified postprocessor to put the CL data in a format compatible with a particular NC machine tool. The postprocessed data are usually transmitted directly to data storage devices at the machine tool or punched onto paper tape, which is read by a tape reader at the machine tool.

This APT system was developed to meet the needs of the Engineering Services Division of Goddard Space Flight Center (GSFC). It is a modified version of the public domain APT IV/SSX8. This modified system runs on DEC VAX computers and contains enhancements that support GSFC machining requirements and make the program more maintainable. A principal functional enhancement is the generalization of the APT "POCKET" statement so that pockets being machined can have concave and

convex interior angles instead of being limited to only concave interior angles.

The APT system software on the DEC VAX is written in FORTRAN for batch and interactive execution on the VAX/VMS operating system. APT is organized into two separate programs: the load complex and the APT processor. The load complex handles the table initiation phase and is usually run only when changes to the APT processor capabilities are made. This phase initializes character recognition and syntax tables for the APT processor by creating FORTRAN block-data programs.

The APT processor consists of four components: The translator, the execution complex, the subroutine library, and the CL editor. The translator examines each APT statement in the part program for recognizable structure and generates a new statement, or series of statements, in an intermediate language. The execution complex processes all of the definition, motion, and related statements to generate CL coordinates. The subroutine library contains routines defining the algorithms required to process the sequenced list of intermediate language commands generated by the translator. The CL editor reprocesses the CL coordinates according to user-supplied commands to generate a final CL file.

A sample postprocessor is also included, which translates a CL file into a form to use with a Wales Stripit Fabromatic Model 30/30, or equivalent, sheet-metal punch. The user should be able to develop postprocessors readily for other NC machine tools.

The most recent enhancements to this version of APT were developed in 1984 by Don Premo of ITE, Inc., under the direction of John Lallande and Lloyd Purves of the Goddard Space Flight Center.

This program was written by Lloyd Purves of Goddard Space Flight Center and Norman Clerman of Computer Sciences Corp. For further information, Circle 63 on the TSP Request Card. GSC-12758

Analysis of Spiral Bevel Gearing

The program can be generalized for automated finite-element-method model generation.

The tedious task of finite-element-method (FEM) model preparation has been greatly reduced by the development of a preprocessing program for automated

model generation. The utility of the program, including its ability to rapidly evaluate parametric changes, has been demonstrated for spiral, helical, and spiral bevel gearing. A postprocessing program has also been developed that aids in the review and interpretation of calculated FEM stresses.

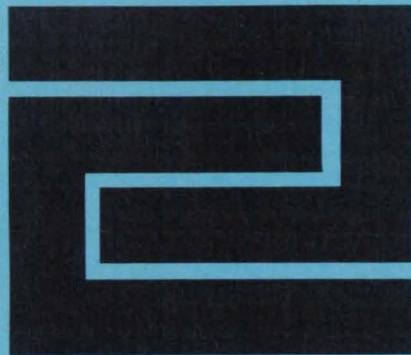
Past experience has shown that current analytical methods do not adequately predict stresses and hence, load-carrying capacity of spiral bevel gears. The limitation of these current methods is observed throughout the size range of gears used in helicopter and V/STOL (Vertical S-TakeOff and Landing) vehicles. However, the problem is particularly acute in the largest size built and tested to date, since this represents the greatest extrapolation from previous successful experience. This inability to accurately predict stresses is in large part due to neglecting the effects of the gear tooth support structure. However, this newly developed program greatly reduces the work associated with utilizing FEM analysis in three-dimensional structures, enabling entire gear configurations to be readily analyzed and thereby improving accuracy significantly.

Four program elements were developed and constitute the software program: The PREPROCESSOR computer program automatically generates a NASTRAN® compatible FORTRAN model of a spur, helical, or spiral bevel gear complete with the necessary NASTRAN® control deck. A SPUR/HELICAL GEAR CONTACT computer program calculates coordinates along the lines of contact between meshing spur or helical gear teeth, and a SPIRAL BEVEL GEAR CONTACT program generates tooth contact lines on the surface of spiral bevel gear teeth. The fourth element is a POST-PROCESSOR code, which was developed to aid in the review and interpretation of the calculated FEM stresses by enabling selective display of pertinent data for analysis.

This new program has been used to evaluate four complex spiral bevel gears, and the results have been compared to experimentally measured stress levels. The correlation obtained between the measured and predicted data was generally in the range of 7 to 12 percent. This program is written in FORTRAN IV for use on an IBM 3033 computer.

This program was written by Raymond J. Drago and Bapa R. Uppaluri of Boeing Vertol Co. for Lewis Research Center. For further information, Circle 60 on the TSP Request Card. LEW-14067





Hardware, Techniques, and Processes

- 152 Pretinning Nickel-Plated Wire Shields
- 152 High-Temperature, High-Pressure Optical Cells
- 153 Making Structural Members From Wire
- 154 Silicone-Rubber Stitching Seal
- 155 Centrifugal Generator of Filled Spherical Shells
- 155 Alining Large Cylinders for Welding
- 156 Prototype Furnace for Automatic Production of Silicon Ribbon
- 157 Fabrication of Slender Struts for Deployable Antennas
- 158 Duplicating Curved Tile Surfaces for Pull Testing
- 159 Adjustable Lid Aids Silicon-Ribbon Growth
- 159 Making Glass-Fiber-Reinforced Coolant Tubes
- 160 Controlling Sample Rotation in Acoustic Levitation

Books and Reports

- 161 Damage and Repair of Composite Structures

Pretinning Nickel-Plated Wire Shields

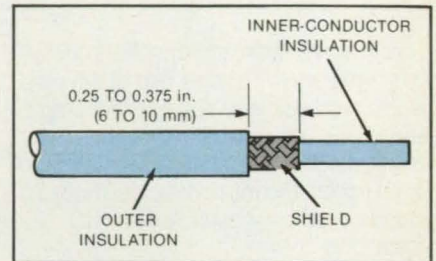
Mild solder flux prevents corrosion.

Lyndon B. Johnson Space Center, Houston, Texas

Nickel-plated copper shielding for wires is pretinned for subsequent soldering with the help of activated rosin flux. Until now, pretinning has not been possible because the acid flux used to clean the shield surface is corrosive and difficult to rinse away. Moreover, the acid flux could be wicked up into the wire insulation sleeve by the braid. In contrast, the rosin flux is easily dissolved and rinsed away by isopropyl alcohol.

In the pretinning procedure, originally developed for assembly of the Space Shuttle payload interrogator, the wire shield is first stripped and trimmed (see figure). It is then brushed with flux and dipped in a solder pot at 500° F (260° C), where it is agitated for 6 to 10 seconds. After removal from the pot, the shield is brushed with isopropyl alcohol and cleaned in a vapor degreaser.

A uniform coating of solder adheres to the shield. If the inner conductors of the wire are protected by polytetrafluoroethylene insulation, they are not adversely affected by



The shield is cut at a point 0.25 to 0.375 in. (6 to 10 mm) from the cut end of the outer jacket. The loosened end of the shield is straightened and pulled toward the cut end. The insulation of the inner wires is kept intact during pretinning.

the heat of the solder pot during their brief immersion.

This work was done by James A. Igawa of TRW, Inc., for Johnson Space Center. For further information, including a process specification, Circle 78 on the TSP Request Card.

MSC-20712

High-Temperature, High-Pressure Optical Cells

Infrared radiation can flow to and from a specimen of HgCdTe semiconductor.

Marshall Space Flight Center, Alabama

An optical cell has been constructed for measurement of the thermal diffusivity of HgCdTe semiconductor by laser pulses. The container allows radiation from the laser to enter one side of the alloy sample, while allowing lower-energy infrared radiation to leave the opposite side of the sample so that the temperature rise can be read by a sensor. The cell withstands the 1,000° C cell-operating temperature and contains the molten alloy at its 100-atmosphere (10^7-N/m^2) vapor pressure. Finally, it allows the alloy to solidify without bursting even though the alloy expands on cooling.

Composed entirely of fused silica, the cell includes two optical windows joined by a tube. The construction procedure is laborious, but the results are reliable.

The windows are made from fused-silica rods 10 mm in diameter, initially sawed into 25-mm lengths. One face of each window —

to become an inside face — is ground and polished. Each window is given a temporary handle (a rod 4 mm in diameter fused to the unpolished face) to aid in manipulating it for further processing.

Cell assembly is started by placing the windows, polished ends inward, in a silica tube about 15 cm long (see figure). The end of each handle is tacked to the inside of the tube to fix the position of the windows 1 or 2 mm apart.

The tube, one end of which is sealed, is placed in a glass-blowing lathe. The open end of the tube is connected to a vacuum pump. A flame is worked along the outside of the rotating tube, toward the vacuum end, and fuses the windows to the tube. The vacuum removes gases given off by the heated silica and thus prevents bubbles from being sealed in.

The ends of the fused tube/window assembly are sawed off near the handles. The assembly is then annealed in an oven.

A hole 2 mm in diameter is drilled radially into the cell interwindow gap, and a stem is fused to the cell over the hole. The stem will later serve as a port for introducing alloy material into the gap.

The cell is cut to a length of 40 mm with a diamond saw. It is annealed once more, then cut to its final length of 18 mm. The ends — that is, the outside faces of the windows — are ground and polished by hand.

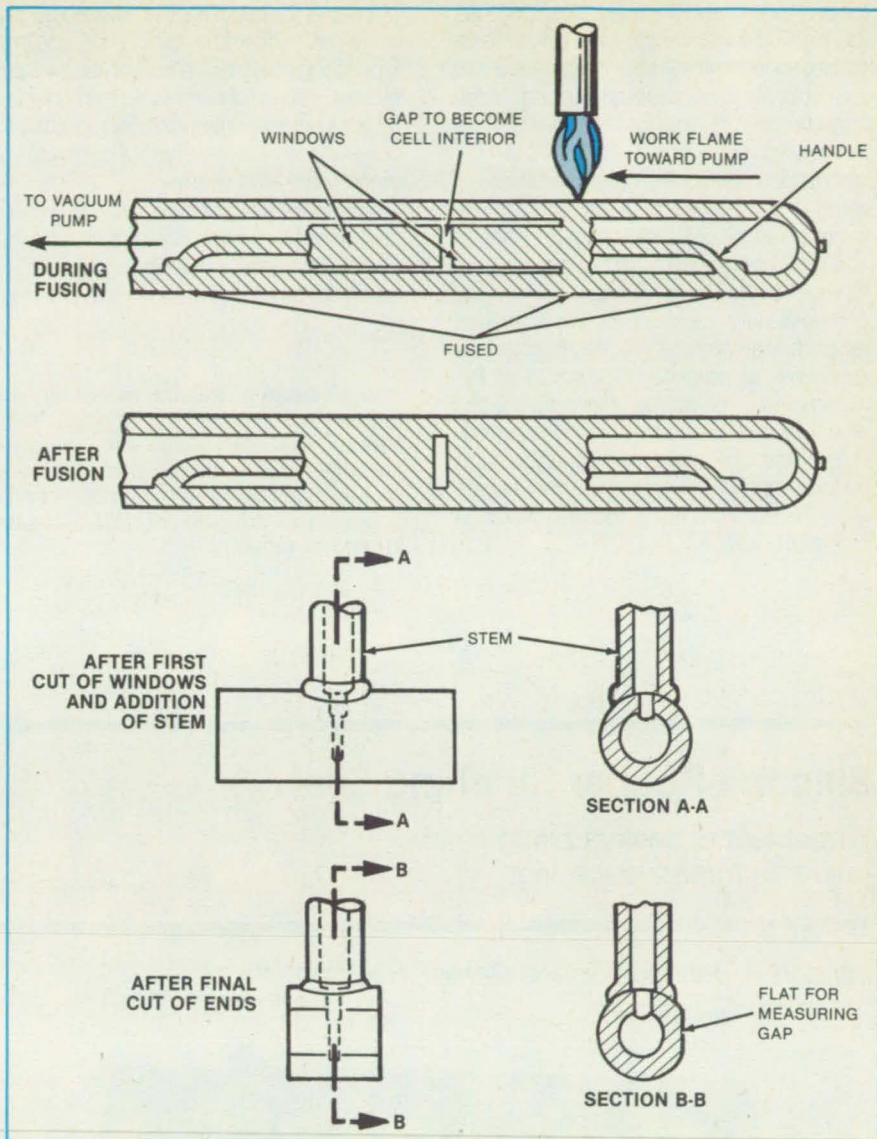
The final size of the gap, after assembly and annealing, is a critical dimension in the thermal diffusivity measurement. To measure the gap, a flat is polished on the side of the cell. A microscope mounted on a micrometer stage is focused through the flat, first on one window wall and then on the other, and the distance between the walls is measured on a micrometer stage.

The cell is filled with the desired proportions of Cd, Te, and Hg and sealed under vacuum. The contents are reacted and homogenized in a rocking furnace with the stem hanging downward. Once homogenization is complete, the stem is tipped up to cast the contents down into the cell. The contents are frozen by cooling from the bottom up.

In operation, the cell is heated to the operating temperature to remelt the contents. A laser beam is directed through the window, and the contents are observed through the opposite window with an infrared-sensitive photovoltaic cell.

This work was done by Ronald P. Harris of Marshall Space Flight Center, and Lawrence R. Holland and Robbie E. Smith of the University of Alabama. For further information, Circle 101 on the TSP Request Card.

This invention is owned by NASA, and a patent application has been filed. Inquiries concerning nonexclusive or exclusive license for its commercial development should be addressed to the Patent Counsel, Marshall Space Flight Center [see page 21]. Refer to MFS-26000.



These Steps in the Fabrication of an optical cell require careful control. During fusion on the glass-blowing lathe, for example, the cell will deform or collapse if the silica is slightly overheated. Cleanliness is critical, since contamination causes devitrification of fused silica.

Making Structural Members From Wire

Beams and columns would be fabricated onsite.

Lyndon B. Johnson Space Center, Houston, Texas

Structural members of any size, consisting of wire gridwork, would be fabricated onsite in a proposed new construction method. Although it was originally intended for manufacturing large structures in space, the technique has potential for use on Earth.

NASA Tech Briefs, Summer 1985

As shown in the figure, a typical cylindrical beam or column is made by assembling equal numbers of evenly-spaced right- and left-handed wire helices about a common axis, along with straight wire longitudinal members. The longitudinal members meet

the helices at their intersections, and all three wire layers are joined together at these points. The layer of longitudinal wires may be placed inside, outside, or between the helices.

The wires form a cylindrical geodesic

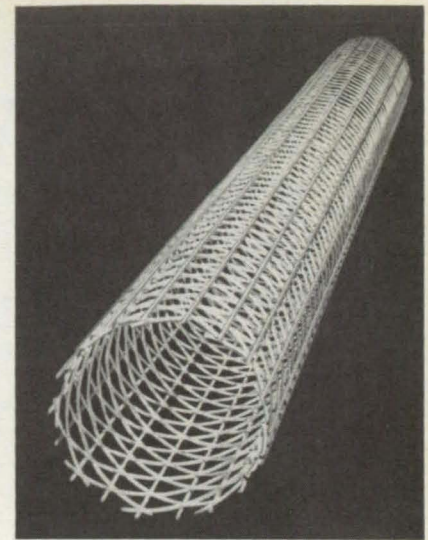
truss of equilateral triangles. The truss has the high rigidity-to-weight ratio characteristic of geodesic structures. It also has a low susceptibility to damage on account of the large number of redundant elements.

A computerized procedure has been developed to optimize the number and size of wires and the column diameter for a selected modulus of elasticity, column length, and axial loading. To maximize the strength-to-weight ratio, graphite-fiber-reinforced composite wire can be used. The technique takes full advantage of the mechanical properties of graphite because all of the high-modulus material is oriented along the wire axis, and the proportions of the ingredients of the composite can be adjusted to minimize the coefficient of thermal expansion, thereby minimizing thermal distortion of the structure.

Further development is needed to produce an automatic beam- or column-fabricating machine. Where metal wire can be used instead of composite, it may be fairly simple to adapt methods now used to produce wire reinforcements for concrete columns, piers, and beams.

This work was done by Thomas J. Dunn of Johnson Space Center. No further documentation is available.
MSC-20175

A **Rigid Beam or Column** is formed from intersecting helices and straight members of relatively flexible wire. The wires are joined at their intersections: The short wire sections between the joints therefore approximate the sides of rigid triangular structural subunits.



Silicone-Rubber Stitching Seal

Placement of sealant along seams prevents thread loosening.

Lyndon B. Johnson Space Center, Houston, Texas

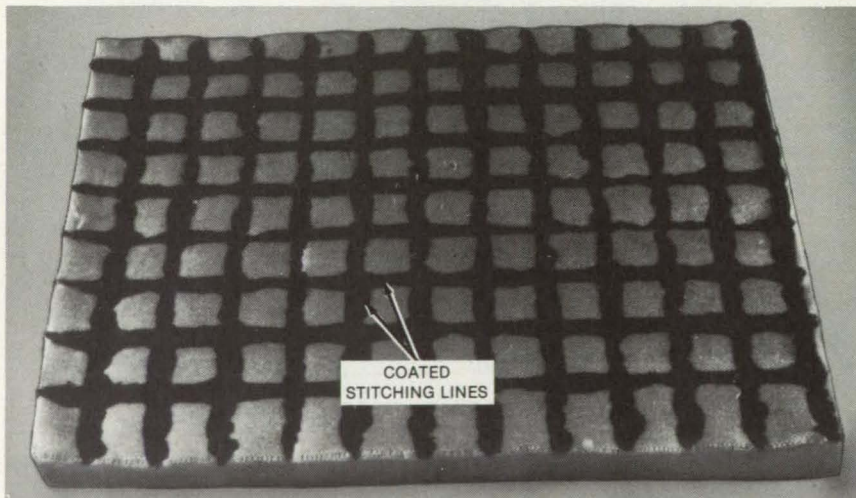


Figure 1. The **Stitches of an Insulating Quilt** are coated with silicone rubber. The rubber anchors the threads, preventing "runs."

Fabric products can be protected from raveling by coating the threads and filling the stitching holes with silicone rubber. The rubber also waterproofs the seam and helps to prevent gas leakage.

The technique is designed to coat a flexible insulating quilt along the stitches on one surface only (see Figure 1). For other products, the technique can be varied as needed, provided that care is taken to keep the silicone rubber in the stitching holes.

Uncured silicone rubber is applied to the stitching lines with an air-pressurized sealant gun (see Figure 2). Next, a plastic release film is placed on the coated side, and the blanket is flipped over so that the release film lies underneath. This allows gravitation to pull the liquid rubber downward, away from the surface not to be coated; and the plastic film prevents the liquid rubber from leaking out of the stitching holes. The blanket may then be bagged and the adhe-

sive cured under a partial vacuum of about 3.5 psi (24 kN/m²) or under pressure.

Possible applications include balloons, parachutes, ultralight aircraft, sails, rescue harnesses, tents, or other fabric products that are highly stressed in use.

This work was done by David S. Wang of Rockwell International Corp. for Johnson Space Center. No further documentation is available.
MSC-20708

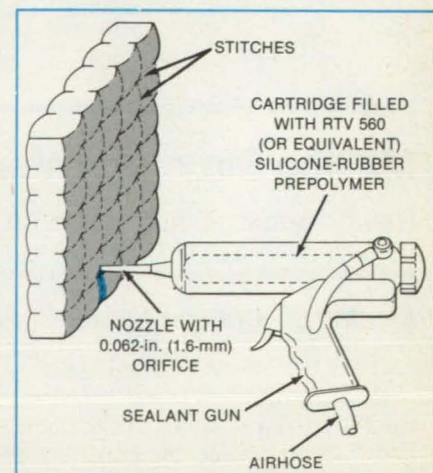


Figure 2. A **Sealant Gun** applies uncured silicone rubber to a row of stitches.

NASA Tech Briefs, Summer 1985

Centrifugal Generator of Filled Spherical Shells

Small bubbles are formed at a controlled rate.

NASA's Jet Propulsion Laboratory, Pasadena, California

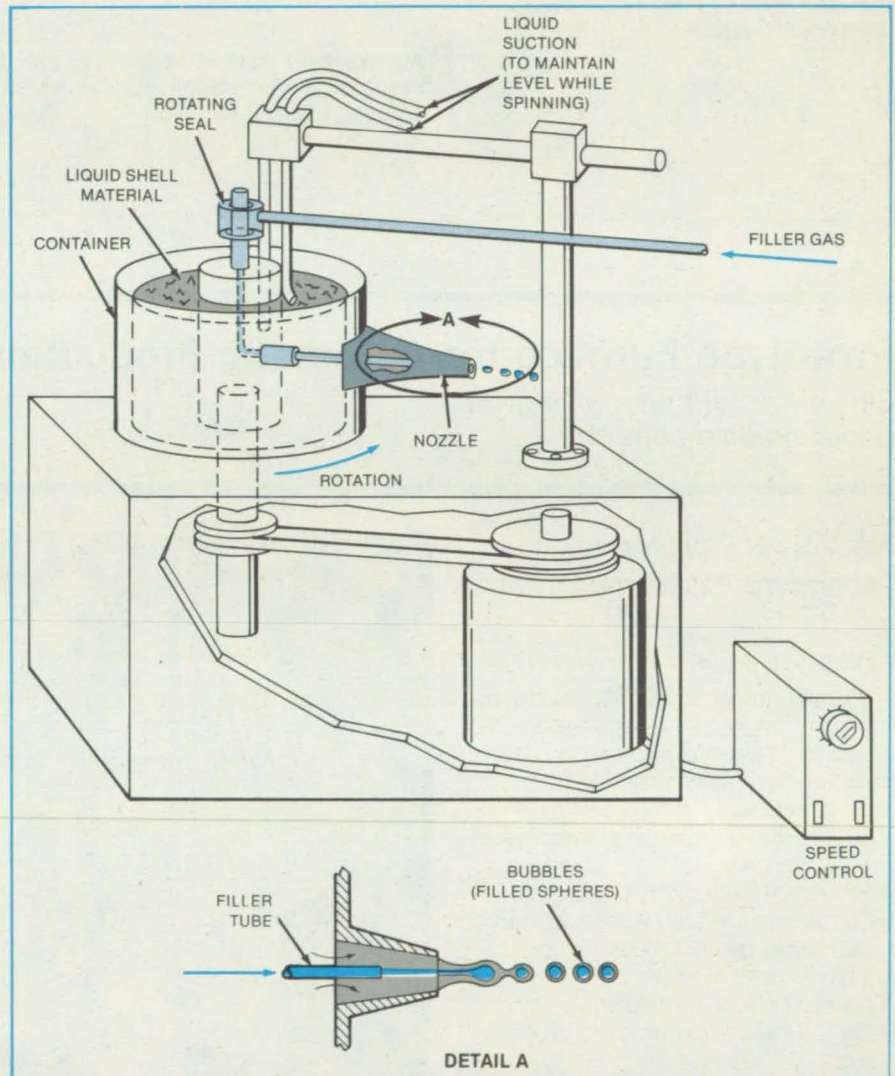
A centrifugal apparatus produces filled spherical shells of about 200- μm diameter for a wide range of industrial and scientific applications. The shells may be made from a variety of materials, including metals. The filler may be gases, liquids, or aerosols.

As shown in the figure, a rotating container has a radially extending nozzle in which centrifugal force draws liquid shell material — for example, molten metal — from the container. The liquid shell material is fed from outside the container and is automatically maintained at a fixed level. Along the axis of the nozzle is a tube that connects through a rotating seal to a source of gas or other filler material.

As the container and nozzle rotate at about 800 rpm, centrifugal force draws the encapsulant and bubbles of filler out of the nozzle in a stream of equally spaced bubbles. The encapsulant hardens into shells around the gas within. One of the advantages of the centrifugal nozzle over a stationary nozzle driven by gas and liquid pressures only is that the rate of bubble formation and the pressure inside the bubbles can be controlled somewhat by varying the rotation rate. Another advantage is that the centrifugally-induced pressure gradient along the nozzle forms small bubbles. (The physical principle of this phenomenon is not completely understood.) The material-flow and rotation rates can be adjusted to change the bubble size.

This work was done by Taylor G. Wang, Dan Granett, and Wesley M. Akutagawa of Caltech for NASA's Jet Propulsion Laboratory. For further information, Circle 30 on the TSP Request Card.

Title to this invention has been waived under the provisions of the National Aeronautics and Space Act [42 U.S.C. 2457(f)], to the California Institute of Technology.



Rotating With a Container, a nozzle fires a stream of bubbles. The nozzle diameter is about 200 micrometers. The filler-tube diameter is less than 100 micrometers.

Alining Large Cylinders for Welding

Brackets with jackscrews match adjacent sections.

Marshall Space Flight Center, Alabama

Special tooling aligns and holds internally-stiffened large-diameter cylindrical parts for welding. The tooling replaces NASA Tech Briefs, Summer 1985

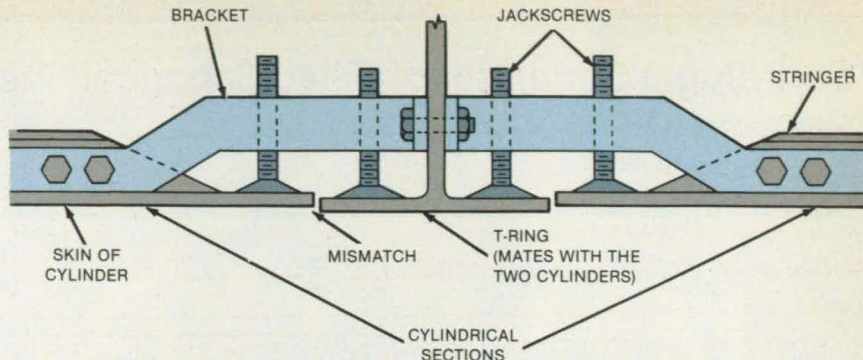
large mandrels. The mandrel tooling was expensive and cumbersome and did not mate the parts precisely.

The new tooling consists of brackets that are bolted to the internal stiffening stringers on the cylindrical sections.

Push/pull jackscrews on the brackets are adjusted to bring the sections into alignment for welding (see figure). The tooling substantially reduces costs while allowing more precise control and improved quality.

This work was done by James H. Ehl of Marshall Space Flight Center. No further documentation is available.

Inquiries concerning rights for the commercial use of this invention should be addressed to the Patent Counsel, Marshall Space Flight Center [see page 21]. Refer to MFS-28001.



Alignment Brackets are attached to strengthening fins on the insides of cylindrical tank sections. Jackscrews on the brackets are then raised or lowered to eliminate mismatches between adjacent sections.

Prototype Furnace for Automatic Production of Silicon Ribbon

Single-crystal material is grown under precise control.

NASA's Jet Propulsion Laboratory, Pasadena, California

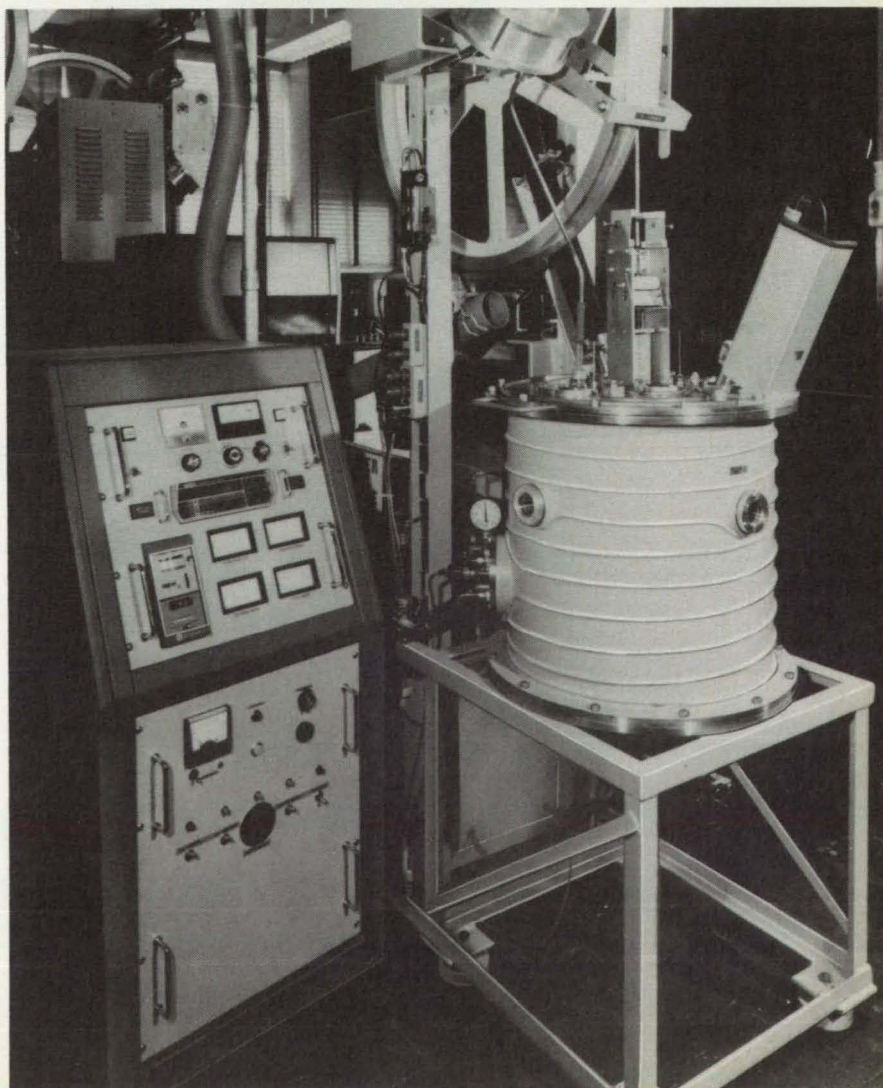
A new furnace permits sustained growth of single-crystal silicon ribbon by the dendritic-web growth process. The furnace (see figure) brings together the mechanisms necessary for continuous automatic operation. The mechanisms provide the following features:

- Programed startup of ribbon growth;
- Constant melt level during ribbon growth, maintained by continuous and precise replenishment of silicon;
- Constant melt temperature;
- Constant width and thickness of ribbon; and
- Constant ribbon-withdrawal speed.

The furnace is used for ribbon-growth experiments as well as for prototype production of ribbon.

This work was done by C. S. Duncan and W. B. Stickel of Westinghouse Electric Corp. for NASA's Jet Propulsion Laboratory. For further information, Circle 14 on the TSP Request Card. NPO-16175

A Reel Takes Up Ribbon from the furnace. Equipment for continuous automatic control is mounted on the furnace.



Fabrication of Slender Struts for Deployable Antennas

High moduli of elasticity are potentially achievable.

Langley Research Center, Hampton, Virginia

The inherent stiffness associated with tetrahedral truss structures makes them particularly well suited for application in large diameter antennas on orbiting spacecraft. Slender struts have been developed for the efficient stowage of such deployable trusses in the spacecraft cargo bay. The strut design includes an overwrap of aluminum foil, which significantly improves the thermal conductivity and has the potential to act as a vapor barrier if necessary. Many elements have been introduced into the fabrication process to reduce the labor-intensive aspects of producing these tubes. Included among these elements are the use of a vertical winding machine, a Teflon® (or equivalent) mandrel, a dry fiber placement, an aluminum foil wound off canted spools, and a prewound creeled fiber array.

Long, slender tubular struts approximately 16 ft (5 m) long and 0.5 in. (1.27 cm) in diameter have been identified by Langley Research Center as elements required for efficient stowage and deployment of large truss-supported antennas. One concept for achieving desired stiffness and thermal stability includes the use of high modulus graphite/epoxy oriented in the longitudinal direction and overwrapped with thin aluminum foil. The foil improves thermal conductivity and provides a vapor barrier. Thermal gradients, which are a result of nonuniform heating, will be reduced as the conductivity is increased. Also, the use of an aluminum surface has been shown to almost completely control the absorption or desorption of moisture, if it is a problem.

Estimated properties have been determined for four types of longitudinal graphite fiber/epoxy struts overwrapped with aluminum foil and based on a 60-percent fiber volume. The effect of a thin aluminum layer is readily evident. For example, as indicated in the figure, the addition of a 1-mil (0.025-mm) layer of aluminum on the surface of a 0.020-in. (0.51-mm) wall of a 75×10^6 psi (0.52×10^{10} N/m²) graphite/epoxy strut yields a transverse thermal conductivity of about 3 Btu/hr-ft-°F ($5 \text{ W/m}\cdot^\circ\text{C}$) compared with $0.1 \text{ Btu/hr}\cdot\text{ft}\cdot^\circ\text{F}$ ($0.17 \text{ W/m}\cdot^\circ\text{C}$) for bare graphite/epoxy. This increase is accomplished with almost no reduction in modulus of elasticity [43 versus 44×10^6 psi (0.296×10^9 versus 0.303×10^9 N/m²)]. In this case, the coefficient of thermal expansion (CTE) is negative [$-0.5/^\circ\text{F}$ ($-0.9/^\circ\text{C}$)]. A zero CTE can be obtained using a 100×10^6

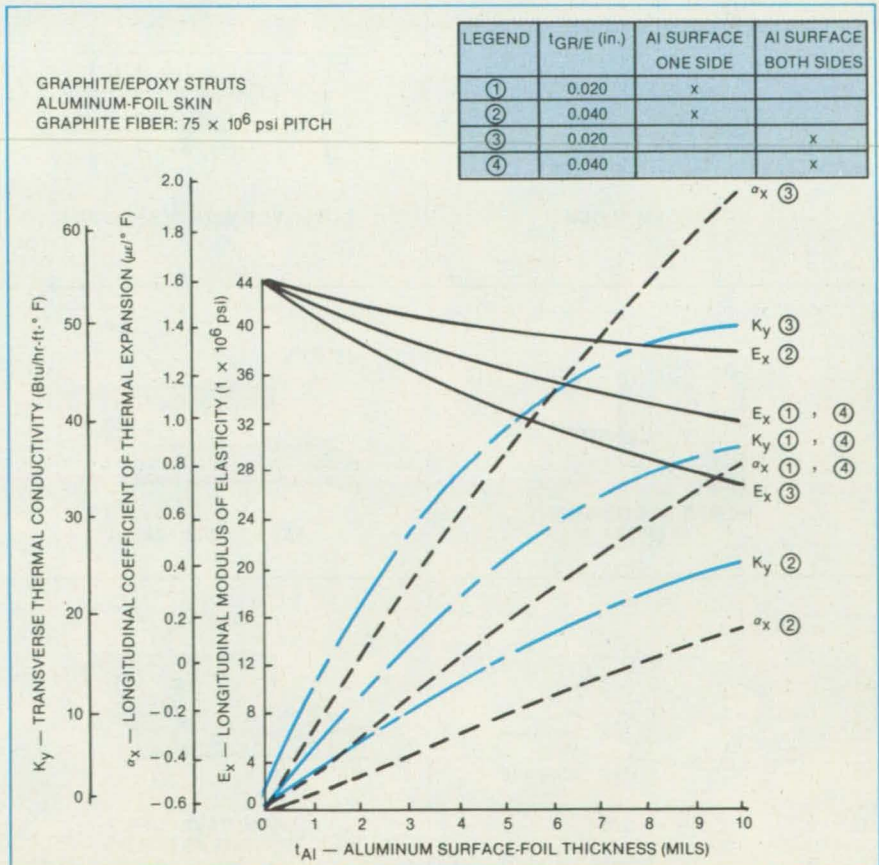
psi ($689 \times 10^9 \text{ N/m}^2$) pitch fiber and 3.5 mils (0.089 mm) of aluminum. The density of such a structure is 0.075 lb/in.^3 (2.08 gm/cm^3). For cases where a slightly negative CTE is desired to compensate for positive CTE joints and fittings, it is possible to obtain higher values of the modulus of elasticity and lighter weight structures.

The fabrication process used can accurately place dry graphite fibers and overwrap them with aluminum foil, resulting in straight, slender graphite tubes. The graphite fibers are pulled out of the creeled spools and fed through ceramic eyelets. The spools of aluminum foil are mounted on a rotating ring and capture the graphite fiber as the vertical winding machine carriage moves upward. The epoxy resin is applied by mechanically spreading the epoxy on a tetrafluoroethylene mandrel by means of a doctor blade attached to the carriage. This

fabrication process has the potential to be an economical way to manufacture tailored tubing and should approach the cost of pultruded elements.

This work was done by Harold G. Bush of Langley Research Center and Ray M. Bluck and Robert R. Johnson of Lockheed Missiles and Space Co., Inc. Further information may be found in NASA CR-172164 [N83-31733/NSP], "Fabrication of Slender Struts for Deployable Antennas" [7]. A copy may be purchased [prepayment required] from the National Technical Information Service, Springfield, Virginia 22161.

This invention is owned by NASA, and a patent application has been filed. Inquiries concerning nonexclusive or exclusive license for its commercial development should be addressed to the Patent Counsel, Langley Research Center [see page 21]. Refer to LAR-13136.



The Aluminum Overwrap Increases Thermal Conductivity with almost no reduction in the modulus of elasticity.

Duplicating Curved Tile Surfaces for Pull Testing

Vacuum chucks can be custom-made at low cost.

Lyndon B. Johnson Space Center, Houston, Texas

The strength of adhesive bonds to fragile objects with complex shapes (for example, curved-contour ceramic tiles) can be tested easily with vacuum chucks. A fast splash-molding technique, originally developed for vacuum chucks used on the silica tiles attached to the outer surface of the Space Shuttle orbiter, is used to custom-fabricate a chuck for a specific tile.

In a bond-strength test, the contact surface of the chuck is pressed against a matching surface of the bonded tile. A vacuum line extending through a fine bore in the chuck creates a vacuum at the chuck-and-tile interface. Thus, when the chuck is pulled away, atmospheric pressure tends to push the tile away with the chuck. If the adhesive resists a predetermined pull exerted by the chuck on the tile, the bond is acceptable.

It is essential, of course, that the contour of the chuck be a close replica of the mating tile contour; otherwise, the vacuum will not

hold. Original plans were for the chuck to be shaped by a milling machine from the same computer-numerical-control tapes used to generate the tile surface. Splash molding, however, made this expensive and time-consuming procedure unnecessary.

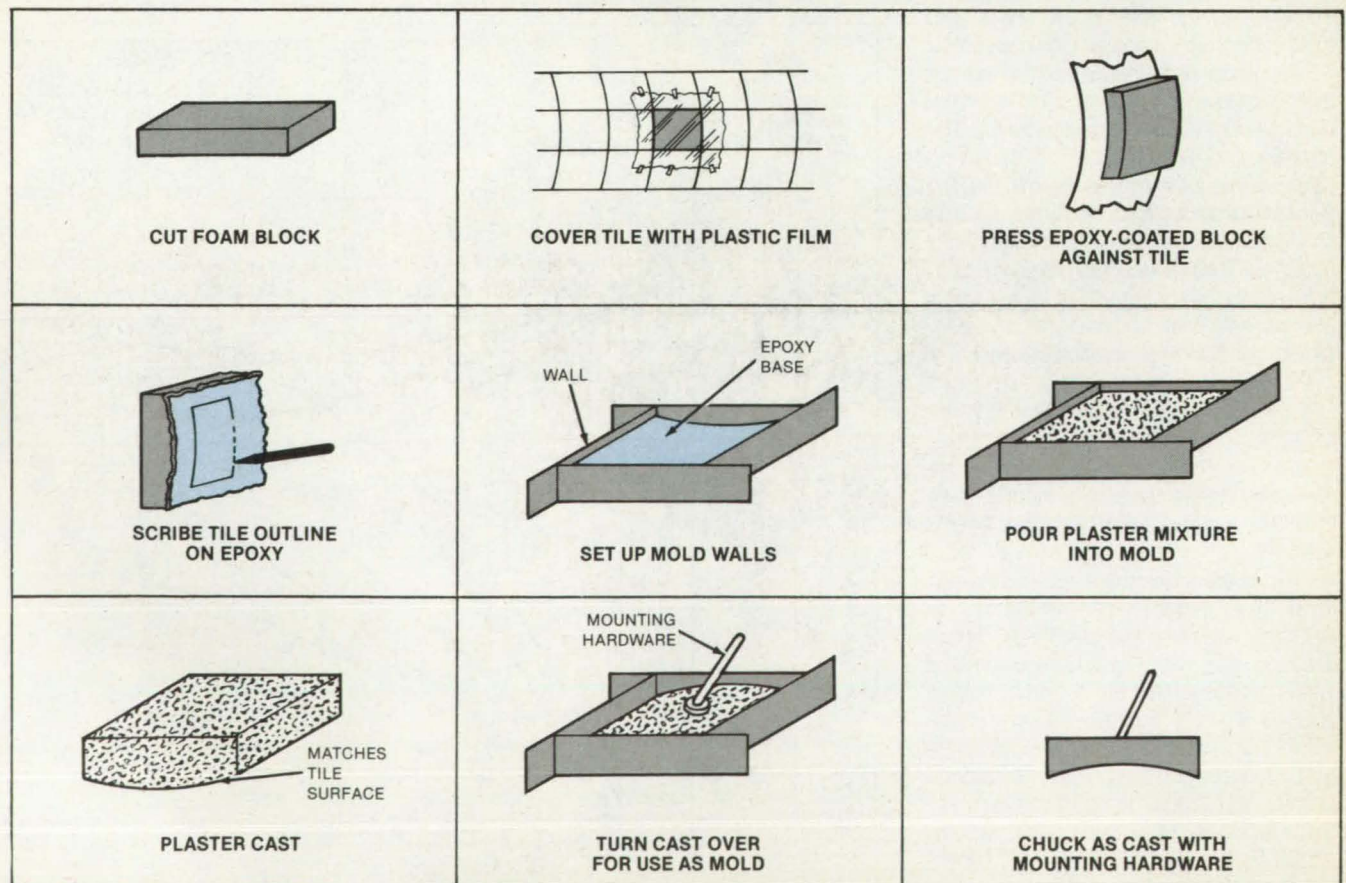
"Splashing" consists of pressing a quickly setting layer of epoxy resin against the tile with a block of flexible polyurethane foam. The epoxy layer hardens, retaining the contour of the tile. The "splashing" and subsequent steps of the technique are illustrated in the figure.

To prevent the epoxy from adhering to the tile, the tile to be splashed is first covered with a plastic film such as that used to wrap food. The film is smoothed to remove creases and air bubbles and is fastened at the edges with tape. The epoxy components are mixed and poured evenly on a foam block large enough to cover the tile. The epoxy-coated block is immediately pressed

by hand against the film-covered tile. The block is removed, and, with the aid of a straightedge, the outline of the tile in the epoxy impression is scribed. The outlined perimeter of the epoxy block is cut with a bandsaw and its edges are sanded smooth.

Four walls are clamped to the plate, forming a mold. A release agent is applied to the mold, and a plaster mixture is poured into it. After hardening for 30 minutes, the plaster cast is removed. The surface of this cast duplicates that of the tile. The plaster cast is turned over and the mold walls placed around it again. The vacuum chuck and its integral mounting hardware are then cast on the plaster duplicate.

This work was done by Richard H. Sebenick of Rockwell International Corp. for Johnson Space Center. No further documentation is available.
MSC-20795



A **Step-by-Step Procedure** for splash molding results in a pull-test chuck contoured for a specific tile. Although the chucks are custom-made, the fabrication process is less expensive than machining.

Adjustable Lid Aids Silicon-Ribbon Growth

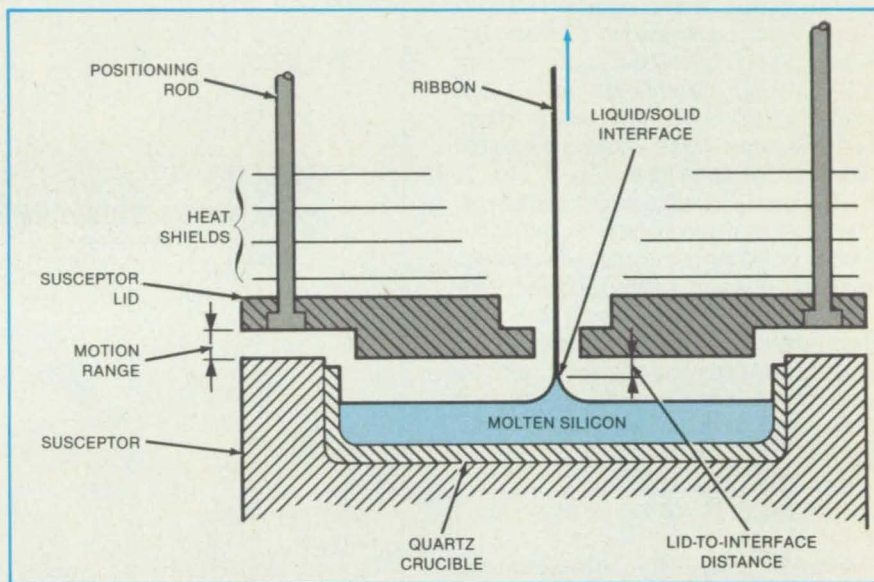
Closely-spaced crucible cover speeds up solidification.

NASA's Jet Propulsion Laboratory, Pasadena, California

The growth rate of dendritic-web silicon ribbon from molten silicon is increased by controlling the distance between the crucible susceptor lid and the liquid/solid interface. The lid is held in a relatively high position when the crucible is newly filled with chunks of polycrystalline silicon. As the silicon melts and forms a pool of liquid at a lower level, the lid is gradually lowered (see figure).

The shorter lid-to-interface distance apparently allows heat to flow from the interface through the solid ribbon, or dendritic web, more rapidly. As a result, the liquid solidifies more quickly, and the solid ribbon can be withdrawn at a faster rate. Whereas with a fixed lid ribbon could be formed at a rate of 1.9 centimeters per minute, the rate for the same crucible with a movable lid was 2.7 centimeters per minute — a 42 percent increase in the production rate. The residual stress in the ribbon was at the same low level in both cases.

The lid and its heat shields are mounted on rods that are raised or lowered as necessary. A total lid travel of only 3.2 millimeters is enough to bring about the large increase in the growth rate.



The **Crucible Lid** is brought close to the solid/liquid interface as clearance develops during the melting of the silicon. Externally controlled positioning rods lower the lid and the heat shields mounted on it.

This work was done by J. P. McHugh, R. G. Seidensticker, and C. S. Duncan of Westinghouse Electric Corp. for NASA's

Jet Propulsion Laboratory. For further information, Circle 58 on the TSP Request Card.
NPO-16354

Making Glass-Fiber-Reinforced Coolant Tubes

A new use is found for heat-shrinkable sleeves.

Lyndon B. Johnson Space Center, Houston, Texas

Smooth, noncontaminating channels for transporting cooling water in the Space Shuttle extravehicular-mobility unit are made of fiberglass tubing with the aid of heat-shrinkable sleeves. Previously, glass fibers from the inner walls of the tubes would contaminate the water.

The new technique forms a hard, glossy, clean, inner surface. Standard polyvinyl chloride (PVC) shrinkable sleeving, ordinarily used for electrical wiring, is first preshrunk on a metal rod to the requisite final channel diameter. The sleeve is then filled with sand

and bent to the design shape of the channel. If the sleeve becomes crimped at sharp bends, it is heated locally to relax the PVC and smooth out the folds.

The fiberglass tube is placed over the PVC sleeve, and the assembly is placed in a mold. Resin is injected into the mold at one end and is then cured.

The tube is removed from the mold, and the sand is poured from the PVC sleeve. The assembly is heated so that the PVC sleeve shrinks further and pulls away from the newly-formed inner wall. The sleeve is

drawn from the tube, and the channel is ready for use.

This work was done by Frank Curtin of United Technologies Corp. for Johnson Space Center. No further documentation is available.

Inquiries concerning rights for the commercial use of this invention should be addressed to the Patent Counsel, Johnson Space Center [see page 21]. Refer to MSC-20677.

Controlling Sample Rotation in Acoustic Levitation

Sample rotation would be stopped or controlled by controlling the phase shift.

NASA's Jet Propulsion Laboratory, Pasadena, California

The rotation of an acoustically levitated object would be stopped or controlled according to a phase-shift monitoring and control concept. The principle applies to a square-cross-section levitation chamber with two perpendicular acoustic drivers operating at the same frequency.

The apparatus is shown schematically in the figure. A microphone is placed at the corner facing the two acoustic-driver ports. The sound waves arriving at the microphone from the X and Y drivers have pressure amplitude P_x and P_y and phases Φ_x and Φ_y , respectively. Assuming plane standing waves in the X and Y modes, the net pressure amplitude at the microphone is given by

$$P = \sqrt{(P_x + P_y \cos \Phi)^2 + (P_y \sin \Phi)^2}$$

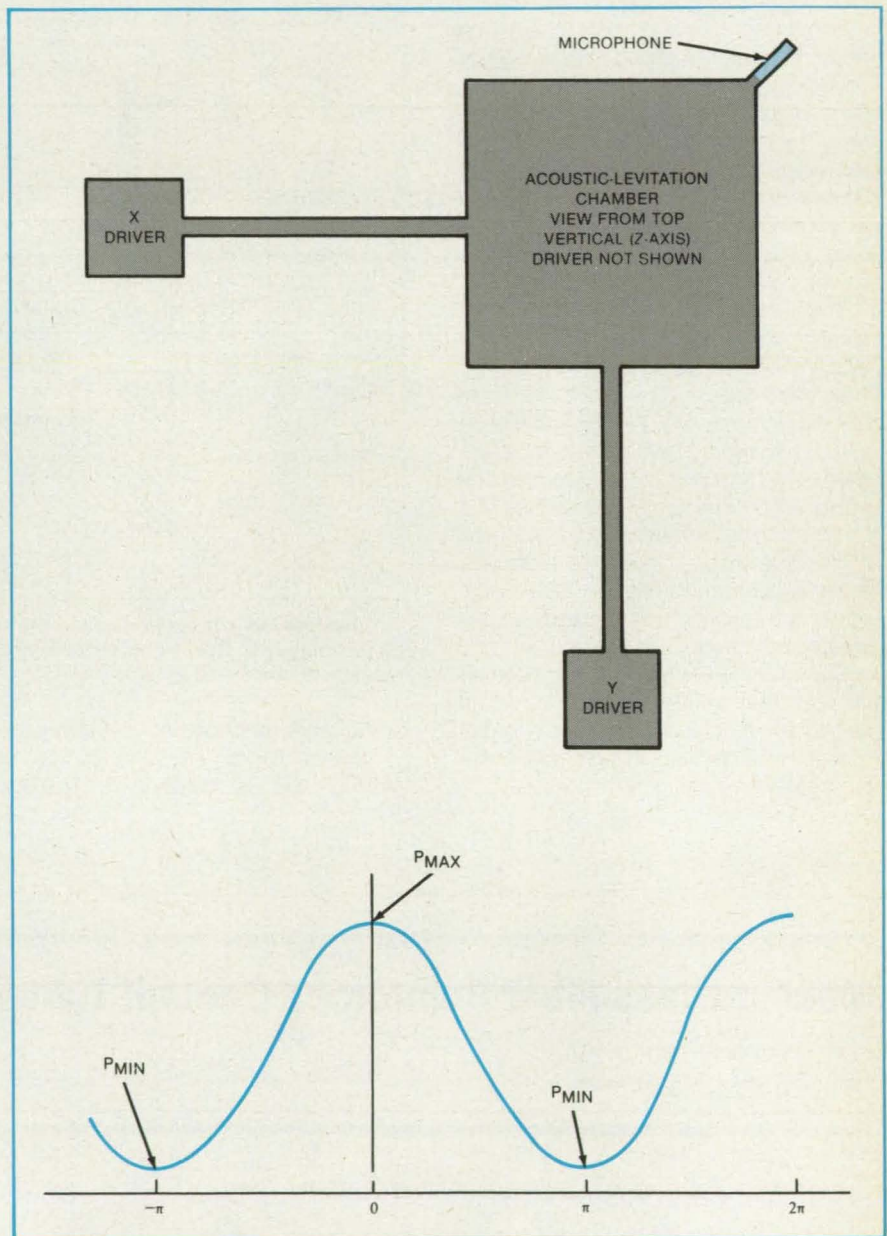
where $\Phi = \pm(\Phi_x - \Phi_y)$. The maximum and minimum pressure amplitudes occur at $\Phi = 0$ and $\pm\pi$, respectively, at which points the viscous acoustic torque is zero, resulting in zero sample rotation.

In a controlled-rotation levitation system, Φ_x would be adjustable so that the phase difference Φ can be manually or automatically controlled. In making a manual adjustment, the operator could be guided by observing the sample rotation (if possible) or by measuring the variation of acoustic amplitude with changes in the phase setting.

In one automatic-control version, the amplitude measurement would be taken while Φ_x is varied to obtain a portion of the P-versus- Φ curve: This would enable extrapolation to the points $\Phi = 0$ or $\pm\pi$ for no rotation or to an intermediate phase difference for controlled rotation.

In another version, repeated amplitude measurements would be taken as Φ_x is dithered about the point of maximum or minimum P. The servosystem would adjust the central value of Φ_x to correct any deviation from the extremum of amplitude, thereby restoring the average phase difference to the value for zero rotation.

This work was done by Martin B. Barmatz and James D. Stoneburner of Caltech for NASA's Jet Propulsion Laboratory. For further information, Circle 69 on the TSP Request Card.
NPO-15962



The Phase Difference Between the X and Y Acoustic Excitation is measured at one corner by measuring the variation of acoustic amplitude sensed by the microphone. The phase of the X driver is adjusted to the value that produces no rotation or controlled rotation of the levitated object.

Books and Reports

These reports, studies, and handbooks are available from NASA as Technical Support Packages (TSP's) when a Request Card number is cited; otherwise they are available from the National Technical Information Service.

Damage and Repair of Composite Structures

Graphite/polyimide and graphite/epoxy panels are tested

A NASA technical memorandum reports on research in the damage and repair of composite-material structures of the types used in airplanes. The research includes:

- Identifying defect areas,
- Determining whether a particular kind of damage weakens a structure in a manner that degrades performance in the intended application,
- Developing repair procedures, and
- Testing to demonstrate that a given repair procedure enables a component to serve during the remainder of its design life.

The investigations involve samples of graphite/epoxy and graphite/polyimide laminates as formed into flat, hat-stiffened, and honeycomb-sandwich panels. Laminates of 6, 8, 12, and 16 plies are being used to determine the effect on compressive strength of interlayer delaminations, surface cracks, delamination between graphite/polyimide and metal inserts, and impact damage.

Test results thus far show that the compressive strength is severely reduced by delamination when the delamination width is an appreciable fraction of the width of the specimen. The results also indicate that impact damage causes a significant reduction in strength, even though the damage may not be visible. Fracture toughness and methods for improving tolerance to damage continue under investigation. The fatigue of notched laminates and the growth of delaminations are also under study.

Various repair procedures are being considered. For graphite/epoxy, these include precured bonded patches, cure-in-place patches, and combinations of the two in both flush and externally protruding configurations. The most effective technique thus far seems to be flush, cure-in-place.

The bonding of graphite/polyimide is not as well established as that of graphite/epoxy. Bonding techniques under investigation include cure-in-place, cure-in-place with adhesive, secondary bonding with one ply of preimpregnated composite, secondary bonding with adhesive, and secondary bonding with adhesive on one ply of glass cloth. Bonded samples are tested in short-beam shear and flexure. Based on preliminary analysis of test results, cure-in-place and secondary bonding with one ply of prepreg are the most promising repair techniques.

The technology of repairs of graphite/epoxy structures is being adapted to the development of repair techniques for graphite/polyimide structures intended for use at higher temperatures. Future work will address work completed and reported in NASA-CR-159056, dated January 1983, the long-term durability of repairs on graphite/epoxy in a 10-year outdoor-exposure program.

This work was done by Jerry W. Deaton of Langley Research Center. Further information may be found in NASA TM-84505 [N82-31447/NAP], "A Repair Technology Program at NASA on Composite Materials" [\$7]. A copy may be purchased [prepayment required] from the National Technical Information Service, Springfield, Virginia 22161. LAR-13146

PSI PRESSURE SCANNERS MAKE TURBINE TESTING A BREEZE.

For fast, accurate and reliable pressure measurement, you can't beat the 780B, today's state of the art in pressure scanning systems.



The 780B gives you faster data acquisition rates. Improved accuracy, with repeatable results. And computer compatibility that offers a friendly interface to nearly any system.

Call or write today for more information on the 780B from PSI... the leaders in digital pressure measurement technology.

- 20,000 measurements per second
± 0.10% F.S. worst case inaccuracy
- ± 1.0 psid to 500 psid ranges
- Automatic on-line calibration
- IEEE-488 compatibility



PRESSURE SYSTEMS

15 Research Drive, Hampton, VA 23666
(804) 865-1243

Circle Reader Action No. 378

SPACE THE NEW FRONTIER

The Equity Research Department of
Shearson Lehman/American Express Inc.

and

The Center for Space Policy, Inc.

advisors to the U.S. Government and Industry
are pleased to announce

SPACE

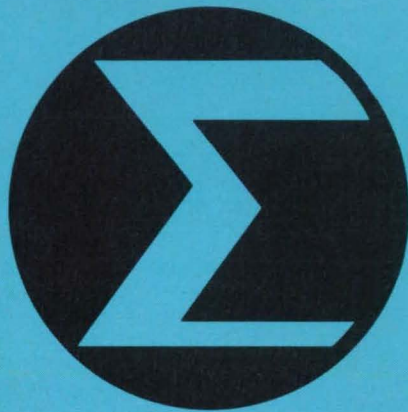
the first monthly analysis of commercial
investment opportunities in space.

The financial expertise of SHEARSON LEHMAN/AMERICAN EXPRESS and the special knowledge of THE CENTER FOR SPACE POLICY have teamed to offer a totally new investment service, to help investors evaluate these and other opportunities in this New Frontier.

For information contact: James P. Samuels, Shearson Lehman/American Express, 2 World Trade Center, New York, NY 10048, (212) 321-5722 or Brad M. Meslin/David Lippy, CENTER FOR SPACE POLICY, INC. 1972 Massachusetts Avenue, Cambridge, MA 02140, (617) 576-2266/2828

Circle Reader Action No. 384

Mathematics and Information Sciences



Hardware, Techniques, and Processes

- 162 Free-Vibration Analysis of Structures
- 162 Prediction of Combustion Gas Deposit Compositions

Computer Programs

- 163 Design Language for Digital Systems
- 164 Manipulation and Display of Panel-Method Geometry
- 164 Analysis of Satellite Communications Antenna Patterns
- 164 An Interactive Plotting Routine
- 164 Processing Digital Imagery Data
- 165 Personal-Computer Video-Terminal Emulator

Books and Reports

- 165 Standard Codes for Telemetry and Telecommand

Free-Vibration Analysis of Structures

An improved numerical procedure is more than twice as fast as previous methods.

NASA's Jet Propulsion Laboratory, Pasadena, California

A unified numerical algorithm efficiently solves free-vibration problems of stationary or spinning structures with or without viscous or structural damping. The algorithm can be used to solve static problems involving multiple loads and to solve the quadratic matrix eigenvalue problems associated with a finite-dynamic-element structural discretization.

Dynamic-response analysis is often important in designing structures as diverse as buildings, rotating machinery, and vehicles. An essential step in such an analysis is the determination of the natural vibration frequencies (eigenvalues) and the associated normal modes (eigenvectors). Both are determined by a standard technique, such as the finite-element method, to discretize the representation of the continuous structure being modeled.

The analysis produces a set of simultaneous algebraic equations that are put in matrix form. The resulting eigenvalue problem yields the vibration frequencies and modes. A general formulation that includes the various eigenvalue problems as special cases is

$$M\ddot{q} + C\dot{q} + Kq = 0$$

where M , C , and K represent the inertia, damping, and stiffness matrices, respectively. For most complicated practical structures, the discretization process results in a rather large number of simultaneous equations, the matrix forms of which are usually highly banded. A special

symmetric-matrix decomposition scheme has been adopted for matrix triangularization, which improves the efficiency and economy of execution. The algorithm also uses a bisection scheme that further accelerates the solution convergence rate, particularly for the case of repeated roots. The individual eigenproblems covered by the algorithm are the following:

- Undamped free vibration and buckling,
- Undamped free vibration of spinning structures,
- Quadratic matrix equations,
- Damped free vibration of spinning structures with or without structural damping,
- Damped free vibration of nonspinning structures with or without structural damping, and
- Simultaneous equations.

The algorithm has been implemented in a computer program called EIGSOL, which is over two times faster than earlier programs based on less-efficient related algorithms. The program fully exploits matrix sparsity, such as bandedness, and may be used to calculate eigenvalues lying within a specified range and the corresponding eigenvectors without having to compute the others. The program listing contains comment statements that show how the program should be configured for each of the cases listed. The program operates in the real or in the complex domain.

This work was done by Kajal K. Gupta of Caltech for NASA's Jet Propulsion Laboratory. For further information, Circle 94 on the TSP Request Card. NPO-15000

Prediction of Combustion Gas Deposit Compositions

Predictions are made for metal and mineral-seeded combustion processes.

Lewis Research Center, Cleveland, Ohio

Fossil-derived fuels are expected to remain a major terrestrial energy source for the remainder of the century. Regardless

of whether these fuels are burned directly or converted to higher quality liquids or gases, the metal or mineral contents can

lead to the formation of deposits during the conversion or combustion process. It is desirable to predict the compositions, amounts, and locations of such deposits in order to assess the magnitude of potential problems such as fouling, corrosion, or particulate emissions associated with the use of these "dirty" fuels.

Deposit compositions are calculated on the basis of the premise that the condensed phases predicted by an equilibrium thermodynamic analysis are the ones likely to appear as deposits. The NASA Lewis Research Center Computer Program for Calculation of Complex Chemical Equilibrium Compositions (CEC) is used in conjunction with the Computer Program for Calculation of Ideal Gas Thermodynamic Data (PAC)

and the resulting Thermodynamic Data Base (THDATA) to predict deposit compositions from metal or mineral-seeded combustion processes. In order to predict deposition rates and locations, the basic thermodynamic analyses must be expanded to include chemical kinetics, heat and mass transfer considerations, and liquid deposit layer flow dynamics.

Although there are some shortcomings with the use of these methods and additional work is desirable, the results are encouraging. It has been demonstrated that the procedure can be used to predict accurately the chemical compositions of complicated deposit mixtures.

This work was done by F. J. Kohl, B. J. McBride, F. J. Zeleznik, and S. Gordon of Lewis Research Center. Further infor-

mation may be found in:

NASA TM-81634 [N81-15069/NSP], "Deposition and Material Response From Mach 0.3 Burner Rig Combustion of SRC-11 Fuels" [\$8.50],

NASA TM-81686 [N81-27258/NSP], "Material Response From Mach 0.3 Burner Rig Combustion of a Coal-Oil Mixture" [\$7], and

NASA TN-D-4097 [N67-3512/NSP], "Fortran IV Program Calculation of the Thermodynamic Data" [\$14.50].

Copies of these reports may be purchased [prepayment required] from the National Technical Information Service, Springfield, Virginia 22161.

LEW-14091

Computer Programs

These programs may be obtained at a very reasonable cost from COSMIC, a facility sponsored by NASA to make raw programs available to the public. For information on program price, size, and availability, circle the reference number on the TSP and COSMIC Request Card in this issue.

Design Language for Digital Systems

It can describe digital systems at the gate, register transfer, and combinational block levels.

Just as software designers use high-level languages to express algorithms in terms of concise language statements, digital hardware designers use hardware description languages to describe the systems they are designing. Hardware description languages are valuable in such applications as hardware design, system documentation, and logic design training.

The Digital Systems Design Language (DDL) is a convenient hardware description language for developing and testing digital designs and for inputting design details into a design automation system. A set of computer programs has been developed that provides the designer with an automatic synthesis system based on DDL. The set includes a DDL translator program, a simulation program, two synthesis programs, and a logic minimization program. These DDL-based programs are being used by NASA

as part of an integrated circuit design and fabrication system for Large Scale Integration (LSI) and Very Large Scale Integration (VLSI) technologies.

DDL is highly suitable for describing digital systems at the gate, register transfer, and major combinational block levels. DDL is a block-structured register-transfer language where the blocks usually correspond to the natural divisions of the hardware being described and allow a nested view of the hardware. For example, a computer may have a major block called an "ALU," which contains a block called "ADDER," which in turn consists of interconnected logic blocks called "FULL-ADDERS." Each block becomes an automation, where the statements describe the state transitions of a finite state machine controlling the processes of the intended algorithm. The DDL language can be used to describe parallel operations as well as both synchronous and asynchronous behaviors.

The DDL translator program (DDLTRN) compiles the DDL description into a facility table, a set of Boolean equations (BE's) (corresponding to the combinational logic portion), and a set of Register Transfer equations (RTE's) (corresponding to the sequential logic portion). The BE's and RTE's are arranged to eliminate duplicate expressions and Boolean constants. The DDL Simulation Program (DDLSIM) is a register-transfer level simulator. It uses the output of the system description and simulates the system according to commands provided by the designer. A simulation performance list is provided as the output. DDLSIM enables the designer to thoroughly test and verify the design of the digital system.

DDLSYN is a hardware synthesizer. Input to DDLSYN consists of the BE's and RTE's output by DDLTRN and a user-

supplied standard cell library. For a modular synthesis, each module can be translated separately and synthesized individually by DDLSYN.

A DDLSYN synthesis generates a list of the standard cells, a cell interconnection list, a cross-reference list, and, for modular synthesis, a module interconnection list. PLASYN is a Programmed Logic Array (PLA) synthesizer that uses the output from DDLTRN to produce a PLA program that implements the combinational logic portion of the system in the DDL description. The PLA program generated is simply a coded representation of the connections on the AND and OR gates of a PLA.

The Multiple-Output Minimization Program, MOMIN, is included in the DDL system for optional use by the designer. The BE's and RTE's as generated by DDLTRN are not completely minimized. Although minimization may not be required during the initial phase of the design cycle, it is usually desirable to apply formal minimization techniques before the design is finalized.

These DDL-based programs are written in FORTRAN IV for batch execution and have been implemented on an SEL-32 computer. The largest program has a central memory requirement of approximately 35k of 32-bit words. These digital systems design aids were developed in 1983.

This program was written by Sajjan G. Shiva of the University of Alabama for Marshall Space Flight Center. For further information, Circle 75 on the TSP Request Card.

Inquiries concerning rights for the commercial use of this invention should be addressed to the Patent Counsel, Marshall Space Flight Center [see page 21]. Refer to MFS-25352.



Manipulation and Display of Panel-Method Geometry

An interactive graphics program can be used with any geometry type that is expressible in the Hess format.

An interactive graphics program, GEOM, manipulates and displays panel-method geometry. Modern aerodynamic panel-method computer programs such as PANAIR often require large and complex geometries. [PANAIR is described in the article "Higher-Order Panel Method for Aerodynamic Flow Analysis" (ARC-11398), page 428, *NASA Tech Briefs*, Vol. 6, No. 4 (Spring/Summer 1982).] These geometries are characterized by an abutting set of networks, where each network is composed of quadrilateral panels described by the coordinates of their corners. However, use of GEOM is not limited to data intended for aerodynamics programs.

GEOM can manipulate and display any geometry data that can be expressed in the Hess format. It provides the user with the capability to manipulate, modify, and view such geometric configurations interactively. GEOM can be used to:

1. Build configurations,
2. Scale and rotate networks,
3. Transpose networks,
4. Graphically display selected networks,
5. Join and split networks,
6. Create wake networks,
7. Produce symmetric images of networks,
8. Repanel and rename networks,
9. Display configuration cross sections, and
10. Output network geometry in Hess and PANAIR formats.

A specialized data-base management system (PAGMS — PANAIR Geometry Management System) facilitates data transfers in the GEOM program.

The GEOM program and the PAGMS data-base management system are written in FORTRAN IV and Assembler for interactive execution. They have been implemented on a CDC CYBER 170 series computer operating under NOS with a central memory requirement of approximately 108k (octal) of 60-bit words. GEOM requires the Tektronix PLOT 10 graphics software for visual displays. The GEOM program was developed in 1983.

This program was written by Jon F. Hall, Dan H. Neuhart, and Kenneth B. Walkley of Kentron International, Inc., for Langley Research Center. For further information, Circle 61 on the TSP Request Card. LAR-13224

Analysis of Satellite Communications Antenna Patterns

The effects of varying geometrical and electrical parameters can be studied.

This computer program accurately and efficiently predicts the far-field patterns of offset, or symmetric, parabolic reflector antennas. These reflectors are used extensively in modern communications satellites and in multiple-beam and low side-lobe antenna systems. The antenna designer can use this program to study the effects of varying geometrical and electrical (RF) parameters of a parabolic reflector and its feed system. Accurate predictions of the far-field patterns can help the designer predict the overall performance of the antenna.

The method of analysis is based on the applications of the physical optics integral, which is evaluated using the Jacobi-Bessel expansion technique. The physical optics vector radiation integral is constructed for an offset reflector illuminated by an arbitrarily located and oriented source. This is accomplished by using the Eulerian angle transformation. A novel procedure is used to express the radiation integral in terms of a summation (series) of Fourier transforms of an "effective" current distribution that includes the effect of the curvature of the surface. This series is biconvergent in nature and can be related to the asymptotic evaluation of the integral. The Fourier transform integrals are expressed in terms of the Jacobi-Bessel series expansion for the numerical analysis. An important feature of this expansion is that the expansion coefficients are independent of the observation points, and they can be used as a pattern signature to construct the pattern at any observation angle.

The program allows the designer to study different reflector configurations for different polarizations, feed positions, beam locations, and reflector parameters. The results of this computer program have been thoroughly tested and compared to measured data with excellent agreement for both copolar and cross-polar patterns.

This program is written in FORTRAN 77 and has been implemented on a UNIVAC 1100-series computer with a central-memory requirement of approximately 47k of 36-bit words. The program includes plotting options that use a supplied relocatable plot library to generate SC 4020 plotter output. This program was completed in 1983.

This work was done by Yaha Rahmat-Samii of Caltech for NASA's Jet Propulsion Laboratory. For further information, Circle 84 on the TSP Request Card. NPO-16400

An Interactive Plotting Routine

Program offers the interactive applications programmer a plug-in routine for graphic displays.

A routine called CRTRPM meets the needs of the applications programmer to plot data in an interactive environment on a Tektronix graphics terminal. CRTRPM is designed specifically for applications where data must be viewed and responded to at the terminal. CRTRPM can produce from one to four grids on the terminal screen at one time, with from one to ten plots of X-Y data on each grid. Inputs to CRTRPM are arrays of X-Y data, scaling parameters, legend information, and other data pertinent to the construction and appearance of the graphs.

CRTRPM is written in FORTRAN V for interactive execution and has been implemented on a CDC CYBER 70 series computer with a memory requirement of approximately 42k (octal) of 60-bit words. The system is designed to be used with the PLOT-10 TCS graphics package and Tektronix 4114, 4014, and 4016 terminals. CRTRPM should be transportable to any system with a FORTRAN 77 compiler, the TCS graphics package, and Tektronix 4000 series terminals. The CRTRPM routine was developed in 1983.

This program was written by Dana W. Bowdish of Rockwell International Corp. for Johnson Space Center. For further information, Circle 99 on the TSP Request Card. MSC-20771

Processing Digital Imagery Data

Program processes remotely sensed, multispectral scanner data.

The Earth Resources Laboratory Applications Software (ELAS) is a geobased information system designed for analyzing and processing digital imagery data. ELAS was developed mainly to process remotely sensed scanner data, especially the multispectral data acquired by the various NASA Landsat satellites. In addition to Landsat multispectral data, ELAS supports the processing of such other data as aircraft-acquired scanner data, the Return Beam Vidicon (RBV) data from Landsat satellites, digitized topographic data, and numerous other ancillary data, such as soil types and rainfall information, that can be stored in digitized form. As an integrated image-processing and data-base

maintenance system, ELAS offers the user of remotely sensed data a wide range of easy to use capabilities in the areas of land cover analysis.

The ELAS system is structured in terms of an operating subsystem and a collection of application modules. The operating system handles all of the required input/output functions, system control functions, and the swapping in and out of applications modules as they are needed. The versatile operating subsystem and the available application modules allow the user to perform a wide range of land cover analyses as well as data-base construction and manipulation. The available ELAS capabilities include: Derivation of training statistics; classification of data using a maximum likelihood scheme; registration of an image to an image and an image to a map; numerous image data display capabilities; manipulations with polygons that define areas within the data; implementation on a point-by-point basis of algorithms coded in an interpreter BASIC programming language instruction set; and the regression, correlation, and other statistical analyses of the multivariate data sets. The ELAS system is also structured so that new applications modules can be easily integrated into the sys-

tem without affecting previously entered modules.

The ELAS system is written in FORTRAN and Assembler for batch or interactive processing and has been implemented on the following computers: Perkin-Elmer 8/32 operating under OS32, Sperry Univac V70 operating under VORTEX II, PRIME 750 operating under PRIMOS, SEL 32/27 operating under MPX 32, and DEC VAX 11/780 operating under VMX 3.1. The ELAS system was developed in 1980 and last updated in 1983.

This program was written by P. K. Conner, B. G. Junkin, M. H. Graham, M. T. Kalcic, and B. R. Seyfarth for Marshall Space Flight Center. For further information, Circle 66 on the TSP Request Card. MFS-25987

Personal-Computer Video-Terminal Emulator

Video terminal with some "intelligent" capabilities is emulated.

An OWL-1200 video terminal emulator has been written for the IBM Personal Computer. The OWL-1200 is a simple user terminal with some intelligent capabilities. These capabilities include screen formatting and block transmission of data. Several programs, such as Systonetics, VISION software for hierarchical scheduling, use this type of terminal. The emulator software provides the IBM Personal Computer with most of the capabilities of the OWL-1200 terminal. Even those features that are implemented in hardware on the OWL-1200 are fully provided by the emulator software.

This emulator is written in PASCAL and Assembler for the IBM Personal Computer operating under DOS 1.1. Minimum machine requirements include one disk drive, a serial communication board, a color graphics adapter, and 128 kbytes of memory. This emulator was developed in 1983.

This program was written by Robert H. Buckley of Kennedy Space Center and Anthony Koromilas, Richard M. Smith, Gary E. Lee, and Edward W. Giering of Boeing Services International. For further information, Circle 105 on the TSP Request Card. KSC-11293

Books and Reports

These reports, studies, and handbooks are available from NASA as Technical Support Packages (TSP's) when a Request Card number is cited; otherwise they are available from the National Technical Information Service.

Standard Codes for Telemetry and Telecommand

Different systems could communicate and development costs would be reduced.

A report discusses efforts to standardize the telemetry and telecommand codes of various space programs. Used to detect and correct bit errors in communication channels with low signal-to-noise ratios, these codes have proliferated in recent years. Each coding/decoding system was

developed to solve a specific problem, but some systems are similar and exhibit similar performance.

Standardization was proposed to reduce the duplication of cost and effort entailed by the custom development of a new coding/decoding scheme for each situation and to enable communication between systems. Though a standard code will not be optimum in every case, it should perform satisfactorily enough to justify the lower cost in most cases.

The guideline for telemetry recommends a convolutional code with a constraint length of 7 and a code rate of $\frac{1}{2}$ bit per symbol. For the greatest error-correcting ability, a more powerful recommended code is obtained by the concatenation of this convolutional code (the "inner" code) with a Reed-Solomon (R-S) code (the "outer" code) of symbol length 8 and code word length of 255 symbols.

The data at the spacecraft or other transmitter are first processed by the R-S encoder, then by the convolutional encoder. At the receiving station, the data stream is deconvolved, then put through an R-S decoder.

The requirement of a low error rate is more demanding in telecommand than in telemetry. The guideline for telecommand requires commands to be divided into command-link transmission units (CLTU's), each of which carries a load of command bits, typically several hundred to several thousand bits long. Each CLTU contains a variable-length preamble needed for bit synchronization, followed by an 8-bit Barker code, followed next by a set of telecommand frames of 48, 56, or 64 bits. The Barker code sets off the preamble from the telecommand frames and establishes the sense of zero and one. Each frame contains a Bose-Chaudhuri-Hocquenghem code, which includes a 7-bit parity byte followed by a zero: This enables each frame to be checked individually for errors.

This work was done by Mervyn L. MacMedan of Caltech for NASA's Jet Propulsion Laboratory. To obtain a copy of the report, "Standard Methods for Telemetry and Telecommand Channel Coding," Circle 37 on the TSP Request Card. NPO-16305

Subject Index



A

ABSORPTION SPECTROSCOPY
Monitoring trace gases in the atmosphere page 69 NPO-16278

ACOUSTIC LEVITATION
Blowing polymer bubbles in an acoustic levitator page 100 NPO-16212
Controlling sample rotation in acoustic levitation page 160 NPO-15962

ACOUSTIC MEASUREMENT
Frequency-discriminating acoustic-event counter page 58 MSC-20467

ADHESION TESTS
Duplicating curved title surfaces for pull testing page 158 MSC-20795

AERODYNAMIC STABILITY
Aerodynamic rear cone for trucks page 109 MFS-28007

AEROSOLS
Airborne DIAL system for remote tropospheric sensing page 71 LAR-13002

AIR SAMPLING
Accurate airborne particle sampler page 110 LAR-13080

AIRCRAFT ENGINES
Miniature rocket motor for aircraft stall/spin recovery page 144 LAR-13199

AIRCRAFT MAINTENANCE
Damage and repair of composite structures page 161 LAR-13146

ALIGNMENT
Adapter helps to align plasma torch page 143 MFS-28024

ALLOWANCES
Effects of bearing clearance on turbopump stability page 148 MFS-27063

ALTERNATING CURRENT
Predicting inverter performance in ac power distribution system page 67 MSC-20769

AMORPHOUS SEMICONDUCTORS
Plasma deposition of doped amorphous silicon page 104 NPO-14955

AMPOULES
High-temperature, high-pressure optical cells page 152 MFS-26000

ANCHORS (FASTENERS)
End restraints for impact-energy-absorbing tube specimens page 109 LAR-13179
Blind-side, high-temperature fastener lock page 140 LAR-13037

ANTENNA RADIATION PATTERNS
Analysis of satellite communications antenna patterns page 164 NPO-16400
Estimating antenna shape from far-field measurements page 74 NPO-16425
Fabrication of slender struts for deployable antennas page 157 LAR-13136

ANVILS
Anvil for flaring PCB guide pins page 148 MSC-20345

ARC LAMPS
Power supply for 25-watt arc lamp page 32 LAR-13202
Orienting arc lamps for longest life page 51 MSC-20562

ATMOSPHERIC DIFFUSION
Exhaust effluent diffusion model page 105 MFS-25940

AUTOMATIC TEST EQUIPMENT
Online tester for a symbol generator page 58 MSC-20357

B

BATTERY CHARGERS
Recharging batteries chemically page 35 NPO-16024

BEAMS (SUPPORTS)
Sequentially-deployable tetrahedral beam page 113 LAR-13098
Making structural members from wire page 153 MSC-20175

BEARING ALLOYS
Ion implantation improves bearing-surface properties page 95 MFS-25995

BEARINGS
Analyses of multishaft rotor-bearing response page 127 LEW-13925
Effects of bearing clearance on turbopump stability page 148 MFS-27063
Low-temperature seal for actuator rod page 118 MSC-20744

BENDING
Testing machine for biaxial loading page 118 MSC-20477

BIONICS
Low-friction joint for robot fingers page 140 NPO-15914

BISTABLE CIRCUITS
Comparator with noise suppression page 43 LAR-13151

BODY-WING CONFIGURATIONS
Retractable end plates for aircraft lifting surfaces page 108 LAR-12946

BONDING
Bonding solar-cell modules page 104 NPO-16399

BRAKES (FOR ARRESTING MOTION)
Gradually acting shaft stop page 147 MSC-20729

BUBBLES
Centrifugal generator of filled spherical shells page 155 NPO-16051
Blowing polymer bubbles in an acoustic levitator page 100 NPO-16212

BURNERS
Modeling a transient catalytic combustor page 104 LEW-13723

C

CARBON FIBERS
Determining fiber orientation in graphite-reinforced composites page 101 MFS-28032

CATALYSIS
Modeling a transient catalytic combustor page 104 LEW-13723

CERAMICS
Duplicating curved surfaces for pull testing page 158 MSC-20795
Production process for strong, light ceramic tiles page 97 MSC-20602

CHEMICAL REACTORS
Windowless high-pressure solar reactor page 68 NPO-16310

CIRCUIT BREAKERS
Remote power controllers for high-power dc switching page 44 LEW-14109

CIRCUIT PROTECTION
Low-voltage protection for volatile computer memories page 42 NPO-15909

CLAMPS
Hand-held power clamp page 147 MSC-20549
Optical mounts for cryogenic beam splitters page 73 GSC-12923

CLOUDS
Accurate airborne particle sampler page 110 LAR-13080
Airborne cloud detector page 63 LAR-13137

CMOS
Latchup in CMOS integrated circuits page 66 NPO-16304

COAL
Corrosive effects of burning fuels page 103 NPO-16345
Coal-sizing auger page 134 NPO-16184
Side shield for wall support page 135 NPO-16188
All-water-jet coal excavator page 133 NPO-16183
Slurry-mixing chamber page 132 NPO-16182
Reducing coal dust with water jets page 131 NPO-16180
Modular pick-and-bucket mining machine page 130 NPO-16179
Pointable auger page 129 NPO-16178
Automated coal-mining system page 128 NPO-16177
Service modules for coal extraction page 134 NPO-16185
Roof shield for advance and retreat mining page 136 NPO-16189
Compact hydraulic excavator and support unit page 136 NPO-16190

CODING
Standard codes for telemetry and telecommand page 165 NPO-16305

COLLIMATION
Adapter helps to align plasma torch page 143 MFS-28024

COMBUSTION PHYSICS
Modeling a transient catalytic combustor page 104 LEW-13723
Prediction of combustion gas deposit compositions page 162 LEW-14091

COMMUNICATION

EQUIPMENT
Communications headgear with protective features page 63 LAR-13156

COMMUTATORS
Commutating permanent-magnet motors at low speed page 46 MFS-25207

COMPARATOR CIRCUITS
Comparator with noise suppression page 43 LAR-13151

COMPOSITE MATERIALS
Determining fiber orientation in graphite-reinforced composites page 101 MFS-28032
Damage and repair of composite structures page 151 GSC-12758
Thermal shock-resistant composite crucible page 143 LEW-14105
Plastic and failure analysis of composites page 105 LAR-13183

COMPUTER DESIGN
Analysis of spiral-bevel gearing page 151 LEW-14067

COMPUTER GRAPHICS
Manipulation and display of panel-method geometry page 164 LAR-13224

An interactive plotting routine page 164 MSC-20771

COMPUTER STORAGE DEVICES
Low-voltage protection for volatile computer memories page 42 NPO-15909

COMPUTER SYSTEMS SIMULATION
Personal computer video-terminal emulator page 165 KSC-11293

CONDENSERS (LIQUIFIERS)
High-performance heat pipe page 70 MSC-20136

CONDUCTIVITY METERS
Measuring soil hydraulic conductivity with microwaves page 70 GSC-12937

CONTROL EQUIPMENT
Experiments with a manipulator sensor system page 149 NPO-16094
Personal computer video-terminal emulator page 165 KSC-11293
Portable temperature set-point controller page 35 MSC-20056

COOLING SYSTEMS
Making glass-fiber-reinforced coolant tubes page 159 MSC-20677

CORROSION
Corrosive effects of burning fuels page 103 NPO-16345

CRACKS
Detecting cracks in rough metal surfaces page 119 MSC-20734

CRAWLER TRACTORS
Improved highway pads for tracked vehicles page 138 NPO-16318

CROSSOVERS
Crossover concept for optical printed circuits page 82 NPO-15131

CRUCIBLES
Thermal shock-resistant composite crucible page 143 LEW-14105
Filament guides for silicon-ribbon growth page 88 NPO-16306
Adjustable lid aids silicon-ribbon growth page 159 NPO-16354

CRUSHERS
Coal-sizing auger page 134 NPO-16184

CRYOGENIC EQUIPMENT
Insulating cryogenic pipes with frost page 141 MSC-20426

CRYSTAL GROWTH
Prototype furnace for automatic production of silicon ribbon page 156 NPO-16175
Filament guides for silicon-ribbon growth page 88 NPO-16306
Adjustable lid aids silicon-ribbon growth page 159 NPO-16354

D

DAMAGE ASSESSMENT
Damage and repair of composite structures page 161 LAR-13146

DEMODULATORS
Pulse-width-to-analog-voltage converter page 53 MSC-20006

DEPOSITION
Plasma deposition of doped amorphous silicon page 104 NPO-14955

DIELECTRICS
Degradation of dielectrics in space page 103 NPO-16003

DIGITAL SYSTEMS
Design language for digital systems page 163 MFS-25352

DIMENSIONAL MEASUREMENT
Hand-held electronic gap-measuring tools page 114 MSC-20176

DISPLACEMENT MEASUREMENT
Fixture for linearly variable displacement transducers page 115 LAR-12937

DRILLING
Precise electrochemical drilling of repeated deep holes page 142 MFS-19767
Pointable auger page 129 NPO-16178

DUCTED FAN ENGINES
Duct-flow analysis page 86 LEW-14000

E

EDDY CURRENTS
Inexpensive eddy-current standard page 116 LAR-13154

ELECTRIC BATTERIES
Recharging batteries chemically page 35 NPO-16024
Improved electrodes for lithium cells page 98 NPO-16397

ELECTRIC CONNECTORS
Electrically connecting to pressure vessels page 51 MSC-20709

ELECTRIC CONTACTS
Rolling-contact rheostat page 36 NPO-15567
Study of contact resistances in integrated circuits page 54 NPO-16248

ELECTRIC HYBRID VEHICLES
Hybrid and electric advanced vehicle systems simulation page 150 LEW-13927

ELECTRIC MOTORS
Commutating permanent-magnet motors at low speed page 46 MFS-25207

ELECTRIC POWER SUPPLIES
Power supply for 25-watt arc lamp page 32 LAR-13202

Incrementally variable high-voltage supply page 38 MFS-28018

ELECTRIC POWER TRANSMISSION

Integrating residential photovoltaics with power lines page 84 NPO-16331

ELECTRIC SWITCHES

Reed-switch position indicator page 49 KSC-11215

ELECTRICAL INSULATION

Lightweight electrical insulation page 92 NPO-16165

ELECTRICAL RESISTANCE

Study of contact resistances in integrated circuits page 54 NPO-16248

ELECTROCHEMICAL CELLS

Recharging batteries chemically page 35 NPO-16024

ELECTROCHEMICAL MACHINING

Precise electrochemical drilling of repeated deep holes page 142 MFS-19767

ELECTRODES

Improved electrodes for lithium cells page 98 NPO-16397

ELECTRON BEAM WELDING

Microfissuring in electron-beam-welded nickel alloy page 96 MFS-27041

ELECTRONIC EQUIPMENT TESTS

Measuring moisture in sealed electronic enclosures page 78 MSC-18866

Analyzing microchips with dark-field negative photo-micrography page 72 NPO-16299

Online tester for a symbol generator page 58 MSC-20357

ELECTRONIC PACKAGING

Measuring moisture in sealed electronic enclosures page 78 MSC-18866

Intercalated-carbon low-resistivity fibers page 94 NPO-16307

ENCAPSULATED MICROCIRCUITS

Analyzing microchips with dark-field negative photo-micrography page 72 NPO-16299

ENERGY CONVERSION EFFICIENCY

Augmenting thrust with waste heat page 86 NPO-16218

Estimating the performance of a concentrating solar array page 80 MFS-28021

ENVIRONMENTAL CONTROL

Portable temperature set-point controller page 35 MSC-20056

EVAPORATORS

High-performance heat pipe page 70 MSC-20136

EXCAVATION

Modular pick-and-bucket mining machine page 130 NPO-16179

EXHAUST DIFFUSERS

Improved exhaust diffuser for jet-engine testing page 146 NPO-16328

EXHAUST GASES

Corrosive effects of burning fuels page 103 NPO-16345

Exhaust effluent diffusion model page 105 MFS-25940

F

FAILURE ANALYSIS

Plastic and failure analysis of composites page 105 LAR-13183

Predicting the fatigue life of structures page 102 MFS-27049

FAR FIELDS

Analysis of satellite communications antenna patterns page 164 NPO-16400

FASTENERS

Hand-held power clamp page 147 MSC-20549

Blind-side, high-temperature fastener lock page 140 LAR-13037

FATIGUE LIFE

Predicting the fatigue life of structures page 102 MFS-27049

Optimizing load spectra for gears page 149 MSC-20487

FIBER COMPOSITES

Fabrication of slender struts for deployable antennas page 157 LAR-13136

Intercalated-carbon low-resistivity fibers page 94 NPO-16307

Determining fiber orientation in graphite-reinforced composites page 101 MFS-28032

FINITE ELEMENT METHOD

Analysis of spiral-bevel gearing page 151 LEW-14067

Airborne cloud detector page 63 LAR-13137

FLOW DISTRIBUTION

Duct-flow analysis page 86 LEW-14000

FLOWMETERS

Flowmeter for clear and translucent fluids page 117 MFS-28030

Centrifugal generator of filled spherical shells page 155 NPO-16051

FLUID FLOW

Flowmeter for clear and translucent fluids page 117 MFS-28030

FLUIDIZED BED PROCESSORS

Fluidized-bed particles scavenge silicon fines page 98 NPO-16034

FLUX PINNING

Paramagnetic precipitates may raise supercurrent page 94 MFS-25925

FOLDING STRUCTURES

Sequentially-deployable tetrahedral beam page 113 LAR-13098

Making structural members from wire page 153 MSC-20175

FOSSIL FUELS

Prediction of combustion gas deposit compositions page 162 LEW-14091

FREQUENCY DISCRIMINATORS

Frequency-discriminating acoustic-event counter page 58 MSC-20467

FREQUENCY MODULATION

Programmable driver for voltage-controlled oscillators page 60 NPO-16364

FREQUENCY SYNCHRONIZATION

Satellite time- and frequency-transfer system page 65 MFS-25991

FUEL CONSUMPTION

Aerodynamic rear cone for trucks page 109 MFS-28007

Retractable end plates for aircraft lifting surfaces page 108 LAR-12946

FURNACES

Prototype furnace for automatic production of silicon ribbon page 156 NPO-16175

G

GAPS

Hand-held electronic gap-measuring tools page 114 MSC-20176

GAS DETECTORS

Monitoring trace gases in the atmosphere page 69 NPO-16278

GAS EXPLOSIONS

Curtain wall creates ventilation channel page 137 NPO-16194

GAS-METAL INTERACTIONS

Measuring hydrogen concentrations in metals page 96 MFS-27020

GEARS

Analysis of spiral-bevel gearing page 151 LEW-14067

Optimizing load spectra for gears page 149 MSC-20487

GLANDS (SEALS)

Low-temperature seal for actuator rod page 118 MSC-20744

Lightweight electrical insulation page 92 NPO-16165

Processing of image data by integrated circuits page 61 NPO-15059

Analyzing microchips with dark-field negative photo-micrography page 72 NPO-16299

Modeling "soft" errors in bipolar integrated circuits page 54 NPO-16293

Integrated CMOS latchup in CMOS integrated circuits page 66 NPO-16304

Study of contact resistances in integrated circuits page 54 NPO-16248

Crossover concept for optical printed circuits page 82 NPO-15131

Blowing polymer bubbles in an acoustic levitator page 100 NPO-16212

Controlling sample rotation in acoustic levitation page 160 NPO-15962

Orienting arc lamps for longest life page 51 MSC-20562

Improved electrodes for lithium cells page 98 NPO-16397

Testing machine for biaxial loading page 111 MSC-20477

Blind-side, high-temperature fastener lock page 140 LAR-13037

Automatically-programmed machine tools page 151 GSC-12758

Magnetron-sputtered amorphous metallic coatings page 100 NPO-16221

Experiments with a manipulator sensor system page 149 NPO-16094

Hand-held electronic gap-measuring tools page 114 MSC-20176

IMAGE PROCESSING

Processing of image data by integrated circuits page 61 NPO-15059

IMAGING TECHNIQUES

Multispectral analysis of NMR imagery page 106 KSC-11301

INDICATING INSTRUMENTS

Reed-switch position indicator page 49 KSC-11215

Airborne cloud detector page 63 LAR-13137

INFRARED SPECTROMETERS

Lens-and-detector array for spectrometer page 80 NPO-16388

High-temperature, high-pressure optical cells page 152 MFS-26000

INJECTION LASERS

High-output injection laser page 45 LAR-13213

INPUT/OUTPUT ROUTINES

Personal computer video-terminal emulator page 165 KSC-11293

INSPECTION

Detecting cracks in rough metal surfaces page 119 MSC-20734

INSULATION

Insulating cryogenic pipes with frost page 141 MSC-20426

Processing of image data by integrated circuits page 61 NPO-15059

Analyzing microchips with dark-field negative photo-micrography page 72 NPO-16299

Modeling "soft" errors in bipolar integrated circuits page 54 NPO-16293

Integrated CMOS latchup in CMOS integrated circuits page 66 NPO-16304

Study of contact resistances in integrated circuits page 54 NPO-16248

Crossover concept for optical printed circuits page 82 NPO-15131

Blowing polymer bubbles in an acoustic levitator page 100 NPO-16212

Controlling sample rotation in acoustic levitation page 160 NPO-15962

Orienting arc lamps for longest life page 51 MSC-20562

Improved electrodes for lithium cells page 98 NPO-16397

Testing machine for biaxial loading page 111 MSC-20477

Blind-side, high-temperature fastener lock page 140 LAR-13037

Automatically-programmed machine tools page 151 GSC-12758

Magnetron-sputtered amorphous metallic coatings page 100 NPO-16221

Experiments with a manipulator sensor system page 149 NPO-16094

Hand-held electronic gap-measuring tools page 114 MSC-20176

ION IMPLANTATION

Ion implantation improves bearing-surface properties page 95 MFS-25995

ION IRRADIATION

Modeling "soft" errors in bipolar integrated circuits page 54 NPO-16293

IONIZING RADIATION

Degradation of dielectrics in space page 103 NPO-16003

J

JET ENGINES

Improved exhaust diffuser for jet-engine testing page 146 NPO-16328

JIGS

Aligning large cylinders for welding page 155 MFS-28001

Holder for ultrasonic evaluation of small-diameter tubes page 138 LAR-13152

End restraints for impact-energy-absorbing tube specimens page 109 LAR-13179

Precise electrochemical drilling of repeated deep holes page 142 MFS-19767

L

LABYRINTH SEALS

Predicting leakage in labyrinth seals page 149 MFS-27051

LAMINATES

Plastic and failure analysis of composites page 105 LAR-13183

LANDFORMS

Processing digital imagery data page 164 MFS-25987

LASER SPECTROMETERS

Monitoring trace gases in the atmosphere page 69 NPO-16278

LASERS

High-output injection laser page 45 LAR-13213

LATCH-UP

Latchup in CMOS integrated circuits page 66 NPO-16304

LEAKAGE

Predicting leakage in labyrinth seals page 149 MFS-27051

LEVITATION

Blowing polymer bubbles in an acoustic levitator page 100 NPO-16212

Controlling sample rotation in acoustic levitation page 160 NPO-15962

LIFE (DURABILITY)

Orienting arc lamps for longest life page 51 MSC-20562

LITHIUM

Improved electrodes for lithium cells page 98 NPO-16397

LOAD TESTING MACHINES

Testing machine for biaxial loading page 111 MSC-20477

LOCKS (FASTENERS)

Blind-side, high-temperature fastener lock page 140 LAR-13037

LOGIC DESIGN

Design language for digital systems page 163 MFS-25352

LOW VOLTAGE

Low-voltage protection for volatile computer memories page 42 NPO-15909

LUGS

Electrically connecting to pressure vessels page 51 MSC-20709

M

MACHINE TOOLS

Automatically-programmed machine tools page 151 GSC-12758

MAGNETRON SPUTTERING

Magnetron-sputtered amorphous metallic coatings page 100 NPO-16221

MANIPULATORS

Experiments with a manipulator sensor system page 149 NPO-16094

MECHANICAL MEASUREMENT

Hand-held electronic gap-measuring tools page 114 MSC-20176

MEDICAL ELECTRONICS

Multispectral analysis of NMR imagery page 106 KSC-11301

METAL COATINGS

Magnetron-sputtered amorphous metallic coatings page 100 NPO-16221

MICROCRACKS

Microfissuring in electron-beam-welded nickel alloy page 96 MFS-27041

MICROWAVES

Programmable driver for voltage-controlled oscillators page 60 NPO-16364

Measuring soil hydraulic conductivity with microwaves page 70 GSC-12937

Recovering microwave cross-polarization losses page 64 NPO-15353

MINING

Curtain wall creates ventilation channel page 137 NPO-16194

Coal-sizing auger page 134 NPO-16184

Side shield for wall support page 135 NPO-16188

All-water-jet coal excavator page 133 NPO-16183

Slurry-mixing chamber page 132 NPO-16182

Reducing coal dust with water jets page 131 NPO-16180

Modular pick-and-bucket mining machine page 130 NPO-16179

Pointable auger page 129 NPO-16178

Automated coal-mining system page 128 NPO-16177

Service modules for coal extraction page 134 NPO-16185

Roof shield for advance and retreat mining page 136 NPO-16189

Compact hydraulic excavator and support unit page 136 NPO-16190

Slurry-mixing chamber page 132 NPO-16182

MOISTURE METERS

Measuring moisture in sealed electronic enclosures page 78 MSC-18866

MULTISPECTRAL BAND SCANNERS
Processing digital imagery data page 164 MFS-25987

N**NICKEL ALLOYS**

Microfissuring in electron-beam-welded nickel alloy page 96 MFS-27041

NOISE SUPPRESSORS

Comparator with noise suppression page 43 LAR-13151

NONDESTRUCTIVE TESTS

Inexpensive eddy-current standard page 116 LAR-13154

Detecting cracks in rough metal surfaces page 119 MSC-20734

NONLINEAR OPTICS

Retrodirective-optical-transponder concept page 50 NPO-16315

NUCLEAR MAGNETIC RESONANCE

Multispectral analysis of NMR imagery page 106 KSC-11301

NUCLEAR POWER PLANTS

Synthetic organic materials in nuclear powerplants page 103 NPO-16424

NUMERICAL ANALYSIS

Free-vibration analysis of structures page 162 NPO-15000

NUMERICAL CONTROL

Automatically-programmed machine tools page 151 GSC-12758

O**OPTICAL COMMUNICATION**

Retrodirective-optical-transponder concept page 50 NPO-16315

OPTICAL DATA PROCESSING

Processing digital imagery data page 164 MFS-25987

Processing of image data by integrated circuits page 61 NPO-15059

OPTICAL WAVEGUIDES

Crossover concept for optical printed circuits page 82 NPO-15131

ORBITS

Interferometry measures elliptical satellite orbits page 66 NPO-16313

ORGANIC MATERIALS

Synthetic organic materials in nuclear powerplants page 103 NPO-16424

P**PACKINGS (SEALS)**

Shaft seal compensates for cold flow page 145 MFS-25678

PAINTS

Diffusely reflecting paints containing TFE page 92 GSC-12883

PANEL METHOD (FLUID DYNAMICS)

Manipulation and display of panel-method geometry page 164 LAR-13224

PANELS

Fixture for linearly variable displacement transducers page 115 LAR-12937

PARABOLIC ANTENNAS

Analysis of satellite-communications antenna patterns page 164 NPO-16400

Estimating antenna shape from far-field measurements page 74 NPO-16425

PARAMAGNETISM

Paramagnetic precipitates may raise supercurrent page 94 MFS-25925

PARTICLE SAMPLING

Accurate airborne particle sampler page 110 LAR-13080

PHASE CONTROL

Controlling sample rotation in acoustic levitation page 160 NPO-15962

PHOTOMETERS

Lens-and-detector array for spectrometer page 80 NPO-16388

Multiband selector for linear photodetector array page 84 GSC-12911

PHOTOVOLTAIC CELLS

Segmented trough reflector page 68 NPO-15026

Tests of low-concentration-ratio photovoltaic elements page 84 MFS-28020

Estimating the performance of a concentrating solar array page 80 MFS-28021

Integrating residential photovoltaics with power lines page 84 NPO-16331

PIGMENTS

Diffusely reflecting paints containing TFE page 92 GSC-12883

PIPELINING (COMPUTERS)

Fast control sequencer page 60 NPO-16116

PIPES (TUBES)

Insulating cryogenic pipes with frost page 141 MSC-20426

Making glass-fiber-reinforced coolant tubes page 159 MSC-20677

PLASMA TORCHES

Adapter helps to align plasma torch page 143 MFS-28024

PLOTTING

An interactive plotting routine page 164 MSC-20771

POSITIONING DEVICES (MACHINERY)

Holder for ultrasonic evaluation of small-diameter tubes page 138 LAR-13152

POTENTIOMETERS

Rolling-contact rheostat page 36 NPO-15567

POWER CONDITIONING

Incrementally variable high-voltage supply page 38 MFS-28018

POWER LINES

Predicting inverter performance in ac power distribution system page 67 MSC-20769

POWER SUPPLY CIRCUITS

Rotary power transformer and inverter circuit page 52 NPO-16270

Remotely-adjustable solid-state high-voltage supply page 48 NPO-15719

PREDICTION ANALYSIS TECHNIQUES

Prediction of combustion gas deposit compositions page 162 LEW-14091

PRESSING (FORMING)

Anvil for flaring PCB guide pins page 148 MSC-20345

PRESSURE VESSELS

High-temperature, high-pressure optical cells page 152 MFS-26000

Electrically connecting to pressure vessels page 51 MSC-20709

PROGRAMMING LANGUAGES

Design language for digital systems page 163 MFS-25352

PROPULSION SYSTEM PERFORMANCE

Hybrid and electric advanced vehicle systems simulation page 150 LEW-13927

PROTECTIVE COATINGS

Diffusely reflecting paints containing TFE page 92 GSC-12883

Magnetron-sputtered amorphous metallic coatings

page 100 NPO-16221

PULSE DURATION

Pulse-width-to-analog-voltage converter page 53 MSC-20006

PULSE WIDTH AMPLITUDE CONVERTERS

Pulse-width-to-analog-voltage converter page 53 MSC-20006

R**RADAR**

Point simulator for synthetic-aperture radar page 62 NPO-16296

RADIATION DAMAGE

Synthetic organic materials in nuclear powerplants page 103 NPO-16424

Degradation of dielectrics in space page 103 NPO-16003

RANDOM ACCESS MEMORY

Modeling "soft" errors in bipolar integrated circuits page 54 NPO-16293

REMOTE CONTROL

Remote power controllers for high-power dc switching page 44 LEW-14109

REMOTE SENSORS

Airborne DIAL system for remote tropospheric sensing page 71 LAR-13002

RESISTORS

Rolling-contact rheostat page 36 NPO-15567

RESONANCE

Ferroresonant circuit with increased efficiency page 30 NPO-16326

ROBOTS

Low-friction joint for robot fingers page 140 NPO-15914

Force sensor for large robot arms page 116 NPO-16097

ROCKET ENGINES

Miniature rocket motor for aircraft stall/spin recovery page 144 LAR-13199

ROCKET EXHAUST

Exhaust effluent diffusion model page 105 MFS-25940

ROTARY WINGS

Blade vibrations page 117 ARC-11444

ROTORS

Analyses of multishaft rotor-bearing response page 127 LEW-13925

S**SAFETY**

Curtain wall creates ventilation channel page 137 NPO-16194

SCAVENGING

Fluidized-bed particles scavenge silicon fines page 98 NPO-16034

SEALS (STOPPERS)

Silicone-rubber switching seal page 154 MSC-20708

Shaft seal compensates for cold flow page 145 MFS-25678

Predicting leakage in labyrinth seals page 149 MFS-27051

Low-temperature seal for actuator rod page 118 MSC-20744

SEAMS (JOINTS)

Silicone-rubber switching seal page 154 MSC-20708

SEMICONDUCTOR LASERS

High-output injection laser page 45 LAR-13213

SEQUENTIAL CONTROL

Fast control sequencer page 60 NPO-16116

SERVICE MODULES

Service modules for coal extraction page 134 NPO-16185

SERVOMECHANISMS

Low-friction joint for robot fingers page 140 NPO-15914

Force sensor for large robot arms page 116 NPO-16097

SETUPS

Aligning large cylinders for welding page 155 MFS-28001

SHAFTS (MACHINE ELEMENTS)

Analyses of multishaft rotor-bearing response page 127 LEW-13925

Gradually acting shaft stop page 147 MSC-20729

Shaft seal compensates for cold flow page 145 MFS-25678

SHEAR STRENGTH

Fixture for linearly variable displacement transducers page 115 LAR-12937

SHOCK RESISTANCE

Thermal shock-resistant composite crucible page 143 LEW-14105

SIGNAL CODING

Standard codes for telemetry and telecommand page 165 NPO-16305

SIGNAL TRANSMISSION

Recovering microwave cross-polarization losses page 64 NPO-15353

SILICON

Fluidized-bed particles scavenge silicon fines page 98 NPO-16034

Prototype furnace for automatic production of silicon ribbon page 156 NPO-16175

Filament guides for silicon-ribbon growth page 88 NPO-16306

Adjustable lid aids silicon-ribbon growth page 159 NPO-16354

Plasma deposition of doped amorphous silicon page 104 NPO-14955

SILICONE RUBBER

Silicone-rubber switching seal page 154 MSC-20708

SIMULATION

Point simulator for synthetic-aperture radar page 62 NPO-16296

SINTERING

Production process for strong, light ceramic tiles page 97 MSC-20602

SOILS

Measuring soil hydraulic conductivity with microwaves page 70 GSC-12937

SOLAR ARRAYS

Multiband selector for linear photodetector array page 84 GSC-12911

Bonding solar-cell modules page 104 NPO-16399

Tests of low-concentration-ratio photovoltaic elements page 84 MFS-28020

Estimating the performance of a concentrating solar array page 80 MFS-28021

Segmented trough reflector page 68 NPO-15026

Bonding solar-cell modules page 104 NPO-16399

Tests of low-concentration-ratio photovoltaic elements page 84 MFS-28020

Integrating residential photovoltaics with power lines page 84 NPO-16331

Windowless high-pressure solar reactor page 68 NPO-16310

Segmented trough reflector page 68 NPO-15026

Windowless high-pressure solar reactor page 68 NPO-16310

Windowless high-pressure solar reactor page 68 NPO-16310

Windowless high-pressure solar reactor page 68 NPO-16310

Windowless high-pressure solar reactor page 68 NPO-16310

Windowless high-pressure solar reactor page 68 NPO-16310

Windowless high-pressure solar reactor page 68 NPO-16310

Windowless high-pressure solar reactor page 68 NPO-16310

Windowless high-pressure solar reactor page 68 NPO-16310

Windowless high-pressure solar reactor page 68 NPO-16310

Windowless high-pressure solar reactor page 68 NPO-16310

SPEED CONTROL
Gradually acting shaft stop page 147 MSC-20729

SPHERICAL SHELLS
Centrifugal generator of filled spherical shells page 155 NPO-16051

STANDARDS
Inexpensive eddy-current standard page 116 LAR-13154

STARTERS
Power supply for 25-watt arc lamp page 32 LAR-13202

STATIC STABILITY
Free-vibration analysis of structures page 162 NPO-15000

STATISTICAL ANALYSIS
Statistical energy analysis program page 120 MFS-27035

STEELS
Measuring hydrogen concentrations in metals page 96 MFS-27020

STRUCTURAL FATIGUE
Predicting the fatigue life of structures page 102 MFS-27049

STRUCTURAL VIBRATION
Statistical energy analysis program page 120 MFS-27035

Free-vibration analysis of structures page 162 NPO-15000

STYROFOAM (TRADEMARK)
Lightweight electrical insulation page 92 NPO-16165

SUPERCONDUCTORS
Paramagnetic precipitates may raise supercurrent page 94 MFS-25925

SUPPORTS
Side shield for wall support page 135 NPO-16188

Roof shield for advance and retreat mining page 136 NPO-16189

Optical mounts for cryogenic beam splitters page 73 GSC-12923

End restraints for impact-energy-absorbing tube specimens page 109 LAR-13179

SURFACE DISTORTION
Estimating antenna shape from far-field measurements page 74 NPO-16425

SWITCHES
Reed-switch position indicator page 49 KSC-11215

SWITCHING CIRCUITS
Remote power controllers for high-power dc switching page 44 LEW-14109

Commutating permanent-magnet motors at low speed page 46 MFS-25207

SYNCHRONISM
Satellite time- and frequency-transfer system page 65 MFS-25991

SYNTHETIC APERTURE RADAR
Point simulator for synthetic-aperture radar page 62 NPO-16296

T

TELEMETRY
Standard codes for telemetry and telecommand page 165 NPO-16305

TEMPERATURE

CONTROL
 Portable temperature set-point controller page 35 MSC-20056
 Orienting arc lamps for longest life page 51 MSC-20562

TEMPERATURE MEASUREMENT

Improved thermal-diffusivity-measuring apparatus page 76 NPO-16280
 Combination heat-flux and temperature gage page 112 MSC-20706

TENSILE TESTS

Testing machine for biaxial loading page 111 MSC-20477

TEST CHAMBERS

Improved exhaust diffuser for jet-engine testing page 146 NPO-16328

TEST PATTERN GENERATORS

Online tester for a symbol generator page 58 MSC-20357

TETRAHEDRONS

Sequentially-deployable tetrahedral beam page 113 LAR-13098

THERMAL DIFFUSIVITY

Improved thermal-diffusivity-measuring apparatus page 76 NPO-16280

THERMOCOUPLES

Combination heat-flux and temperature gage page 112 MSC-20706

TILES

Duplicating curved tile surfaces for pull testing page 158 MSC-20795
 Production process for strong, light ceramic tiles page 97 MSC-20602

TIME SIGNALS

Satellite time- and frequency-transfer system page 65 MFS-25991

TOOLS

Hand-held power clamp page 147 MSC-20549
 Anvil for flaring PCB guide pins page 148 MSC-20345

TORQUE

Experiments with a manipulator sensor system page 149 NPO-16094

TRACKED VEHICLES

Improved highway pads for tracked vehicles page 138 NPO-16318

TRANSDUCERS

Force sensor for large robot arms page 116 NPO-16097
 Flowmeter for clear and translucent fluids page 117 MFS-28030

TRANSFORMERS

Rotary power transformer and inverter circuit page 52 NPO-16270

TRANSMISSION LOSS

Recovering microwave cross-polarization losses page 64 NPO-15353

TRANSMISSIONS (MACHINE ELEMENTS)

Hybrid and electric advanced vehicle systems simulation page 150 LEW-13927

TRANSPONDERS

Retrodirective-optical-transponder concept page 50 NPO-16315

TROPOSPHERE

Airborne DIAL system for remote tropospheric sensing page 71 LAR-13002

TRUCKS

Aerodynamic rear cone for trucks page 109 MFS-28007

TRUSSES

Fabrication of slender struts for deployable antennas page 157 LAR-13136
 Making structural members from wire page 153 MSC-20175

TUNNELING (EXCAVATION)

Automated coal-mining system page 128 NPO-16177

Compact hydraulic excavator and support unit page 136 NPO-16190

TURBINE PUMPS

Effects of bearing clearance on turbopump stability page 148 MFS-27063

TURBOMACHINERY

Duct-flow analysis page 86 LEW-14000

U**ULTRASONIC TESTS**

Holder for ultrasonic evaluation of small-diameter tubes page 138 LAR-13152

V**VACUUM FURNACES**

Improved thermal-diffusivity-measuring apparatus page 76 NPO-16280

VEHICULAR TRACKS

Improved highway pads for tracked vehicles page 138 NPO-16318

VERY LONG BASELINE INTERFEROMETRY

Interferometry measures elliptical satellite orbits page 66 NPO-16313

VIBRATION DAMPING

Tabs reduce helicopter-blade vibrations page 117 ARC-11444

VIBRATIONAL SPECTRA

Statistical energy analysis program page 120 MFS-27035

VOLTAGE REGULATORS

Programmable driver for voltage-controlled oscillators page 60 NPO-16364
 Ferroresonant circuit with increased efficiency page 30 NPO-16326

W**WASTE ENERGY UTILIZATION**

Augmenting thrust with waste heat page 86 NPO-16218

WEAR

Ion implantation improves bearing-surface properties page 95 MFS-25995
 Optimizing load spectra for gears page 149 MSC-20487

Are You a Subscriber?

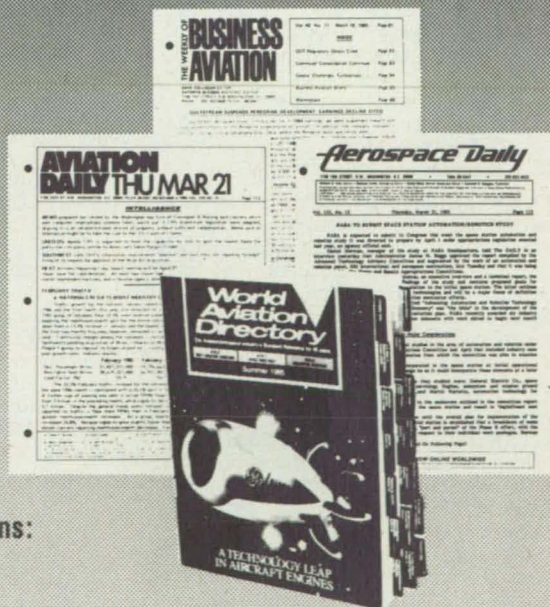
The most relied-upon
 "intelligence/communications"
 network serving the
 aviation/aerospace industry
 worldwide.

Write on company letterhead or call for FREE trial subscriptions:

- 3 weeks of Aerospace Daily*
- 3 weeks of Aviation Daily
- 4 weeks of Business Aviation
- 30 day inspection of World Aviation Directory

*Aerospace Daily is now on-line as part of a comprehensive network of electronic databases called **Aerospace Online**. Call 202-822-4691 for a one month test.

Murdoch Magazines • 1156 15th St., NW • Washington, DC 20005 • 202-822-4600



Letters

The "Letters" column is designed to encourage a wide exchange of ideas among NASA Tech Briefs readers. To contribute a request for information or to respond to such a request, use the feedback cards in this issue, or write or call: Manager/Technology Transfer Division, P.O. Box 8757, Baltimore/Washington International Airport, MD 21240; (301) 859-5300. While we can print only a small number of letters, we will endeavor to select those that are varied and of wide interest.

ROBOTICS APPLICATIONS

I want to build some robotic-controlled tools for use in my wood laboratory. I intend to build my own equipment since it is unlikely my school district will buy such equipment. Where can I get information?

Truman J. Siple
Industrial Arts Instructor
Bensalem Township School District
Bensalem, PA

You may wish to write directly to the following NASA office for additional information about the services it offers: NASA Headquarters, Office of External Relations, Code LE, Washington, DC 20546. This office can provide you with information concerning educational materials, curriculum assistance, youth programs (e.g., model building, science fairs), professional education conferences, instructional resources, and teacher education courses.

IDEAS, IDEAS

I am an innovator, an idea man, and in some respects a refiner of ideas. In other words, I create concepts for others to develop into products. In some cases, I can develop alternate concepts from existing concepts or products.

I would like to be able to find a place where I can "dump" ideas, concepts, etc. I am willing to talk to anyone who is receptive to ideas, and to develop mutually acceptable terms of agreement.

Donald Kellerstrass
D & R Innovators
Washington, IL

The following NASA office provides information and assistance to inventors, and others with specific discoveries, innovations, new concepts, or ideas they wish NASA to note, comment on, accept, or buy. Please contact this office for additional information regarding the services it provides: Office of Management Operations, Inventions and Contributions Board, Code NB, NASA Headquarters, Washington, DC 20546.

VARIABLE TRANSMISSION UPDATE

I was sorry to read that more information on the continuously variable transmission design by Mr. David C. Grana is currently unavailable [see NASA Tech Briefs, Spring 1985, p. 128]. This makes it hard to judge his idea and compare it with the continuously variable transmission which was designed and produced by DAF Automobiel Fabriken in Einhoven, the Netherlands, over 20 years ago.

DAF used the "variomatic" in passenger cars for over 10 years before they sold the car manufacturing plant to Volvo. Volvos are still available with the variomatic in Europe.

A new design by DAF is the "transmatic," which, contrary to the system previously used by DAF and similar to the system described by Mr. Grana, does not use a pull-

ing force, but rather a pushing force, to transmit the power from one axle to the other. This system is currently manufactured in the Netherlands and will be used in cars manufactured in Europe as well as in Japan and the United States.

I am quite sure that DAF would be willing to supply Mr. Grana, or for that matter anyone interested, with more information on their system.

Evert Osterman
Former DAF employee
Valencia, CA

I am seeking information on flywheel energy storage variable transmissions and portable energy cells.

Douglas G. Thorpe
Irvine, KY

You may wish to purchase the following documents from the American Institute of Aeronautics and Astronautics (see address below): A80-47199, *Designing Optimal Closed-Circuit Variable-Speed Power Transmissions*; A80-42158, *Continuously Variable Ratio Transmissions for Single-Shaft Gas Turbines*.

In addition, the following publications are available from the National Technical Information Service (see address below): N81-19459, *Advanced Continuously Variable Transmissions For Electric And Hybrid Vehicles*; N81-13357, *Design Studies Of Continuously Variable Transmissions For Electric Vehicles*; N80-25668, *Continuously Variable Transmissions: Theory And Practice*.

COMPUTER-ASSISTED TOMOGRAPHY

I would like more information on inspection techniques like computer-assisted tomography.

H.T. Morgan
Aerojet Strategic Propulsion Co.
Sacramento, CA

The following publications are available for purchase from the American Institute of Aeronautics and Astronautics (see address below): A84-22936, *Computer Tomography in the Diagnosis of Neoplasms in the Accessory Nasal Sinuses*; A84-20898, *Prospects for the Use of Computer Controlled Tomography in Otolaryngology*; A84-15047, *Computer-Assisted Tomography for the Diagnosis of Cerebral Insult*; A84-15041, *The Use of Computer Tomography in Diagnosing the Wounds from Bullets that Penetrate the Skull and Brain*; A84-13003, *Computer Assisted Tomography Applied to Ballistics*; A83-41440, *Scintigraphy with (Tc-99)-Pyrophosphate and Computer Tomography in the Diagnosis of Tumors of the Cranial Bone*.

For extensive literature search services in your area of interest, you may wish to contact the NASA Industrial Applications Center nearest you. These Centers offer computerized access to a comprehensive collection of scientific and technical documents produced by NASA, by other government agencies, and by corporate and academic research organizations around the world. Each Center also has a professional staff that can help you evaluate your information needs and assist you with solutions to specific technical problems. For the location of the Industrial Applications Center nearest you, see page 21, this issue.

CATCHING UP

The Spring '84 issue was the last copy of

NASA Tech Briefs that I received. I would appreciate continuing to receive NASA Tech Briefs. Please provide me with Summer & Winter '84 issues and future issues.

G.A. Smart
American Home Products Corp.
New York, NY

Due to the recent commercialization of the journal there will be no Fall 1984 and Winter 1984 issues of NASA Tech Briefs.

Past issues of Tech Briefs have been released behind schedule. The decision by NASA and Associated Business Publications, Inc. to begin the new commercialized version of the journal with Vol. 9, No. 1, Spring 1985, was made in an effort to catch up and ensure timely release on a quarterly basis in the future. We want to assure you that you have not missed any Tech Briefs and they will continue to be free to qualified subscribers.

PHOTO RESEARCH

I am engaged in research on the reefs of Cozumel, Mexico, and am searching for aerial or satellite photos of those reefs. I have already contacted the EROS center, but their photos do not show enough detail, being about 1,300,000. I would prefer something covering a smaller area. The area I am interested in is at 87°W and 20°15'N to 20°30'N. Would you have any photos available that would show anything in the shallow water off the southwest coast of the island? If you do not have such photos, do you know who might?

Douglas Fenner, Ph.D.
Seattle, WA

We regret that the information you requested is not available from this office. However, you may wish to write to the following office for information on the service it provides: National Climatic Center, NOAA Environmental Data Service, Federal Building, Asheville, NC 28801.

MEMORABILIA

I've enjoyed and benefitted from NASA Tech Briefs for five years. It keeps me informed and up-to-date. Keep up the good work.

I would like to know if there is a catalog of memorabilia items which use the NASA logo or commemorate the space shuttle, etc.—items like ties, tie clasps, cufflinks, and such—so that I might order some.

Peter W. Mauer
Federal Systems Division, IBM
Owego, NY

For information on purchasing emblems, patches, etc., please write to one of the following offices: Space Age Enterprises, P.O. Box 58127, Houston, TX 77058; National Medallion Company, Inc., P.O. Box 58127, Houston, TX 77058; Visitor Information Center, Johnson Space Center, Houston TX 77058.

To inquire about the availability and cost of documents published by the American Institute of Aeronautics and Astronautics, write: AIAA, Technical Information Services, 555 West 57th Street, New York, NY 10019. To purchase publications from the National Technical Information Service, write: NTIS, 5285 Port Royal Road, Springfield, VA 22161.

Advertiser's Index

Atlantis Securities Corp.(RAC 402*)	65
Bell Helicopter	47
Celerity Computing(RAC 352)	31
Center for Space Policy(RAC 384)	161
Data General Corp.(RAC 353)	4-5
Du Pont-KAPTON(RAC 399,400,401) ...	97,99,101
EMR Photoelectric(RAC 352)	81
Fairchild Control Systems Co.(RAC 357)	17
Fisher Pen Company(RAC 358)	28
GAF Corporation(RAC 359)	87
General Dynamics Convair Div. (RAC 360)	57
General GE Electric(RAC 361) ... Cov.II-1	
Gould, Inc.(RAC 362)	11
Grumman Data Systems(RAC 363)	8-9
Honeywell Inc. Space and Strategic Avionics Division ..(RAC 364)	174, Cov.III
Interstellar Communications Corporation(RAC 366)	12
Lake Shore Cryotronics, Inc.(RAC 369)	48
Leach Relay(RAC 370)	23
Lockheed California Company	27
McDonnell Douglas Corporation(RAC 372,373,374) ...	29, 93, Cov.IV
Outer Space Laboratories, Inc.(RAC 376)	12
Post Offers	107
Pressure Systems, Incorporated (RAC 378)	161
Rockwell International Corporation/Rocketdyne Division(RAC 380)	37
Scanivalve Corporation(RAC 381)	55
Schott Glass Technologies Inc.(RAC 383)	91
Shearson Lehman Brother Inc.(RAC 384)	161
SPACECOM (Space Communication Company) ..(RAC 385)	171
Space Genetics Research Corporation(RAC 386)	12
Space Metallurgy, Inc.(RAC 387)	12
Space Shuttle Cargo Corporation(RAC 388)	12
Sperry Corporation, Systems Management Group ..	59
Systonetics, Inc.(RAC 391)	25
Texas Instruments(RAC 393)	33
Tex-Tech Industries, Inc.(RAC 392)	86
United States International Trading Co., Inc.(RAC 409)	12-13
Verdix(RAC 398)	75
Vitro Corporation(RAC 394)	2
Wintek Corporation(RAC 411)	85
World Aviation Directory	169
Wyle Laboratories Scientific Services & Systems Group ..(RAC 396)	7
Zero Gravity Enterprises, Inc.(RAC 397)	12

*RAC stands for **Reader Action Card**. For further information on these advertisers, please circle the RAC number on the Reader Action Card elsewhere in this issue. This index has been compiled as a service to our readers and advertisers. Every precaution is taken to ensure its accuracy, but the publisher assumes no liability for errors or omissions.

Classifieds

Classified advertising rates and specifications are as follows: Set in 6 point light type face, with up to five words at beginning of copy in bold caps. Count box numbers as six words.

50 words or less \$ 125
100 words \$ 175

Check or money order must accompany order to: Classified Advertising Manager, NASA Tech Briefs, Suite 921, 41 East 42nd Street, New York, NY 10017-5391.

FINALLY! A CONCISE, MONTHLY SOURCE providing authoritative coverage of all space affairs: the internationally read SPACE PRESS. Our worldwide reports have been quoted by aerospace publications, Office of Technology Assessment, etc. Bonus: subscribers may place free notices of positions/services available or sought. \$25 yearly. SPACE PRESS, 645 W.E. Ave. NYC 10025.

DRIVE YOUR OWN ELECTRIC CAR. Be one of the first with a modern 21st Century Car. For assistance in converting from gasoline to electricity or help in purchasing an electric car, write ELECTRIC AUTO ASSOCIATION NEWS, 1249 Lane St., Belmont, CA 94002. Please send SAS #10 Envelope.

CORRECTION

On page 85 of the Spring '85 issue of *NASA Tech Briefs* there is an error in the formula for estimating the latent heat in clouds. The correct formula is:

$$Q_0^* = \frac{\sum \frac{Q_i}{d_i}}{\sum \frac{1}{d_i}}$$

Success is an Exciting Journey Go with SPACECOM

Our company philosophy reminds us, "We will go together to greater successes, knowing that success is a continuing journey—not a destination." At SPACECOM, we're traveling into new and exciting communications territories, guided by past successes, spurred by a sense of adventure, and assured to repeat success along the way.

SPACECOM (Space Communications Company) is owner and operator of the most advanced satellite communications system in existence today, the Tracking and Data Relay Satellite System (TDRSS). And we're further extending our expertise into the military space arena with responsibility for internal and external communications capabilities for the Air Force Consolidated Space Operations Center. Our innovative spirit is guiding us through ever greater successes.

Now we are seeking a **Director, Business Development** to further expand our involvement with C3I and NASA programs in DOD and special agencies.

You will identify new business opportunities, in an Eastern region, for all company capabilities, and will follow through on pursuit, pricing strategies, and proposal development. In addition, you will serve as a primary liaison between SPACECOM components and customers.

You must be a real entrepreneur with a success record of marketing to the Federal government. A BSEE/BSAeE degree and 10-15 years experience are required; MSEE/MSAeE or MBA a definite plus.

Make the journey with SPACECOM. Pack your briefcase with experience—and don't forget those valuable ideas. We offer excellent compensation and benefits, plus the challenge which every professional demands.

Send your resume with salary history, for a confidential review, to Steve Parker, SPACECOM, Dept. NTB-0601, 1300 Quince Orchard Boulevard, Gaithersburg, Maryland 20878.

The courage to lead

SPACECOM.

SPACE COMMUNICATIONS COMPANY

a partnership affiliated with Continental Telecom Inc. and Fairchild Industries, Inc.

U. S. Citizenship Required
We are an Equal Opportunity Employer

Circle Reader Action No. 385

ABOUT THE NASA TECHNOLOGY UTILIZATION PROGRAM


Subject Index

 **NASA TU Services**


 **New Product Ideas**

 **Electronic Components and Circuits**

 **Electronic Systems**

 **Physical Sciences**

 **Materials**


 **Life Sciences**

 **Mechanics**

 **Machinery**

 **Fabrication Technology**

 **Mathematics and Information Sciences**

 **Subject Index**

This document was prepared under the sponsorship of the National Aeronautics and Space Administration. NASA Tech Briefs is published quarterly and is free to engineers in U.S. industry and to other domestic technology transfer agents. It is both a current-awareness medium and a problem-solving tool. Potential products... industrial processes... basic and applied research... shop and lab techniques... computer software... new sources of technical data... concepts... can be found here. The short section on New Product Ideas highlights a few of the potential new products contained in this issue. The remainder of the volume is organized by technical category to help you quickly review new developments in your areas of interest. Finally, a subject index makes each issue a convenient reference file.

Further information on innovations—Although some new technology announcements are complete in themselves, most are backed up by Technical Support Packages (TSP's). TSP's are available without charge and may be ordered by simply completing a TSP Request Card, found at the back of this volume. Further information on some innovations is available for a nominal fee from other sources, as indicated. In addition, Technology Utilization Officers at NASA Field Centers will often be able to lend necessary guidance and assistance.

Patent Licenses—Patents have been issued to NASA on some of the inventions described, and patent applications have been submitted on others. Each announcement indicates patent status and availability of patent licenses if applicable.

Other Technology Utilization Services—To assist engineers, industrial researchers, business executives, Government officials, and other potential users in applying space technology to their problems, NASA sponsors Industrial Applications Centers. Their services are described on pages 20-22. In addition, an extensive library of computer programs is available through COSMIC, the Technology Utilization Program's outlet for NASA-developed software.

Applications Program—NASA conducts applications engineering projects to help solve public-sector problems in such areas as safety, health, transportation, and environmental protection. Two applications teams, staffed by professionals from a variety of disciplines, assist in this effort by working with Federal agencies and health organizations to identify critical problems amenable to solution by the application of existing NASA technology.

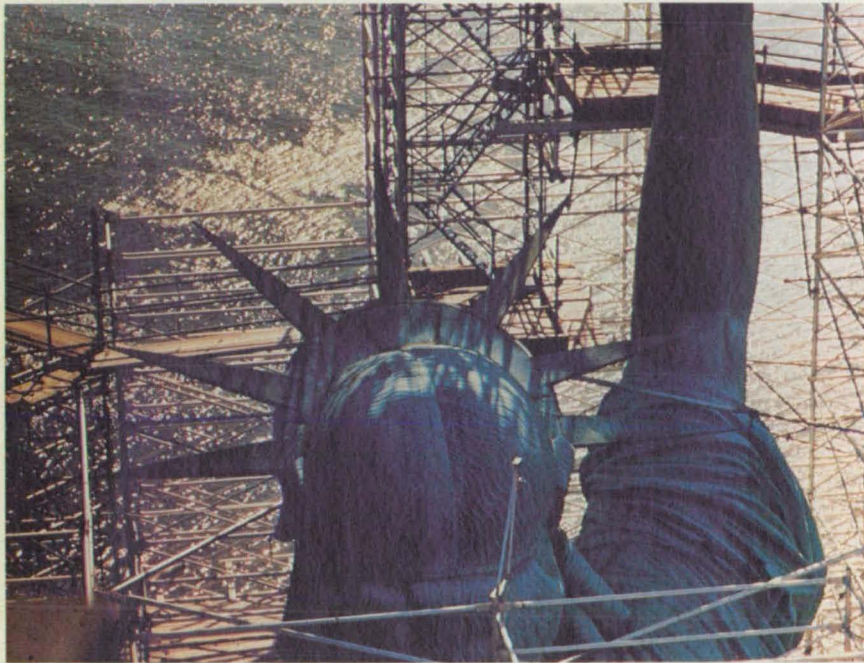
Reader Feedback—We hope you find the information in *NASA Tech Briefs* useful. A reader-feedback card has been included because we want your comments and suggestions on how we can further help you apply NASA innovations and technology to your needs. Please use it; or if you need more space, write to the Manager, Technology Transfer Division, P.O. Box 8757, Baltimore/Washington International Airport, Maryland 21240.

Advertising Reader Service—Reader Action Card (RAC): For further information on the advertisers, please circle the RAC number on the separate Reader Action Card in this issue.

Change of Address—If you wish to have *NASA Tech Briefs* forwarded to your new address, use the Subscription Card enclosed at the back of this volume of *NASA Tech Briefs*. Be sure to check the appropriate box indicating change of address, and also fill in your identification number (T number) in the space indicated. You may also call the Manager, Technology Utilization Office, at (301) 859-5300, ext. 242 or 243.

This document was prepared under the sponsorship of the National Aeronautics and Space Administration. Neither Associated Business Publications, Inc., nor anyone acting on behalf of Associated Business Publications, Inc., nor the United States Government nor any person acting on behalf of the United States Government assumes any liability resulting from the use of the information contained in this document, or warrants that such use will be free from privately owned rights. The U. S. Government does not endorse any commercial product, process, or activity identified in this publication.

Mission **A**ccomplished



Almost a century after assuming her post at the entrance to New York Harbor, the Statue of Liberty began to yield to the effects of time and the elements. Her offshore location had exposed her vulnerable copper exterior to the corrosive action of salt spray, wind and fog, and water had collected in the folds of Liberty's robes, in the curls of her hair and elsewhere—sometimes corroding all the way through.

Millions upon millions of visitors had left their various marks on the statue's interior, and leakage and corrosion combined to create the unsafe conditions which forced the closing of Liberty's torch, before indicating the need for a full-scale renovation. In 1984, such a project was undertaken, and plans call for its completion in time for the statue's 1986 centennial celebration.

The fast-paced rehabilitation has been aided by a variety of new technologies, including an anti-corrosion paint, originally developed by NASA, which is being used to coat Liberty's iron skeleton. More than 500 gallons of the water-based paint have been donated to the Statue of Liberty Foundation by Inorganic Coatings, Inc. of

Malvern, Pennsylvania, sole manufacturer of the NASA-patented compound. This donation, valued at \$20,000, along with numerous others, is helping to offset the renovation's \$31 million price tag.

The paint which will help give new life to Liberty was developed by researchers at NASA's Goddard Space Flight Center in the early 1970s, for use on the launch structures at Kennedy Space Center. Like Liberty, these structures had been extensively corroded by salt spray, wind and fog, and the cost of maintaining them with commercially available coatings was hefty both in terms of cost and labor. Available anti-corrosion coatings, formulated with zinc dust and either organic or inorganic bases, provided protection, but required two or three coats and lengthy curing periods. The Goddard researchers sought to develop a superior anti-corrosion coating which would resist salt and water, as well as protect the launch structures from the hot rocket exhaust and thermal shock created by rapid temperature changes during launches.

The successful research effort yielded breakthrough silicate chemistry and resulted in a new water-

Through the technology transfer process, many of the new systems, methods and products pioneered by NASA are reapplied in the private sector, obviating duplicate research and making a broad range of new products and services available to the public.

based inorganic zinc coating, which provides long-term protection with only one coat and dries in 30 minutes. The new coating also offers cost advantages in terms of both materials and labor.

To encourage private sector utilization of the new coating technology, NASA licensed it to Shane Associates of Wynnewood, Pennsylvania in 1981. The following year, Inorganic Coatings signed an agreement with Shane Associates to become sole manufacturer and sales agent of the compound, K-Zinc 531.

When Inorganic Coatings' president Parke Schaffer learned of the planned rehabilitation of the Statue of Liberty, he contacted the National Parks Administration to suggest the use of K-Zinc 531 on the statue's iron skeleton. After evaluating the product, the NPA determined that K-Zinc 531 was the best commercial coating available.

Among K-Zinc 531's assets is its water base, which renders the coating non-toxic and non-flammable. Since it has no organic solvent emissions, K-Zinc 531 is also ideal for application in poorly ventilated or enclosed areas, such as the statue's interior.

K-Zinc 531 has been utilized in a number of other refurbishing projects, among them San Francisco's Golden Gate Bridge. Currently, the U.S. Navy uses the coating in renovating older ships and for protecting newly-built ships. A variety of offshore drilling companies protect their rigs with K-Zinc 531, which adheres even in extreme marine environments. Inorganic Coatings is also receiving numerous inquiries from the railroad, automobile and heavy equipment industries.

However widely K-Zinc 531 is used, its most memorable role will undoubtedly be that of protecting the iron infrastructure of the Statue of Liberty, and upholding the promise made by Grover Cleveland at the statue's 1886 dedication: "We will not forget that Liberty has here made her home; nor shall her chosen altar be neglected."



Honeywell, Martin Marietta and Orbital to create a new privately financed



Commercial Space

In the early 1960's, Honeywell pioneered Ring Laser Gyro technology. Now we are working together with Orbital Sciences Corporation and Martin Marietta to pioneer the opening of space as a commercial frontier.

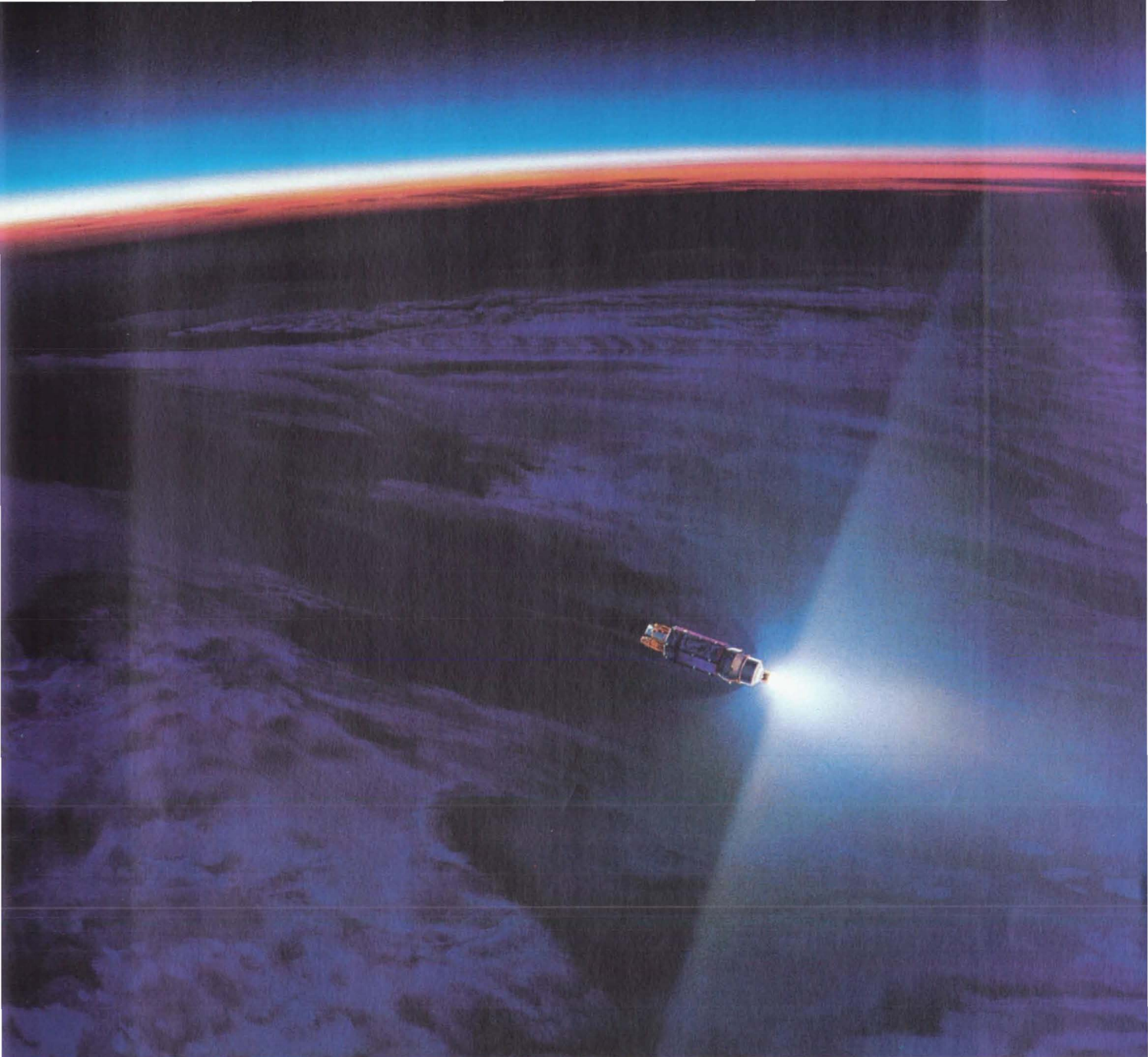
Orbital Sciences Corporation (OSC) recognized that something could be done to reduce the high cost of space transportation. So they developed a vehicle with Martin Marietta

for the purpose of low cost, highly reliable commercial space transportation.

Reliability

OSC, as the entrepreneurial firm responsible for making this project a success, needed team members who would be able to perform to the extreme demands of technical challenge, fixed cost and on-time delivery with a system that worked the first time. And every time.

That's why OSC and Martin Marietta came to Honeywell. We have demonstrated 25 years of



Orbital Sciences Corporation and Honeywell are working together on a commercial space vehicle.

reliable high performance on virtually every major American space program. From Project Mercury to



the Space Shuttle, Honeywell reliability has been a part of over 740 flights into space. The selection of Honeywell's Ring Laser Gyro technology was based on its low cost, exceptional performance capabilities, and its highly reliable operation in over 1500 Laser Inertial Navigation Systems (LINS).

Teamwork

If you would like to know more about our work with Orbital Sciences Corporation and Martin Marietta or how we could work with you, contact: Larry N. Speight, Space and Strategic Avionics Division, 13350 U.S. Highway 19 South, Clearwater, Florida 33546. Phone 813/539-5502.

Together, we can find the answers.

Honeywell

©1985 Honeywell Inc.
Above photo used with permission of Orbital Sciences Corporation ©1984 Orbital Sciences Corporation

BREAKTHROUGH: USE JETS OF WATER TO MAKE LIGHTER, STRONGER JETS.

By using composite materials—layers of carbon fiber cloth bonded together—we make Harrier II airplane parts that are lighter and stronger. But to make sure the layers are properly bonded, we needed a way to look deep inside each part.

To give us this inner view, McDonnell Douglas engineers developed a new method of ultrasonic testing—one that's completely automated.

They programmed water jets to follow the shape of a composite part exactly, adjusting to any change in thickness and automatically scanning every millimeter, quickly and precisely. With this "window to the inside," our quality and productivity are higher, while our costs are significantly lower.

We're creating breakthroughs not only in aerospace, but also in information systems and transportation.

We're McDonnell Douglas.

© 1985, McDonnell Douglas Corporation

MCDONNELL DOUGLAS



Circle Reader Action No. 372